Supplementary Information

Synthesis of Monophosphines Directly from White Phosphorus

Daniel J. Scott,* Jose Cammarata, Maximilian Schimpf and Robert Wolf*

Institute of Inorganic Chemistry, University of Regensburg, 93040 Regensburg, Germany

E-mail: robert.wolf@ur.de, daniel.scott@chemie.uni-regensburg.de

Table of contents

Supplementary Methods

Hydrostannylation of P_4

Supplementary Method 1: Effect of wavelength on the hydrostannylation of P_4 using Bu_3SnH and LED irradiation (0.01 mmol scale)

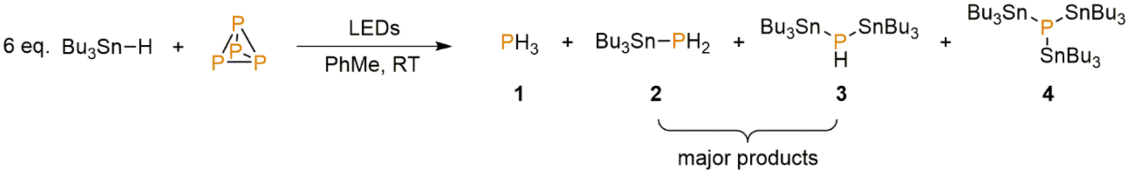

To 10 mL, flat-bottomed, stoppered tubes were added PhMe (500 µL), P_4 (0.01 mmol, as a stock solution in 86.0 µL PhH) and Bu_3SnH (16.1 µL, 0.06 mmol). The tubes were sealed, placed in a water-cooled block to maintain near-ambient temperature, and irradiated with blue light (455 nm (±15 nm), 3.2 V, 700 mA, Osram OSLON SSL 80) or near UV (365 nm) or green (528 nm) light of comparable intensity, for 45 minutes. The resulting mixtures were analysed by $^{31}P\{^{1}H\}$ spectroscopy, as shown in Supplementary Figure 1, below.

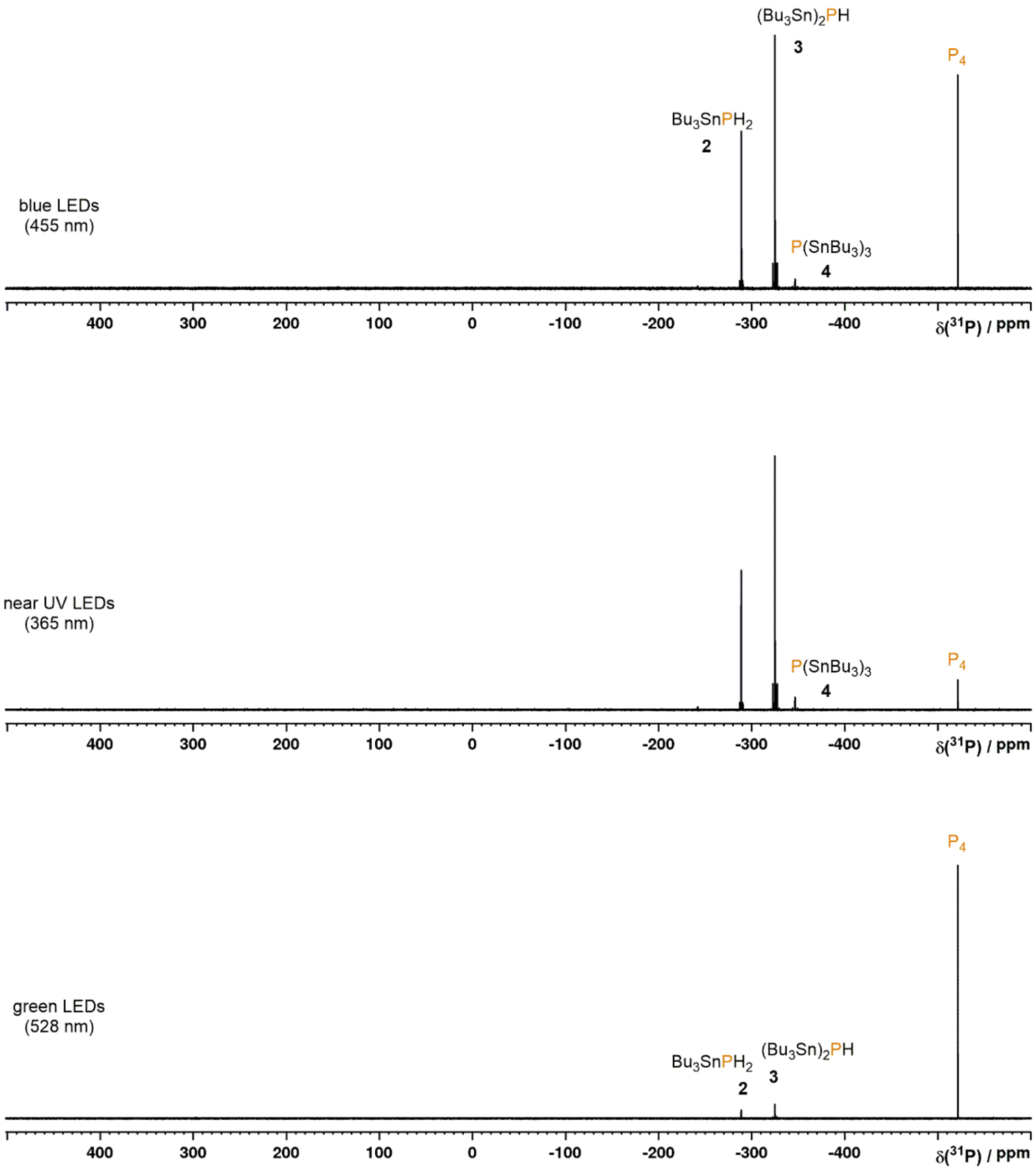

Supplementary Figure 1. ${}^{31}P\{{}^{1}H\}$ NMR spectra for the reaction of P_4 and 6 eq. Bu_3SnH in PhMe, driven by LED irradiation at various wavelengths for 45 minutes.

The spectra clearly show that faster reactivity is observed using near UV LEDs than blue LEDs, which in turn give a significantly faster reaction than green LEDs. Based on these observations, as well as on the fact that none of the reaction components absorbs light appreciably in the visible region (including in the combined reaction mixture; Supplementary Figure 2), we speculate that the observed photoreaction may not be driven by blue light *per se*, but rather by trace amounts of higher energy light being generated by the LED apparatus. Alternatively, Nakajima, Nemoto and colleagues have recently suggested that heavy atom-containing compounds may sometimes undergo direct S_0 to T_n photoexcitation at visible wavelengths, even if no appreciable absorption is observed at these frequencies in standard UV-vis experiments.[1]

Note also that, despite partial conversions, the spectra do not display any resonances other than those for the final products and starting material, suggesting an absence of stable intermediate products.

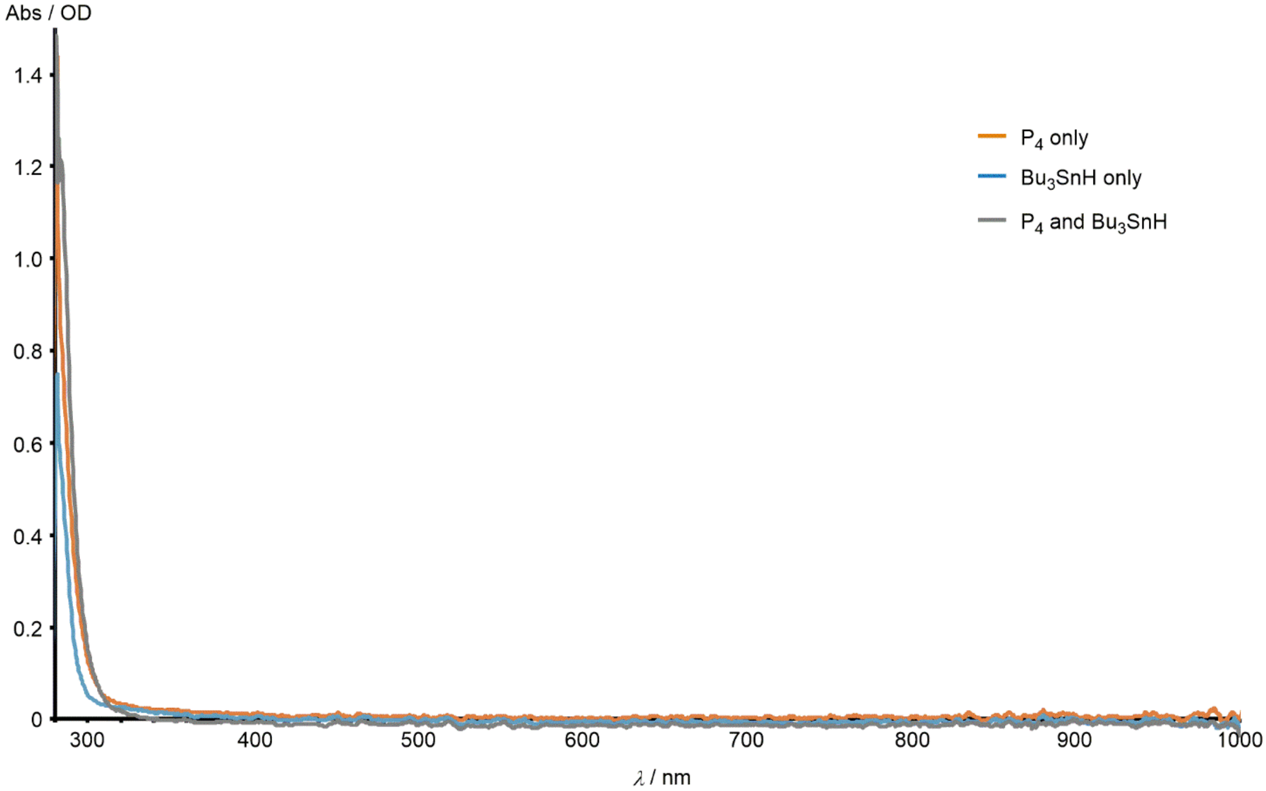

Supplementary Figure 2. UV-vis spectra for solutions of P_4 (0.02 M) and/or Bu_3SnH (0.12) in PhMe. These concentrations correlate to those typically used in P_4 hydrostannylation reactions.

The precise mechanism(s) for initial photochemical generation of $Bu_3Sn\cdot$ radicals in this reaction (as indicated in Fig. 2b) is a topic of ongoing investigation. However, previous studies into light-driven hydrostannylation reactions have suggested that initiation can proceed *via* initial photoinduced electron transfer from the relatively electron-rich tin hydride moiety to an electron-deficient substrate,[2] and an analogous pathway may be operative in this case, for example as illustrated in Supplementary Figure 3, below.

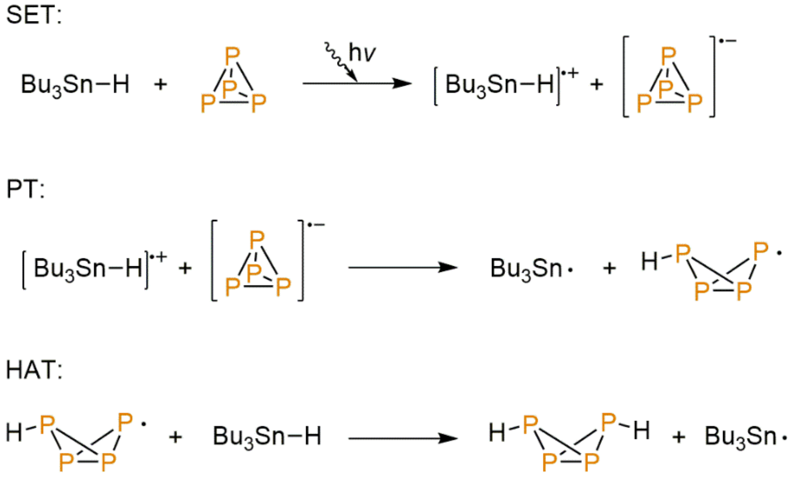

Supplementary Figure 3. A possible mechanism by which $Bu_3Sn\cdot$ radicals might be formed upon photoirradiation of a combination of Bu_3SnH and P_4, through a combination of photinduced single electron transfer (SET), proton transfer (PT) and hydrogen atom transfer (HAT) steps. Alternatively, the initial SET and PT steps could occur as a single, concerted, photoinduced HAT step.

Supplementary Method 2: Hydrostannylation of P_4 using Ph_3SnH under blue LED irradiation

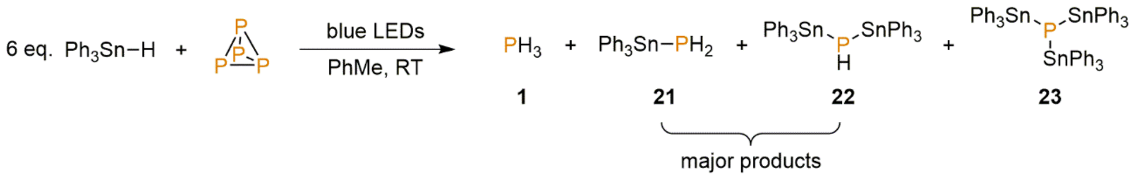

To a 10 mL, flat-bottomed, stoppered tube were added PhMe (500 µL), P_4 (0.01 mmol, as a stock solution in 77.4 µL PhH) and Ph_3SnH (21.1 mg, 0.06 mmol). The tube was sealed, placed in a water-cooled block to maintain near-ambient temperature, and irradiated with blue light (455 nm (±15 nm), 3.2 V, 700 mA, Osram OSLON SSL 80) for 18 h. The resulting mixture was analysed by ^{1}H, $^{31}P\{^{1}H\}$, ^{31}P and $^{119}Sn\{^{1}H\}$ NMR spectroscopy, as shown in Supplementary Figures 4-7, below.

Compared to the analogous reaction using Bu_3SnH (Extended Data Figures 2 and 3), a more appreciable amount of unreacted P_4 was seen to remain at the end of the reaction, although it remains a minor component of the mixture. Analysis of the $^{119}Sn\{^{1}H\}$ spectrum suggests this is probably due to competing generation of the distannane Sn_2Ph_6,[3-5] which could arise through dimerisation of $Ph_3Sn\cdot$ radicals. Alternatively, this could be due to direct reaction of Ph_3SnH with stannylated (oligo)phosphorus species to generate new Sn–Sn and P–H bonds. Such reactions have precedent in the literature,[6] and are expected to be more facile for Ph_3SnH than Bu_3SnH. It must be noted, however, that direct addition of a further 6 eq. of Ph_3SnH at the end of the reaction was not observed to lead to any change in the $^{31}P\{^1H\}$ NMR spectrum of the product mixture, even after 24 h (similarly, no change was observed upon addition of further Bu_3SnH to the analogous reaction mixture produced using Bu_3SnH). The final reaction products $(Ph_3Sn)_xPH_{3-x}$ (x = 1, **21**; x = 2, **22** ; x = 3, **23**) thus do not seem to participate in such reactivity (at least under the relevant reaction conditions).

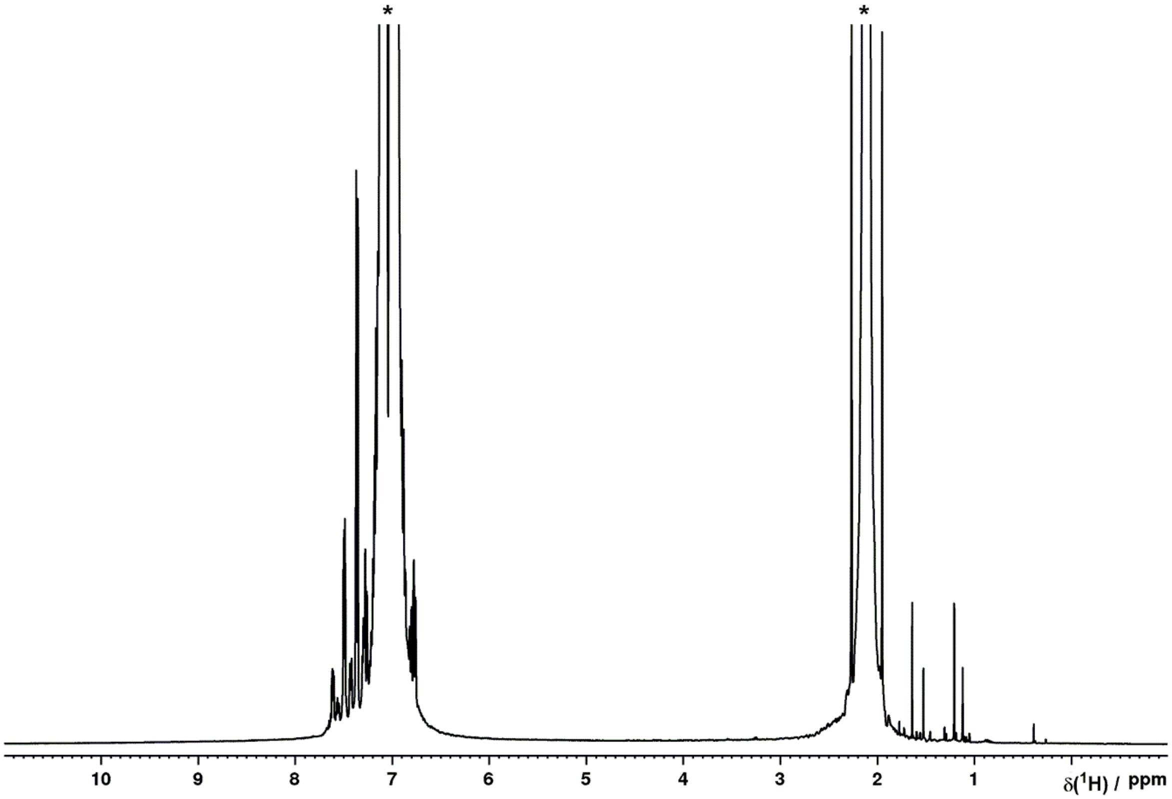

Supplementary Figure 4. ^1H NMR spectrum for the reaction of P_4 and 6 eq. Ph_3SnH in PhMe, driven by 455 nm LED irradiation for 18 h. Solvent resonances (*) truncated for clarity.

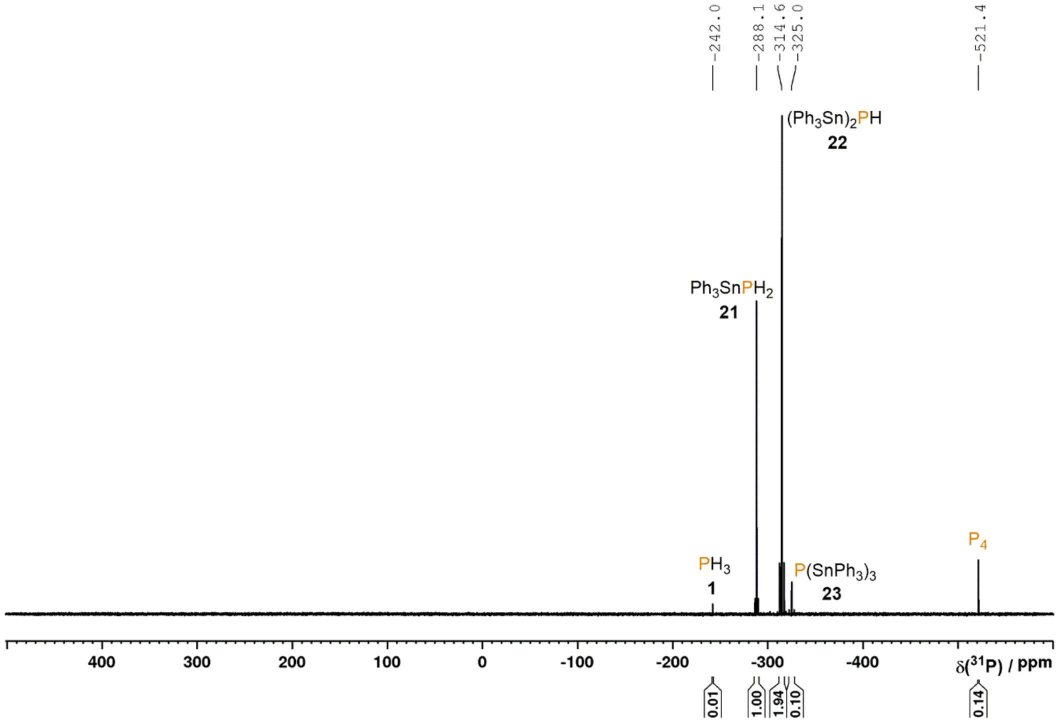

Supplementary Figure 5. $^{31}P\{^1H\}$ NMR spectrum for the reaction of P_4 and 6 eq. Ph_3SnH in PhMe, driven by 455 nm LED irradiation for 18 h.

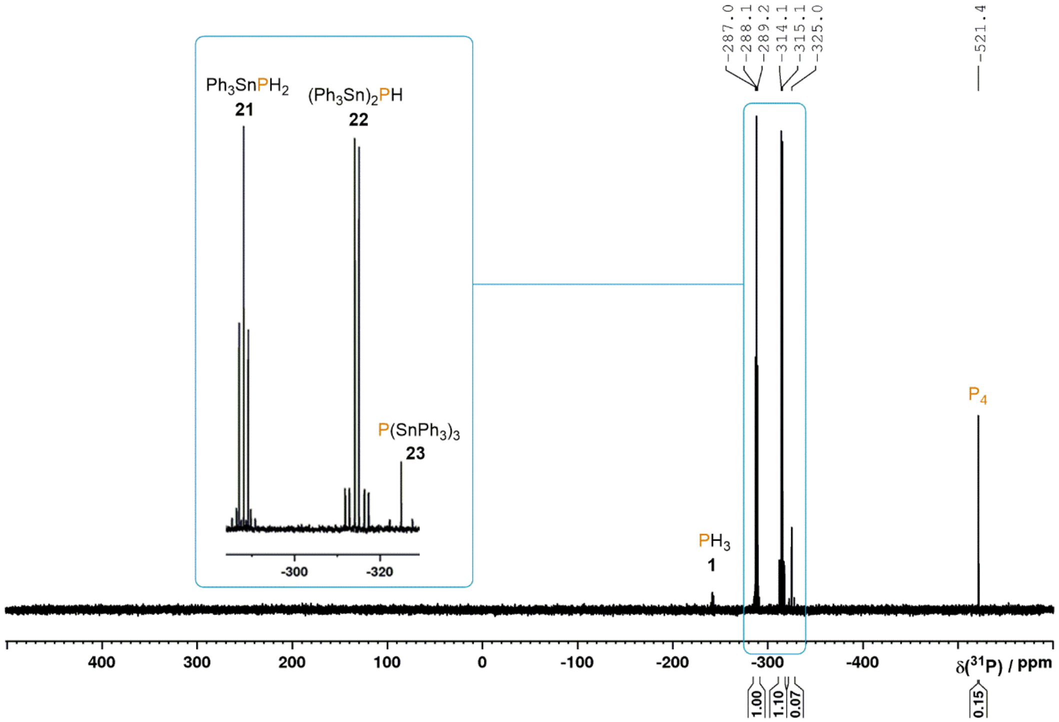

Supplementary Figure 6. ^{31}P NMR spectrum for the reaction of P_4 and 6 eq. Ph_3SnH in PhMe, driven by 455 nm LED irradiation for 18 h.

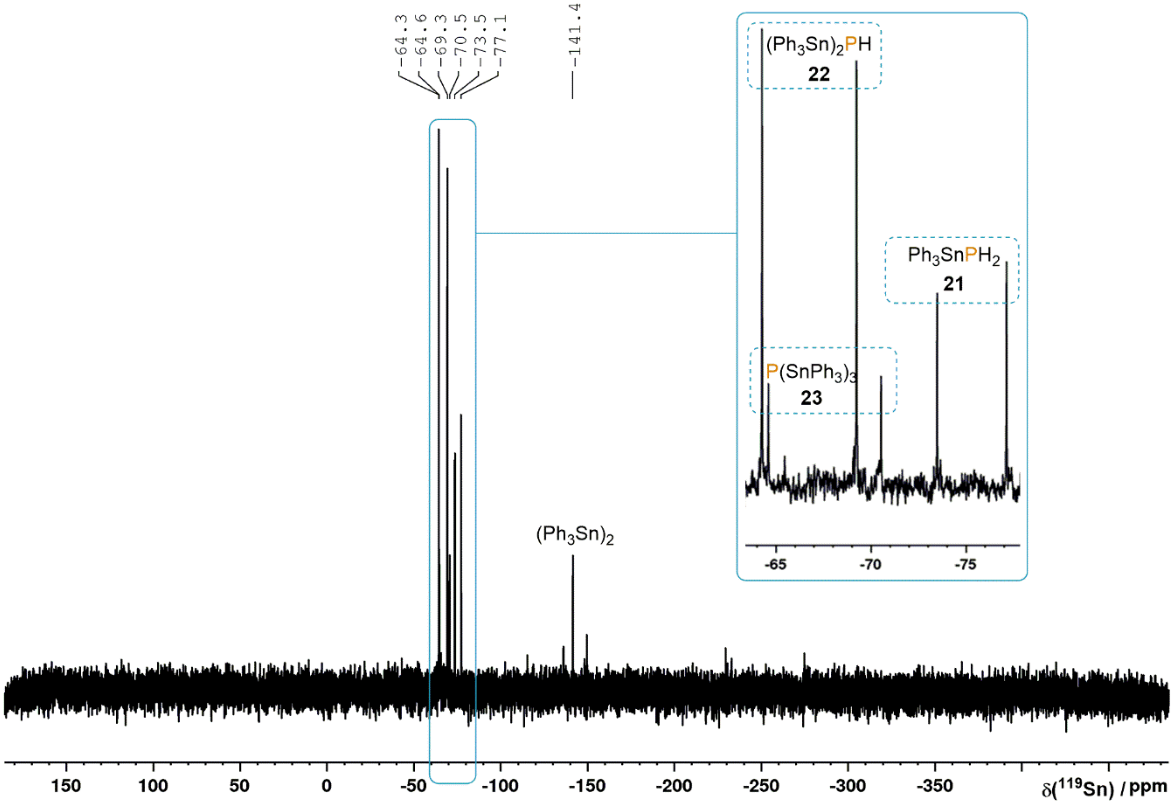

Supplementary Figure 7. $^{119}Sn\{^1H\}$ NMR spectrum for the reaction of P_4 and 6 eq. Ph_3SnH in PhMe, driven by 455 nm LED irradiation for 18 h.

	Ph_3SnPH_2 (**21**)	$(Ph_3Sn)_2PH$ (**22**)	$P(SnPh_3)_3$ (**23**)
$\delta(^{31}P)$ / ppm	–288.1	–314.6	–325.0
$\delta(^{119}Sn)$ / ppm	–75.3	–66.8	–67.6
$^1J(^{31}P\text{-}^1H)$ / Hz	173	162	-
$^1J(^{119}Sn\text{-}^{31}P)$ / Hz	545	741	883

Supplementary Table 1. Selected NMR parameters for compounds $(Ph_3Sn)_xPH_{3\text{-}x}$ (extracted from Supplementary Figures 10-12).

Supplementary Method 3: Hydrostannylation of P_4 using Bu_3SnH under blue LED irradiation (0.5 mmol scale), and isolation and stability of Bu_3SnPH_2 (2) and $(Bu_3Sn)_2PH$ (3)

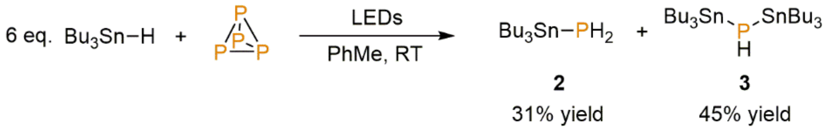

To a 50 mL flat-bottomed Schlenk tube were added P_4 (61.5 mg, 0.5 mmol) and PhMe (25 mL). After stirring to obtain a homogeneous solution Bu_3SnH was added (801 µL, 3.0 mmol). The resulting homogeneous, colorless solution was stirred under irradiation with blue LED light (7X Osram OSLON SSL80, 455 nm (±15 nm), 20.3 V 1000mA) for 18 h, during which time the Schlenk tube was placed in a block cooled by circulating water to maintain near-ambient temperature. Following removal of PhMe under vacuum, the major reaction products were separated by distillation under vacuum (*ca.* 105 °C, 10^{-2} mbar). Bu_3SnPH_2 (**2**) was collected as the volatile fraction (200 mg, 31%) as a colorless oil. $(Bu_3Sn)_2PH$ (**3**) remained as the non-volatile fraction (555 mg, 45%), which was also collected as a colorless oil.

The $(Bu_3Sn)_2PH$ (**3**) isolated in this manner is typically found to be *ca.* 90% pure (as assessed by $^{31}P\{^1H\}$ NMR spectroscopy), containing minor amounts of Bu_3SnPH_2 (**2**) and/or $P(SnBu_3)_3$ (**4**).

Note that the yields and purities obtained for the individual major products are highly dependent on the conditions (temperature and duration) used during the distillation step. If performed too slowly, or at especially high temperature, significant scrambling of the substituents on the P atoms can be observed. This leads to reduced purity of the $(Bu_3Sn)_2PH$ product, due to increased contamination with $P(SnBu_3)_3$. At the same time, this can increase the yield of isolated Bu_3SnPH_2 (which remains clean if kept cold), as more of this compound is formed during scrambling of $(Bu_3Sn)_2PH$. To obtain good yields and purities of both products it is recommended to use as high a vacuum as possible during distillation. For example, using a significantly higher vacuum of *ca.* 10^{-5} mbar allows for a significantly lower distillation temperature (*ca.* 70 °C).

Slow scrambling (over the course of several days) is also observed at room temperature for isolated samples of both products (which suggests that these are kinetic products of the hydrostannylation reaction, with the thermodynamic products being PH_3 and $P(SnBu_3)_3$, presumably due to loss of the former as a gas). However, both are stable for extended periods (at least several months) if stored at –35 °C.

*For Bu_3SnPH_2 (**2**):*

^{1}H NMR (400 MHz, 300 K, C_6D_6): δ = 1.63-1.41 (2H, m), 1.38-1.22 (2H, m), 1.07-0.84 ppm (5H, m).

^{31}P{^{1}H} NMR (121 MHz, 300 K, C_6D_6): δ = –288.4 ppm (s).

^{31}P NMR (121 MHz, 300 K, CD_3CN) : δ = –288.4 ppm (t, $^1J(^{31}P-^1H)$ = 171 Hz).

^{119}Sn{^{1}H} (149 MHz, 300 K, C_6D_6) δ = 18.2 ppm (d, $^1J(^{31}P-^{119}Sn)$ = 522 Hz).

^{13}C{^{1}H} NMR (101 MHz, 300 K, C_6D_6): δ = 29.4 (s), 27.1 (s), 13.5 (s) 11.8 ppm (d, $J(^{31}P-^{13}C)$ = 3.5 Hz).

Analysis of Bu_3SnPH_2 by mass spectrometry has thus far only revealed molecular ion peaks attributable to $(Bu_3Sn)_2PH$ (see below), which we attribute to rapid scrambling in the instrument during the experiment.

Similar NMR data have been reported previously for the related compound Me_3SnPH_2.[7]

*For $(Bu_3Sn)_2PH$ (**3**):*

^{1}H NMR (400 MHz, 300 K, C_6D_6): δ = 1.84-1.53 (12H, m), 1.53-1.33 (12H, m), 1.32-1.04 (12H, m), 1.02-0.86 (18H, m), 0.43 ppm (1H, d, $^1J(^{31}P-^1H)$ = 158 Hz).

^{31}P{^{1}H} NMR (121 MHz, 300 K, C_6D_6): δ = –324.8 ppm (s).

^{31}P NMR (121 MHz, 300 K, CD_3CN) : δ = –324.8 ppm (d, $^1J(^{31}P-^1H)$ = 158 Hz).

^{119}Sn{^{1}H} (149 MHz, 300 K, C_6D_6) δ = 31.7 ppm (d, $^1J(^{31}P-^{119}Sn)$ = 731 Hz).

^{13}C{^{1}H} NMR (101 MHz, 300 K, C_6D_6): δ = 29.5 (d, $J(^{31}P-^{13}C)$ = 0.9 Hz), 27.4 (s), 13.6 (s), 13.2 ppm (d, $J(^{31}P-^{13}C)$ = 0.9 Hz).

MS (EI, PhMe): *m/z* = 612.2053 (M^+).

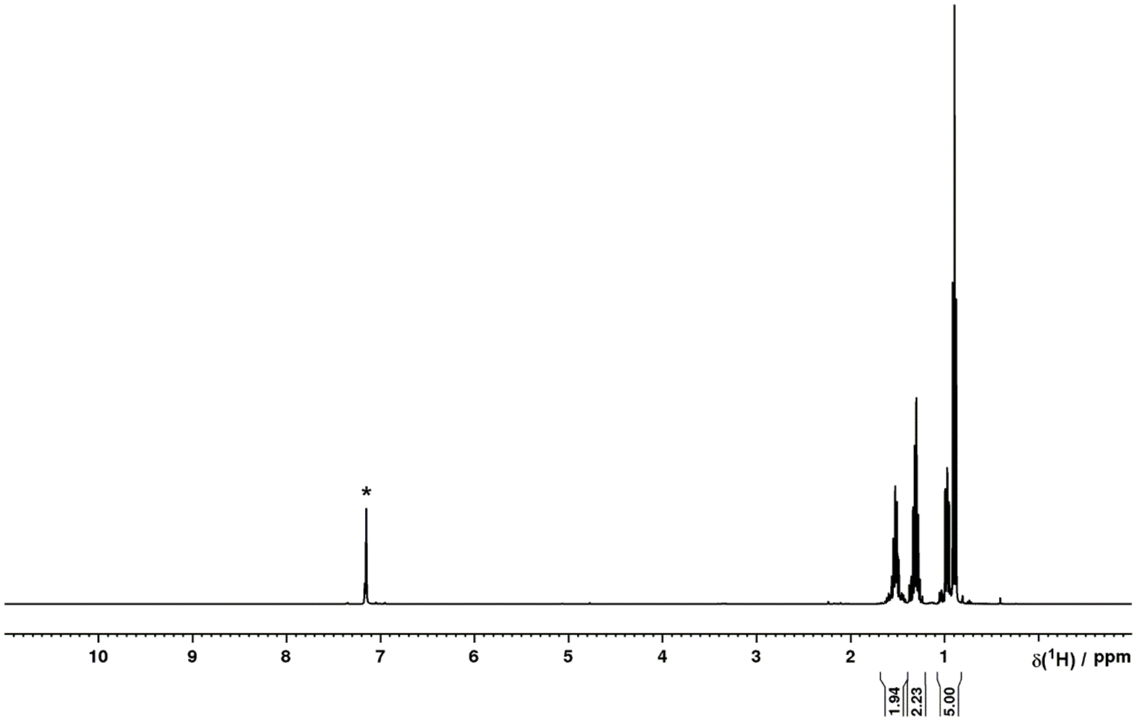

Supplementary Figure 8. ^{1}H NMR spectrum of Bu_3SnPH_2 (**2**) in C_6D_6 (*).

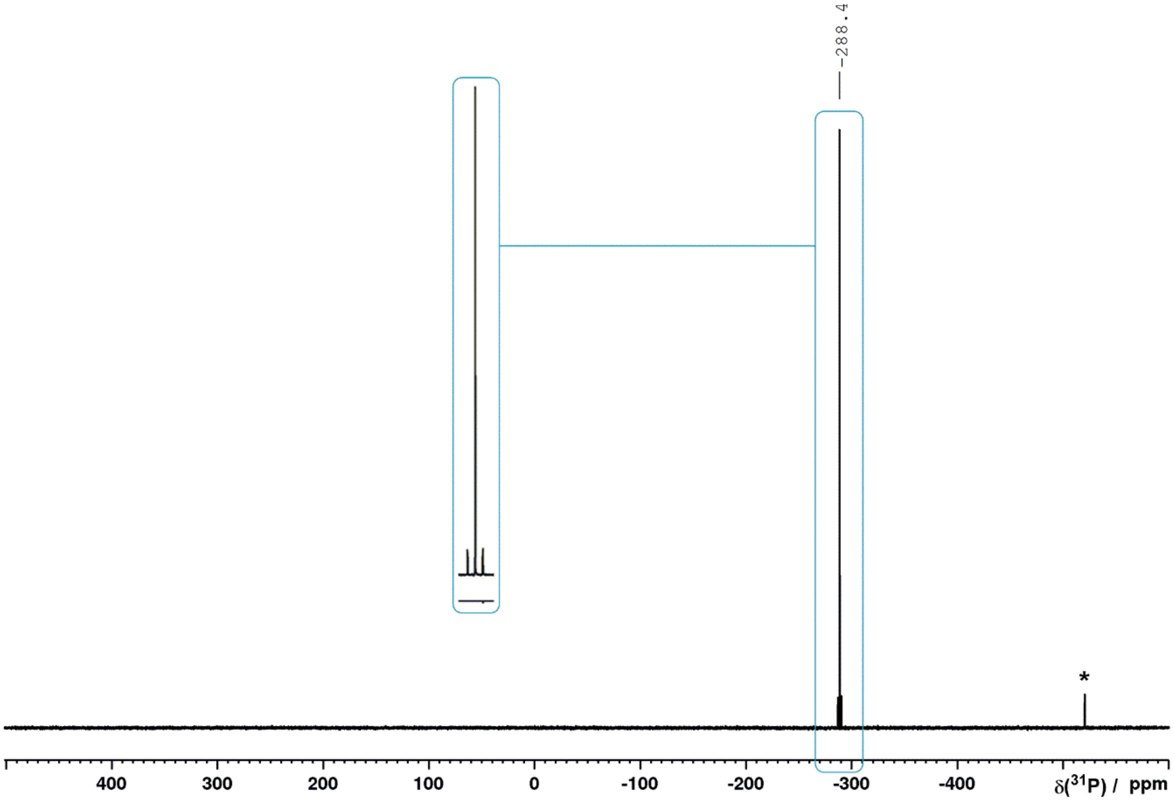

Supplementary Figure 9. $^{31}P\{^1H\}$ NMR spectrum of Bu_3SnPH_2 (**2**) in C_6D_6 (*trace residual P_4).

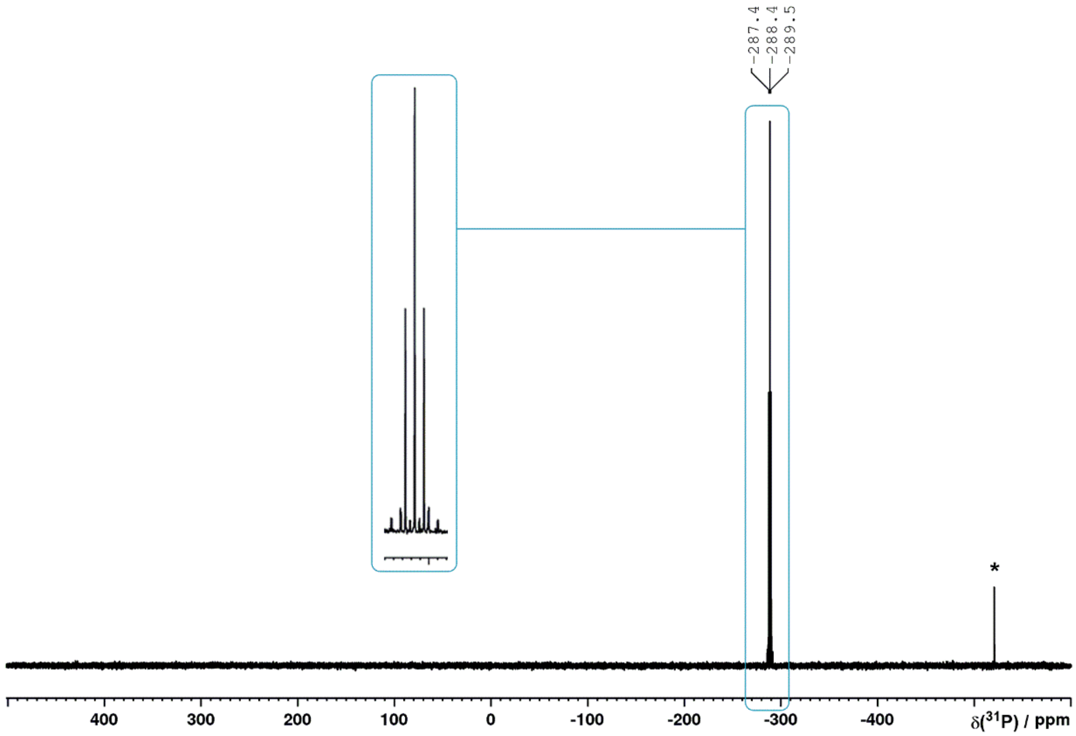

Supplementary Figure 10. ^{31}P NMR spectrum of Bu_3SnPH_2 (**2**) in C_6D_6 (*trace residual P_4).

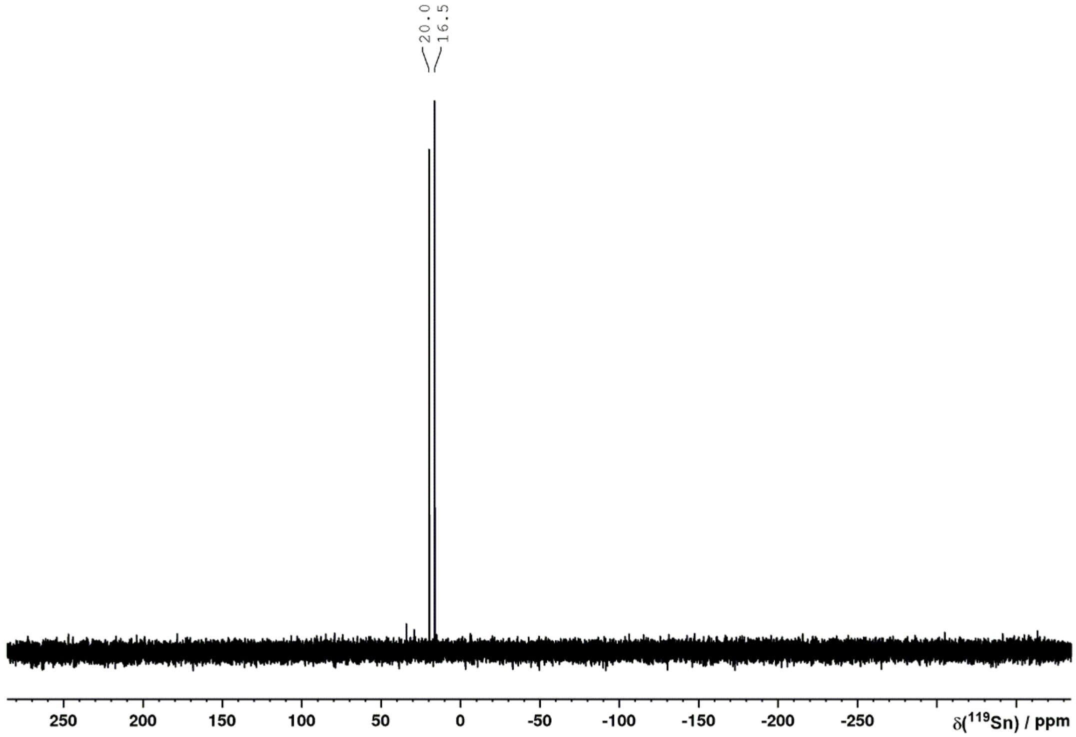

Supplementary Figure 11. $^{119}Sn\{^1H\}$ NMR spectrum of Bu_3SnPH_2 (**2**) in C_6D_6.

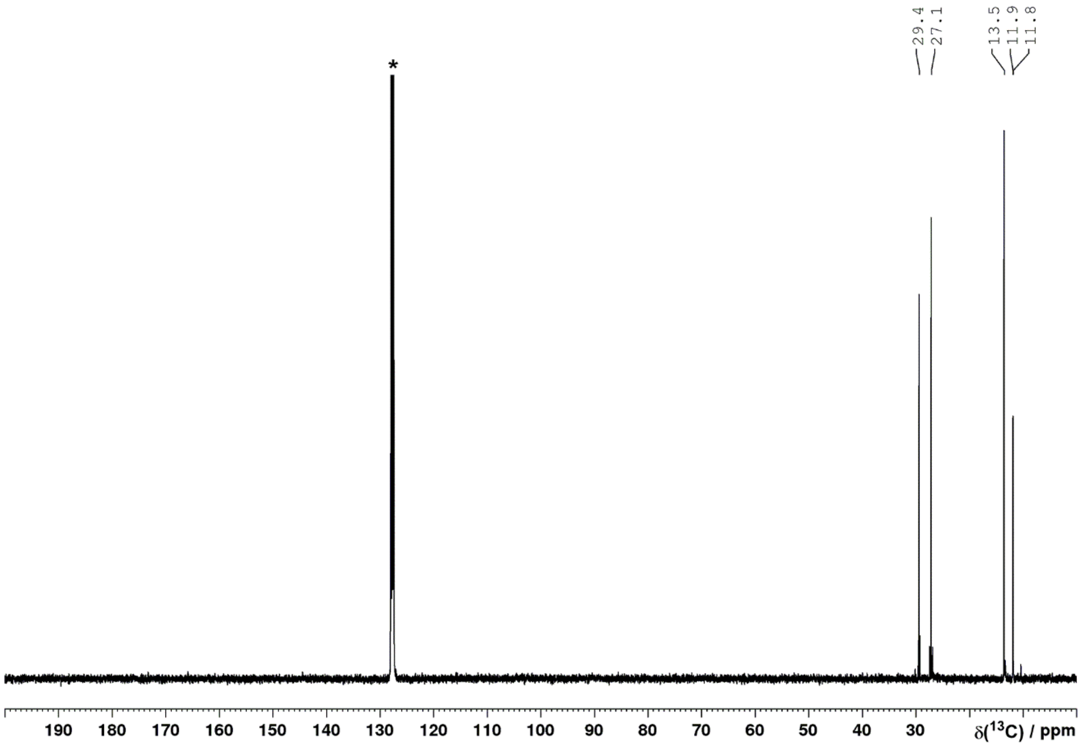

Supplementary Figure 12. $^{13}C\{^1H\}$ NMR spectrum of Bu_3SnPH_2 (**2**) in C_6D_6. Solvent resonance (*) truncated for clarity.

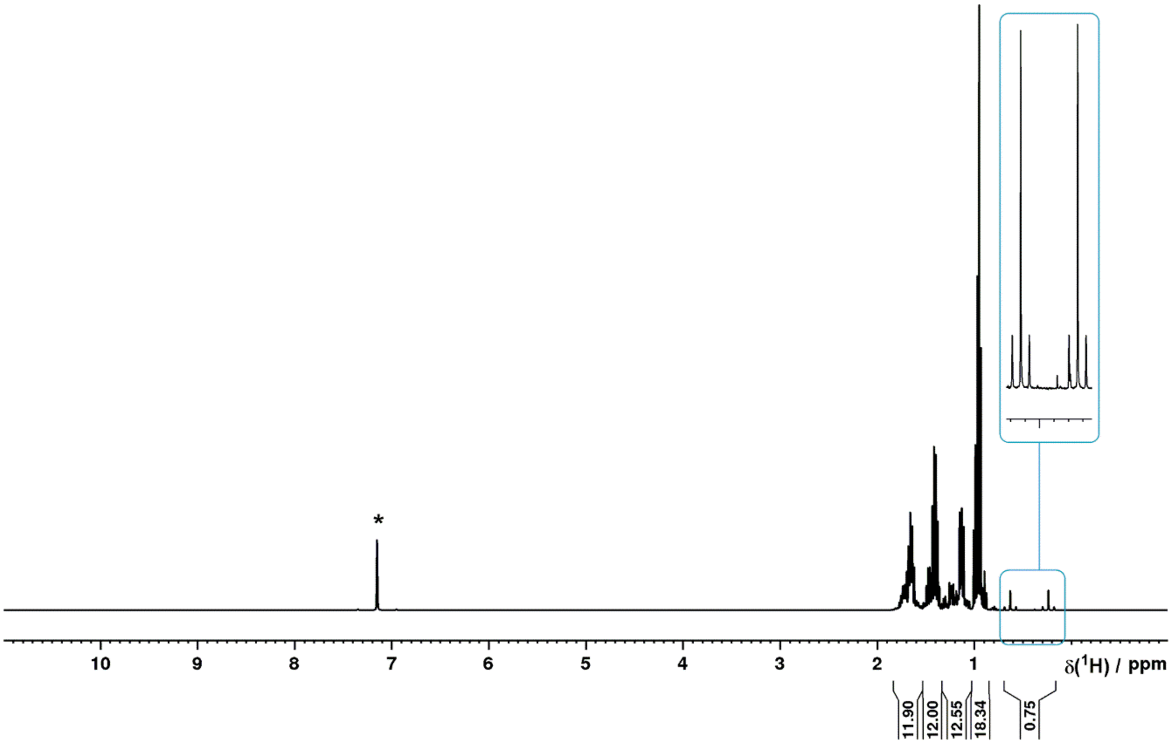

Supplementary Figure 13. ^1H NMR spectrum of $(Bu_3Sn)_2PH$ (**3**) in C_6D_6 (*).

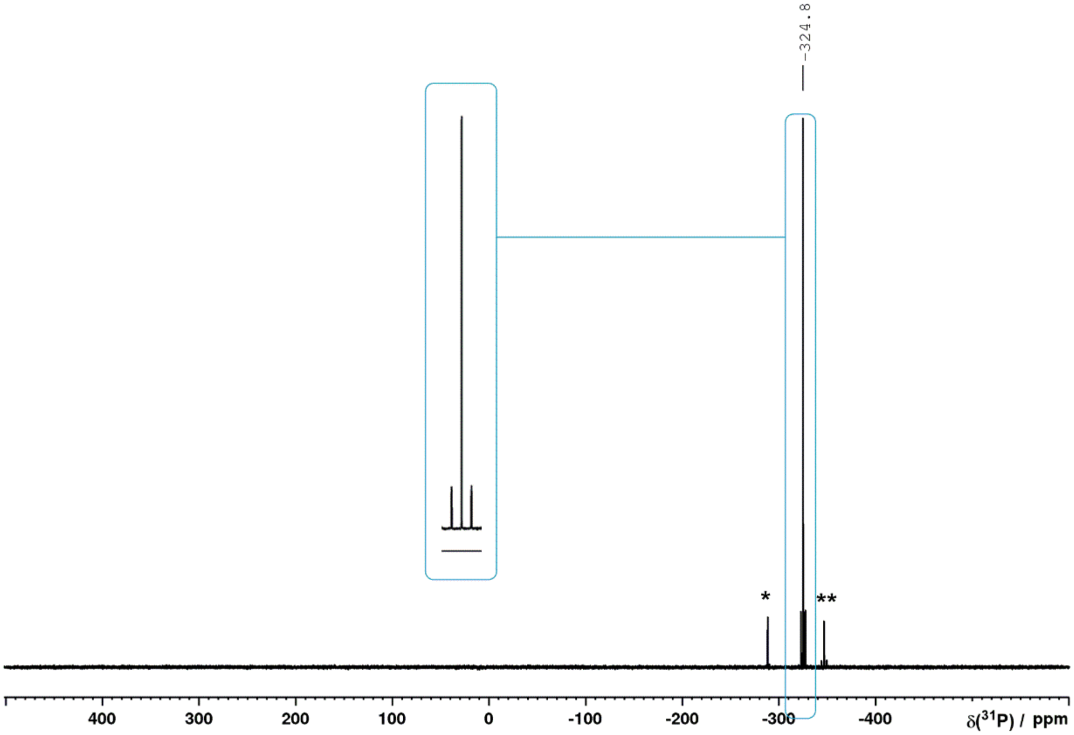

Supplementary Figure 14. $^{31}P\{^{1}H\}$ NMR spectrum of $(Bu_3Sn)_2PH$ (**3**) in C_6D_6, also containing minor Bu_3SnPH_2 (*) and $P(SnBu_3)_3$ (**).

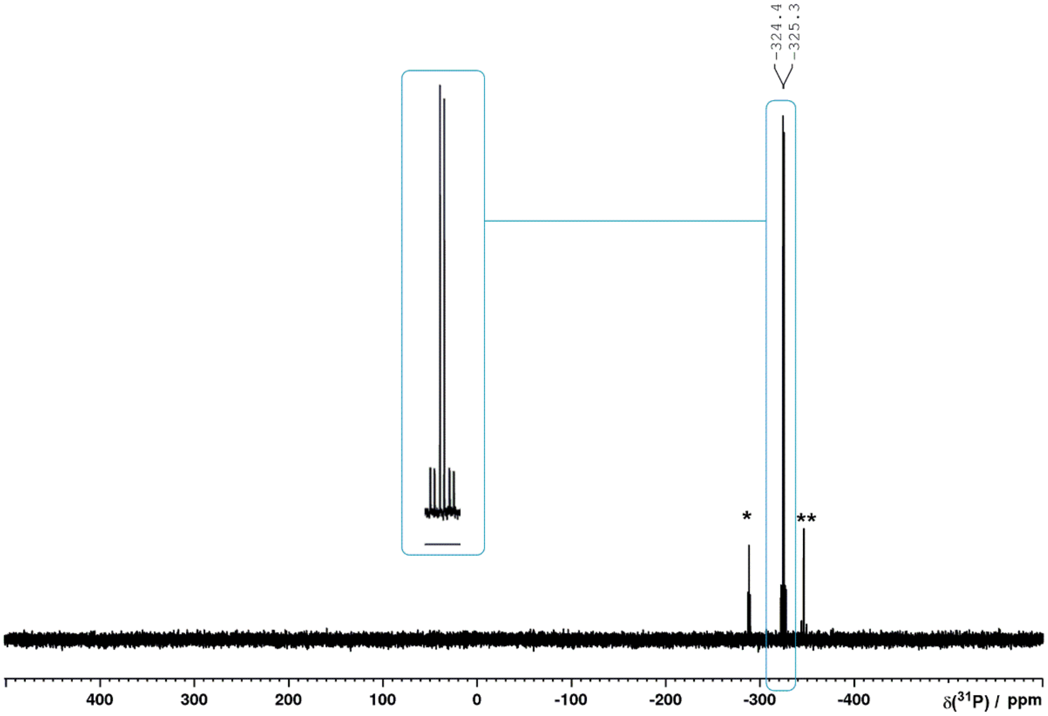

Supplementary Figure 15. ^{31}P NMR spectrum of $(Bu_3Sn)_2PH$ (**3**) in C_6D_6, also containing minor Bu_3SnPH_2 (*) and $P(SnBu_3)_3$ (**).

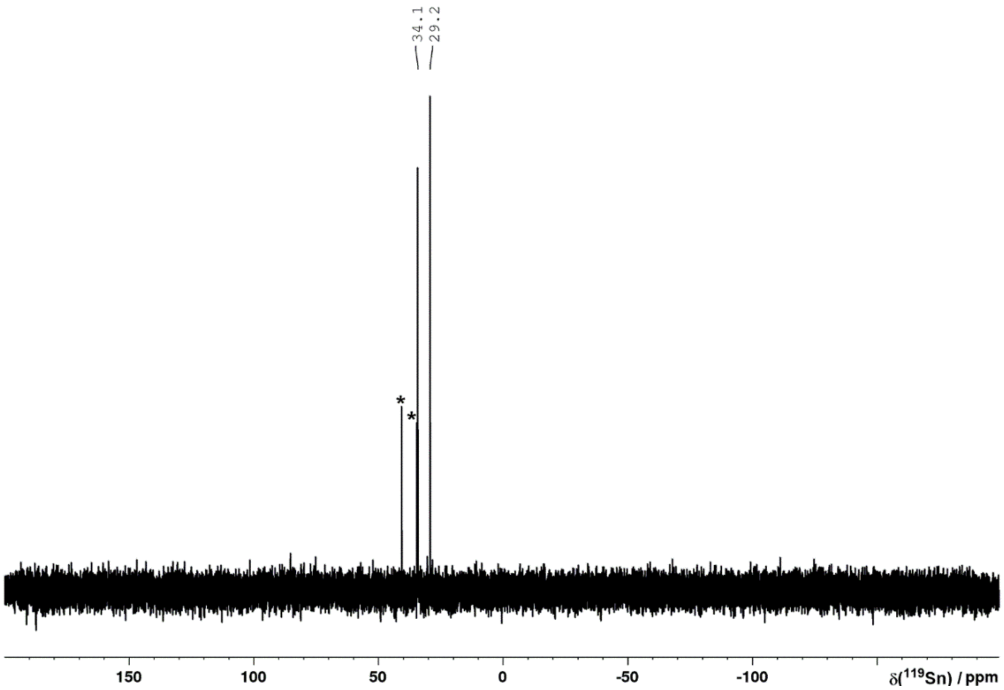

Supplementary Figure 16. $^{119}Sn\{^{1}H\}$ NMR spectrum of $(Bu_3Sn)_2PH$ (**3**) in C_6D_6, also containing minor $P(SnBu_3)_3$ (*).

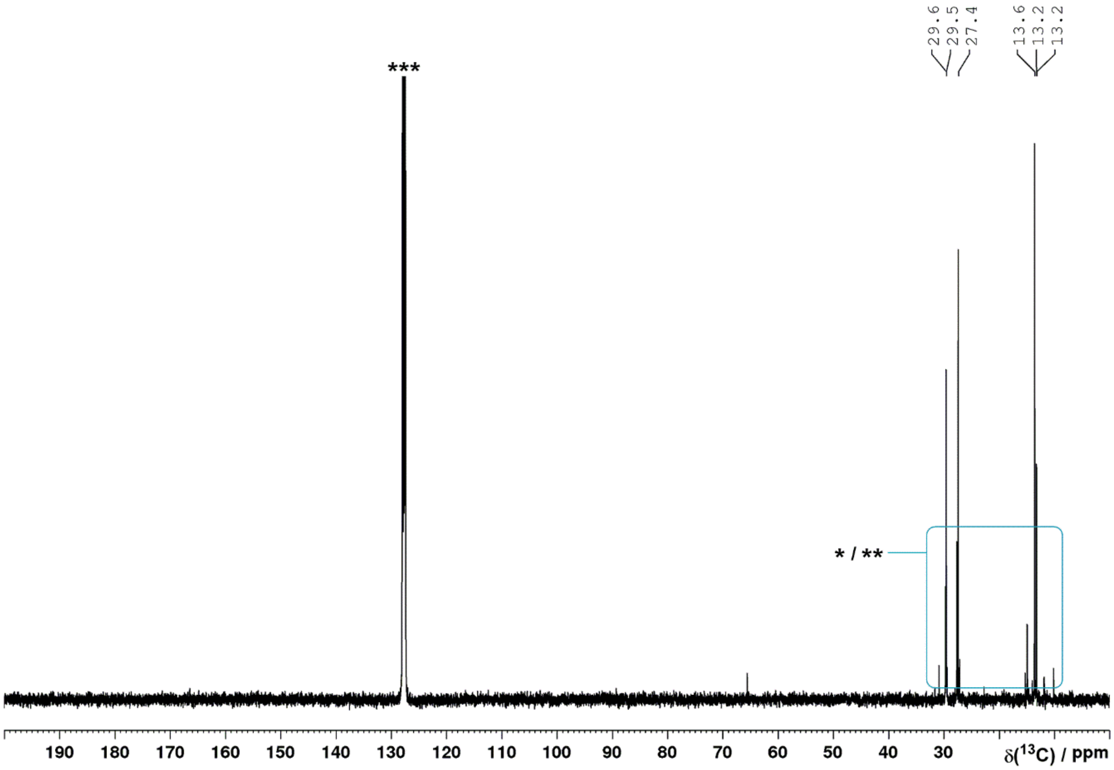

Supplementary Figure 17. $^{13}C\{^{1}H\}$ NMR spectrum of $(Bu_3Sn)_2PH$ (**3**) in C_6D_6, also containing minor Bu_3SnPH_2 (*) and $P(SnBu_3)_3$ (**). Solvent resonance (***) truncated for clarity.

Supplementary Method 4: Air-stability of the products $(Bu_3Sn)_xPH_{3-x}$ (x = 1-3)

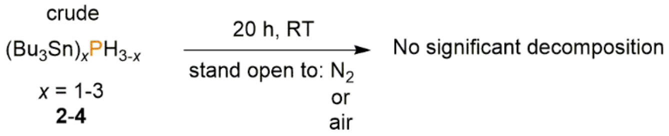

To a pair of 10 mL, flat-bottomed, stoppered Schlenks were added PhMe (500 µL), P_4 (0.01 mmol, as a stock solution in 86.0 µL PhH) and Bu_3SnH (16.1 µL, 0.06 mmol). The tubes was sealed, placed in a water-cooled block to maintain near-ambient temperature, and irradiated with blue light (455 nm (±15 nm), 3.2 V, 700 mA, Osram OSLON SSL 80) for 18 h. Volatiles were then removed under vacuum to give identical colourless oils. One Schlenk was back-filled with dry N_2 and sealed. The other was back-filled with air and left open to the atmosphere. Both tubes were left to stand fo 20 h. Dry, degassed PhMe (500 µL) was then added to both, followed by Ph_3PO (0.02 mmol, as a stock solution in 245 µL MeCN) to act as in internal standard for $^{31}P\{^1H\}$ NMR spectroscopy. The resulting solutions were analysed by $^{31}P\{^1H\}$ NMR spectroscopy, as shown in Supplementary Figure 18, below. The spectra show no appreciable difference between the two samples, indicating that the Bu_3Sn-substituted phosphine products are all appreciably air-stable.

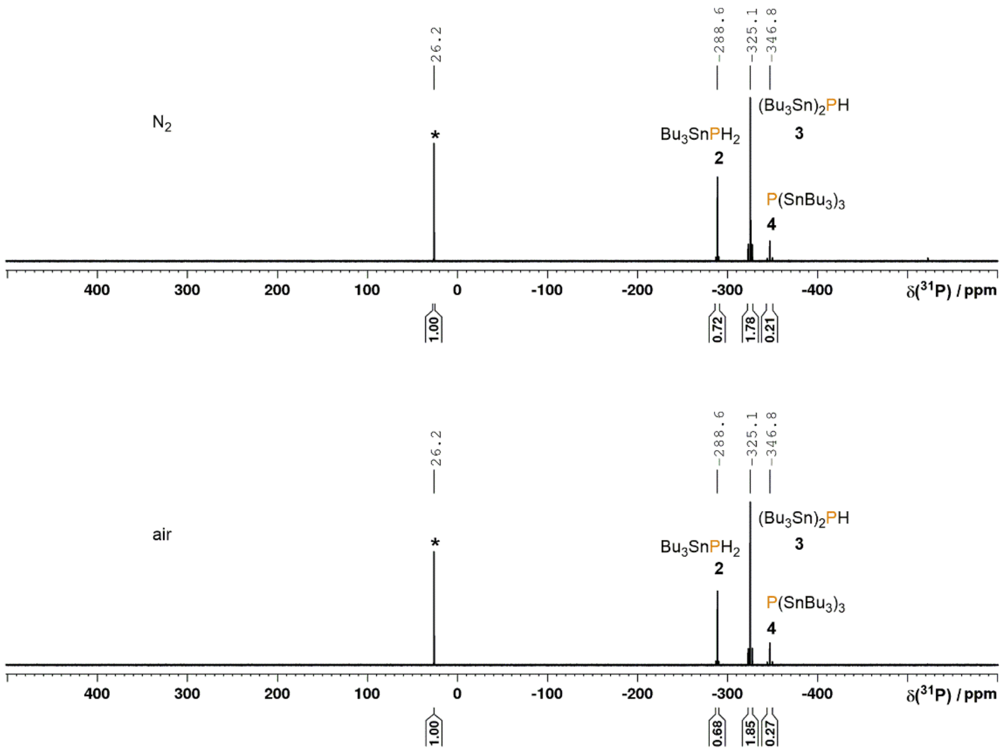

Supplementary Figure 18. $^{31}P\{^1H\}$ NMR spectra in PhMe of a crude P_4 hydrostannylation mixture, after standing neat overnight under N_2 or under air. Spectra acquired in PhMe, also containing Ph_3PO (*) as an internal standard.

Supplementary Method 5: Hydrostannylation of P_4 using Bu_3SnH initiated by AIBN (0.01 mmol scale)

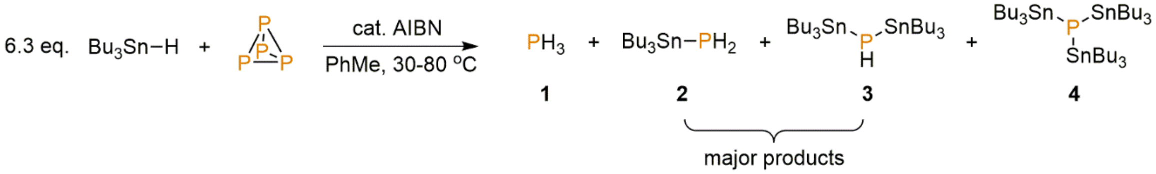

To a 10 mL, flat-bottomed, stoppered tube were added PhMe (500 µL), P_4 (0.01 mmol, as a stock solution in 77.4 µL PhH), AIBN (0.001 mmol, as a stock solution in 49.3 µL PhH) and Bu_3SnH (16.9 µL, 0.063 mmol). The tube was sealed, wrapped in Al foil to exclude light, and heated to 30 °C for 18 h. The resulting mixture was analysed by $^{31}P\{^1H\}$ NMR spectroscopy, as shown in Supplementary Figure 19, below.

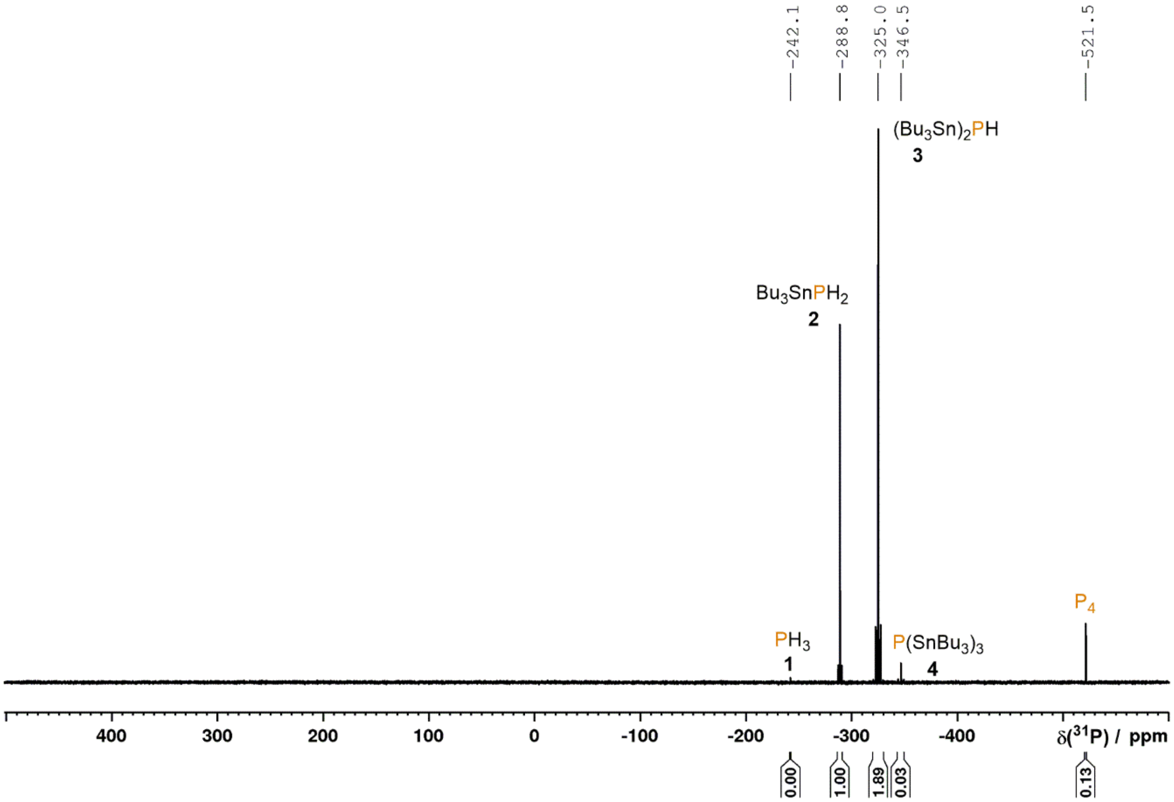

Supplementary Figure 19. $^{31}P\{^1H\}$ NMR spectrum for the reaction of P_4 and 6.3 eq. Bu_3SnH in PhMe, driven by AIBN initiation (2.5 mol% per P) at 30 °C for 18 h.

Otherwise equivalent reactions could be driven to completion with shorter reaction times or reduced catalyst loadings by using elevated temperatures (Supplementary Figures 20-23).

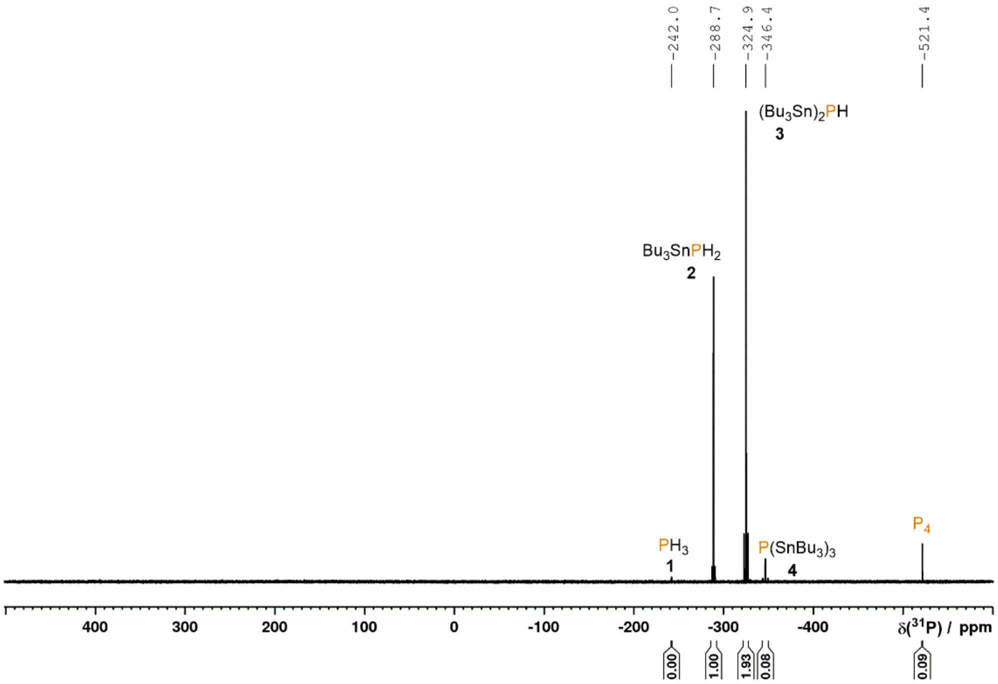

Supplementary Figure 20. $^{31}P\{^{1}H\}$ NMR spectrum for the reaction of P_4 and 6.3 eq. Bu_3SnH in PhMe, driven by AIBN initiation (2.5 mol% per P) at 60 °C for 2 h.

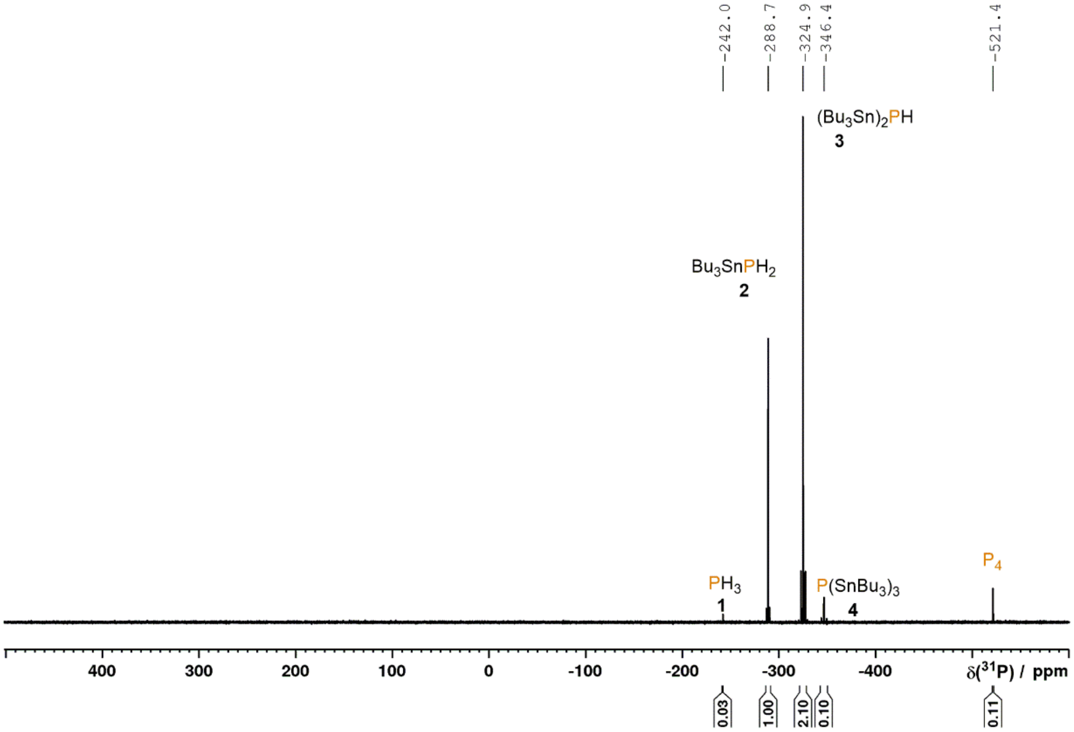

Supplementary Figure 21. $^{31}P\{^{1}H\}$ NMR spectrum for the reaction of P_4 and 6.3 eq. Bu_3SnH in PhMe, driven by AIBN initiation (2.5 mol% per P) at 80 °C for 1 h.

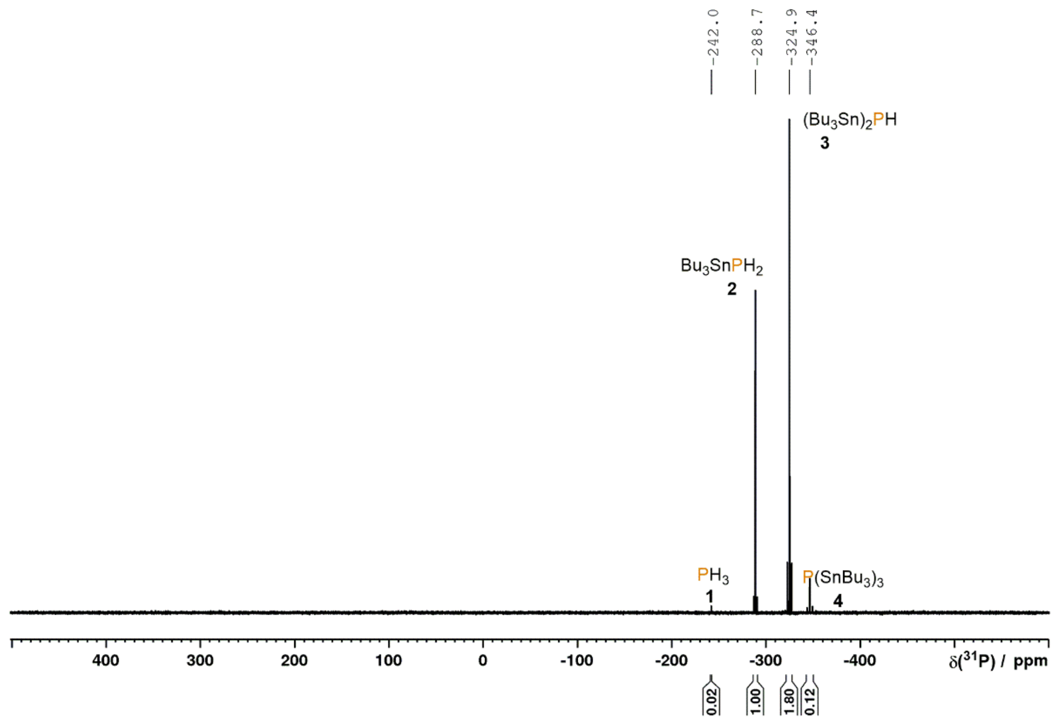

Supplementary Figure 22. $^{31}P\{^1H\}$ NMR spectrum for the reaction of P_4 and 6.3 eq. Bu_3SnH in PhMe, driven by AIBN initiation (0.25 mol% per P) at 60 °C for 19 h.

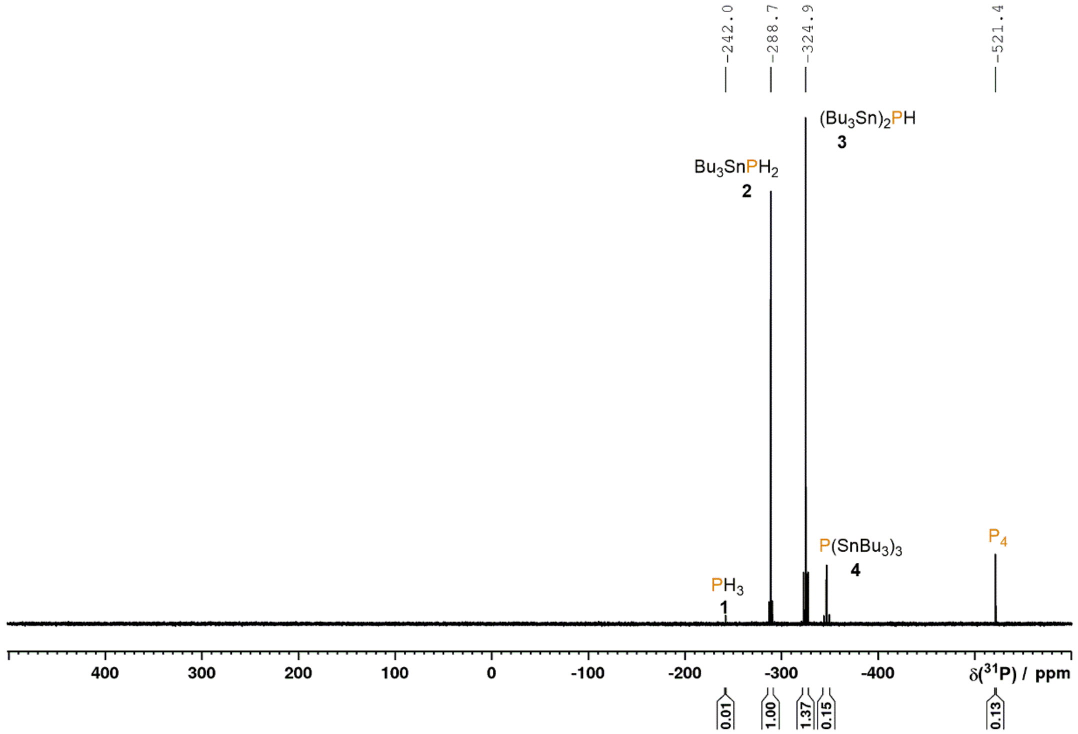

Supplementary Figure 23. $^{31}P\{^1H\}$ NMR spectrum for the reaction of P_4 and 6.3 eq. Bu_3SnH in PhMe, driven by AIBN initiation (0.025 mol% per P) at 80 °C for 18 h.

Supplementary Method 6: Hydrostannylation of P_4 using Bu_3SnH initiated by ACN (0.01 mmol scale)

To a 10 mL, flat-bottomed, stoppered tube were added PhMe (500 µL), P_4 (0.01 mmol, as a stock solution in 86.0 µL PhH), ACN (1.2 mg, 0.005 mmol) and Bu_3SnH (26.9 µL, 0.1 mmol). The tube was sealed, wrapped in Al foil to exclude light, and heated to 60 °C for 16 h. The resulting mixture was analysed by $^{31}P\{^1H\}$ NMR spectroscopy, as shown in Supplementary Figure 24, below.

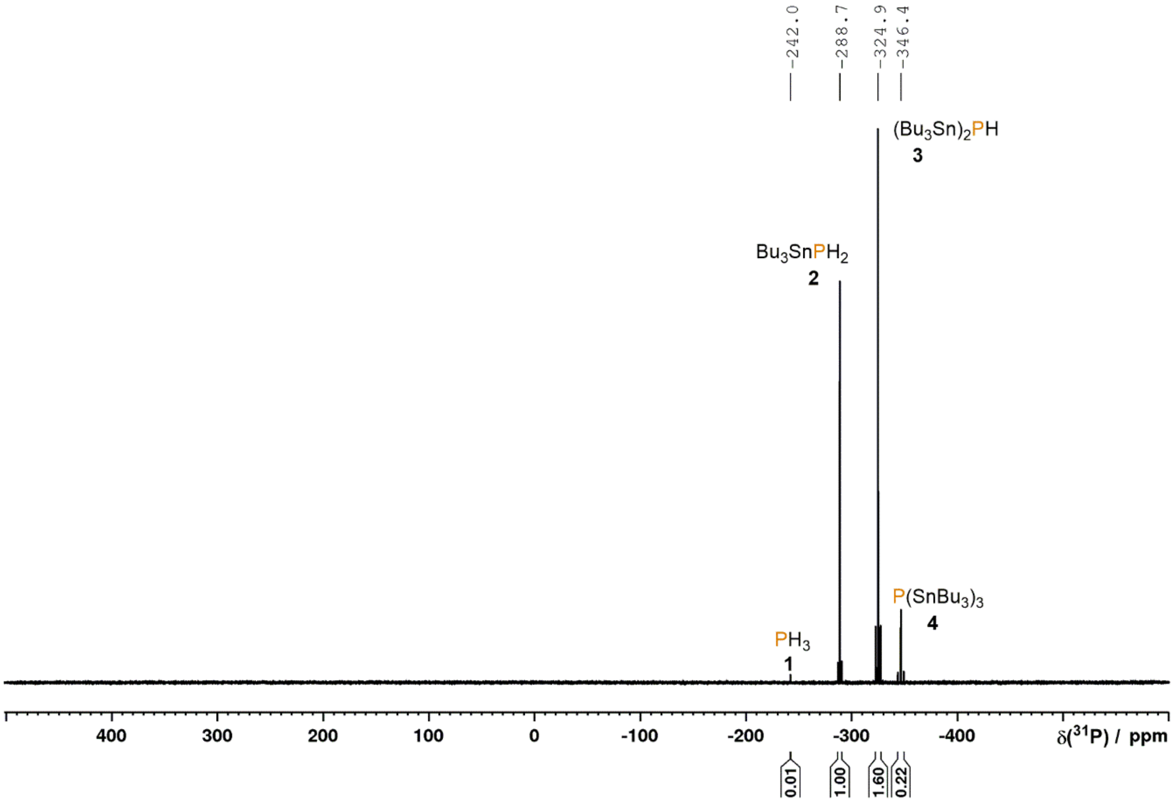

Supplementary Figure 24. $^{31}P\{^1H\}$ NMR spectrum for the reaction of P_4 and 10 eq. Bu_3SnH in PhMe, driven by ACN initiation at 60 °C for 16 h.

Supplementary Method 7: Hydrostannylation of P_4 using Bu_3SnH initiated by TEMPO and attempted hydrostannylation in the presence of a catalytic amount of galvinoxyl (0.01 mmol scale)

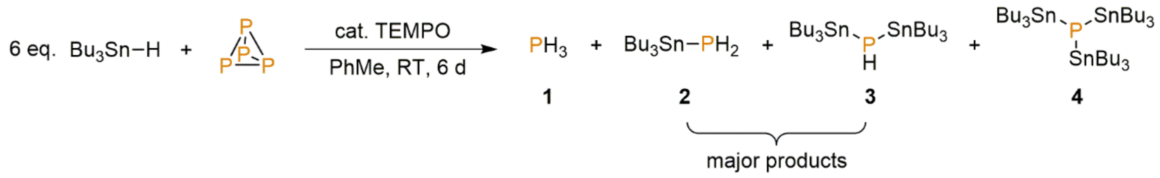

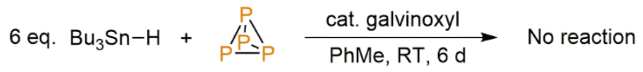

To a 10 mL, flat-bottomed, stoppered tube were added PhMe (500 µL), P_4 (0.01 mmol, as a stock solution in 86.0 µL PhH), TEMPO (1.6 mg, 0.01 mmol) and Bu_3SnH (16.1 µL, 0.06 mmol). The tube was placed in a sealed, opaque container to exclude light, and stirred at RT for 6 d. The resulting mixture was analysed by $^{31}P\{^1H\}$ NMR spectroscopy, as shown in Supplementary Figure 25, below.

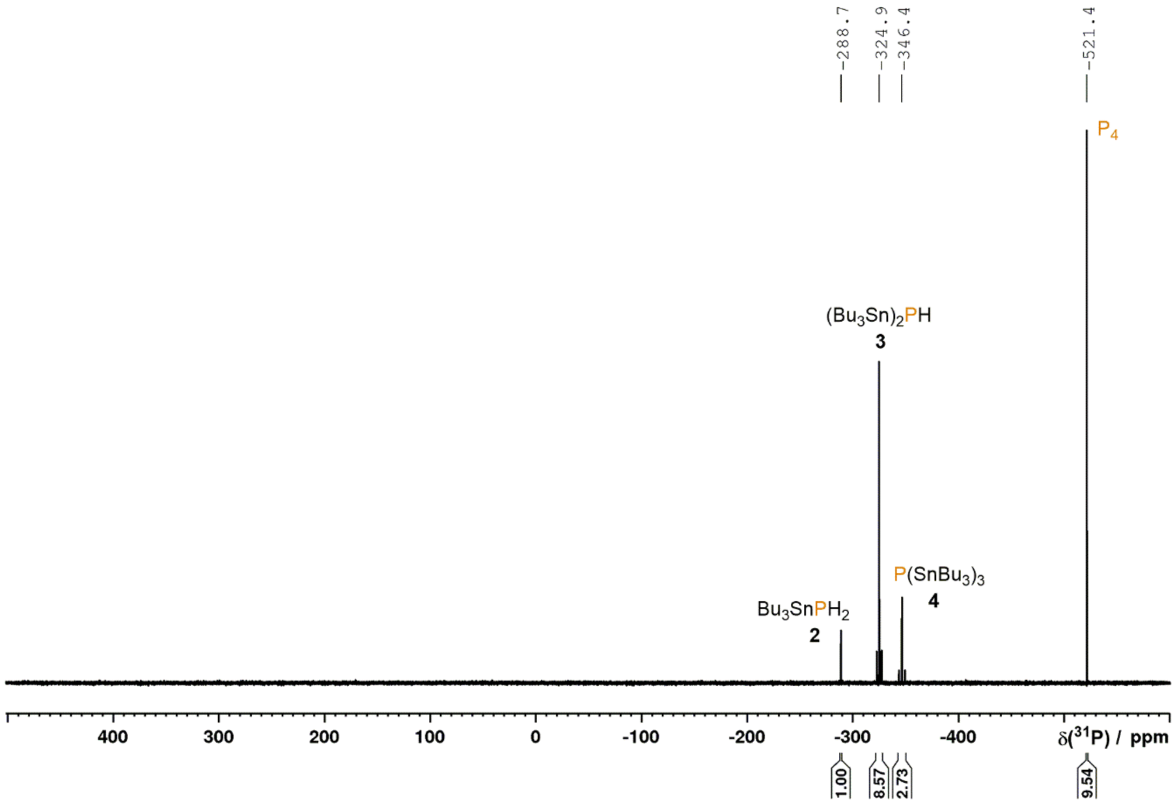

Supplementary Figure 25. $^{31}P\{^1H\}$ spectrum for the reaction of P_4 and 6 eq. Bu_3SnH in PhMe, driven by TEMPO initiation at RT for 6 d.

An analogous reaction was also performed using galvinoxyl (4.2 mg, 0.01 mmol) in place of TEMPO. The resulting $^{31}P\{^1H\}$ spectrum did not indicate any P_4 hydrostannylation (Supplementary Figure 26).

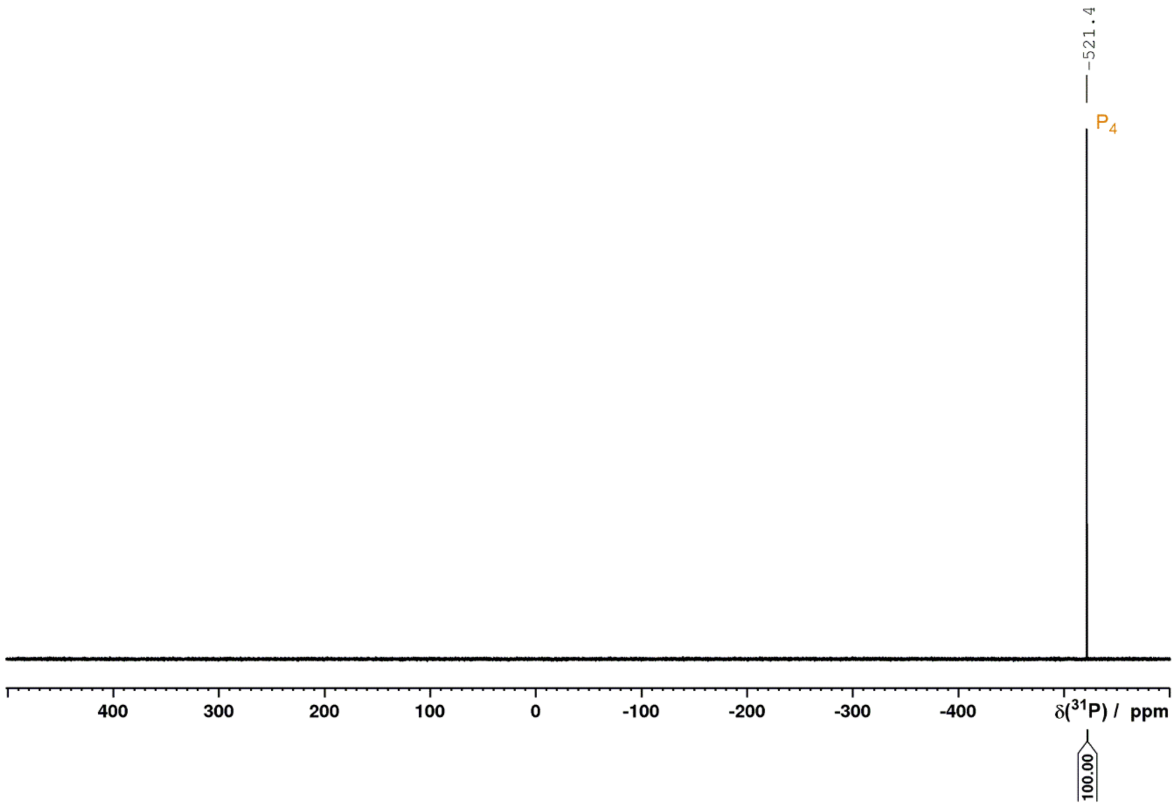

Supplementary Figure 26. $^{31}P\{^1H\}$ spectrum for the attempted reaction of P_4 and 6 eq. Bu_3SnH in PhMe, in the presence of a catalytic amount of galvinoxyl at RT for 6 d.

Supplementary Method 8: Inhibition by TEMPO of hydrostannylation of P_4 using Bu_3SnH under blue LED irradiation

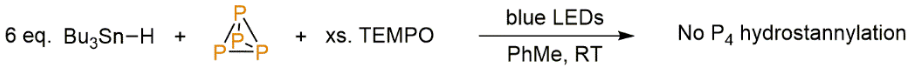

To a 10 mL, flat-bottomed, stoppered tube was added PhMe (500 µL), TEMPO (0.2 mmol, 31.3 mg), P_4 (0.01 mmol, as a stock solution in 86.0 µL PhH) and Bu_3SnH (16.1 µL, 0.06 mmol). The tube was sealed, placed in a water-cooled block to maintain near-ambient temperature, and irradiated with blue light (455 nm (±15 nm), 3.2 V, 700 mA, Osram OSLON SSL 80) for 18 h. The resulting mixture was analysed by ^1H, $^{31}P\{^1H\}$ and $^{119}Sn\{^1H\}$ NMR spectroscopy, as shown in Supplementary Figures 27-29, below.

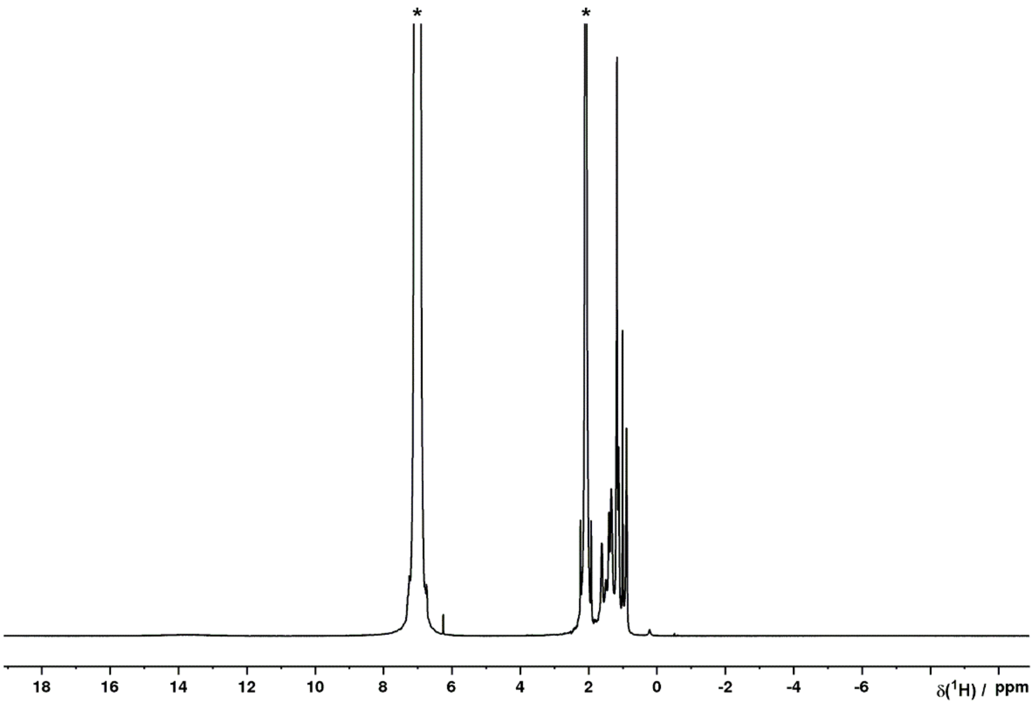

Supplementary Figure 27. ^{1}H NMR spectrum for the reaction of P_4 and 6 eq. Bu_3SnH in the presence of 20 eq. TEMPO in PhMe, driven by 455 nm LED irradiation for 18 h. Solvent resonances (*) truncated for clarity.

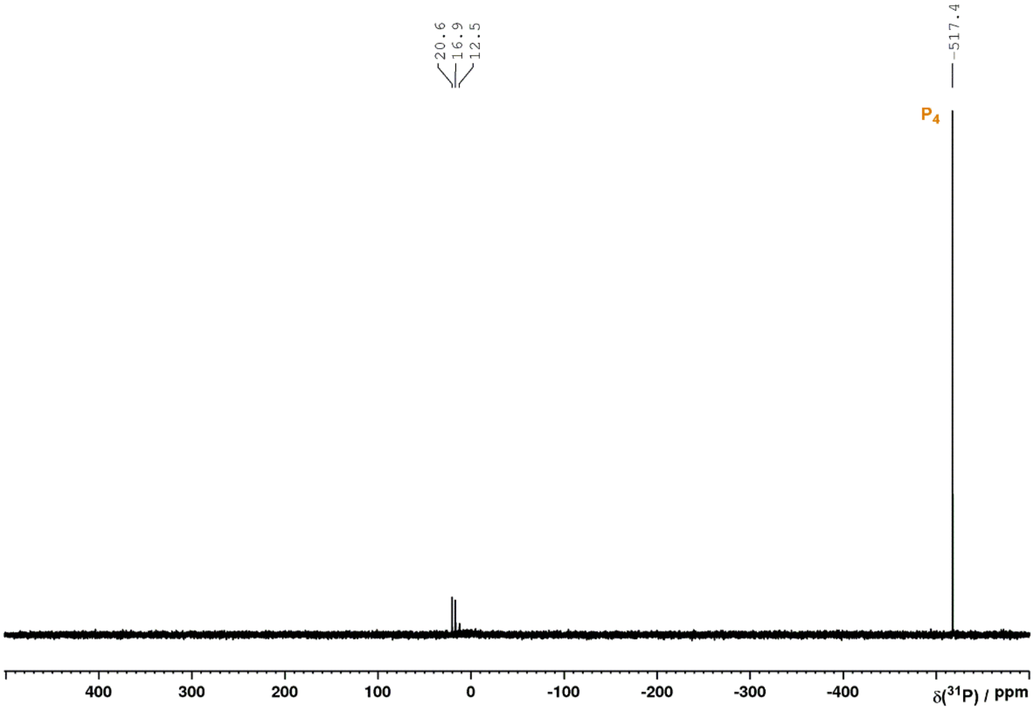

Supplementary Figure 28. $^{31}P\{^1H\}$ NMR spectrum for the reaction of P_4 and 6 eq. Bu_3SnH in the presence of 20 eq. TEMPO in PhMe, driven by 455 nm LED irradiation for 18 h.

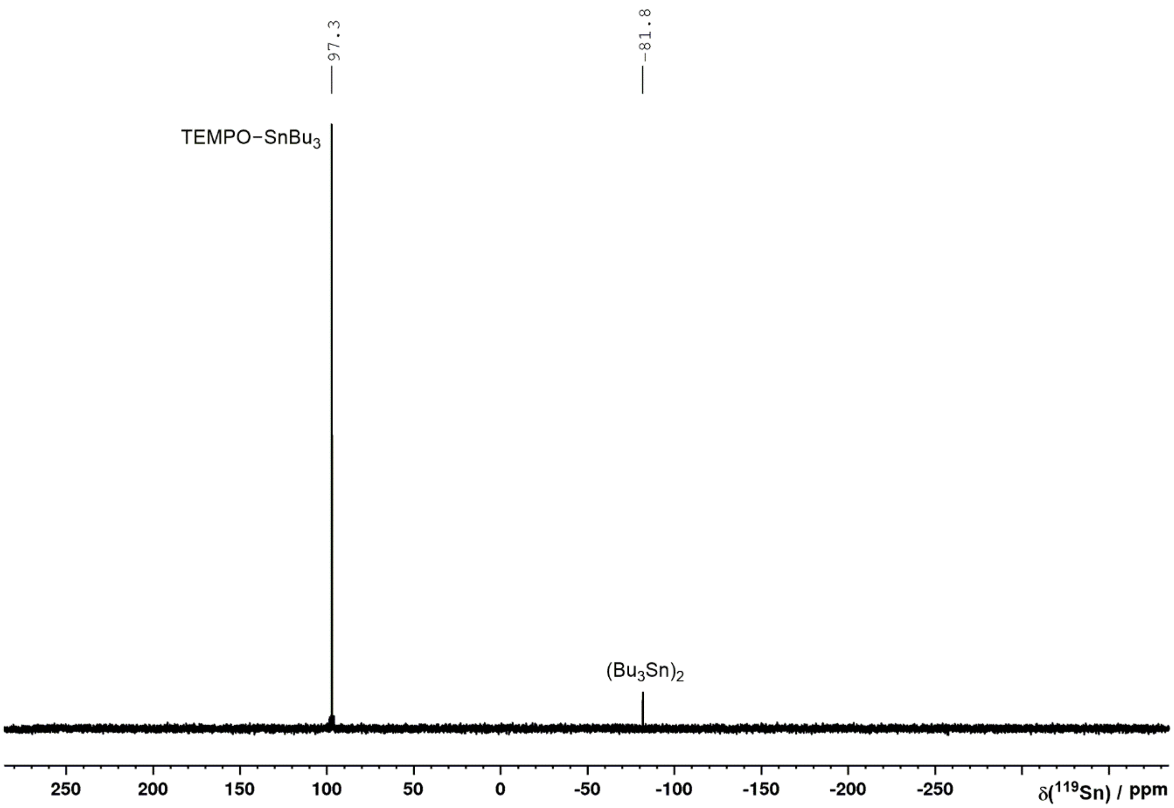

Supplementary Figure 29. ^{119}Sn{^{1}H} NMR spectrum for the reaction of P_4 and 6 eq. Bu_3SnH in the presence of 20 eq. TEMPO in PhMe, driven by 455 nm LED irradiation for 18 h.

The spectra clearly show that the addition of TEMPO has an inhibitory effect on the P_4 hydrostannylation reaction that would be observed in its absence. The ^{31}P{^{1}H} spectrum indicates that the P_4 starting material is the only significant P-containing compound present, with no formation of the phosphines $(Bu_3Sn)_xPH_{3-x}$. The ^{1}H NMR spectrum shows full consumption of Bu_3SnH (through disappearance of the hydride resonance that would otherwise be observed at *ca*. 5 ppm), and the single major ^{119}Sn{^{1}H} resonance is consistent with formation of TEMPO–SnBu$_3$.[8]

These observations are fully consistent with the mechanism proposed in Fig. 2 of the main manuscript, with TEMPO trapping the initially-formed $Bu_3Sn\cdot$ radicals before they can appreciably propagate the productive radical chain. Nevertheless, it should be noted that control experiments in which the above procedure was repeated in the dark (i.e. in the absence of any deliberate source of initiation) showed an essentially identical outcome (Supplementary Figures 30 and 31). This indicates that TEMPO is able to react directly with Bu_3SnH (presumably *via* initial H atom abstraction to form TEMPO–H, and subsequent trapping of $Bu_3Sn\cdot$ by a second equivalent of TEMPO), and that this reaction proceeds to completion within the timeframe of the experiment. These results should therefore be interpreted with appropriate caution.

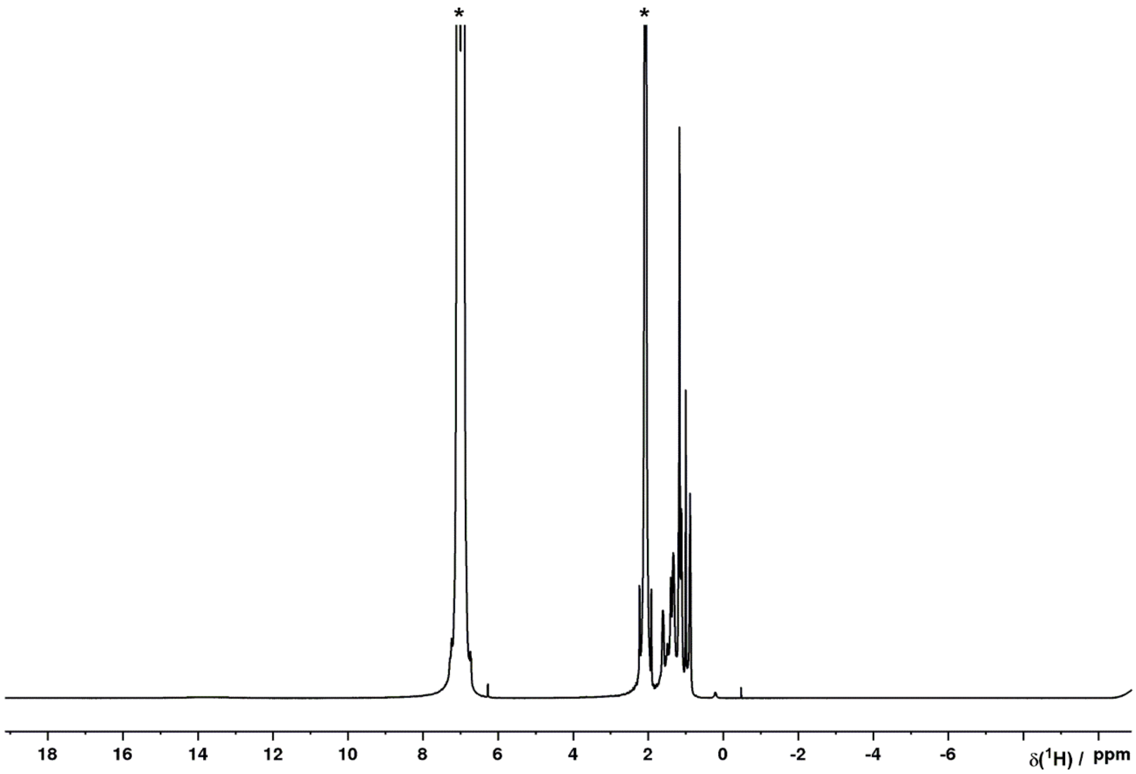

Supplementary Figure 30. ^{1}H NMR spectrum for the reaction between P_4, 6 eq. Bu_3SnH and 20 eq. TEMPO in PhMe, stirred in the dark for 18 h. Solvent resonances (*) truncated for clarity.

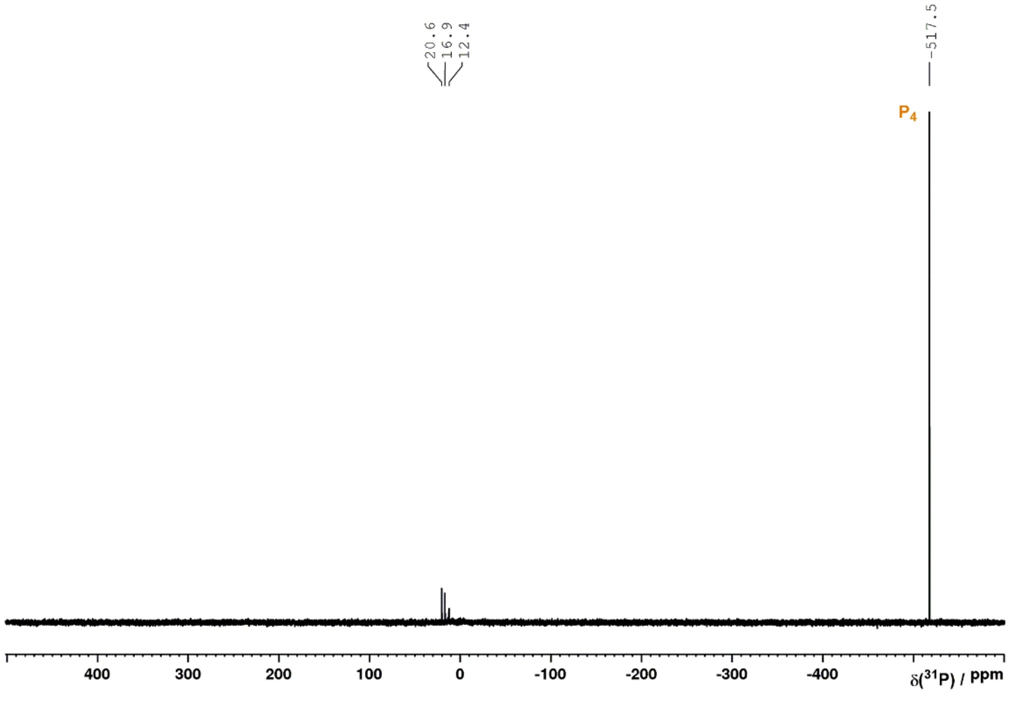

Supplementary Figure 31. $^{31}P\{^1H\}$ NMR spectrum for the reaction between P_4, 6 eq. Bu_3SnH and 20 eq. TEMPO in PhMe, stirred in the dark for 18 h.

For the sake of completeness, it should also be noted that TEMPO appears to react directly with the phosphines $(Bu_3Sn)_xPH_{3-x}$ that are the usual products of the P_4 hydrostannylation reaction. This is illustrated when TEMPO (20 eq. relative to initial P_4) is added at the conclusion of the blue light-driven hydrostannylation reaction (as described in the Methods section of the main manuscript) instead of at the start, and the resulting mixture is stirred for 20 h at room temperature (identical results are obtained when this second step is performed under 455 nm irradiation, or in the dark). $^{31}P\{^1H\}$ NMR analysis of the final product mixture shows full consumption of $(Bu_3Sn)_xPH_{3-x}$ (with the exception of a small amount of $P(Bu_3Sn)_3$), and formation of a new major product characterized by a resonance at 17.0 ppm that has not yet been identified (this resonance does not split in the proton-coupled ^{31}P spectrum but appears to possess $^{117/119}Sn$ satellites, with $J(^{31}P\text{-}^{119}Sn)$ = 49 Hz, which is smaller than would be expected for a ^1J coupling).

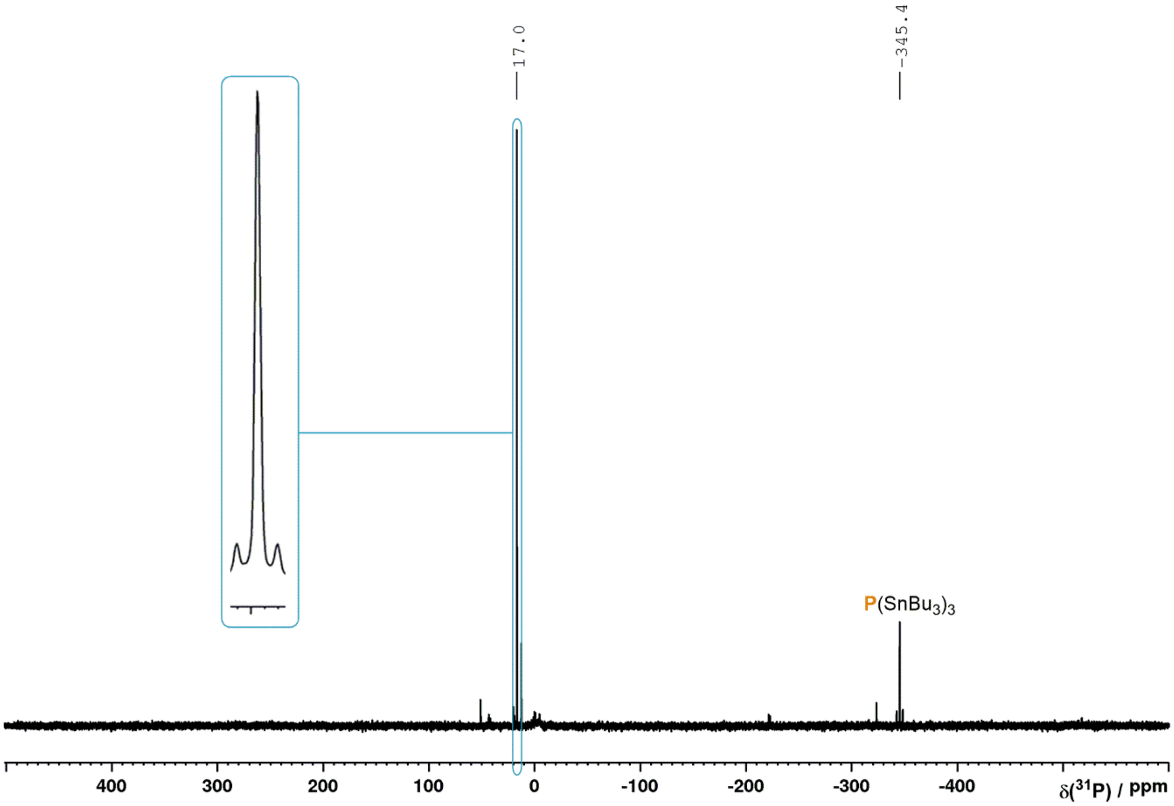

Supplementary Figure 32. $^{31}P\{^1H\}$ NMR spectrum for the reaction of P_4 and 6 eq. Bu_3SnH in PhMe, driven by 455 nm LED irradiation for 18 h, followed by addition of TEMPO (20 eq.) and stirring at room temperature for 20 h.

Supplementary Method 9: Inhibition by TEMPO of hydrostannylation of P_4 using Bu_3SnH initiated by AIBN

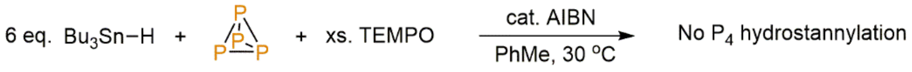

To a 10 mL, flat-bottomed, stoppered tube was added PhMe (500 µL), TEMPO (0.2 mmol, 31.3 mg), P_4 (0.01 mmol, as a stock solution in 93.9 µL PhH), AIBN (0.001 mmol, as a stock solution in 49.3 µL PhH) and Bu_3SnH (16.9 µL, 0.063 mmol). The tube was sealed, wrapped in Al foil to exclude light, and heated to 30 °C for 19 h. The resulting mixture was analysed by ^1H and $^{31}P\{^1H\}$ NMR spectroscopy, as shown in Supplementary Figures 33 and 34, below.

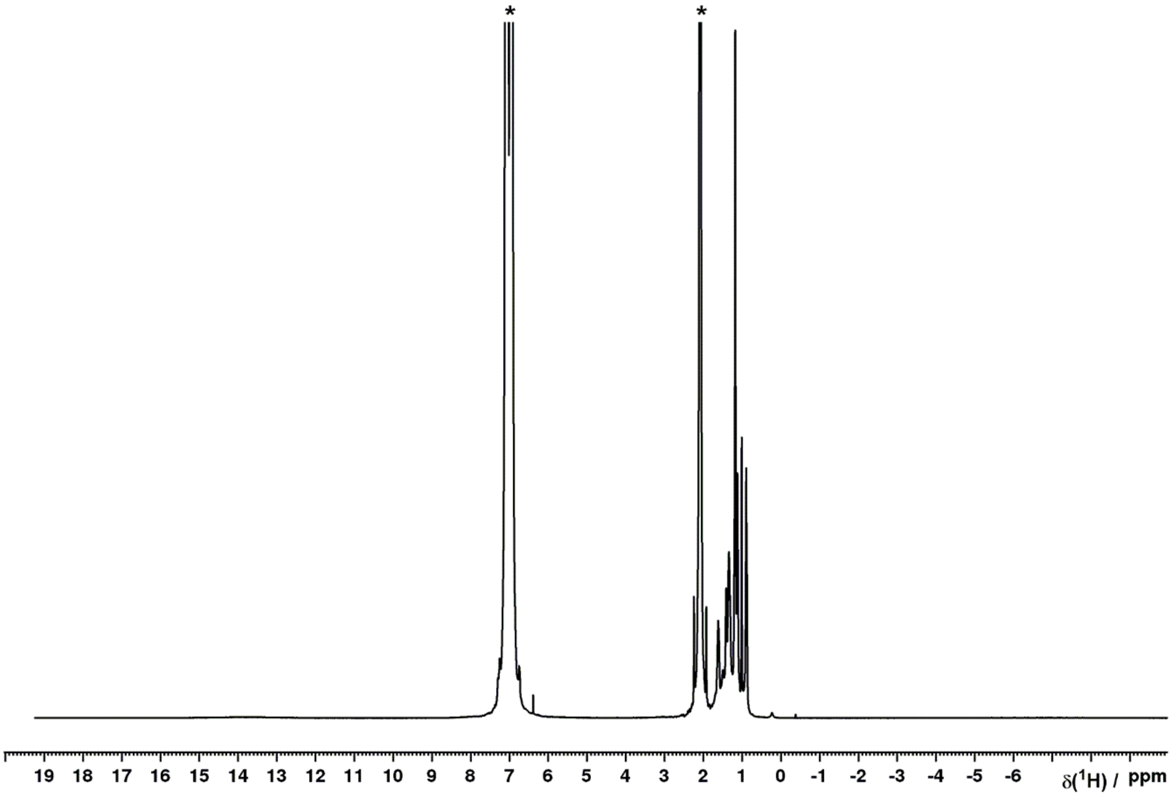

Supplementary Figure 33. ^1H NMR spectrum for the reaction of P_4 and 6 eq. Bu_3SnH in the presence of 20 eq. TEMPO in PhMe, driven by AIBN initiation at 30 °C for 19 h. Solvent resonances (*) truncated for clarity.

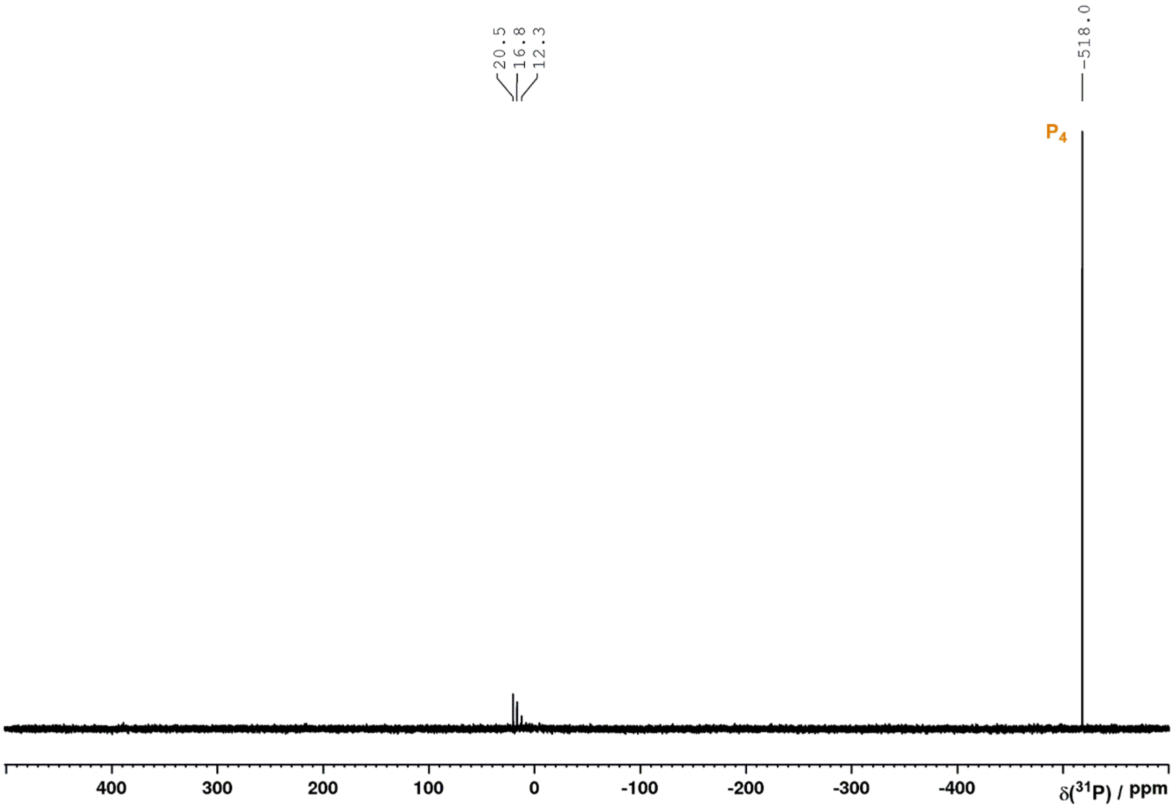

Supplementary Figure 34. $^{31}P\{^{1}H\}$ NMR spectrum for the reaction of P_4 and 6 eq. Bu_3SnH in the presence of 20 eq. TEMPO in PhMe, driven by AIBN initiation at 30 °C for 19 h.

The spectra show that, as for the analogous light-driven reaction (Supplementary Method 8), the addition of excess TEMPO effectively inhibits P_4 stannylation. These results should be interpreted with caution for the same reasons, however.

Supplementary Method 10: Inhibition by galvinoxyl of hydrostannylation of P_4 using Bu_3SnH under blue LED irradiation

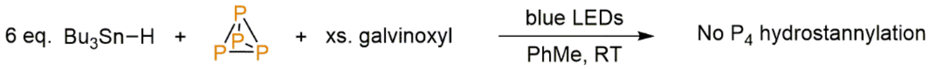

To a 10 mL, flat-bottomed, stoppered tube was added PhMe (500 µL), galvinoxyl (0.2 mmol, 84.3 mg), P_4 (0.01 mmol, as a stock solution in 93.9 µL PhH) and Bu_3SnH (16.1 µL, 0.06 mmol). The tube was sealed, placed in a water-cooled block to maintain near-ambient temperature, and irradiated with blue light (455 nm (±15 nm), 3.2 V, 700 mA, Osram OSLON SSL 80) for 19 h. The resulting mixture was analysed by ^{1}H and $^{31}P\{^{1}H\}$ NMR spectroscopy, as shown in Supplementary Figures 35 and 36, below.

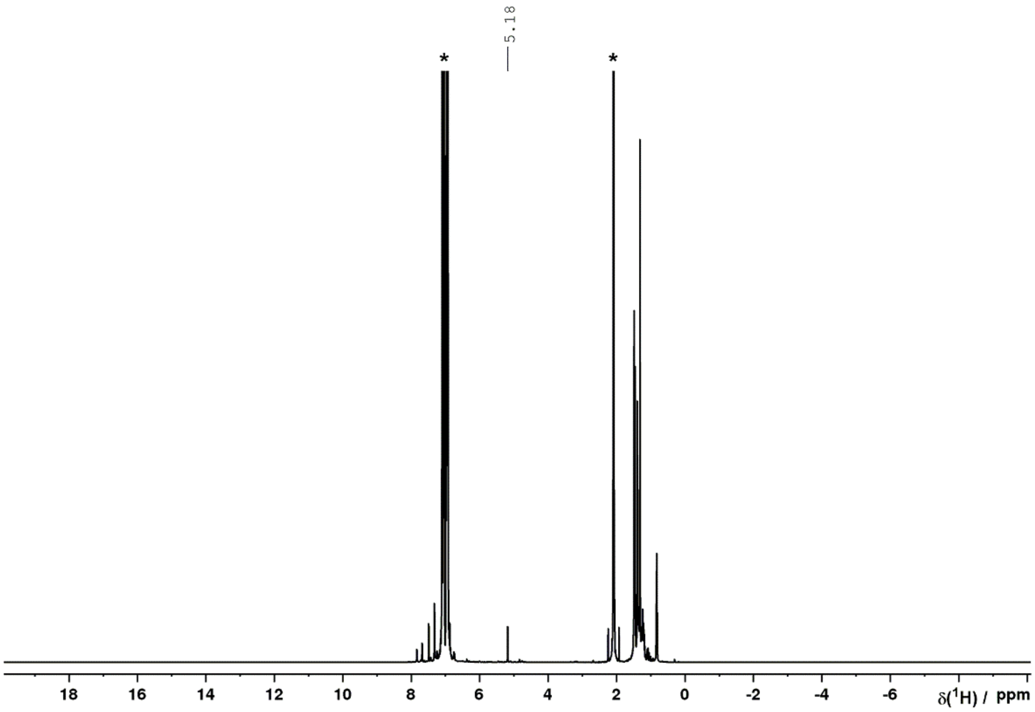

Supplementary Figure 35. ^{1}H NMR spectrum for the reaction of P_4 and 6 eq. Bu_3SnH in the presence of 20 eq. galvinoxyl in PhMe, driven by 455 nm LED irradiation for 19 h. Solvent resonances (*) truncated for clarity.

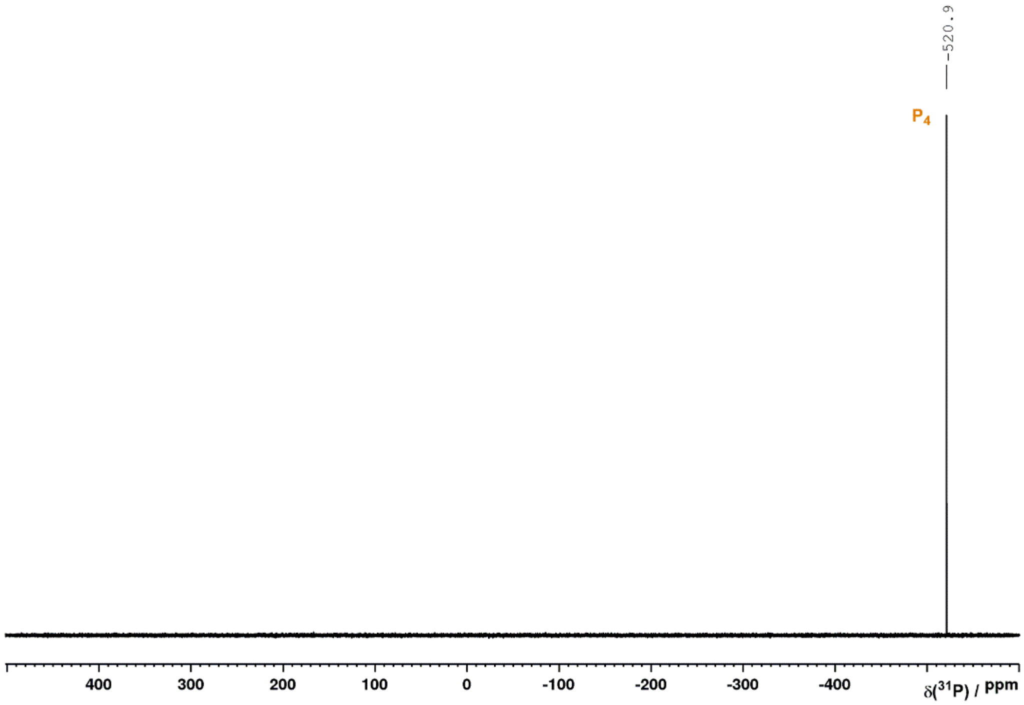

Supplementary Figure 36. $^{31}P\{^1H\}$ NMR spectrum for the reaction of P_4 and 6 eq. Bu_3SnH in the presence of 20 eq. galvinoxyl in PhMe, driven by 455 nm LED irradiation for 19 h.

As with TEMPO (Supplementary Method 8), the spectra clearly show that addition of galvinoxyl has an inhibitory effect on P_4 hydrostannylation, with the $^{31}P\{^1H\}$ spectrum again showing P_4 as the only P-containing compound. The same caution should be used when interpreting these results, however.

Control experiments in which the above procedure is repeated in the dark give a very broad, paramagnetic feature in the ^1H spectrum that overlaps with the expected location of the diagnostic $Bu_3Sn\underline{H}$ resonance (Supplementary Figures 37 and 38). Nevertheless, the sharp signal expected for this starting material is not observed, which suggests that (as with TEMPO) it is consumed by direct reaction with the stable radical even in the absence of another source of initiation. Note that while a reasonably sharp feature can be observed at 5.15 ppm, this is *ca.* 0.15 ppm downfield from the chemical shift observed for the $Bu_3Sn\underline{H}$ resonance in closely related spectra (for example, during analysis of the attempted galvinoxyl-mediated hydrostannylation of P_4 described in Supplementary Method 7, the $Bu_3Sn\underline{H}$ resonance was observed at 4.99 ppm), and given also the lack of obvious $^1J\,^{117/119}Sn$ satellites or $J(^1H\text{-}^1H)$ couplings, this signal is presumed to arise from a galvinoxyl-derived product (a similar resonance is also easily resolved in Supplementary Figure 35).

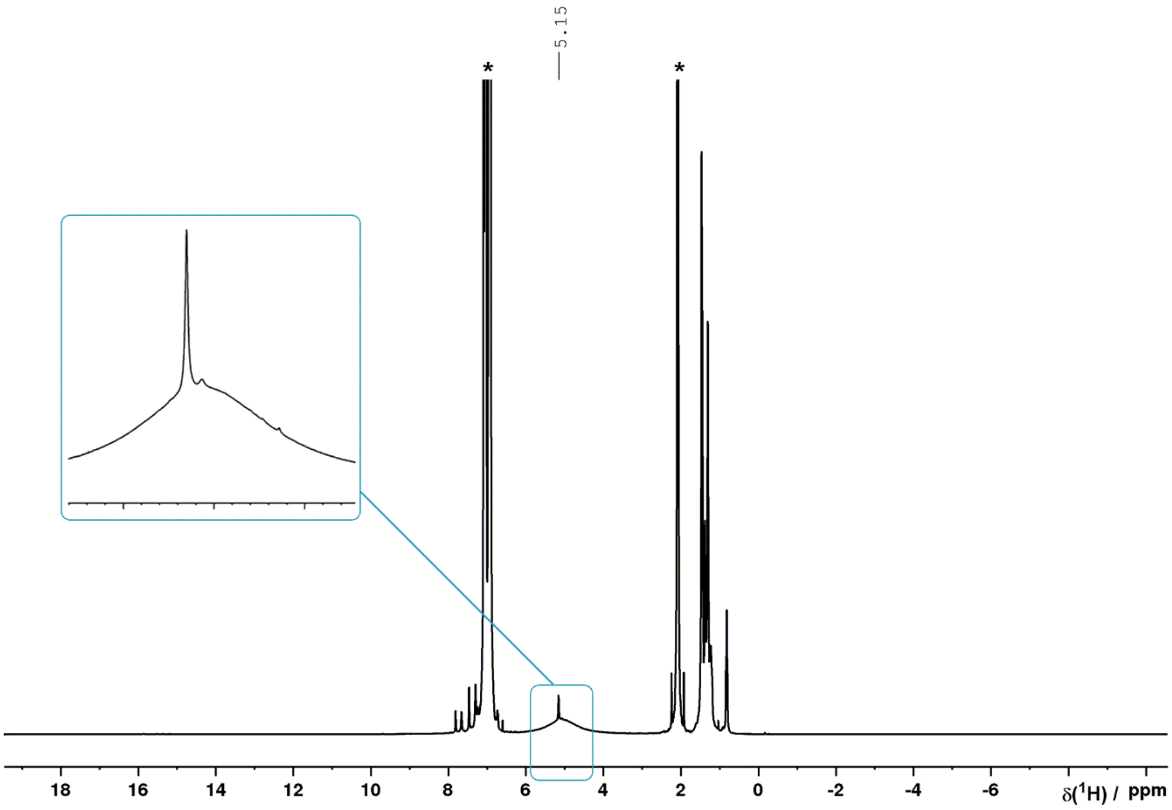

Supplementary Figure 37. ^1H NMR spectrum for the reaction between P_4, 6 eq. Bu_3SnH and 20 eq. galvinoxyl in PhMe, stirred in the dark for 19 h. Solvent resonances (*) truncated for clarity.

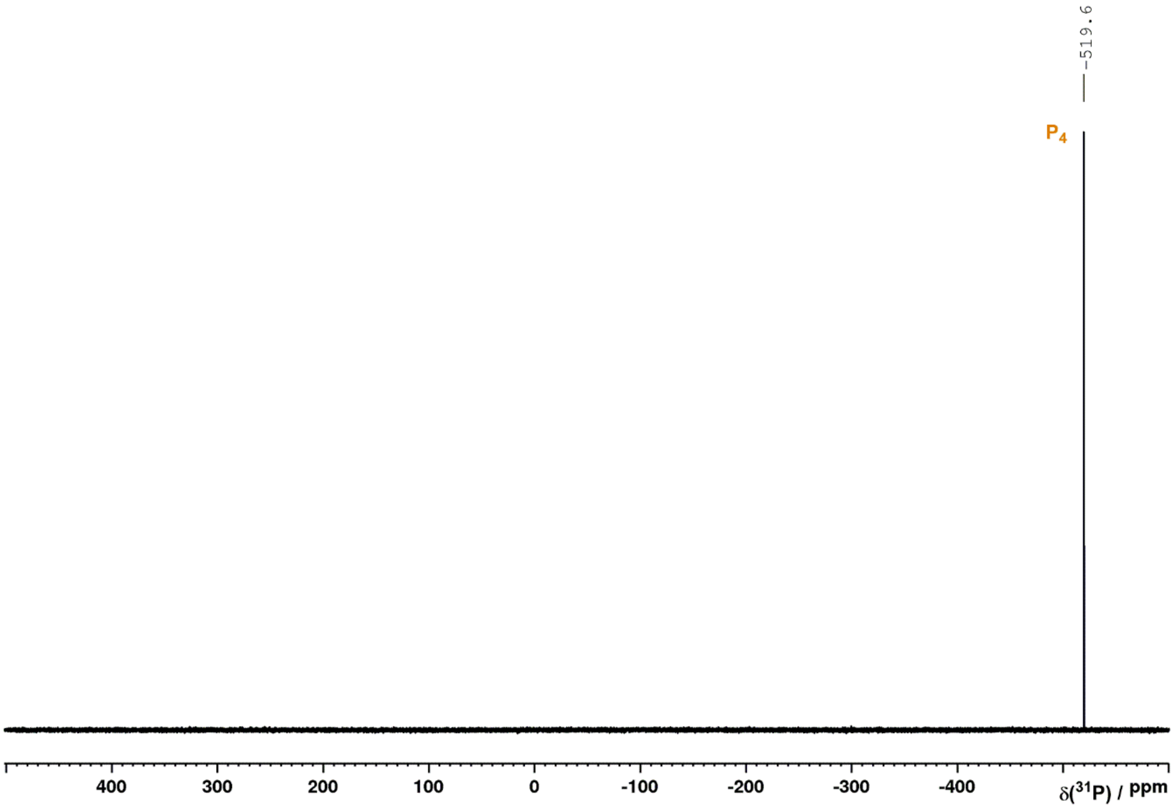

Supplementary Figure 38. $^{31}P\{^1H\}$ NMR spectrum for the reaction between P_4, 6 eq. Bu_3SnH and 20 eq. galvinoxyl in PhMe, stirred in the dark for 19 h.

For the sake of completeness, it should also be noted that, like TEMPO, galvinoxyl appears to react directly with the phosphines $(Bu_3Sn)_xPH_{3-x}$ that are the usual products of the P_4 hydrostannylation reaction. This is illustrated when galvinoxyl (20 eq. relative to initial P_4) is added at the conclusion of the blue light-driven hydrostannylation reaction (as described in the Methods section of the main manuscript) instead of at the start, and the resulting mixture is stirred for 21 h at room temperature (comparable results are obtained when this second step is performed under 455 nm irradiation, or in the dark). $^{31}P\{^1H\}$ NMR analysis of the final product mixture shows full consumption of $(Bu_3Sn)_xPH_{3-x}$. Unlike the analogous case using TEMPO, no major $^{31}P\{^1H\}$ product resonances can be observed in the range between ±500 ppm, which may suggest the formation of unidentified, paramagnetic products.

Supplementary Method 11: Inhibition by galvinoxyl of hydrostannylation of P_4 using Bu_3SnH initiated by AIBN

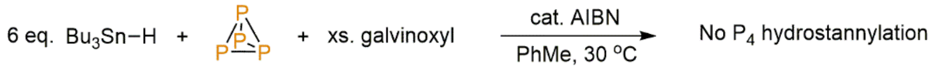

To a 10 mL, flat-bottomed, stoppered tube was added PhMe (500 µL), galvinoxyl (0.2 mmol, 84.3 mg), P_4 (0.01 mmol, as a stock solution in 93.9 µL PhH), AIBN (0.001 mmol, as a stock solution in 49.3 µL PhH) and Bu_3SnH (16.9 µL, 0.063 mmol). The tube was sealed, wrapped in Al foil to exclude light, and heated to 30 °C for 19 h. The resulting mixture was analysed by ^1H and $^{31}P\{^1H\}$ NMR spectroscopy, as shown in Supplementary Figures 39 and 40, below.

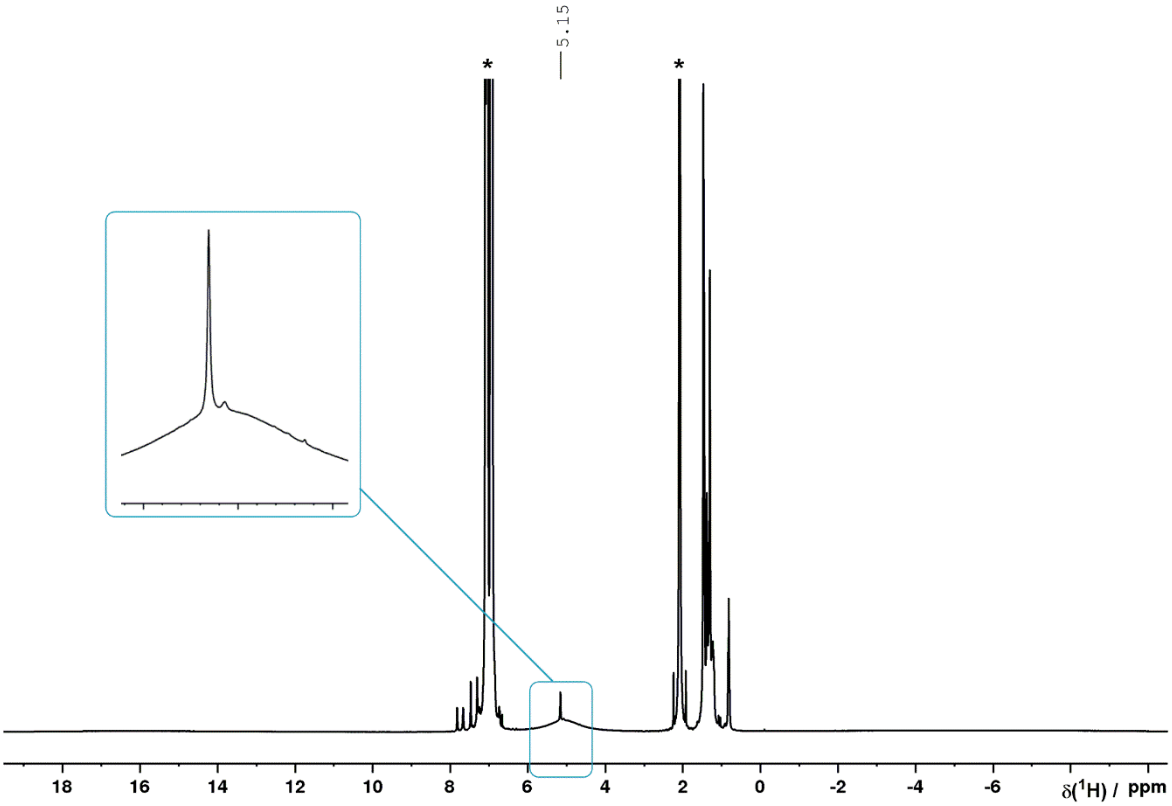

Supplementary Figure 39. ^1H NMR spectrum for the reaction of P_4 and 6 eq. Bu_3SnH in the presence of 20 eq. galvinoxyl in PhMe, driven by AIBN initiation at 30 °C for 19 h. Solvent resonances (*) truncated for clarity.

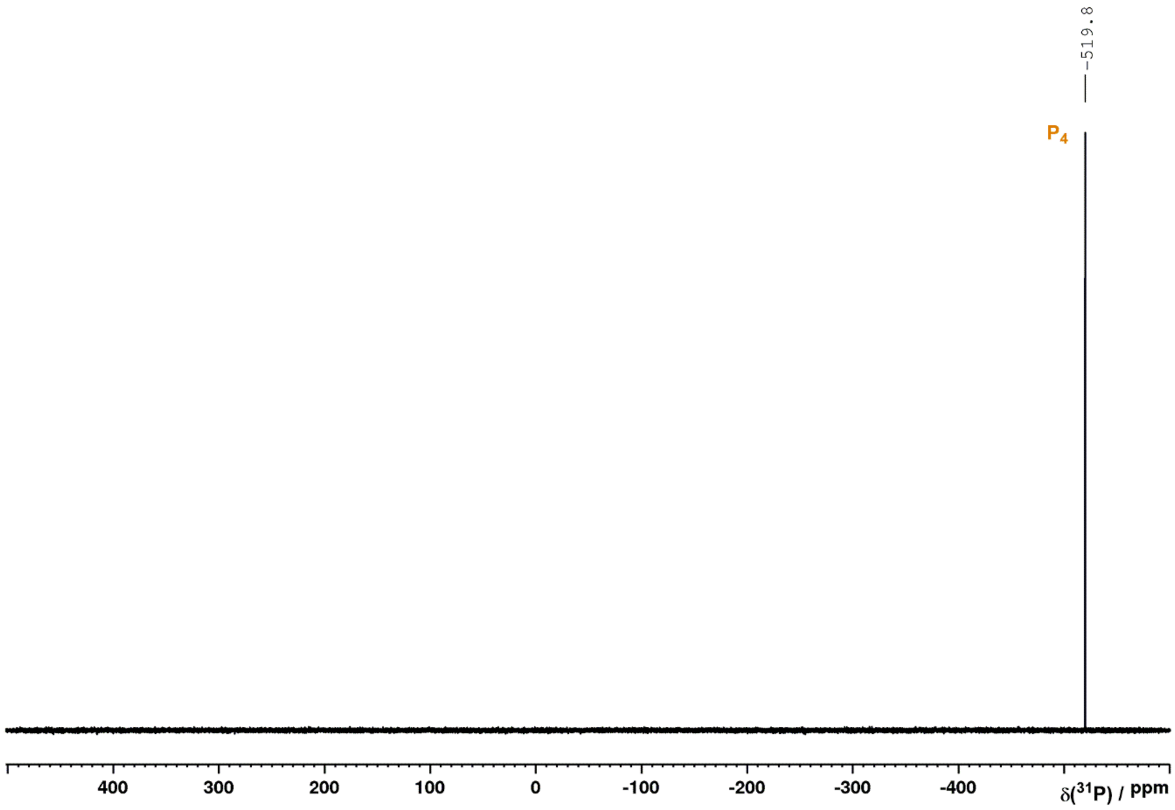

Supplementary Figure 40. $^{31}P\{^{1}H\}$ NMR spectrum for the reaction of P_4 and 6 eq. Bu_3SnH in the presence of 20 eq. alvinoxylg in PhMe, driven by AIBN initiation at 30 °C for 19 h.

The spectra show that, as for the analogous light-driven reaction (Supplementary Method 10), the addition of excess galvinoxyl effectively inhibits P_4 stannylation. These results should be interpreted with caution for the same reasons, however.

Supplementary Method 12: Hydrostannylation of P_2Ph_4 using Bu_3SnH under blue LED irradiation (0.02 mmol scale)

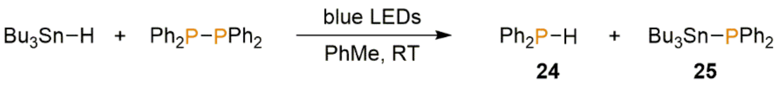

$$Bu_3Sn{-}H + Ph_2P{-}PPh_2 \xrightarrow[\text{PhMe, RT}]{\text{blue LEDs}} \underset{\mathbf{24}}{Ph_2P{-}H} + \underset{\mathbf{25}}{Bu_3Sn{-}PPh_2}$$

To a 10 mL, flat-bottomed, stoppered tube were added PhMe (500 µL), P_2Ph_4 (7.4 mg, 0.02 mmol) and Bu_3SnH (5.4 µL, 0.02 mmol). The tube was sealed, placed in a water-cooled block to maintain near-ambient temperature, and irradiated with blue light (455 nm (±15 nm), 3.2 V, 700 mA, Osram OSLON SSL 80) for

20 h. The resulting mixture was analysed by ^{1}H, $^{31}P\{^{1}H\}$ and ^{31}P NMR spectroscopy, as shown in Supplementary Figures 41-43, below.

The $^{31}P\{^{1}H\}$ spectrum reveals full consumption of the starting material and formation of two new resonances with roughly equal intensity. The more downfield signal at –40.0 ppm splits into a doublet in the ^{1}H-coupled ^{31}P spectrum with a large $^{1}J(^{31}P-^{1}H)$ coupling constant of 215 Hz, consistent with formation of Ph_2PH (**24**).[9] The more upfield signal at –55.3 ppm remains a singlet in the ^{1}H-coupled ^{31}P spectrum, but shows $^{117/119}Sn$ satellites in both spectra with large $^{1}J(^{117}Sn-^{1}H)$ and $^{1}J(^{119}Sn-^{1}H)$ coupling constants of 645 Hz and 675 Hz, respectively, and is consistent with formation of Ph_2PSnBu_3 (**25**).[10]

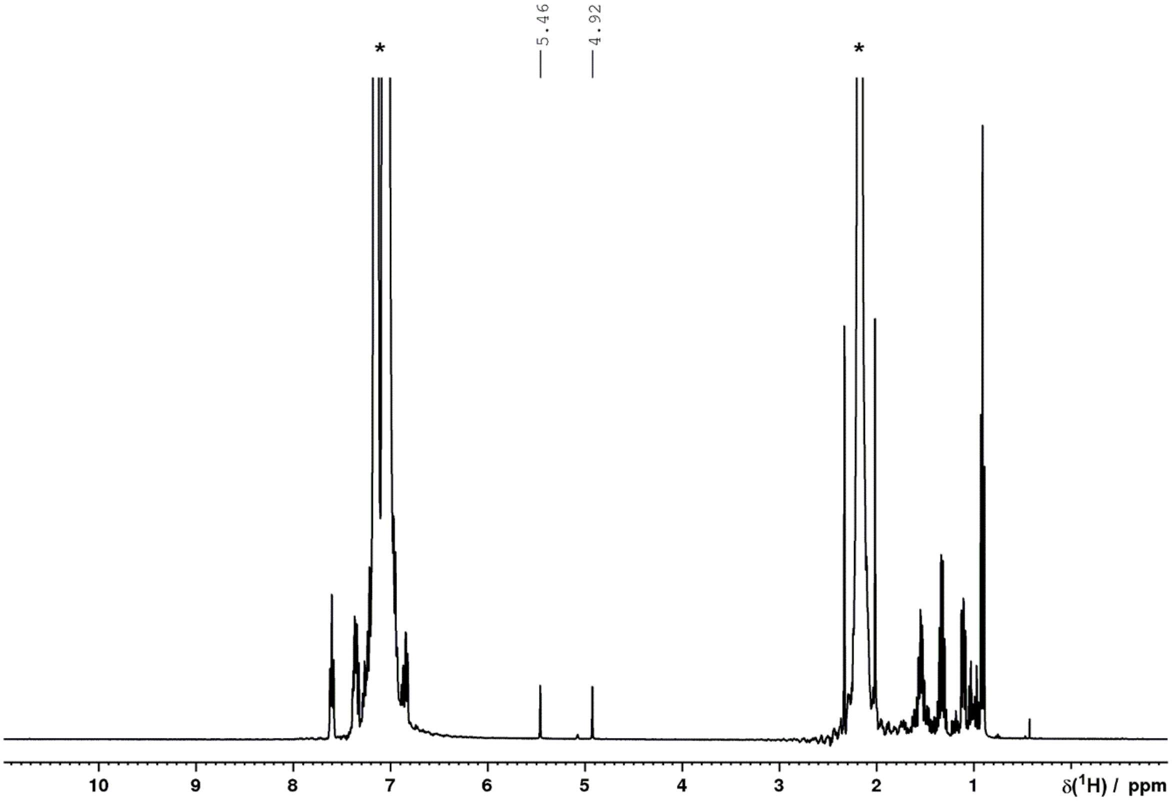

Supplementary Figure 41. ^{1}H NMR spectrum for the reaction of P_2Ph_4 and 1 eq. Bu_3SnH in PhMe, driven by 455 nm LED irradiation for 20 h. Solvent resonances (*) truncated for clarity.

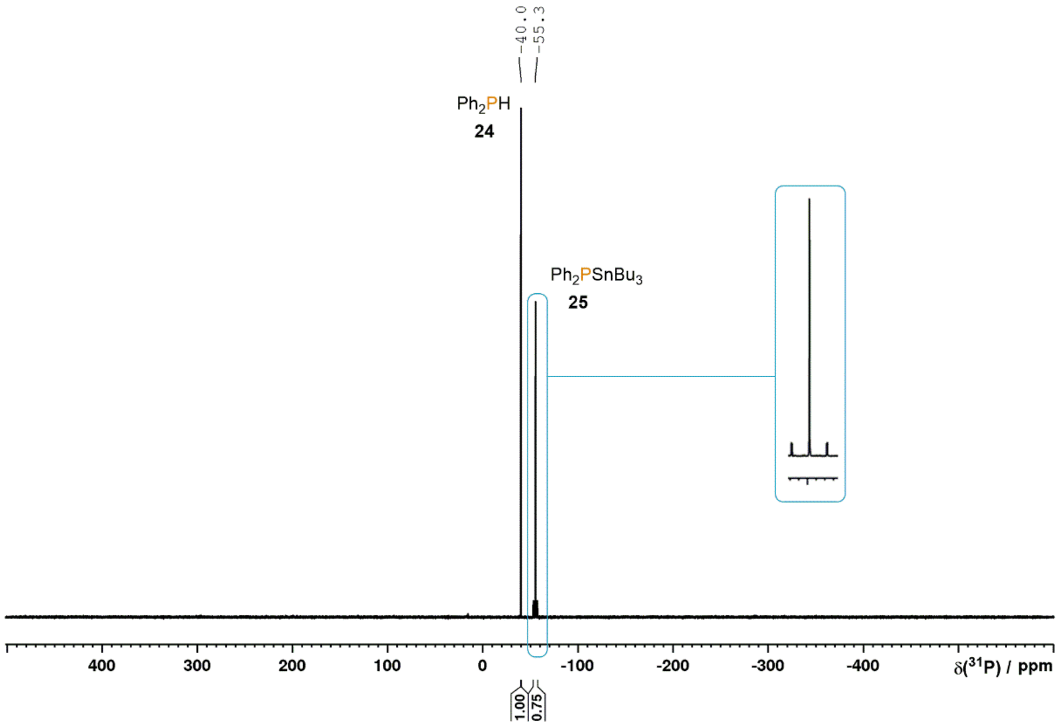

Supplementary Figure 42. $^{31}P\{^1H\}$ NMR spectrum for the reaction of P_2Ph_4 and 1 eq. Bu_3SnH in PhMe, driven by 455 nm LED irradiation for 20 h.

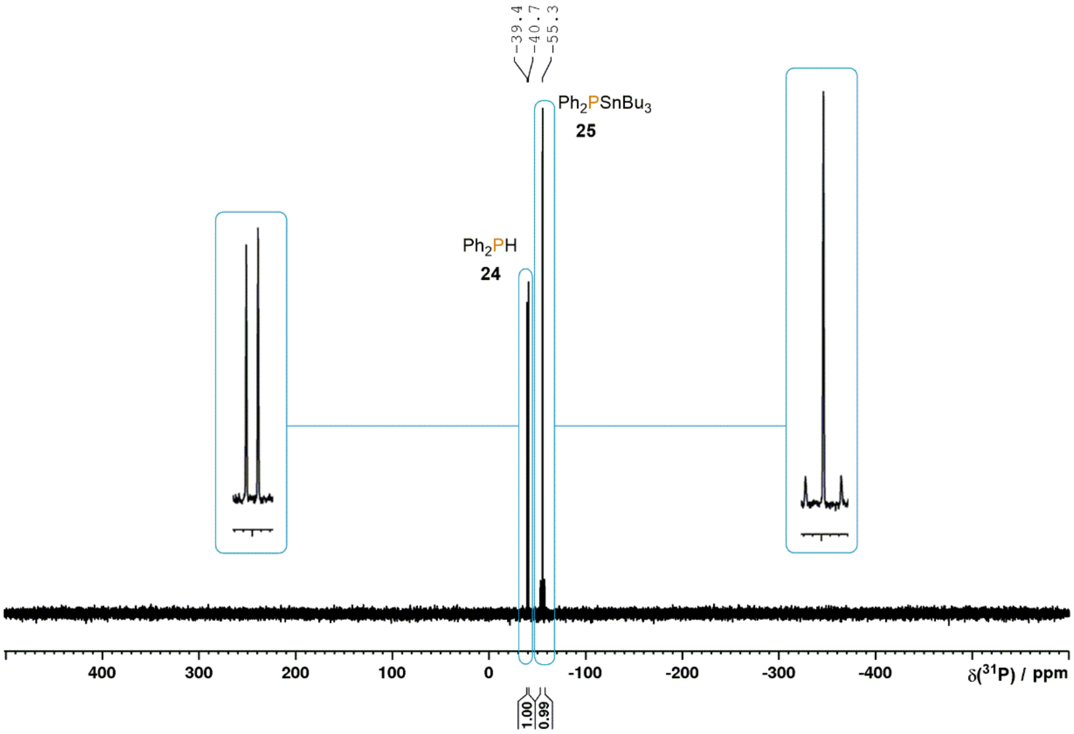

Supplementary Figure 43. ^{31}P NMR spectrum for the reaction of P_2Ph_4 and 1 eq. Bu_3SnH in PhMe, driven by 455 nm LED irradiation for 20 h.

Supplementary Method 13: Hydrostannylation of P_5Ph_5 using Bu_3SnH under blue LED irradiation (0.008 mmol scale)

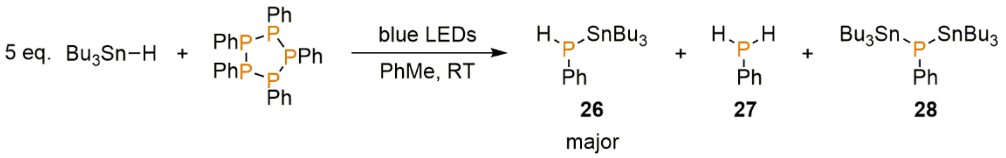

To a 10 mL, flat-bottomed, stoppered tube were added PhMe (500 µL), P_5Ph_5 (4.3 mg, 0.008 mmol) and Bu_3SnH (10.8 µL, 0.04 mmol). The tube was sealed, placed in a water-cooled block to maintain near-ambient temperature, and irradiated with blue light (455 nm (±15 nm), 3.2 V, 700 mA, Osram OSLON SSL 80) for 18 h. The resulting mixture was analysed by ^{1}H, ^{31}P{^{1}H} and ^{31}P NMR spectroscopy, as shown in Supplementary Figures 44-46, below.

The ^{31}P{^{1}H} spectrum reveals full consumption of the starting material and formation of one major new resonance, alongside two more minor resonances with roughly equal intensity.

The major signal at –148.3 ppm splits into a doublet in the ^{1}H-coupled ^{31}P spectrum with a large ^{1}J(^{31}P-^{1}H) coupling constant of 188 Hz. It also displays $^{117/119}$Sn satellites in both spectra with large ^{1}J(^{117}Sn-^{1}H) and ^{1}J(^{119}Sn-^{1}H) coupling constants of 578 Hz and 604 Hz, respectively. This signal is therefore assigned to the product $PhP(H)SnBu_3$ (**26**; the related $PhP(H)SnMe_3$ has been reported previously).[11] Of the minor resonances, the more downfield signal at –123.5 ppm splits into a triplet in the ^{1}H-coupled ^{31}P spectrum with a large ^{1}J(^{31}P-^{1}H) coupling constant of 198 Hz, consistent with formation of $PhPH_2$ (**27**).[12] The more upfield-shifted signal at –167.9 ppm remains a singlet in the ^{1}H-coupled ^{31}P spectrum, but shows $^{117/119}$Sn satellites in both spectra with large ^{1}J(^{117}Sn-^{1}H) and ^{1}J(^{119}Sn-^{1}H) coupling constants of 769 Hz and 804 Hz, respectively. This signal is therefore assigned to $PhP(SnBu_3)_2$ (**28**).

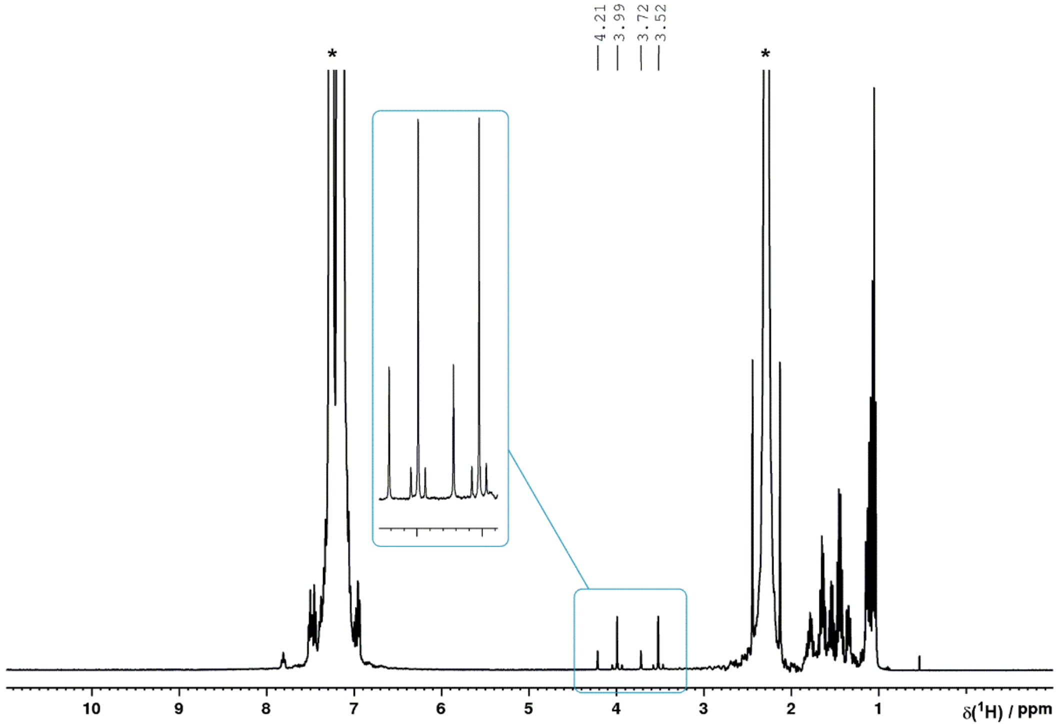

Supplementary Figure 44. ^{1}H NMR spectrum for the reaction of P_5Ph_5 and 5 eq. Bu_3SnH in PhMe, driven by 455 nm LED irradiation for 18 h. Solvent resonances (*) truncated for clarity.

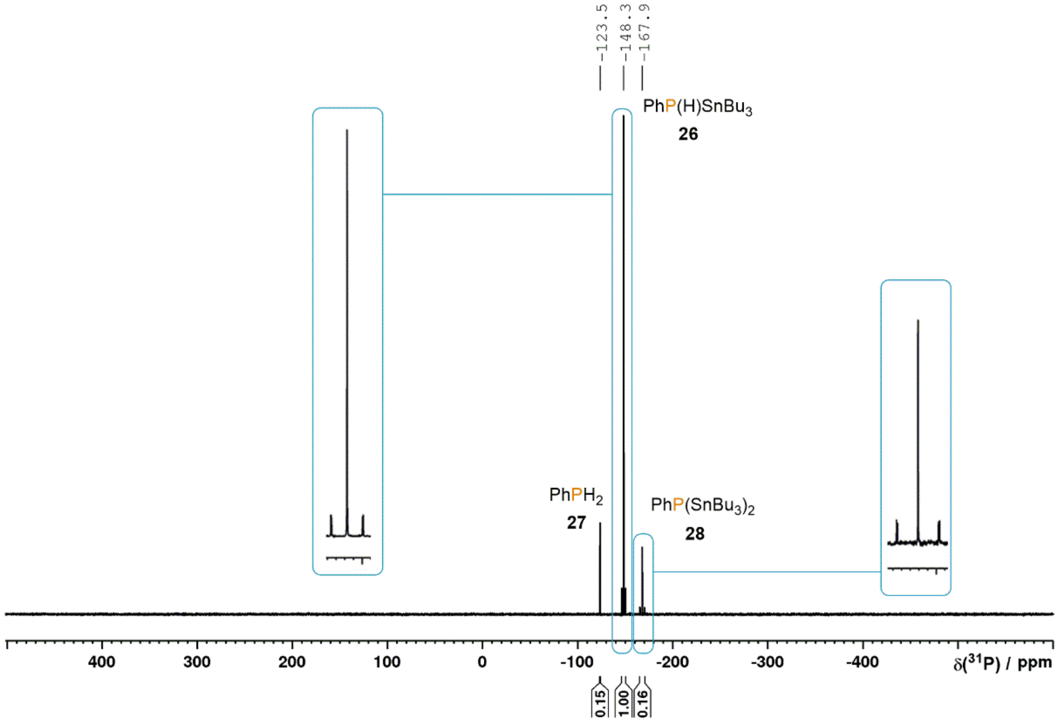

Supplementary Figure 45. ^{31}P{^{1}H} NMR spectrum for the reaction of P_5Ph_5 and 5 eq. Bu_3SnH in PhMe, driven by 455 nm LED irradiation for 18 h.

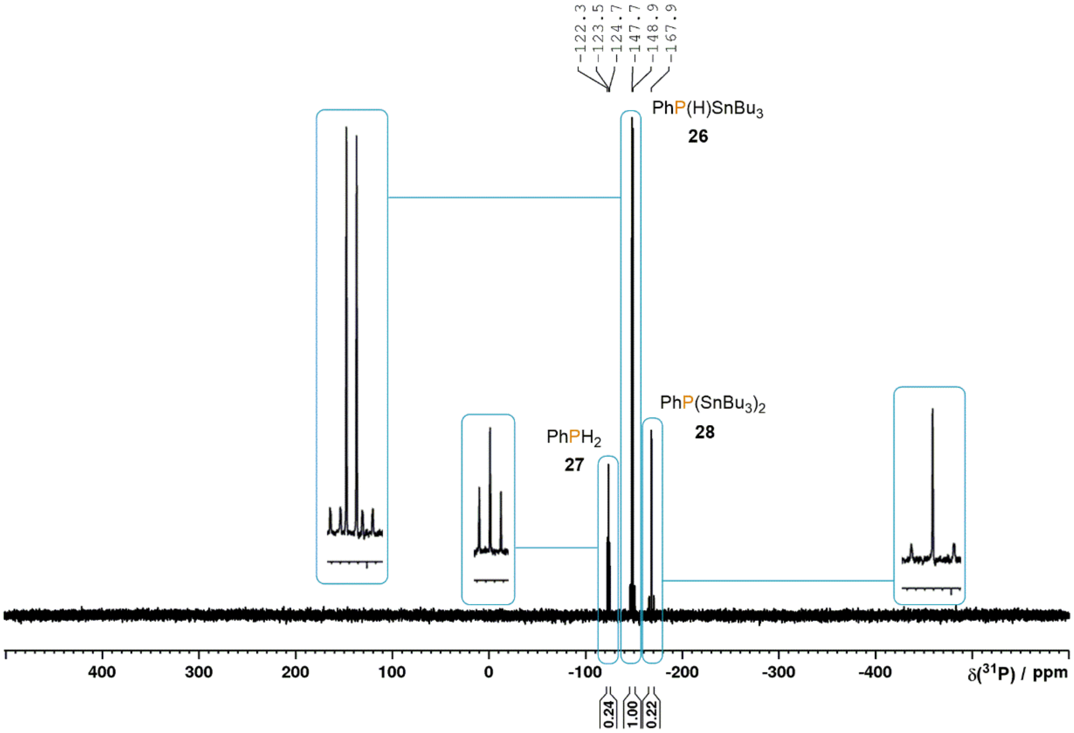

Supplementary Figure 46. ^{31}P NMR spectrum for the reaction of P_5Ph_5 and 5 eq. Bu_3SnH in PhMe, driven by 455 nm LED irradiation for 18 h.

Synthesis and Isolation of Products Derived from $(Bu_3Sn)_xPH_{3-x}$

Supplementary Method 14: Synthesis and quantification of *t*BuC(O)PH₂ (5)

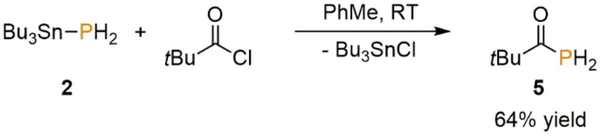

*Note: The product tBuC(O)PH_2 (**5**) was found to be light-sensitive. During the preparation, handling and characterization described below, great care was taken to exclude ambient light as far as possible.*

In a 10 mL stoppered tube were combined Bu_3SnPH_2 (16.2 mg, 0.05 mmol), PhMe (500 μL), and *t*BuC(O)Cl (5.8 μL, 0.048 mmol). The tube was immediately and thoroughly wrapped in Al foil, and the reaction mixture was stirred at room temperature for 16 h. Following trap-to-trap distillation (RT, *ca*. 10^{-2} mbar, receiving vessel cooled in liquid nitrogen), the product was obtained as a colorless solution. In order to assess the yield, Ph_3PO (9.4 mg, 0.034 mmol) was added, and the resulting mixture was analysed by ^{1}H, $^{31}P\{^{1}H\}$, ^{31}P and $^{13}C\{^{1}H\}$ NMR spectroscopy. Quantitative relative integration of the Ph_3PO and *t*BuC(O)PH_2 resonances in the ^{31}P NMR spectrum (using D1 = 30 s; T_1 = 5.8 s for *t*BuC(O)PH_2) indicated a yield of 64% (0.031 mmol).

^{1}H NMR (400 MHz, 300 K, PhMe): δ = 3.49 (2H, d, $^{1}J(^{31}P-^{1}H)$ = 215 Hz), 0.84 ppm (9H, s).

$^{31}P\{^{1}H\}$ NMR (121 MHz, 300 K, PhMe): δ = –122.9 ppm (s).

^{31}P NMR (121 MHz, 300 K, PhMe): δ = –122.9 ppm (t, $^{1}J(^{31}P-^{1}H)$ = 215 Hz).

$^{13}C\{^{1}H\}$ NMR (101 MHz, 300 K, PhMe): δ = 225.0 (d, $J(^{31}P-^{13}C)$ = 40.9 Hz), 48.9 (d, $J(^{31}P-^{13}C)$ = 22.3 Hz), 25.9 ppm (d, $J(^{31}P-^{13}C)$ = 3.0 Hz).

NMR data are consistent with previous reports.[13]

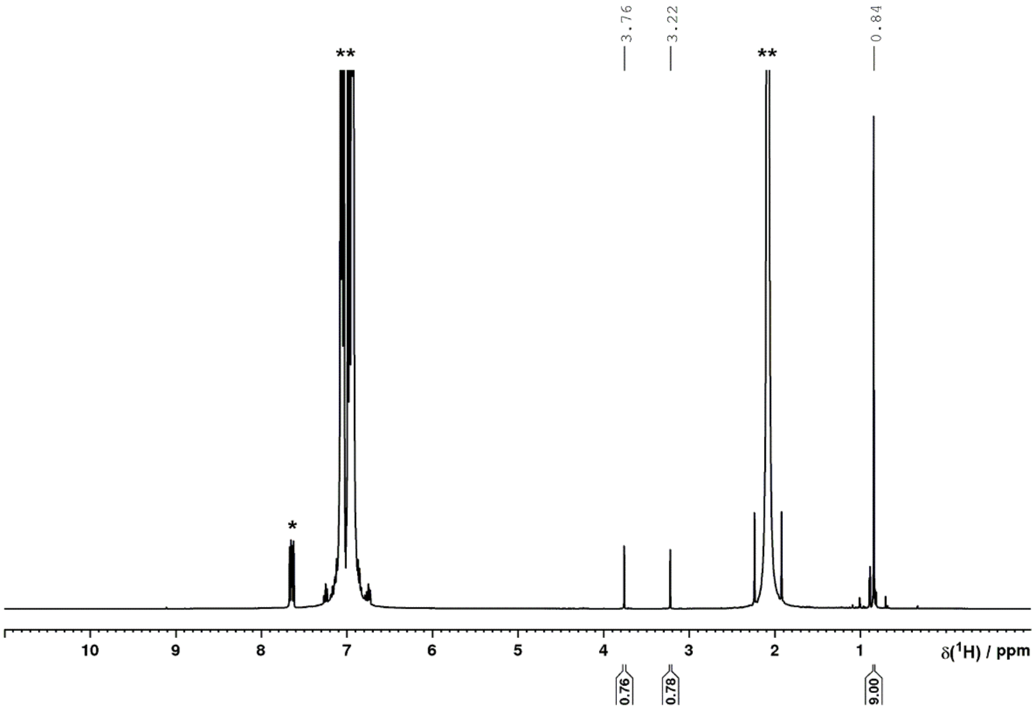

Supplementary Figure 47. ^{1}H NMR spectrum of a solution of *t*BuC(O)PH$_2$ (**5**) in PhMe, also containing Ph$_3$PO (*). Solvent resonances (**) truncated for clarity.

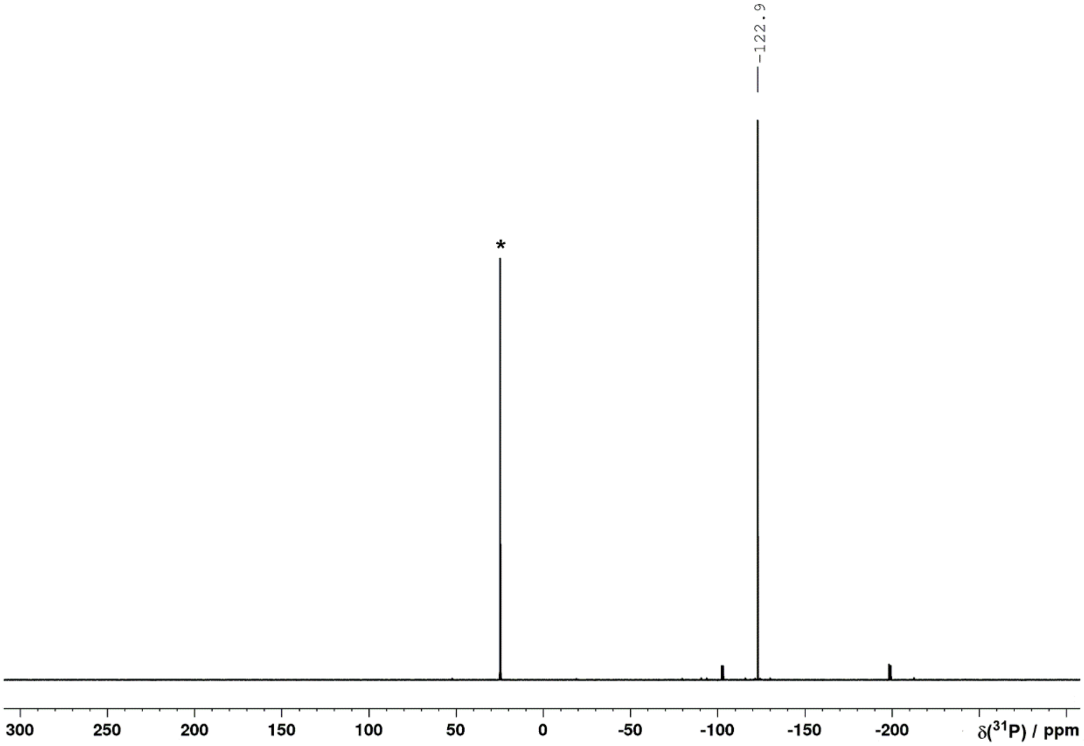

Supplementary Figure 48. ^{31}P{^{1}H} NMR spectrum of a solution of *t*BuC(O)PH$_2$ (**5**) in PhMe, also containing Ph$_3$PO (*).

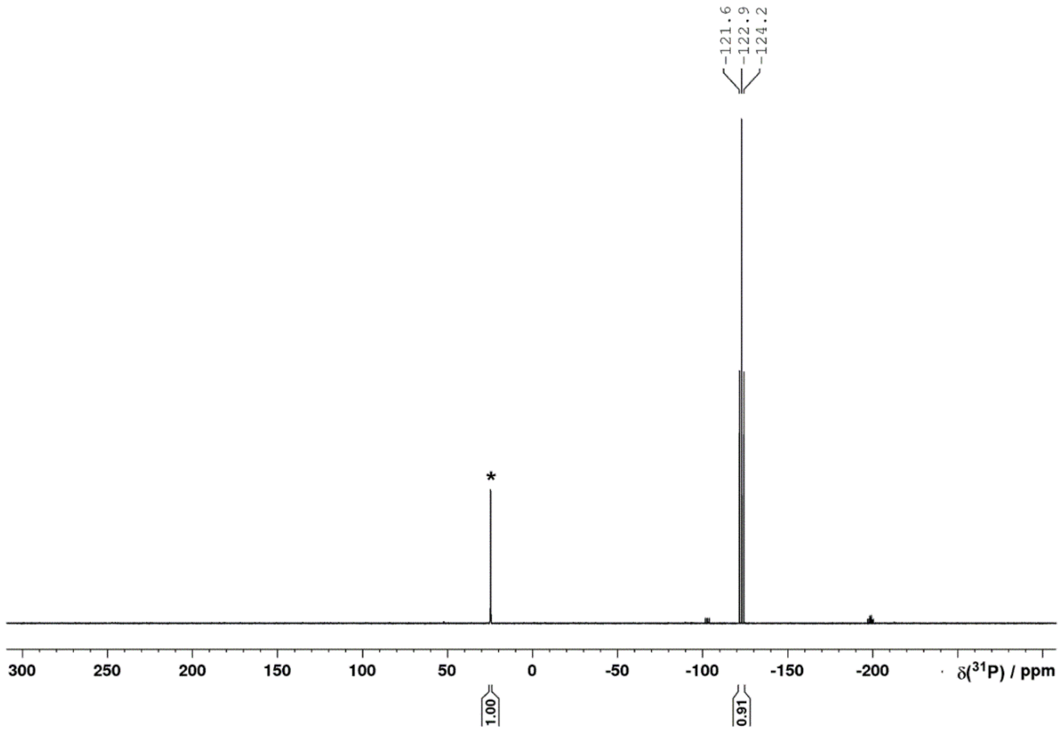

Supplementary Figure 49. ^{31}P NMR spectrum of a solution of *t*BuC(O)PH$_2$ (**5**) in PhMe, also containing Ph$_3$PO (*).

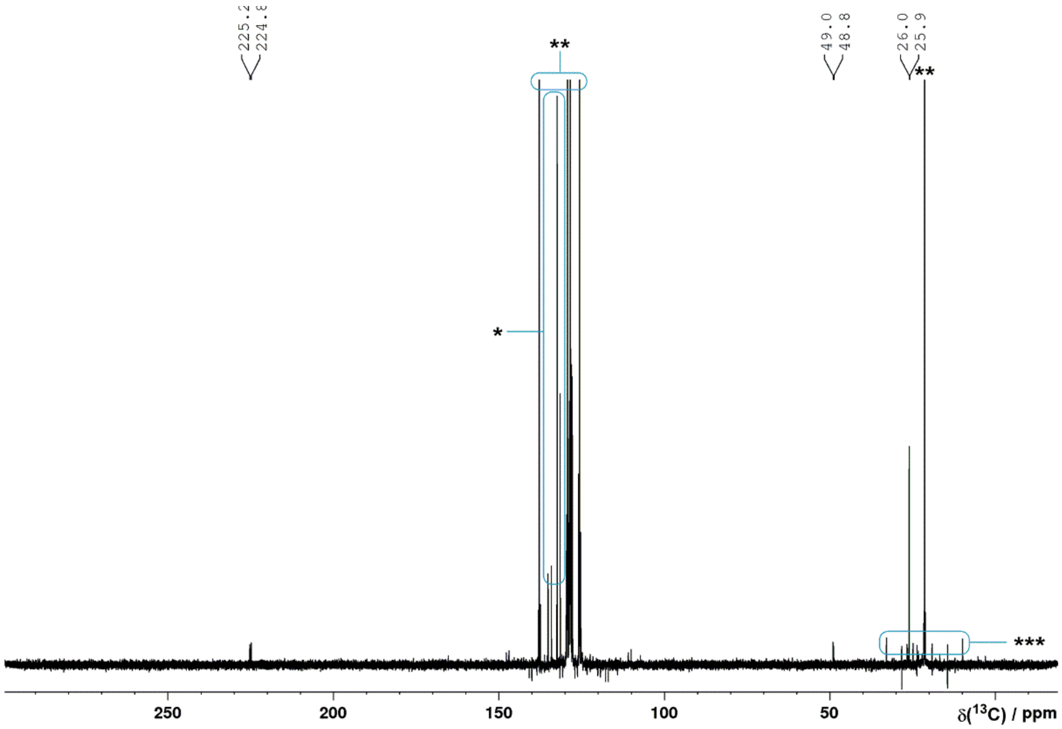

Supplementary Figure 50. $^{13}C\{^1H\}$ NMR spectrum of a solution of *t*BuC(O)PH$_2$ (**5**) in PhMe, also containing Ph$_3$PO (*). Solvent resonances (**) truncated for clarity (***decoupling artefacts).

Supplementary Method 15: Single and double acylation of $(Bu_3Sn)_2PH$ (3)

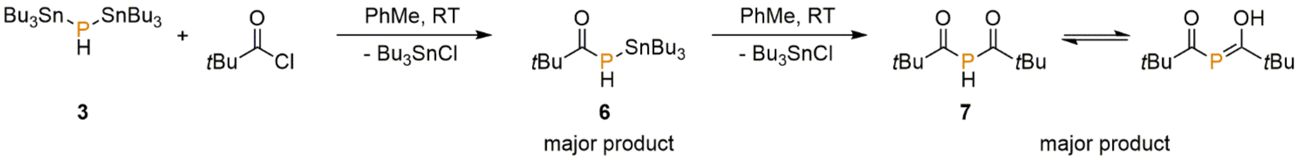

To a stirred solution of $(Bu_3Sn)_2PH$ (**3**, 30.6 mg, 0.05 mmol) in C_6D_6 (500 µL) was added *t*BuC(O)Cl (6.2 µL, 0.05 mmol). The resulting mixture was then analysed by ^{1}H, $^{31}P\{^{1}H\}$ and ^{31}P NMR spectroscopy, as shown in Supplementary Figures 51-53, below.

The $^{31}P\{^{1}H\}$ spectrum clearly indicates formation of a single major species, characterised by a singlet resonance at –140.4 ppm, with $^{117/119}Sn$ satellites ($^{1}J(^{119}Sn\text{-}^{31}P) = 553$ Hz), and which splits into a doublet in the ^{31}P spectrum ($^{1}J(^{31}P\text{-}^{1}H) = 193$ Hz). Given the very similar chemical shift to *t*BuC(O)PH_2, this species can confidently be assigned as *t*BuC(O)P(H)$SnBu_3$ (**6**). Several minor product resonances can also be observed. Those at 52.2 ppm and –36.5 ppm are consistent with previous reports of the two tautomeric forms of the doubly-acylated product HP(C(O)*t*Bu)$_2$ (**7**),[14] and the signal at –122.3 ppm can similarly be assigned to *t*BuC(O)PH_2 (**5**; Supplementary Method 14). The unassigned signal at –125.2 ppm, which has $^{117/119}Sn$ satellites ($^{1}J(^{119}Sn\text{-}^{31}P) = 700$ Hz) but remains a singlet in the ^{31}P spectrum, is attributed to *t*BuC(O)P($SnBu_3$)$_2$, by analogy with *t*BuC(O)PH_2 and *t*BuC(O)P(H)$SnBu_3$. Finally, the signal arising at 10.2 ppm is assumed to be due to formation of Bu_3SnP(C(O)*t*Bu)$_2$, based on the chemical shift (between the two tautomers of HP(C(O)*t*Bu)$_2$), $^{117/119}Sn$ satellites ($^{1}J(^{119}Sn\text{-}^{31}P) = 547$ Hz), and lack of splitting in the ^{31}P spectrum.

When the reaction was repeated using 2 eq. *t*BuC(O)Cl under otherwise identical conditions (Supplementary Figures 54-56), the double acylation product **7** (in equilibrium with its tautomer) was observed to be the major product in the $^{31}P\{^{1}H\}$ spectrum, alongside minor Bu_3SnP(C(O)*t*Bu)$_2$ and *t*BuC(O)P(H)$_x$($SnBu_3$)$_{2-x}$ (x = 0-2).

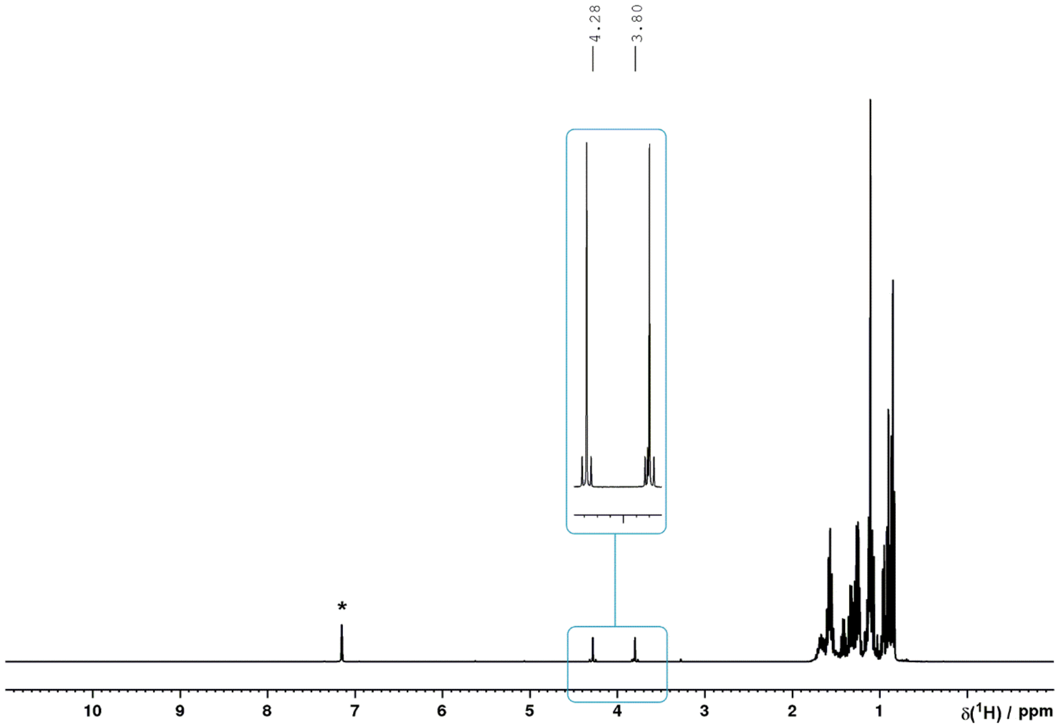

Supplementary Figure 51. ^{1}H NMR spectrum for the reaction of $(Bu_3Sn)_2PH$ (**3**) with 1 eq. *t*BuC(O)Cl in C_6D_6 (*).

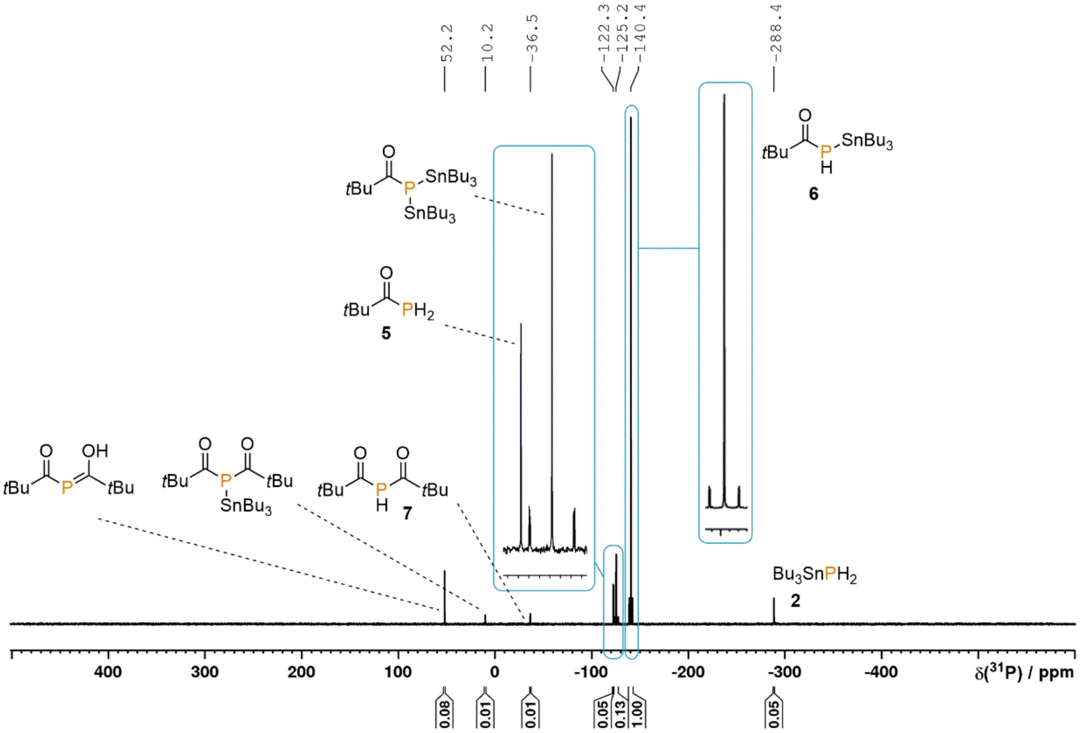

Supplementary Figure 52. $^{31}P\{^1H\}$ NMR for the reaction of $(Bu_3Sn)_2PH$ (**3**) with 1 eq. *t*BuC(O)Cl in C_6D_6.

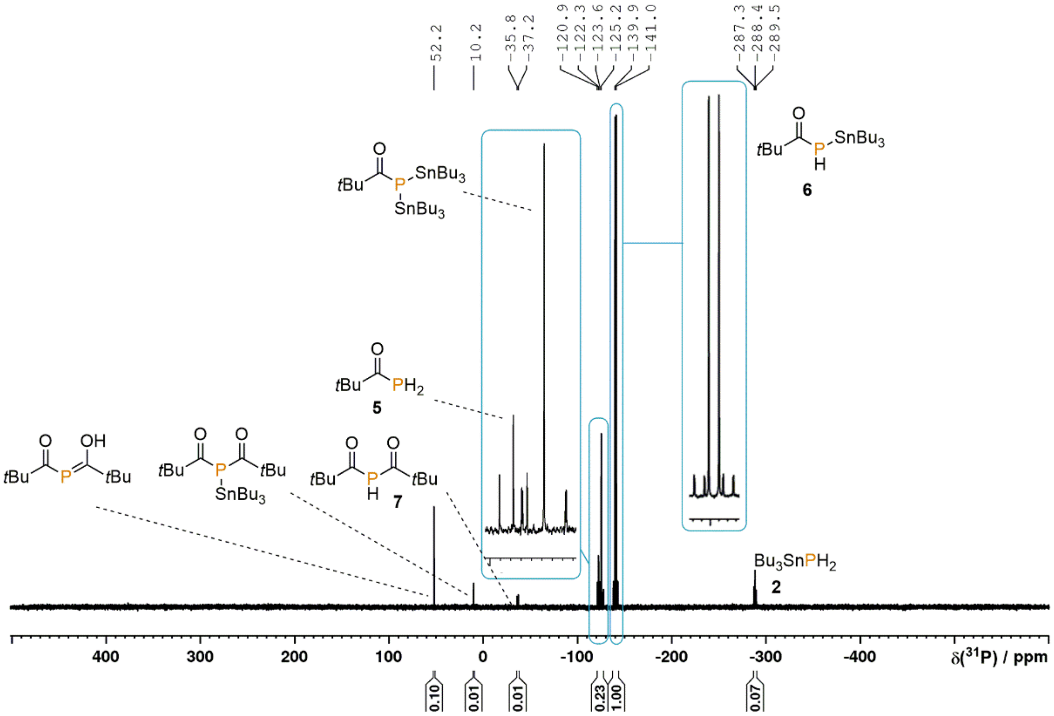

Supplementary Figure 53. ^{31}P NMR spectrum for the reaction of $(Bu_3Sn)_2PH$ (**3**) with 1 eq. *t*BuC(O)Cl in C_6D_6.

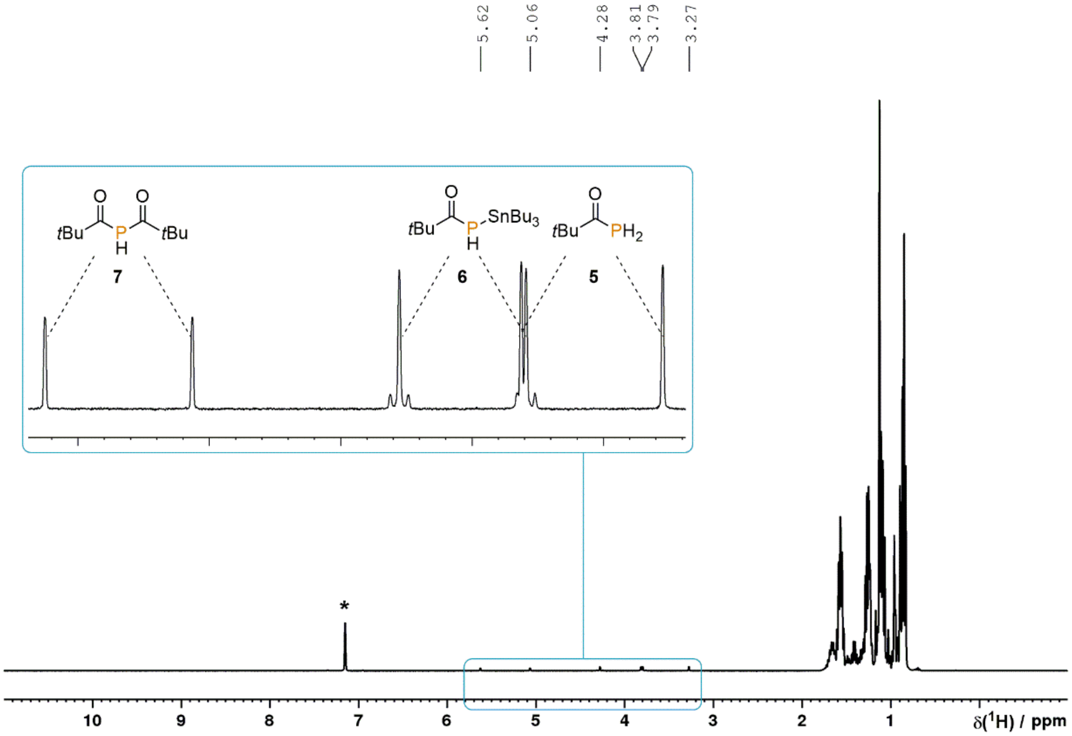

Supplementary Figure 54. ^{1}H NMR spectrum for the reaction of $(Bu_3Sn)_2PH$ (**3**) with 2 eq. *t*BuC(O)Cl in C_6D_6 (*).

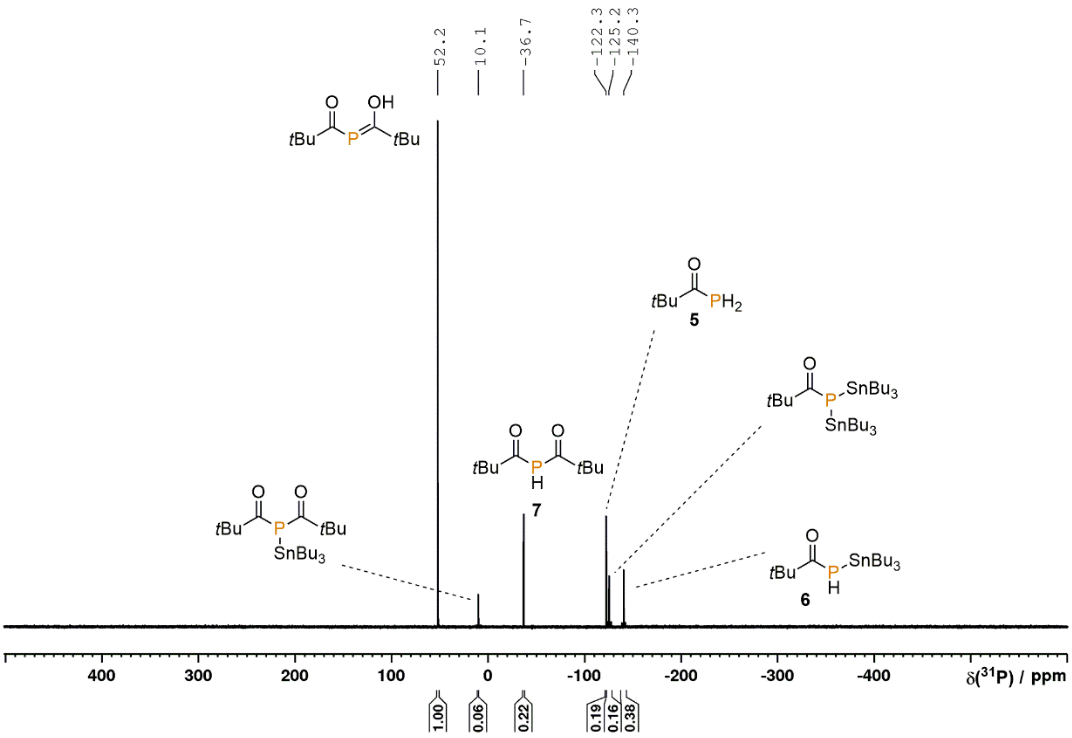

Supplementary Figure 55. $^{31}P\{^1H\}$ NMR for the reaction of $(Bu_3Sn)_2PH$ (**3**) with 2 eq. *t*BuC(O)Cl in C_6D_6.

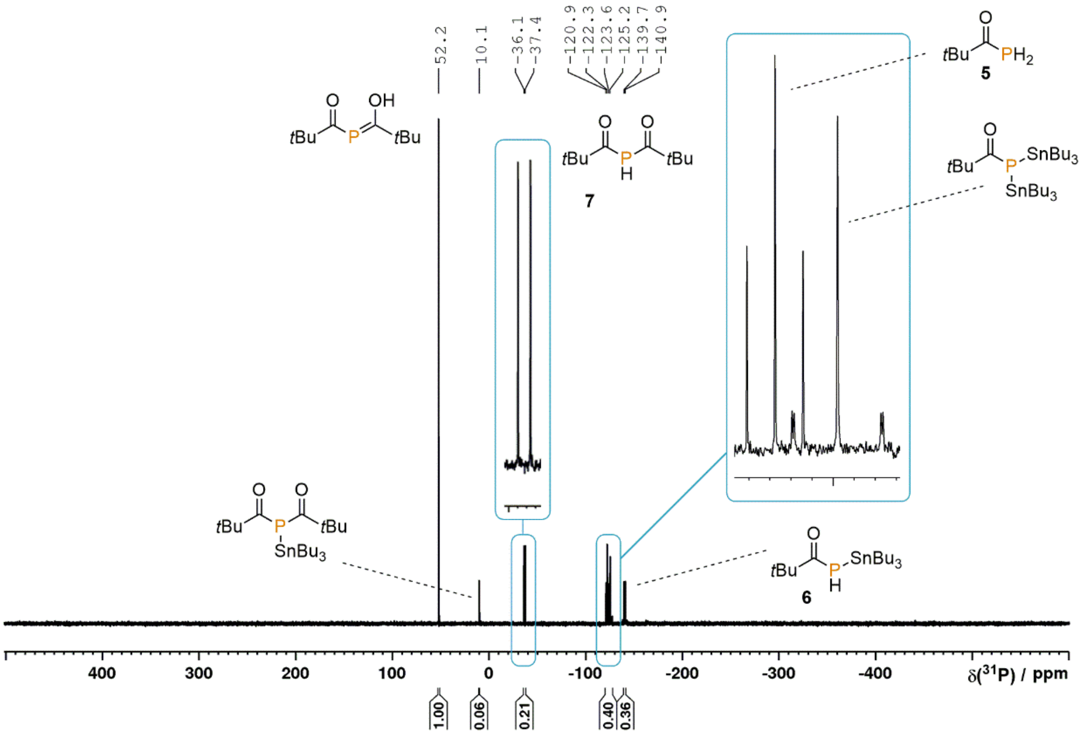

Supplementary Figure 56. ^{31}P NMR spectrum for the reaction of $(Bu_3Sn)_2PH$ (**3**) with 2 eq. *t*BuC(O)Cl in C_6D_6.

Supplementary Method 16: Synthesis and quantification of PH_3 (1)

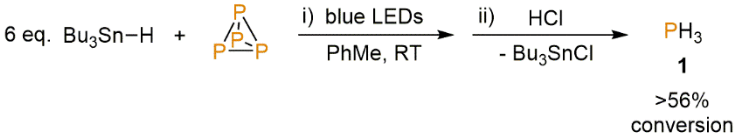

To an NMR tube fitted with a J. Young valve were added PhMe (500 µL), P_4 (0.01 mmol, as a stock solution in 77.4 µL PhH), Ph_3PO (14.2 mg, 0.051 mmol) and Bu_3SnH (16.1 µL, 0.06 mmol). The NMR tube was sealed, placed in thermal contact with a water-cooled block to maintain near-ambient temperature (by placing in a water-filled, flat-bottomed glass tube, which was in turn placed in the block and wrapped in Al foil), and irradiated with blue light (455 nm (±15 nm), 3.2 V, 700 mA, Osram OSLON SSL 80) for 17 h. The resulting colourless solution was frozen by placing the NMR tube in a bath of liquid nitrogen, and HCl (0.4 mmol, 4.0 M in 1,4-dioxane) was added (while still maintaining an inert atmosphere). The NMR tube was sealed and its contents were then thawed, agitated briefly, and analysed by ^1H, $^{31}P\{^1H\}$ and ^{31}P NMR spectroscopy. The resulting spectra indicated clean conversion to PH_3,[15] as shown in Supplementary Figures 57-59, below.

In order to accurately quantify the amount of PH_3 in solution, a proton-coupled ^{31}P spectrum was acquired with a 20 s delay between scans (which was confirmed to be $> 5 \times T_1$), and the intensity of the PH_3 resonance was integrated relative to that of Ph_3PO (which had been added specifically to act as an internal standard). This indicated 56% of the theoretical maximum conversion to PH_3 (Supplementary Figure 60), which provides a lower bound for the actual conversion (this value does not include any PH_3 present in the NMR tube headspace).

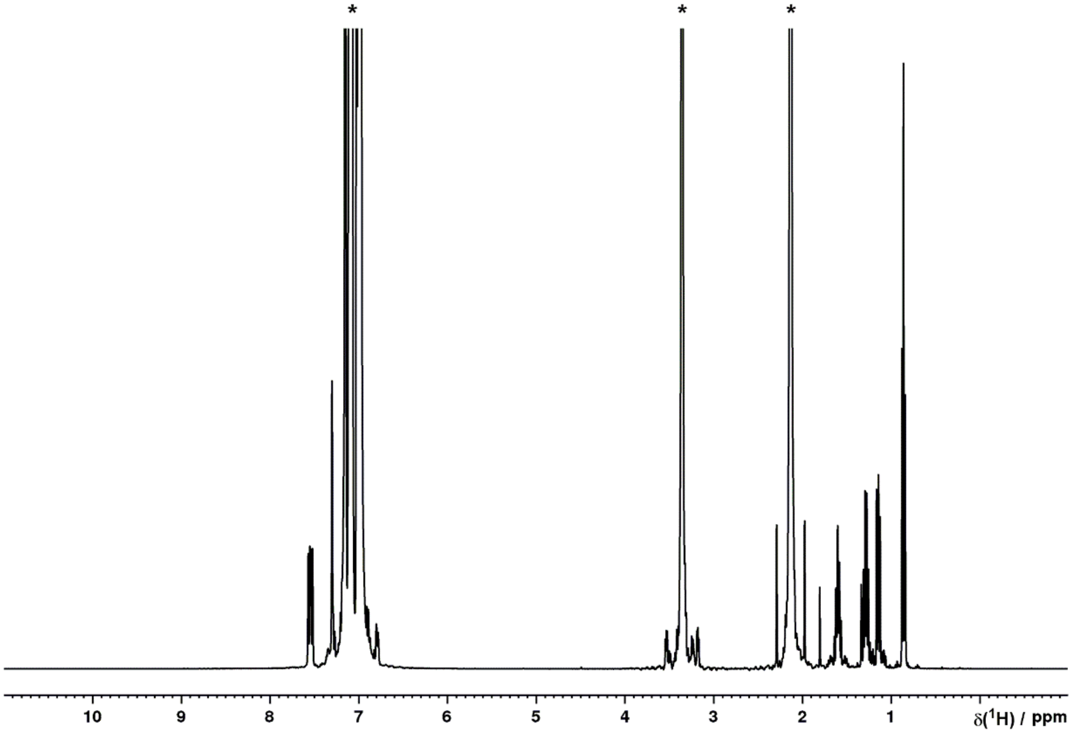

Supplementary Figure 57. ^{1}H NMR spectrum of a solution of PH_3 (**1**) generated *via* hydrostannylation of P_4 in PhMe, followed by acidification. Solvent resonances (*) truncated for clarity.

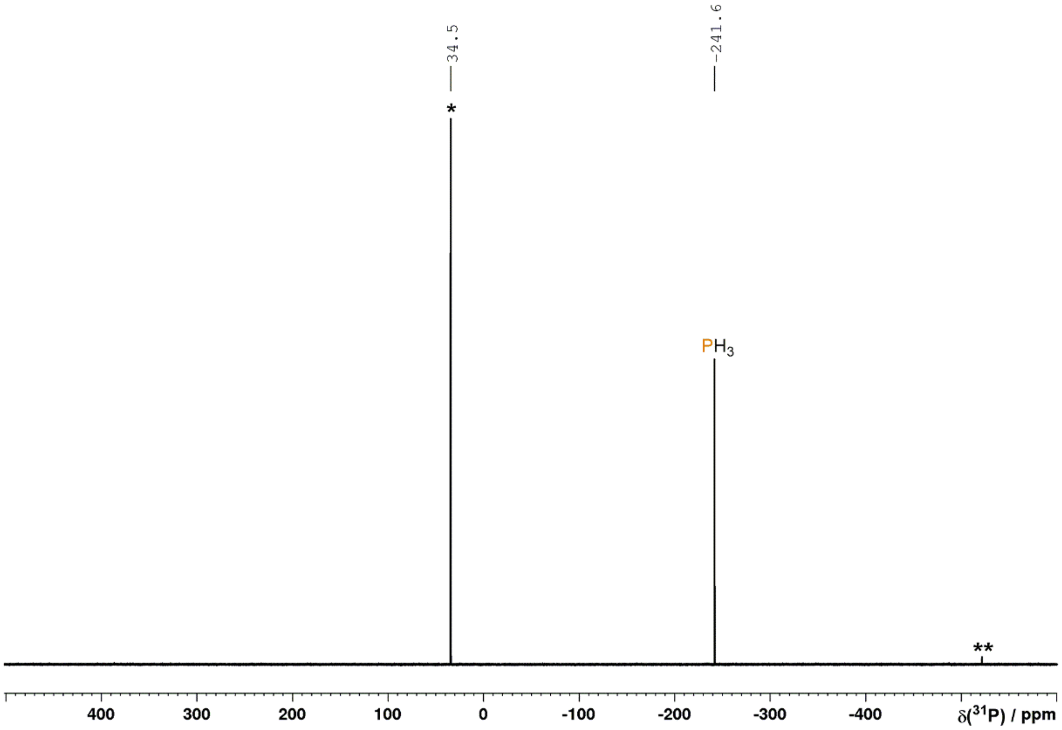

Supplementary Figure 58. $^{31}P\{^1H\}$ NMR spectrum of PH_3 (**1**) generated *via* hydrostannylation of P_4 in PhMe, followed by acidification, in the presence of Ph_3PO (*) as an internal standard (**trace residual P_4).

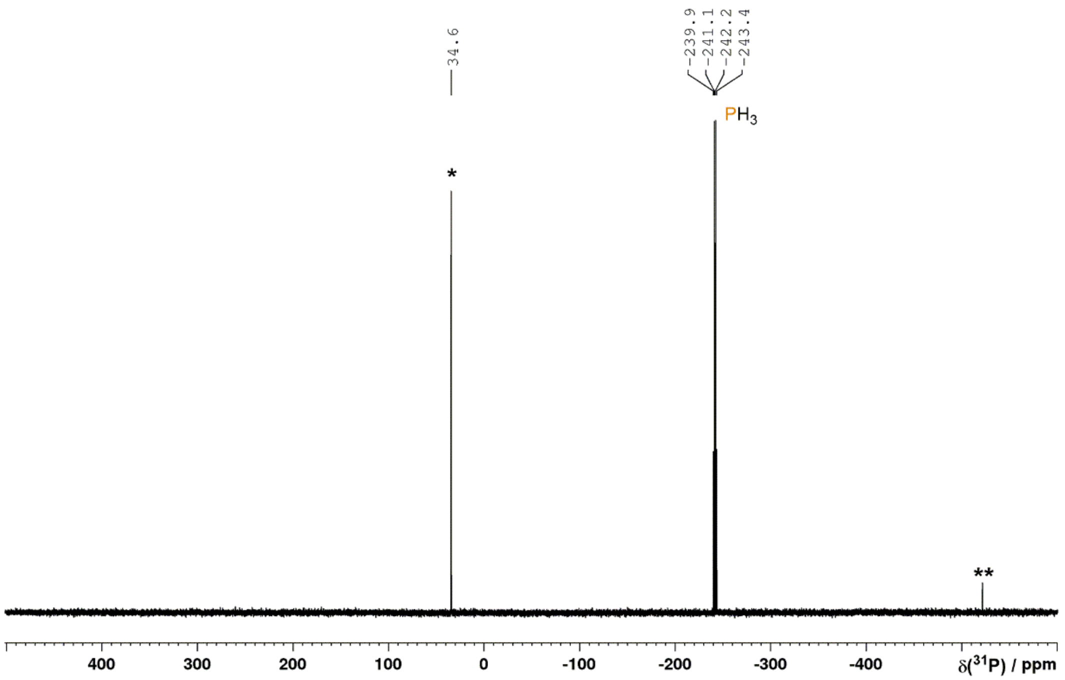

Supplementary Figure 59. ^{31}P NMR spectrum of PH_3 (**1**) generated *via* hydrostannylation of P_4 in PhMe, followed by acidification, in the presence of Ph_3PO (*) as an internal standard (** trace residual P_4).

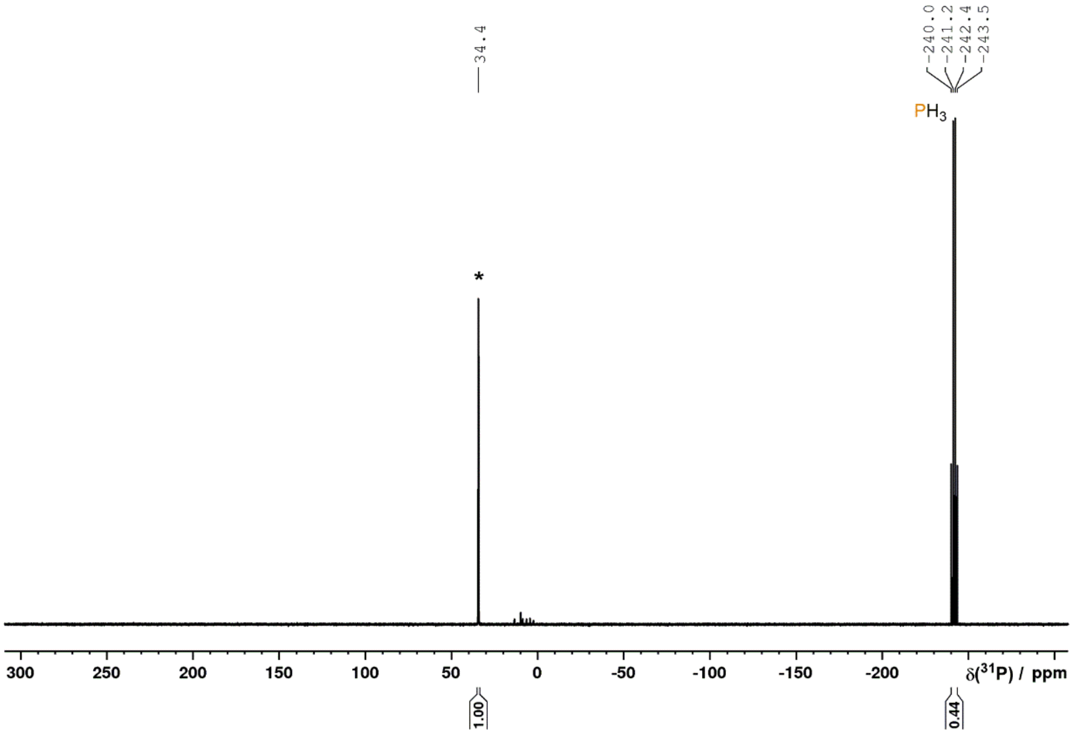

Supplementary Figure 60. Quantitative ^{31}P NMR spectrum (D1 = 20 s) of PH_3 (**1**) generated *via* hydrostannylation of P_4 in PhMe, followed by acidification, in the presence of Ph_3PO (*) as an internal standard.

Supplementary Method 17: Synthesis and isolation of $P(SnBu_3)_3$ (4)

To a 50 mL, flat-bottomed Schlenk tube were added P_4 (61.9 mg, 0.5 mmol) and PhMe (25 mL). After stirring to obtain a homogeneous solution, Bu_3SnH (807 µL, 3.0 mmol) and Bu_3SnOMe (864 µL, 3.0 mmol) were added. The resulting colourless, homogeneous mixture was stirred in a water-cooled block (to maintain near-ambient temperature) and irradiated with blue light (7X Osram OSLON SSL80, 455 nm (±15 nm), 20.3 V 1000 mA) for 16 h. Following removal of volatiles under vacuum, the resulting yellowish oil was stirred at 100 °C for 16 h. After distillation under vacuum (*ca.* 105 °C, 10^{-2} mbar), the product was obtained as a colourless oil (1.53 g, 85%).

^{1}H NMR (400 MHz, 300 K, C_6D_6): δ = 1.81-1.61 (2H, m), 1.51-1.40 (2H, m), 1.1-1.13 (2H, m), 0.98 ppm (3H, t, $^3J(^1H\text{-}^1H)$ = 7.3 Hz).

$^{31}P\{^1H\}$ NMR (121 MHz, 300 K, C_6D_6): δ = –346.5 ppm (s).

^{31}P NMR (121 MHz, 300 K, C_6D_6): δ = –346.5 ppm (s).

$^{119}Sn\{^1H\}$ (149 MHz, 300 K, C_6D_6) δ = 37.6 ppm (d, $^1J(^{31}P\text{-}^{119}Sn)$ = 912 Hz, $^2J(^{119}Sn\text{-}^{117}Sn)$ = 279 Hz).

$^{13}C\{^1H\}$ NMR (101 MHz, 300 K, C_6D_6): δ = 29.7 (d, $J(^{31}P\text{-}^1H)$ = 1.4 Hz), 27.6 (s), 14.9 (d, $J(^{31}P\text{-}^1H)$ = 3.7 Hz), 13.5 ppm (s).

MS (LIFDI, PhMe): m/z = 900.2518 (M^+).

$P(SnBu_3)_3$ has been referenced in one previous paper of which we are aware, but no synthetic procedure or characterisation data appear to have been reported.[16] Nevertheless, the above ^{31}P NMR data are similar to those reported previously for the related compound $P(SnPh_3)_3$.[17]

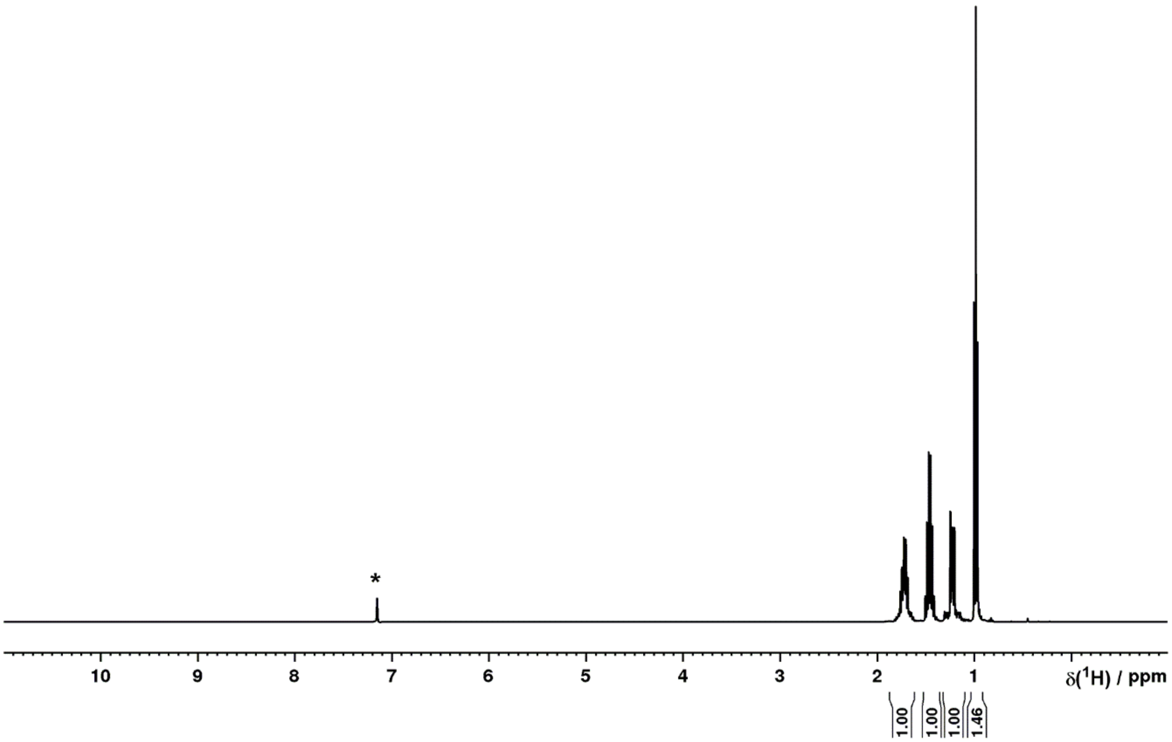

Supplementary Figure 61. ^{1}H NMR spectrum of P(SnBu$_3$)$_3$ (**4**) in C_6D_6 (*).

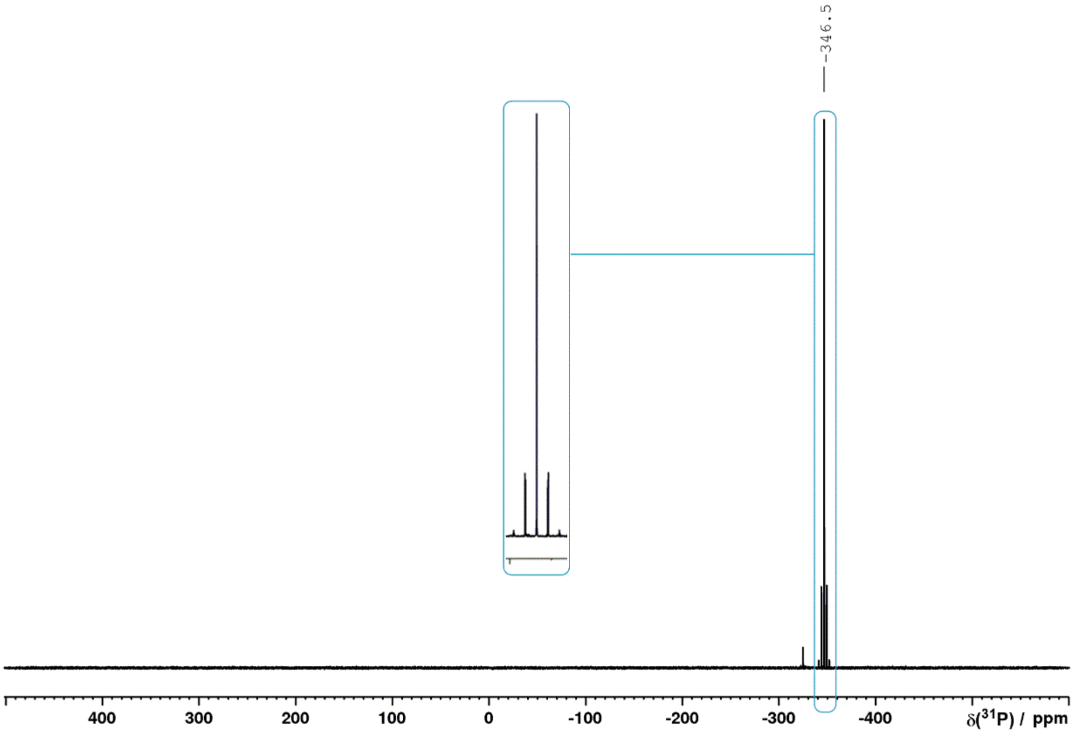

Supplementary Figure 62. ^{31}P{^{1}H} NMR spectrum of P(SnBu$_3$)$_3$ (**4**) in C_6D_6.

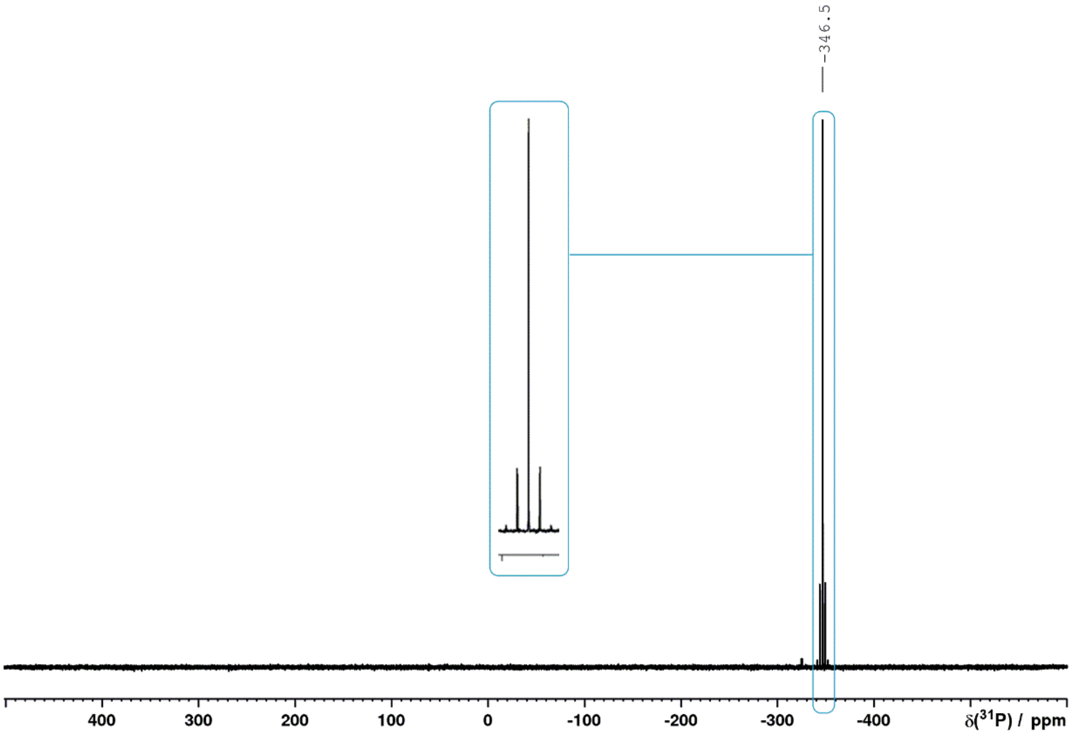

Supplementary Figure 63. ^{31}P NMR spectrum of P(SnBu$_3$)$_3$ (**4**) in C_6D_6.

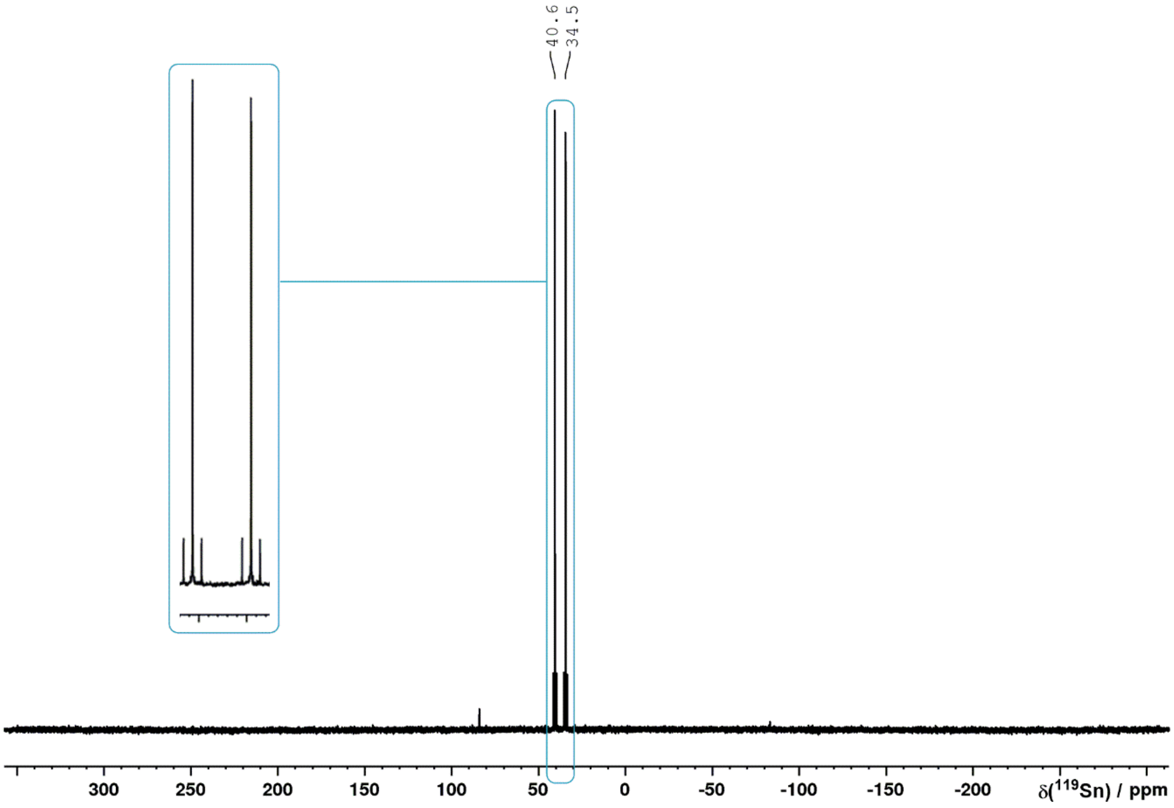

Supplementary Figure 64. ^{119}Sn{^{1}H} NMR spectrum of P(SnBu$_3$)$_3$ (**4**) in C_6D_6.

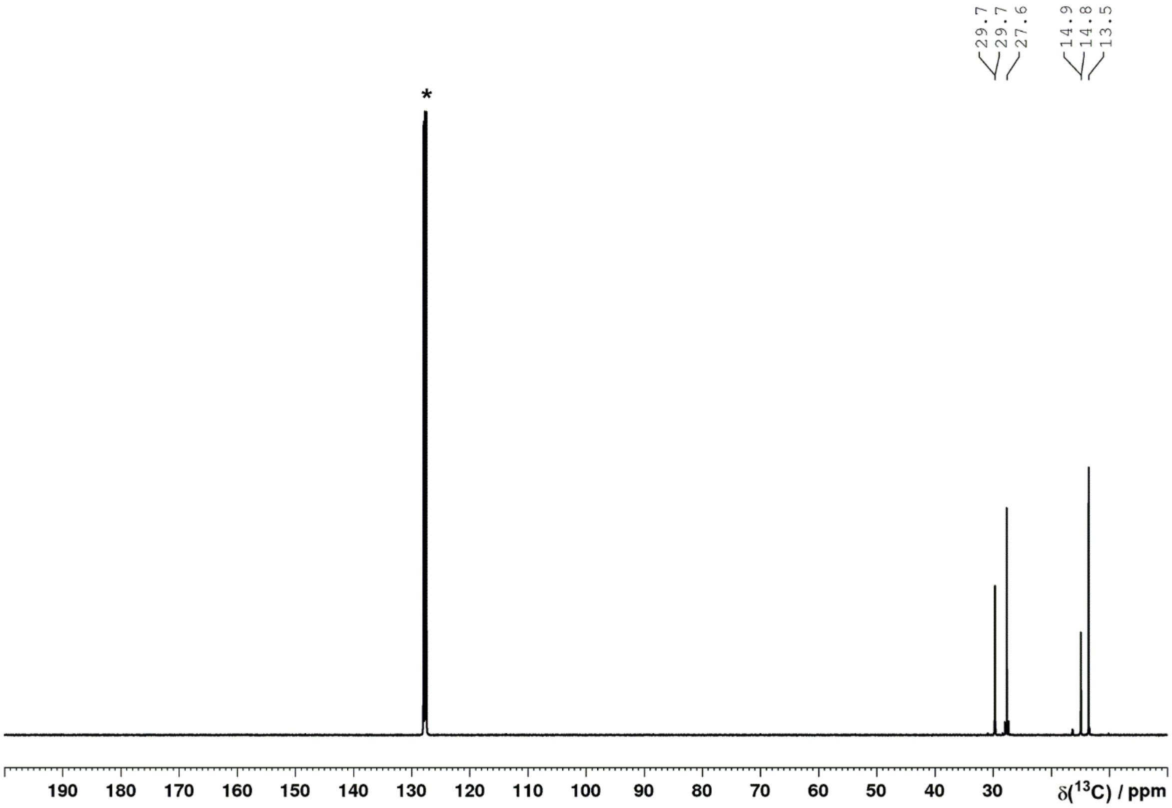

Supplementary Figure 65. $^{13}C\{^{1}H\}$ NMR spectrum of $P(SnBu_3)_3$ (**4**) in C_6D_6 (*).

Supplementary Method 18: Synthesis and isolation of P(C(O)*t*Bu)₃ (8)

8

57% yield

The product P(C(O)*t*Bu)$_3$ (**8**) was prepared as described in the Methods section of the main manuscript. Characterisation data are provided below:

^{1}H NMR (400 MHz, 300 K, C_6D_6): δ = 1.07 ppm (s).

$^{31}P\{^{1}H\}$ NMR (121 MHz, 300 K, C_6D_6): δ = 51.6 ppm (s).

^{31}P NMR (121 MHz, 300 K, C_6D_6): δ = 51.6 ppm (s).

$^{13}C\{^1H\}$ NMR (101 MHz, 300 K, C_6D_6): δ = 221.3 (d, $^1J(^{31}P\text{-}^1H)$ = 47.9 Hz), 49.7 (d, $^2J(^{31}P\text{-}^1H)$ = 30.3 Hz), 25.4 ppm (d, $^3J(^{31}P\text{-}^1H)$ = 3.7 Hz).

MS (APCI, PhMe): m/z = 304.2044 ($[M+NH_4]^+$).

NMR data are consistent with previous reports.[18]

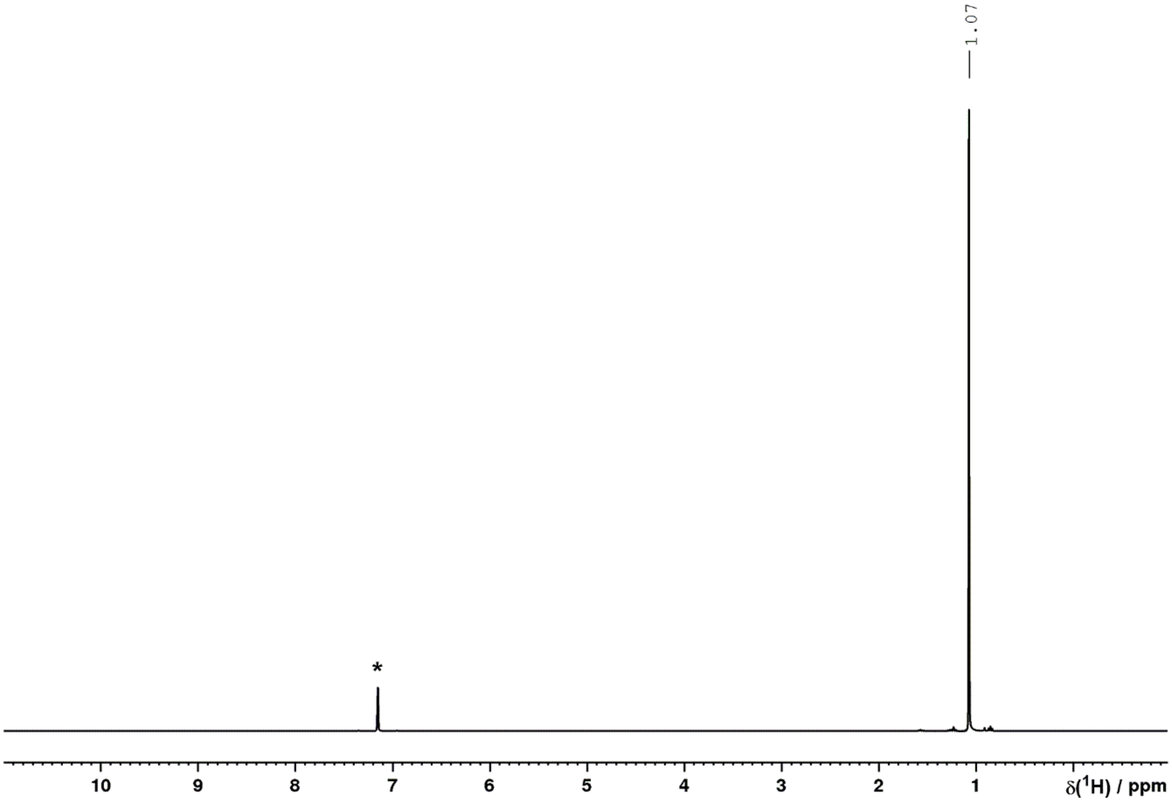

Supplementary Figure 66. ^1H NMR spectrum of $P(C(O)tBu)_3$ (**8**) in C_6D_6 (*).

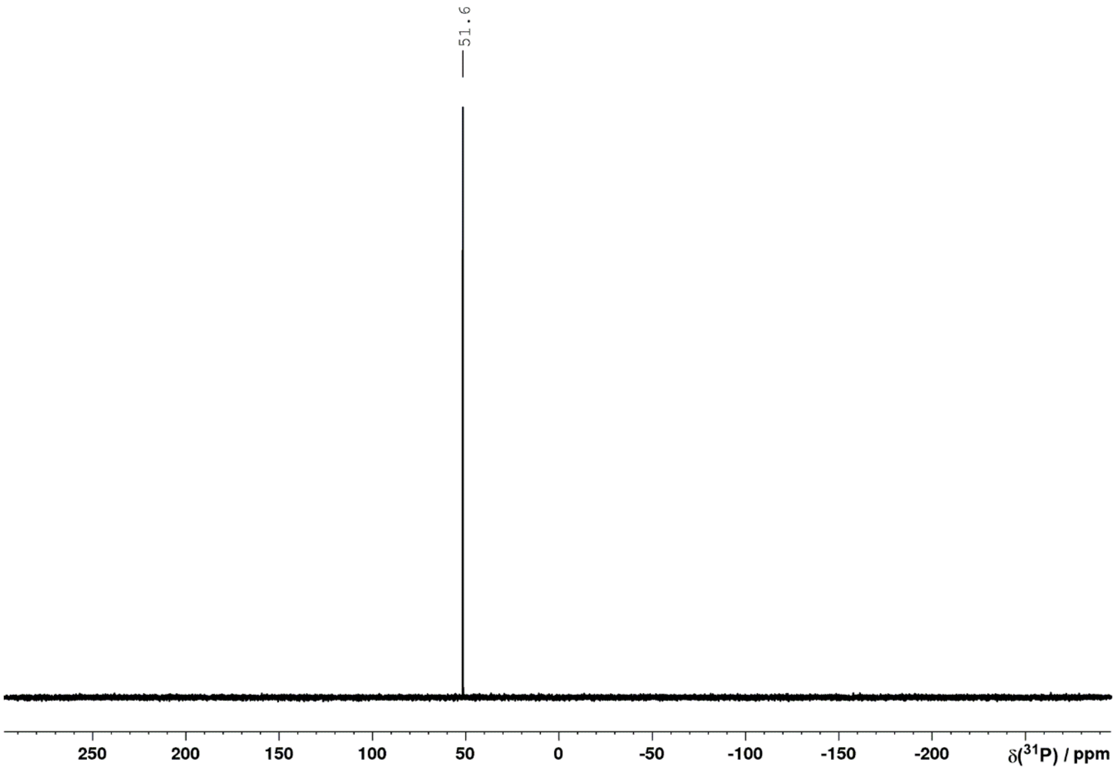

Supplementary Figure 67. $^{31}P\{^{1}H\}$ NMR spectrum of $P(C(O)tBu)_3$ (**8**) in C_6D_6.

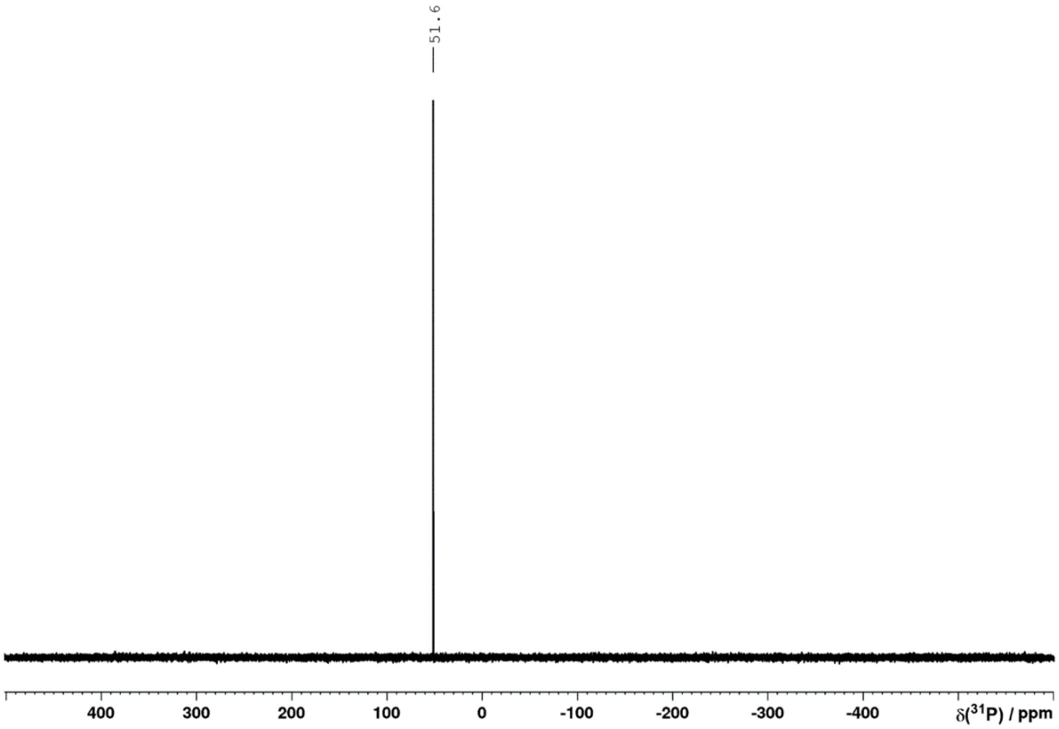

Supplementary Figure 68. ^{31}P NMR spectrum of $P(C(O)tBu)_3$ (**8**) in C_6D_6.

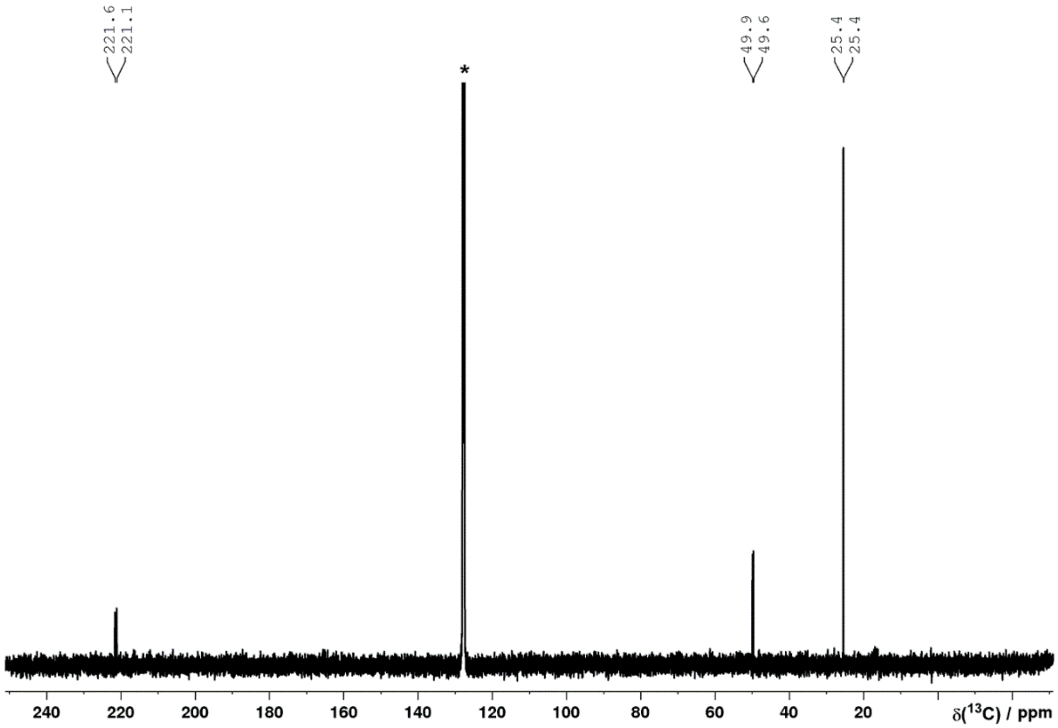

Supplementary Figure 69. $^{13}C\{^1H\}$ NMR spectrum of P(C(O)*t*Bu)$_3$ (**8**) in C_6D_6. Solvent resonance (*) truncated for clarity.

Supplementary Method 19: Synthesis and isolation of P(C(O)Ph)$_3$ (9)

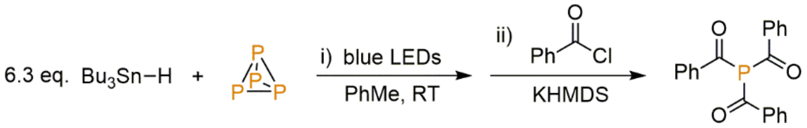

9

51% yield

To a 50 mL flat-bottomed Schlenk tube were added P_4 (62.0 mg, 0.5 mmol) and PhMe (25 mL). After stirring to obtain a homogeneous solution Bu_3SnH was added (847 µL, 3.15 mmol). The resulting colorless solution was stirred under irradiation with blue LED light (7X Osram OSLON SSL80, 455 nm (±15 nm), 20.3 V 1000mA) for 22 h, during which time the Schlenk tube was placed in a block cooled by circulating water to maintain near-ambient temperature. PhC(O)Cl (929 µL, 8.0 mmol) and KHMDS (599 mg, 3.0 mmol) were added, and the reaction mixture was stirred at room temperature for 16 h. The resulting yellow suspension was filtered, volatiles were removed under vacuum, and the remaining solid was washed with *n*-hexane (4 x 20 mL). The remaining yellow residue was recrystallized from THF/*n*-hexane at –35 °C, to afford the desired product as yellow needles (355 mg, 51%).

^{1}H NMR (400 MHz, 300 K, C_6D_6): δ = 7.98 ppm (2H, m), 7.03 ppm (1H, tt, $^3J(^1H-^1H)$ =7.3 Hz, $^5J(^1H-^1H)$ =1.4 Hz), 6.96 ppm (2H, m).

$^{31}P\{^1H\}$ NMR (121 MHz, 300 K, C_6D_6): δ = 54.4 ppm (s).

^{31}P NMR (121 MHz, 300 K, C_6D_6): δ = 54.4 ppm (s).

$^{13}C\{^1H\}$ NMR (101 MHz, 300 K, C_6D_6): δ = 205.8 (d, $J(^{31}P-^1H)$ = 32.9 Hz), 140.9 (d, $J(^{31}P-^1H)$ = 35.2 Hz), 133.9 (d, $J(^{31}P-^1H)$ = 1.4 Hz), 129.0 (d, $J(^{31}P-^1H)$ = 8.0 Hz), 128.9 ppm (d, $J(^{31}P-^1H)$ = 0.8 Hz).

MS (ESI, PhMe): *m/z* = 347.0840 ([M+H]$^+$).

NMR data are consistent with previous reports.[19]

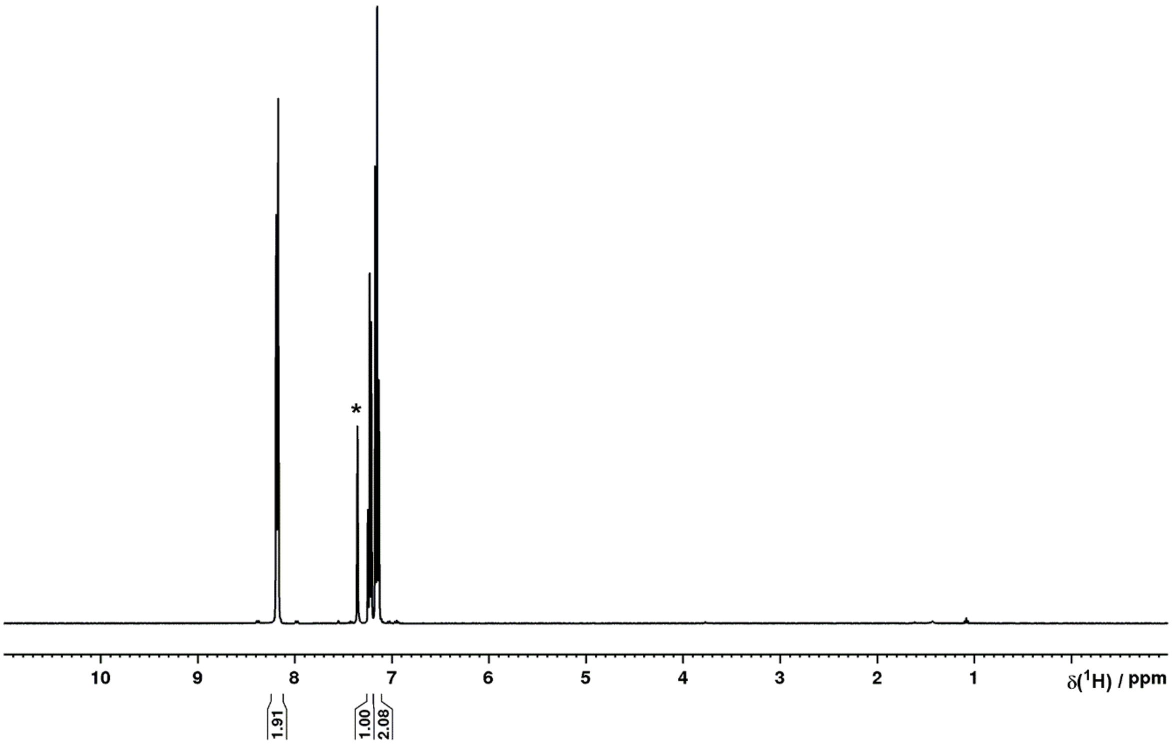

Supplementary Figure 70. ^{1}H NMR spectrum of $P(C(O)Ph)_3$ (**9**) in C_6D_6 (*).

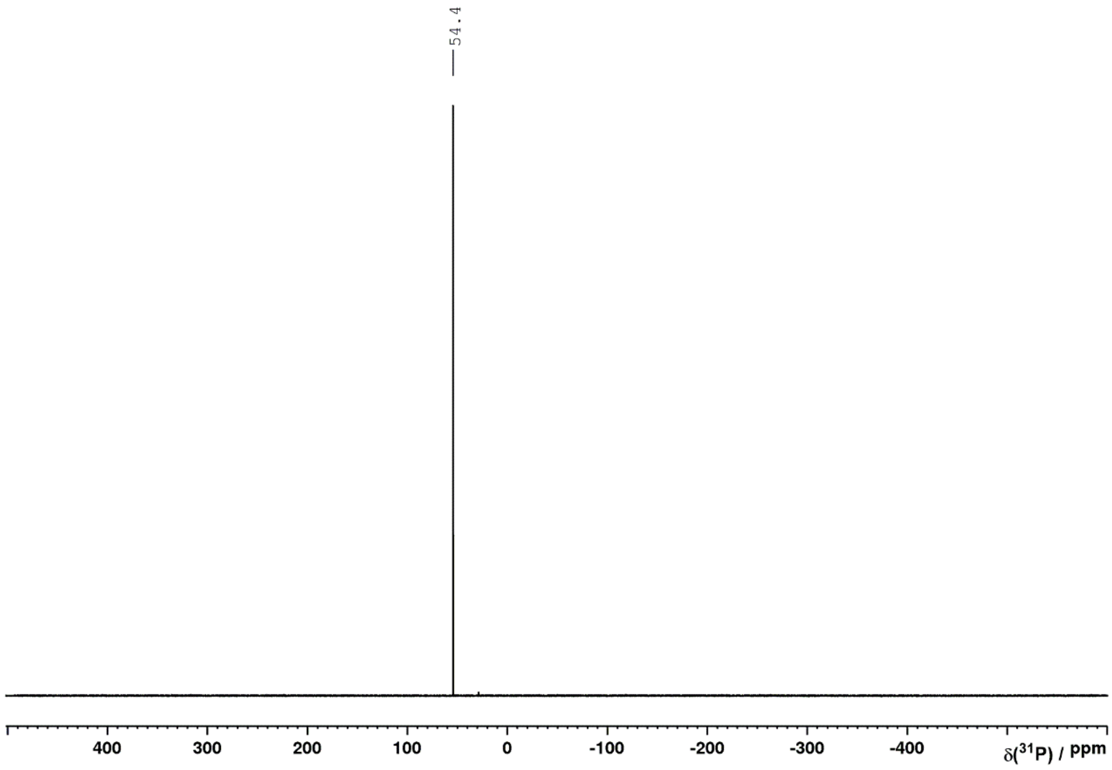

Supplementary Figure 71. $^{31}P\{^{1}H\}$ NMR spectrum of $P(C(O)Ph)_3$ (**9**) in C_6D_6.

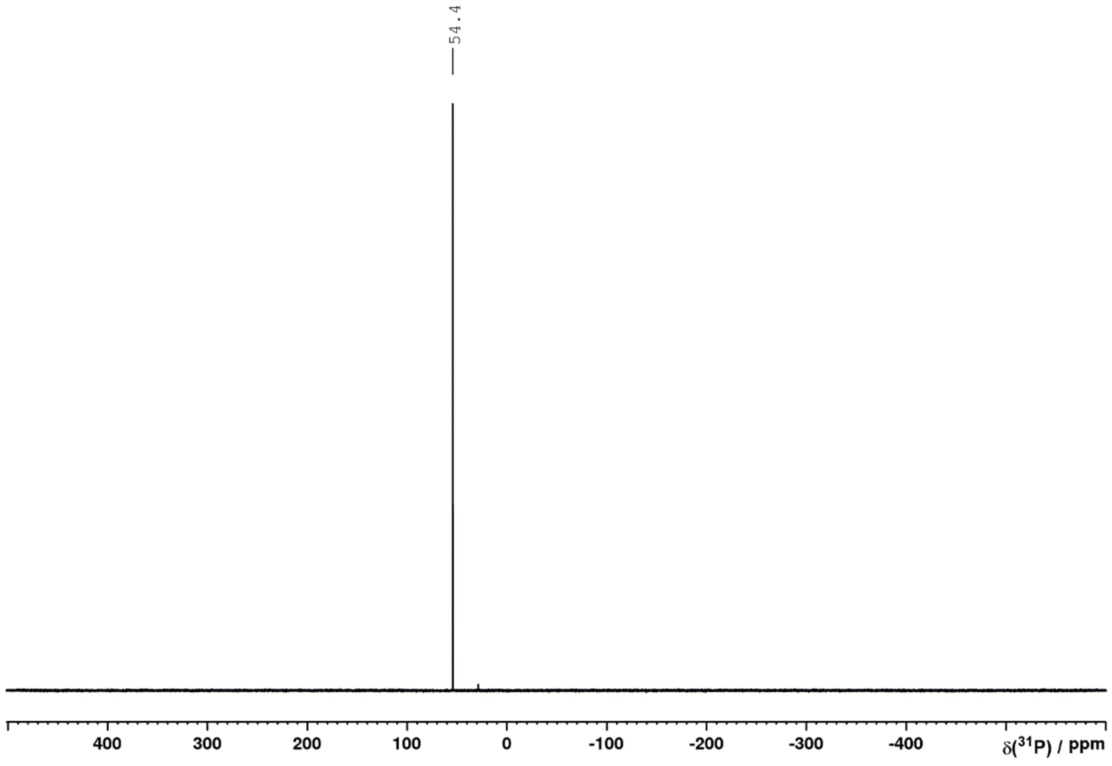

Supplementary Figure 72. ^{31}P NMR spectrum of $P(C(O)Ph)_3$ (**9**) in C_6D_6.

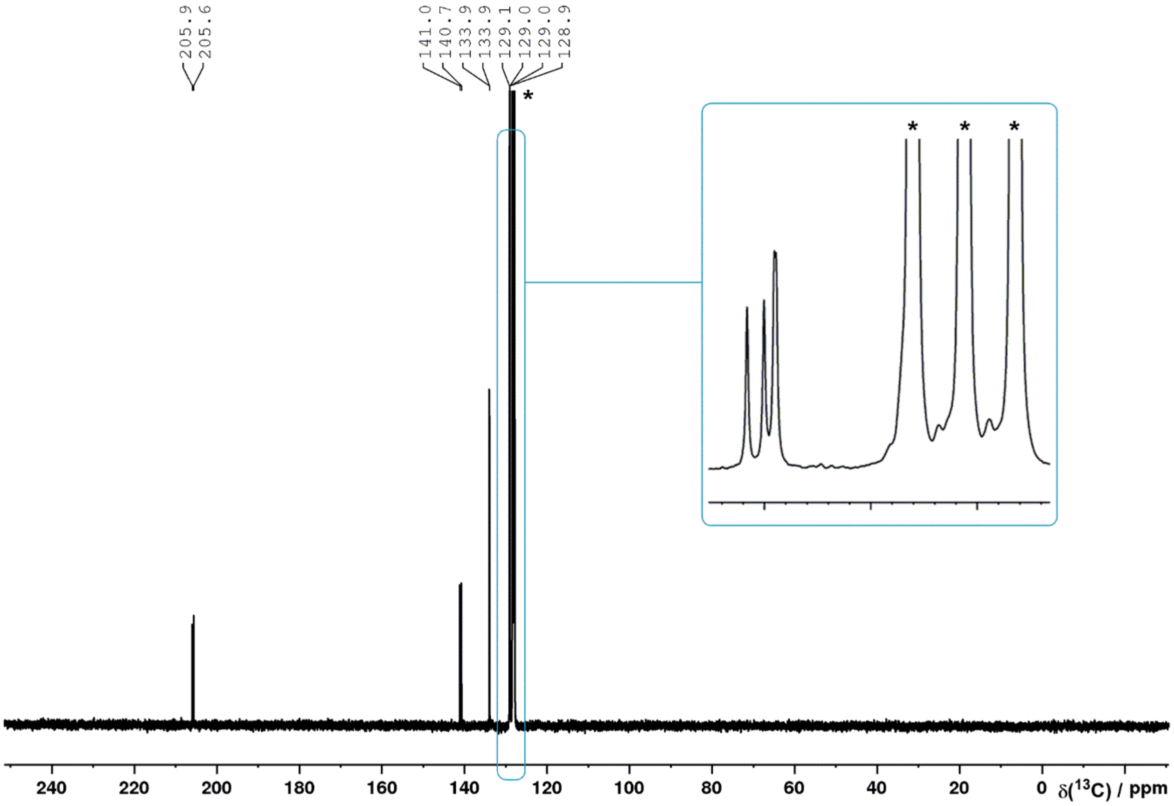

Supplementary Figure 73. $^{13}C\{^{1}H\}$ NMR spectrum of $P(C(O)Ph)_3$ (**9**) in C_6D_6. Solvent resonance (*) truncated for clarity.

Supplementary Method 20: Synthesis and isolation of $P(C(O)\textit{i}Pr)_3$ (10)

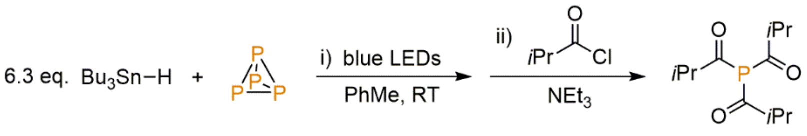

10

70% yield

To a 50 mL flat-bottomed Schlenk tube were added P_4 (62.0 mg, 0.5 mmol) and PhMe (25 mL). After stirring to obtain a homogeneous solution Bu_3SnH was added (847 µL, 3.15 mmol). The resulting colorless solution was stirred under irradiation with blue LED light (7X Osram OSLON SSL80, 455 nm (±15 nm), 20.3 V 1000mA) for 22 h, during which time the Schlenk tube was placed in a block cooled by circulating water to maintain near-ambient temperature. *i*PrC(O)Cl (838 µL, 8.0 mmol) and NEt_3 (418 µL, 3.0 mmol) were added, and the reaction mixture was stirred at room temperature for 16 h. The resulting light yellow suspension was evaporated to dryness, and the remaining solid was extracted with *n*-hexane (3 x 20 mL). The combined extracts were again evaporated to dryness, and the remaining residue was distilled under vacuum (*ca.* 45 °C, 10^{-5} mbar) to afford the desired product as a yellowish oil (341 mg, 70%).

^{1}H NMR (400 MHz, 300 K, C_6D_6): δ = 3.17 ppm (1H, septet, $^{3}J(^{1}\text{H-}^{1}\text{H})$ = 6.9 Hz), 1.03 ppm (6H, d, $^{3}J(^{1}\text{H-}^{1}\text{H})$ = 6.9 Hz).

^{31}P{^{1}H} NMR (121 MHz, 300 K, C_6D_6): δ = 54.1 ppm (s).

^{31}P NMR (121 MHz, 300 K, C_6D_6): δ = 54.1 ppm (s).

^{13}C{^{1}H} NMR (101 MHz, 300 K, C_6D_6): δ = 219.6 (d, $^{1}J(^{31}\text{P-}^{1}\text{H})$ = 49.6 Hz), 46.6 (d, $^{2}J(^{31}\text{P-}^{1}\text{H})$ = 31.1 Hz), 17.8 ppm (d, $^{3}J(^{31}\text{P-}^{1}\text{H})$ = 3.8 Hz).

MS (APCI, PhMe): m/z = 245.1304 ([M+H]$^{+}$).

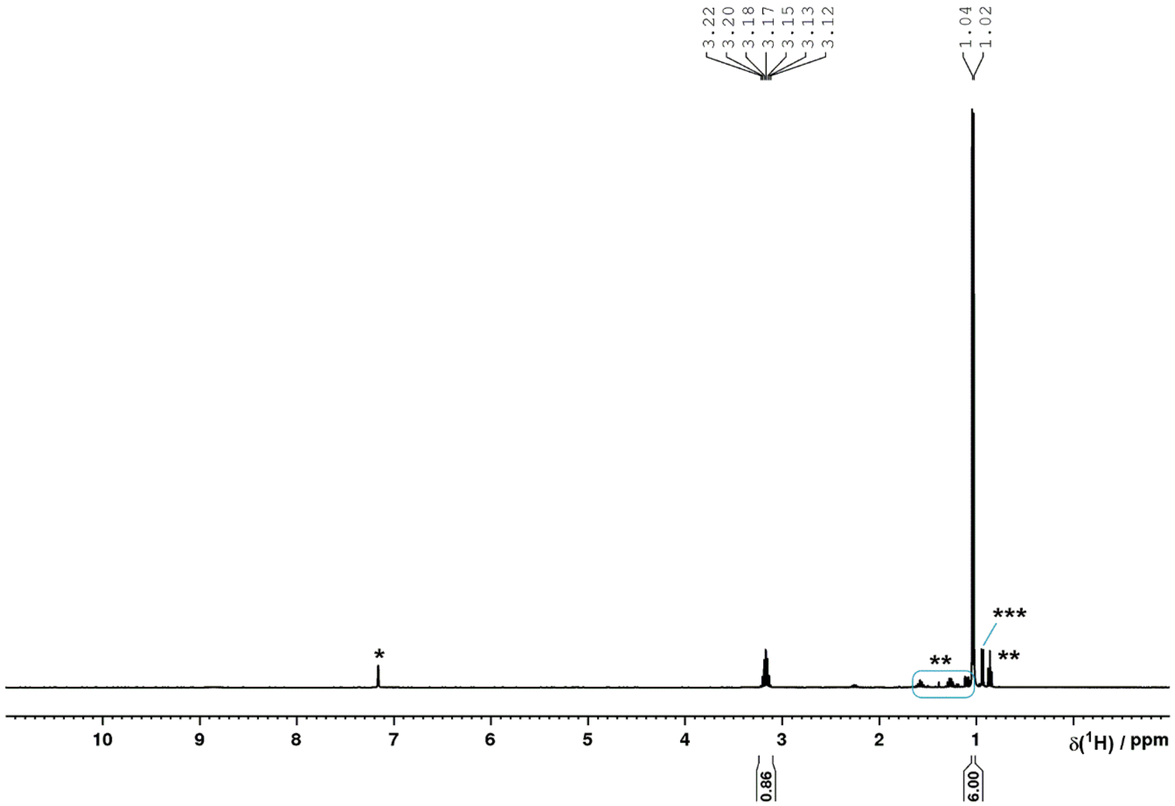

Supplementary Figure 74. ^{1}H NMR spectrum of P(C(O)*i*Pr)$_3$ (**10**) in C_6D_6 (*solvent, **minor Bu_3SnCl, ***unidentified minor impurity).

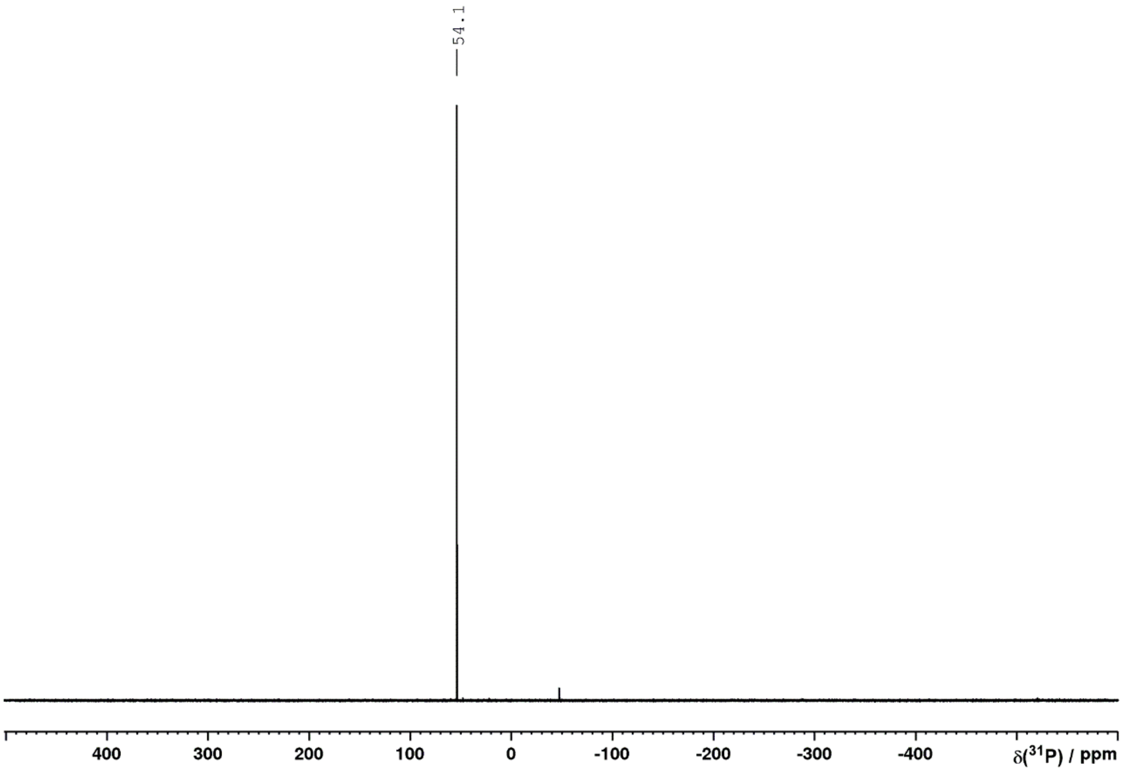

Supplementary Figure 75. $^{31}P\{^1H\}$ NMR spectrum of $P(C(O)iPr)_3$ (**10**) in C_6D_6.

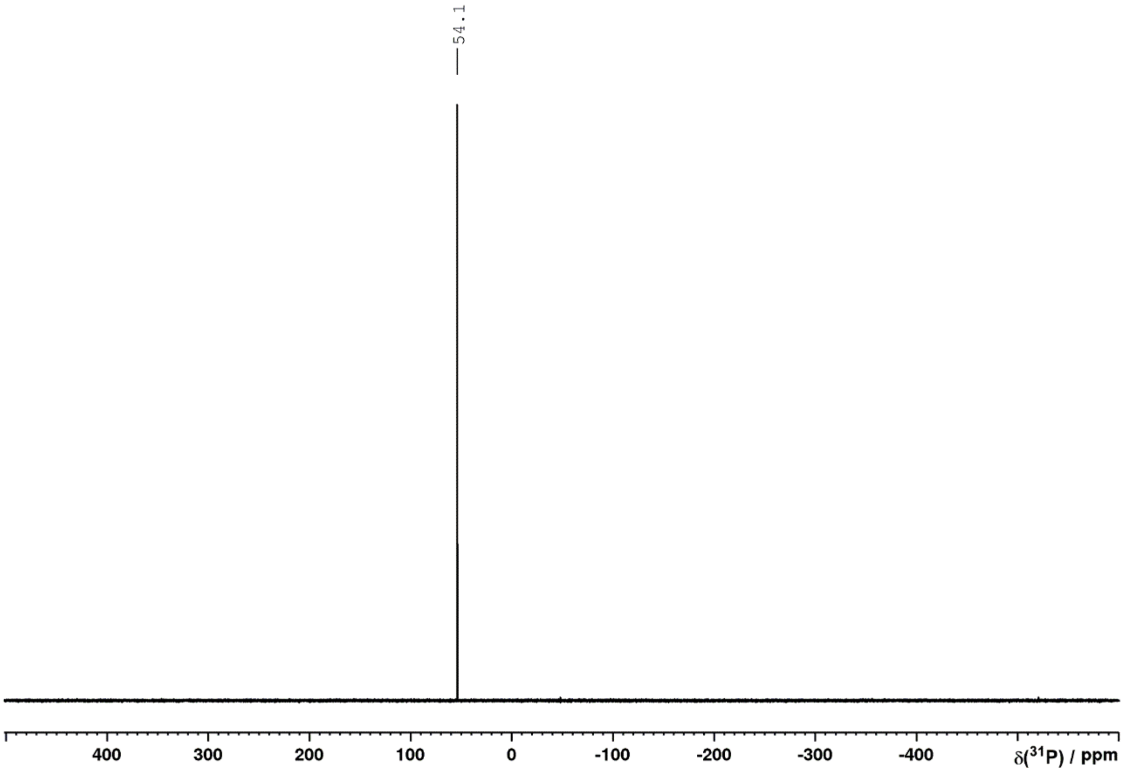

Supplementary Figure 76. ^{31}P NMR spectrum of $P(C(O)iPr)_3$ (**10**) in C_6D_6.

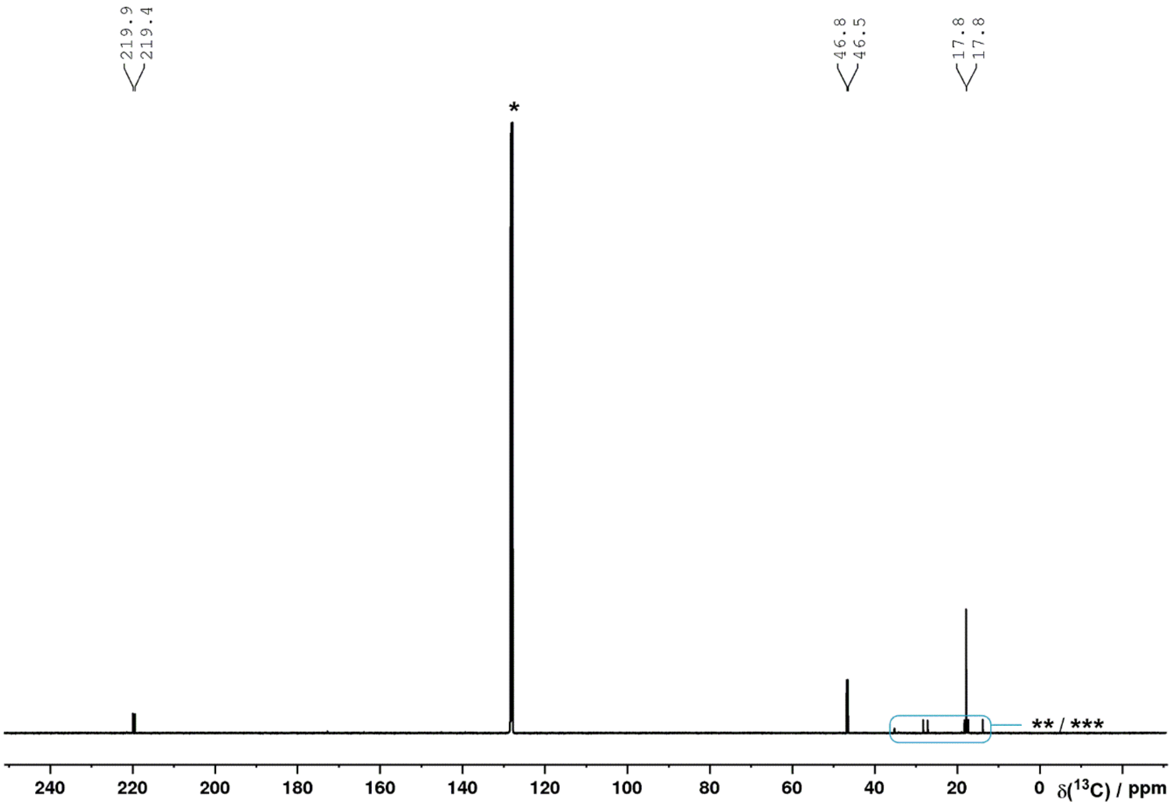

Supplementary Figure 77. $^{13}C\{^{1}H\}$ NMR spectrum of $P(C(O)\mathit{i}Pr)_3$ (**10**) in C_6D_6. Solvent resonance (*) truncated for clarity (**minor Bu_3SnCl, ***unidentified minor impurity).

Supplementary Method 21: Synthesis and quantification of $P(C(O)Cy)_3$ (11)

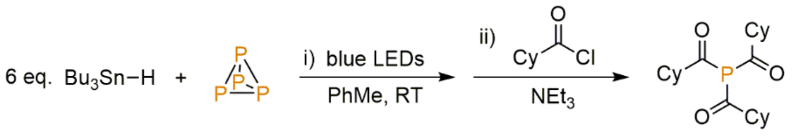

11

56% conversion

To a 10 mL, flat-bottomed, stoppered tube were added PhMe (500 µL), P_4 (0.01 mmol, as a stock solution in 77.4 µL PhH) and Bu_3SnH (16.1 µL, 0.06 mmol). The resulting colorless solution was stirred under irradiation with blue LED light (455 nm (±15 nm), 3.2 V, 700 mA, Osram OSLON SSL 80) for 18 h, during which time the tube was placed in a block cooled by circulating water to maintain near-ambient temperature. CyC(O)Cl (21.4 µL, 0.16 mmol) and Et_3N (8.4 µL, 0.06 mmol) were added, and the reaction mixture was stirred at room temperature for 16 h. Ph_3PO (13.1 mg, 0.047 mmol) was added, and the resulting mixture was analysed by ^{1}H, ^{31}P{^{1}H} and ^{31}P NMR spectroscopy (Supplementary Figures 78-80). Conversion to P(C(O)Cy)$_3$ (56%) was determined using quantitative ^{31}P{^{1}H} spectroscopy (D1 = 22 s, Supplementary Figure 81), by relative integration of the resonances assigned to Ph$_3$PO and P(C(O)Cy)$_3$.

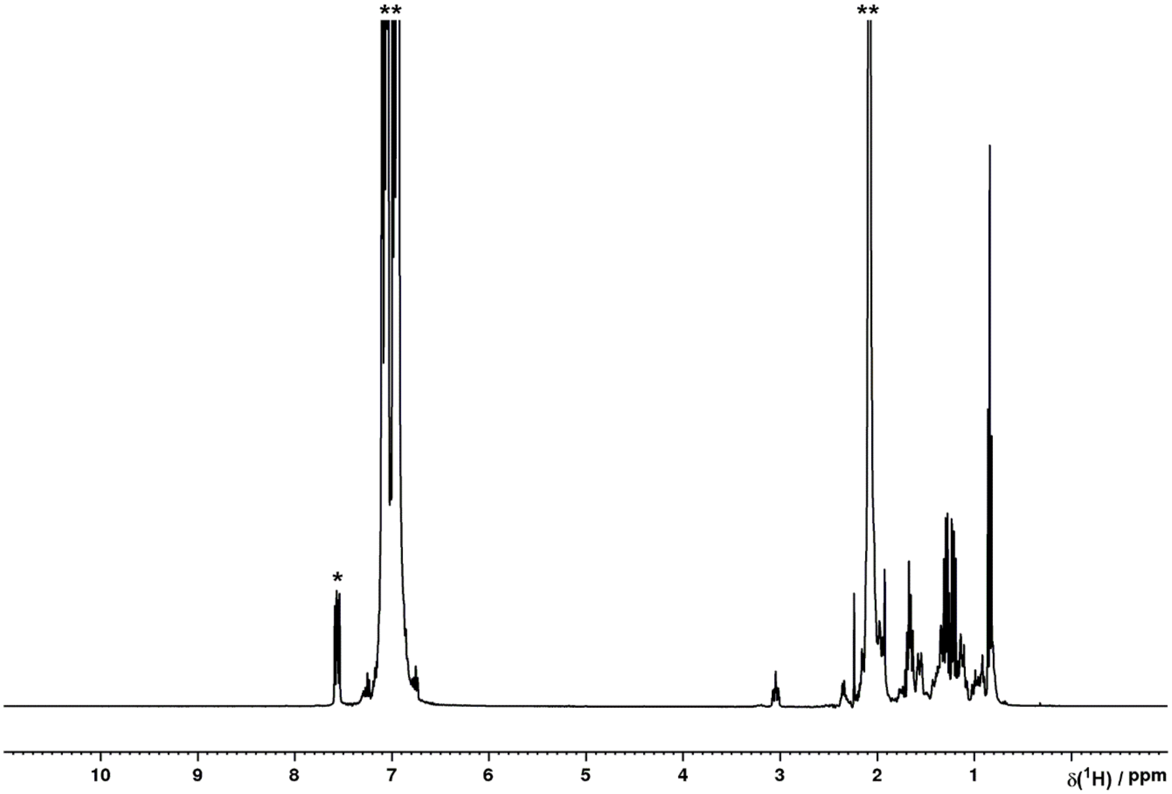

Supplementary Figure 78. ^{1}H NMR spectrum of P(C(O)Cy)$_3$ (**11**) generated *via* hydrostannylation of P$_4$ in PhMe followed by acylation, in the presence of Ph$_3$PO (*) as an internal standard. Solvent resonances (**) truncated for clarity.

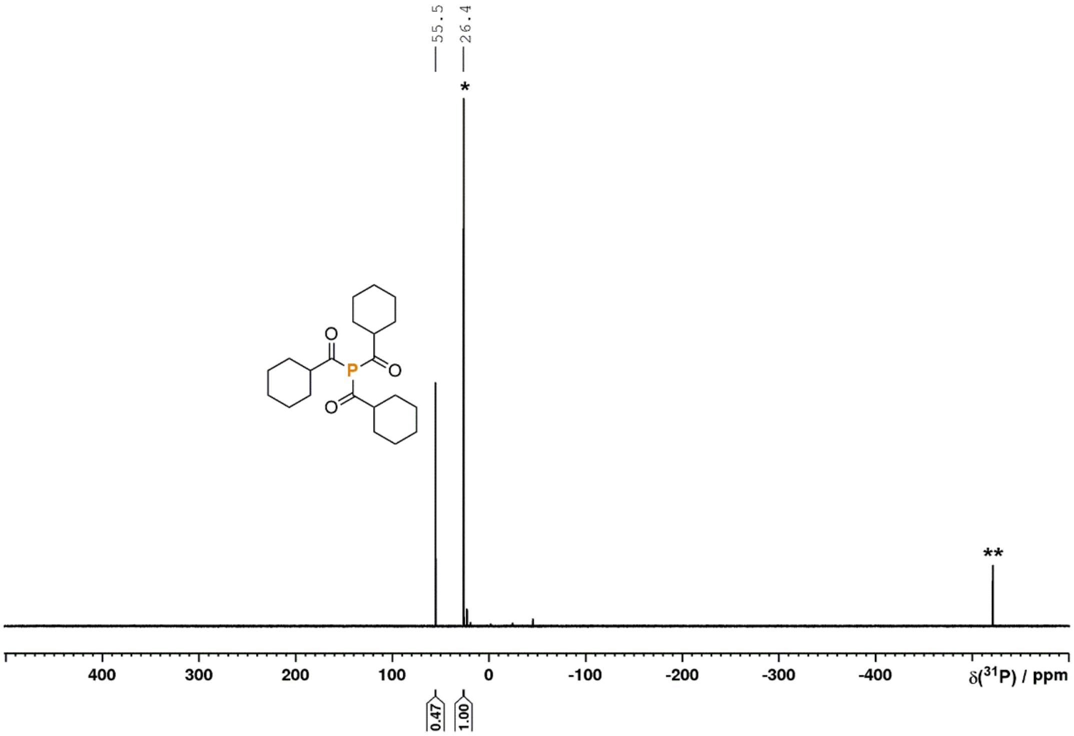

Supplementary Figure 79. $^{31}P\{^1H\}$ NMR spectrum of $P(C(O)Cy)_3$ (**11**) generated *via* hydrostannylation of P_4 in PhMe followed by acylation, in the presence of Ph_3PO (*) as internal standard (**minor residual P_4).

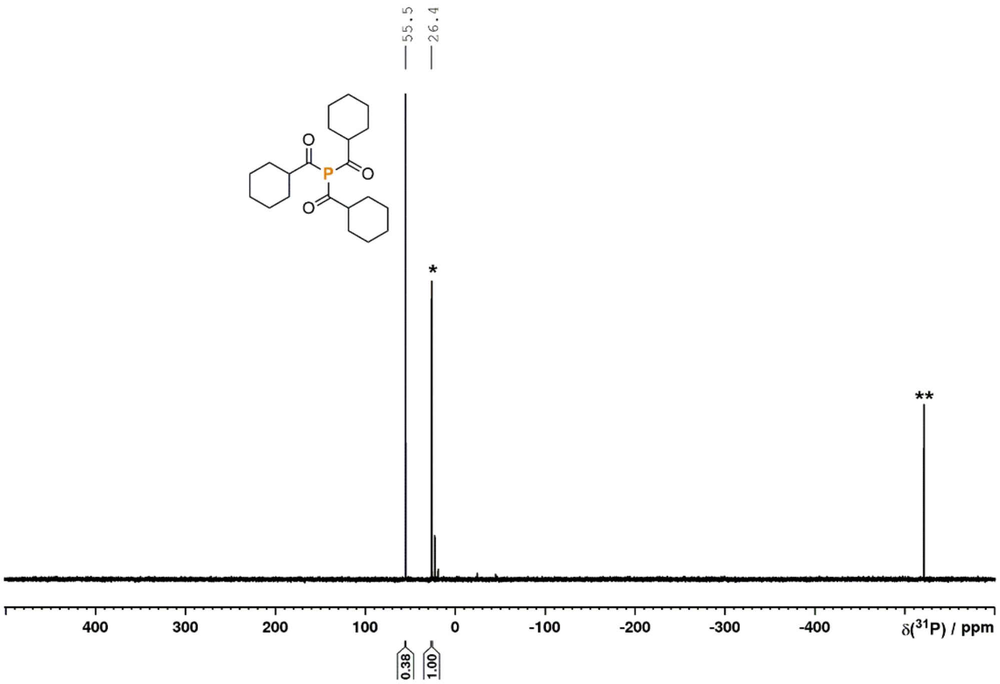

Supplementary Figure 80. ^{31}P NMR spectrum of $P(C(O)Cy)_3$ (**11**) generated *via* hydrostannylation of P_4 in PhMe followed by acylation, in the presence of Ph_3PO (*) as an internal standard (**minor residual P_4).

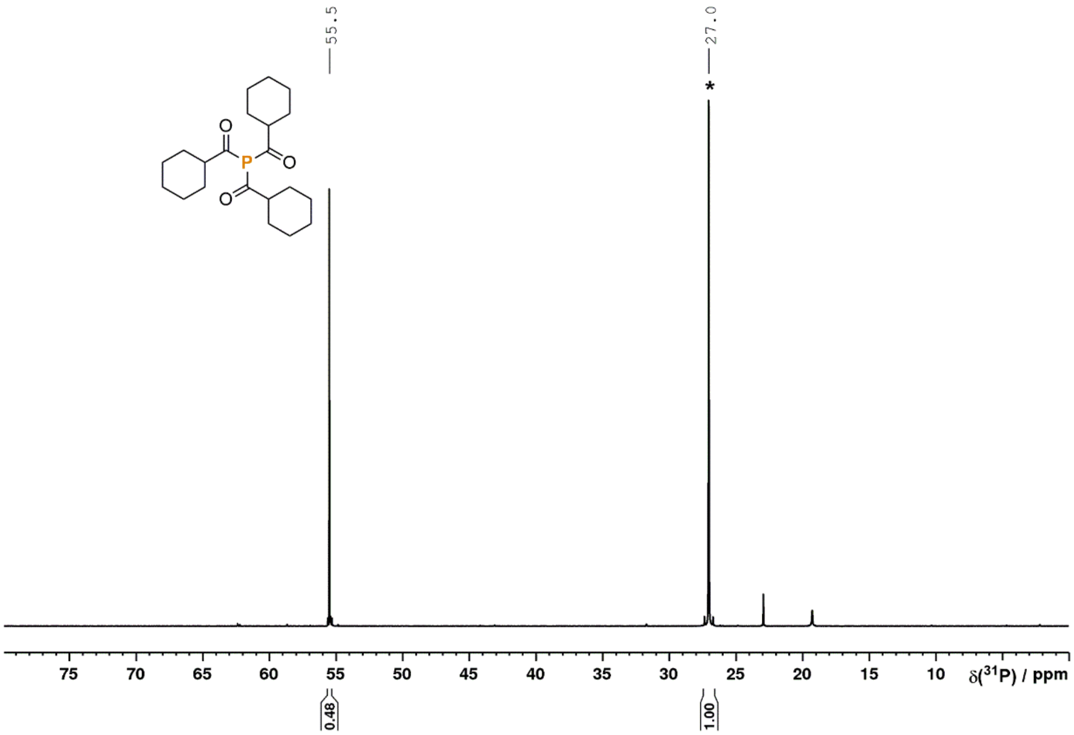

Supplementary Figure 81. Quantitative ^{31}P{^{1}H} NMR spectrum (D1 = 22 s) of P(C(O)Cy)$_3$ (**11**) generated *via* hydrostannylation of P_4 in PhMe followed by acylation, in the presence of Ph_3PO (*) as an internal standard.

Supplementary Method 22: Synthesis and quantification of P(C(O)Bu)$_3$ (12)

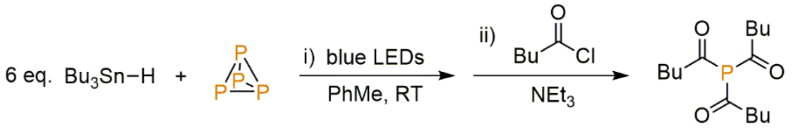

12

43% conversion

To a 10 mL, flat-bottomed, stoppered tube were added PhMe (500 µL), P_4 (0.01 mmol, as a stock solution in 77.4 µL PhH) and Bu_3SnH (16.1 µL, 0.06 mmol). The resulting colorless solution was stirred under irradiation with blue LED light (455 nm (±15 nm), 3.2 V, 700 mA, Osram OSLON SSL 80) for 18 h, during which time the tube was placed in a block cooled by circulating water to maintain near-ambient temperature. BuC(O)Cl (19.0 µL, 0.16 mmol) and Et_3N (8.4 µL, 0.06 mmol) were added, and the reaction mixture was stirred at room temperature for 16 h. Ph_3PO (13.0 mg, 0.047 mmol) was added, and the resulting mixture was analysed by ^{1}H, ^{31}P{^{1}H} and ^{31}P NMR spectroscopy (Supplementary Figures 82-84).

Conversion to $P(C(O)Bu)_3$ (43%) was determined using quantitative $^{31}P\{^1H\}$ spectroscopy (D1 = 22 s, Supplementary Figure 85), by relative integration of the resonances assigned to Ph_3PO and $P(C(O)Bu)_3$.

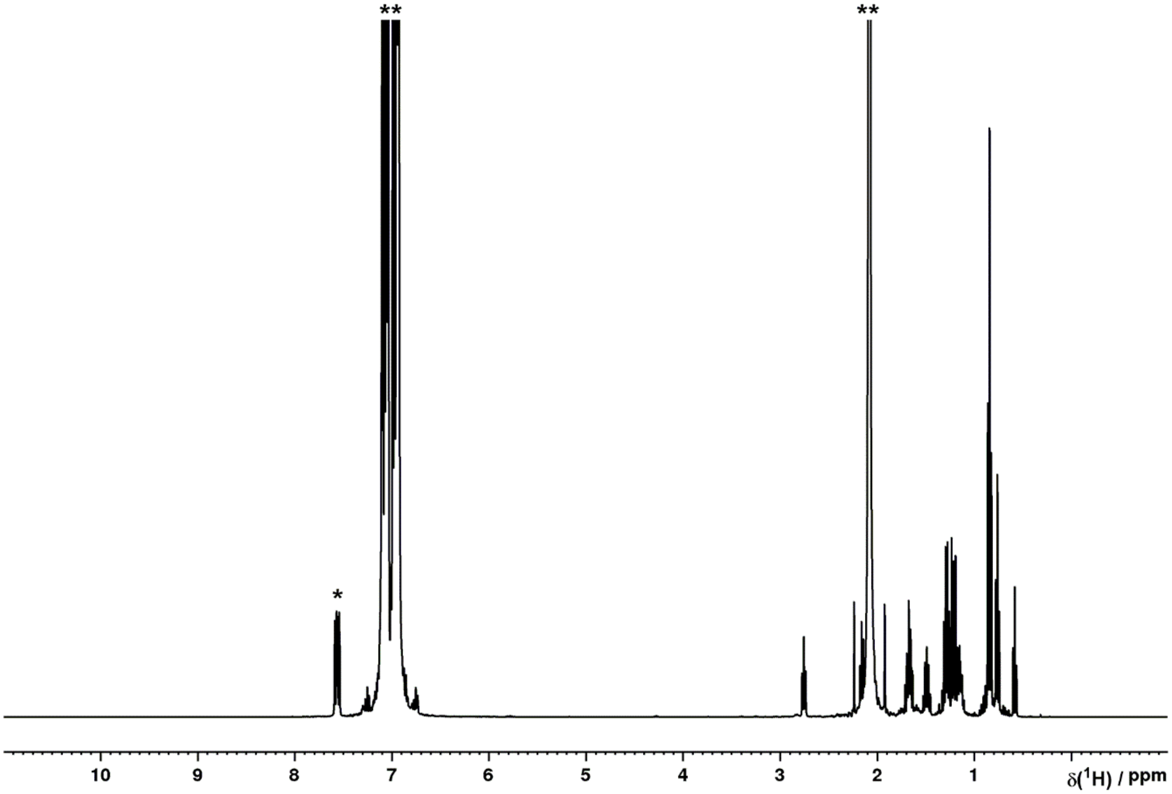

Supplementary Figure 82. ^1H NMR spectrum of $P(C(O)Bu)_3$ (**12**) generated *via* hydrostannylation of P_4 in PhMe followed by acylation, in the presence of Ph_3PO (*) as an internal standard. Solvent resonances (**) truncated for clarity.

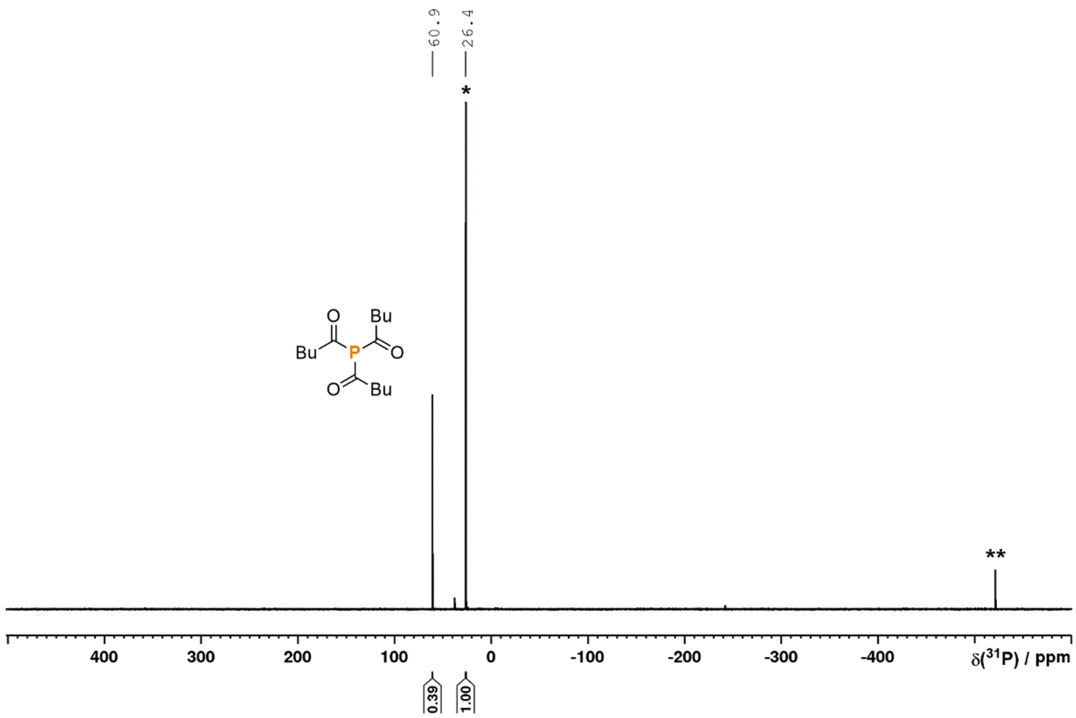

Supplementary Figure 83. $^{31}P\{^{1}H\}$ NMR spectrum of $P(C(O)Bu)_3$ (**12**) generated *via* hydrostannylation of P_4 in PhMe followed by acylation, in the presence of Ph_3PO (*) as internal standard (**minor residual P_4).

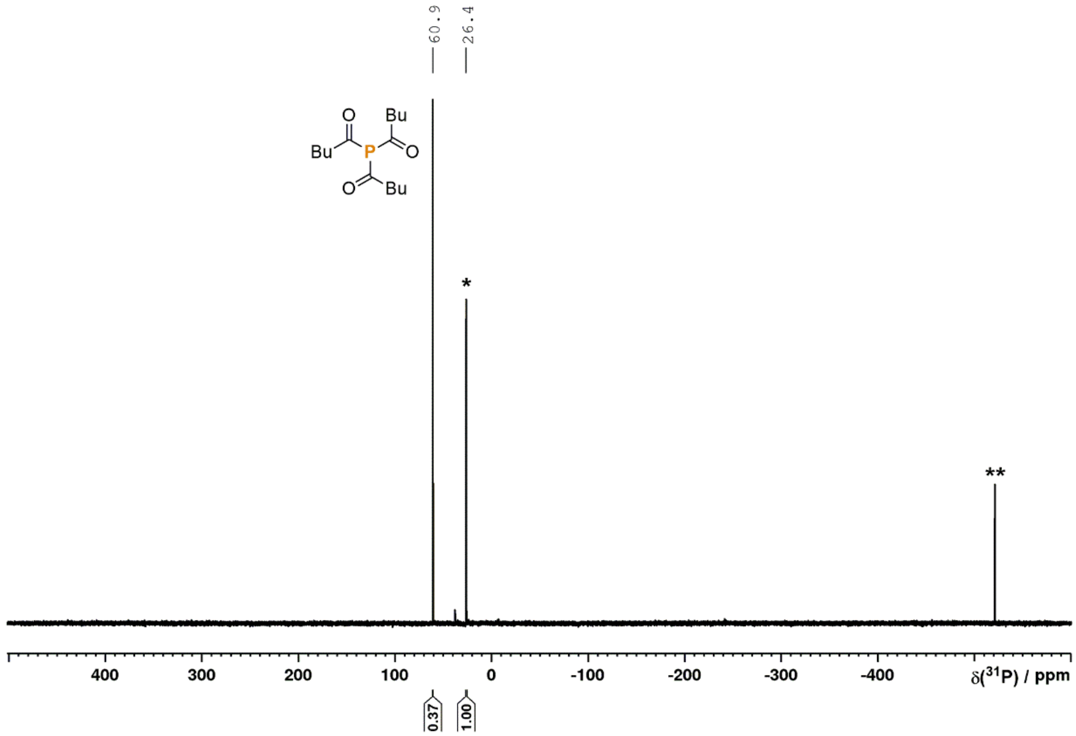

Supplementary Figure 84. ^{31}P NMR spectrum of $P(C(O)Bu)_3$ (**12**) generated *via* hydrostannylation of P_4 in PhMe followed by acylation, in the presence of Ph_3PO (*) as an internal standard (**minor residual P_4).

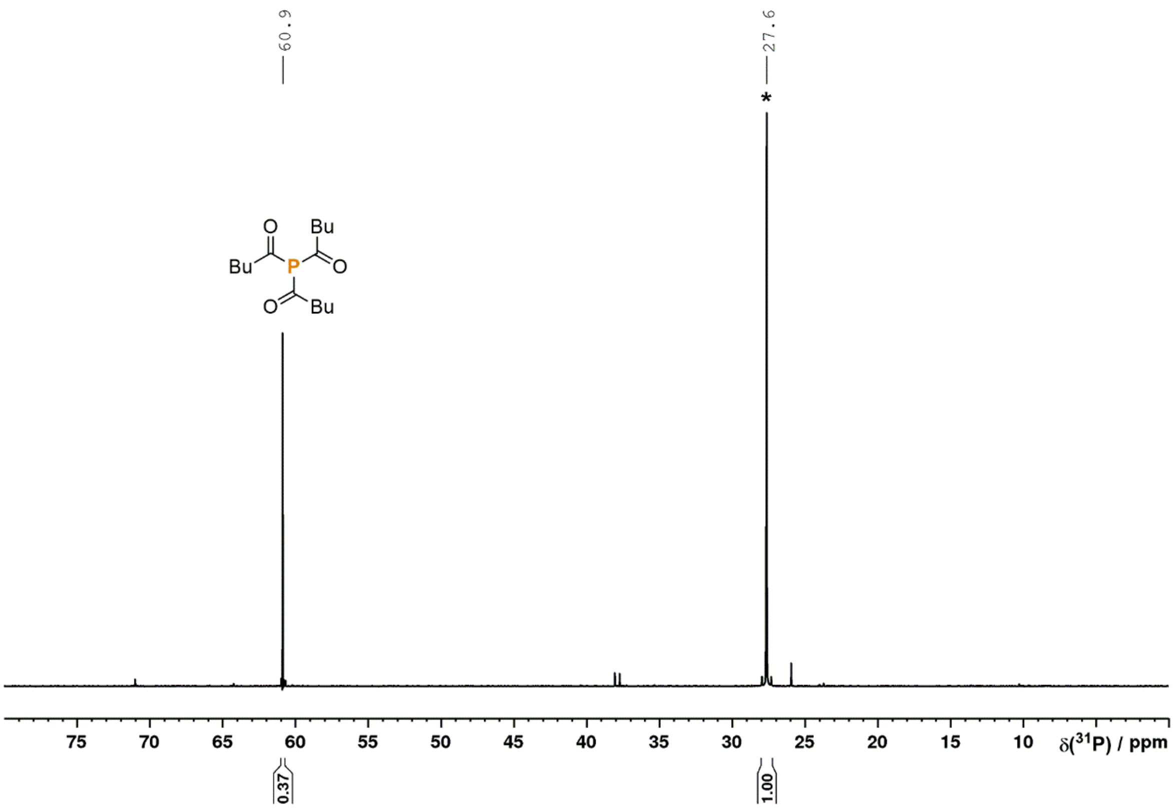

Supplementary Figure 85. Quantitative $^{31}P\{^{1}H\}$ NMR spectrum (D1 = 22 s) of $P(C(O)Bu)_3$ (**12**) generated *via* hydrostannylation of P_4 in PhMe followed by acylation, in the presence of Ph_3PO (*) as an internal standard.

Supplementary Method 23: Synthesis and quantification of $P(C(O)Me)_3$ (13)

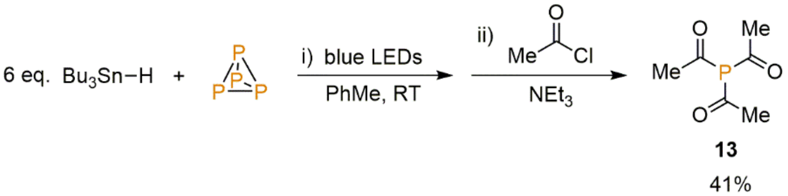

13
41%
conversion

To a 10 mL, flat-bottomed, stoppered tube were added PhMe (500 µL), P_4 (0.01 mmol, as a stock solution in 77.4 µL PhH) and Bu_3SnH (16.1 µL, 0.06 mmol). The resulting colorless solution was stirred under irradiation with blue LED light (455 nm (±15 nm), 3.2 V, 700 mA, Osram OSLON SSL 80) for 18 h, during which time the tube was placed in a block cooled by circulating water to maintain near-ambient temperature. MeC(O)Cl (11.4 µL, 0.16 mmol) and Et_3N (8.4 µL, 0.06 mmol) were added, and the reaction mixture was stirred at room temperature for 16 h. Ph_3PO (10.6 mg, 0.038 mmol) was added, and the resulting mixture was analysed by ^{1}H, ^{31}P{^{1}H} and ^{31}P NMR spectroscopy (Supplementary Figures 86-88). Conversion to P(C(O)Me)$_3$ (41%) was determined using quantitative ^{31}P{^{1}H} spectroscopy (D1 = 22 s, Supplementary Figure 89), by relative integration of the resonances assigned to Ph$_3$PO and P(C(O)Me)$_3$.

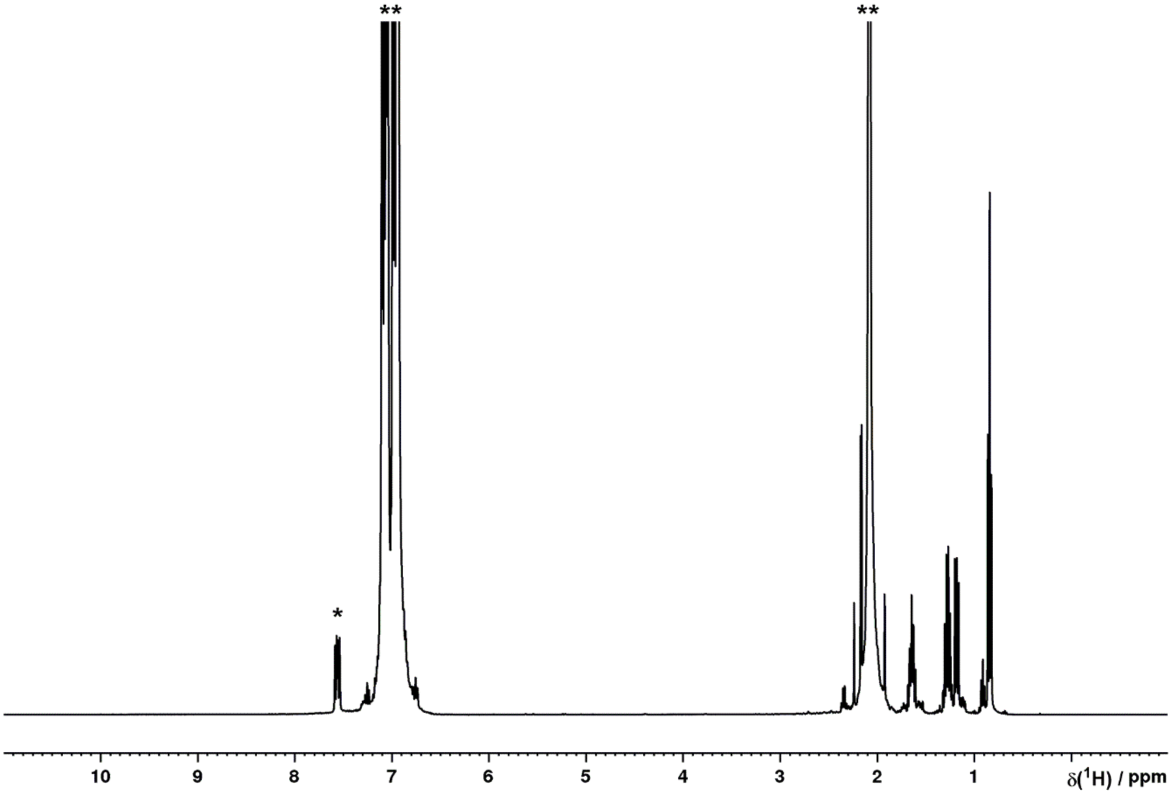

Supplementary Figure 86. ^{1}H NMR spectrum of P(C(O)Me)$_3$ (**13**) generated *via* hydrostannylation of P$_4$ in PhMe followed by acylation, in the presence of Ph$_3$PO (*) as an internal standard. Solvent resonances (**) truncated for clarity.

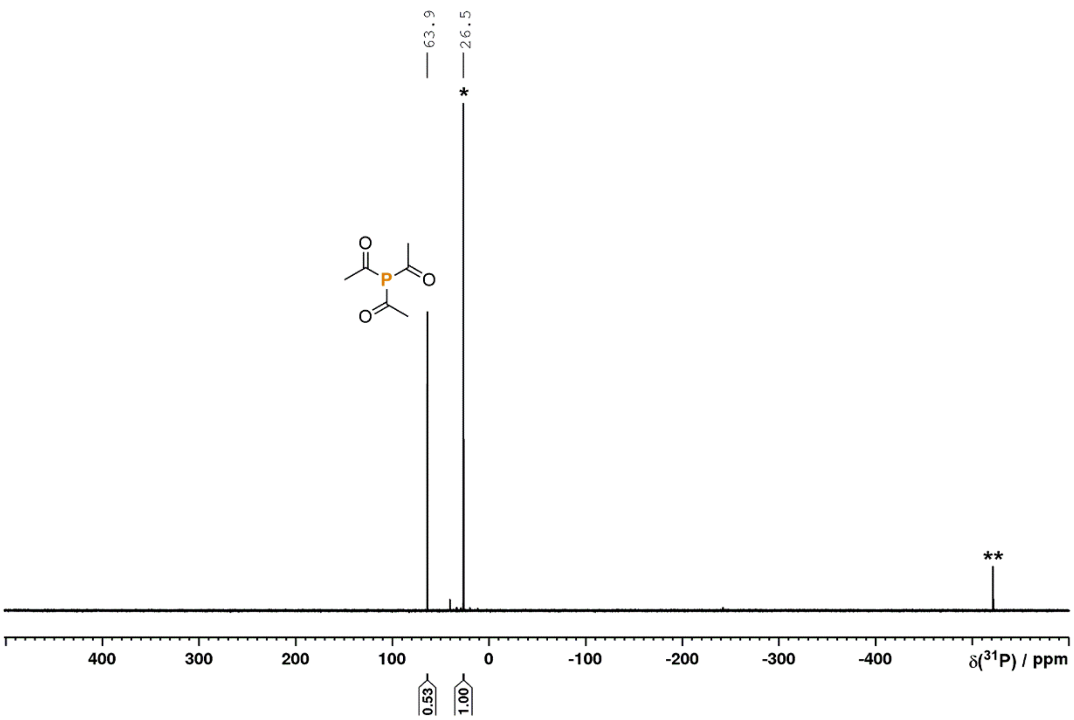

Supplementary Figure 87. $^{31}P\{^1H\}$ NMR spectrum of $P(C(O)Me)_3$ (**13**) generated *via* hydrostannylation of P_4 in PhMe followed by acylation, in the presence of Ph_3PO (*) as internal standard (**minor residual P_4).

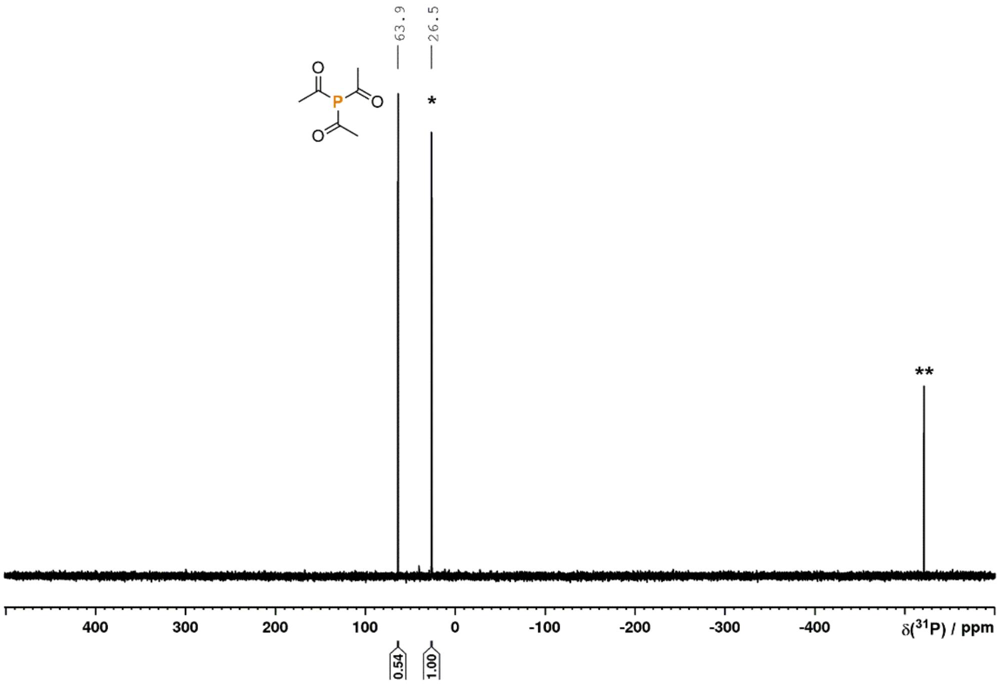

Supplementary Figure 88. ^{31}P NMR spectrum of $P(C(O)Me)_3$ (**13**) generated *via* hydrostannylation of P_4 in PhMe followed by acylation, in the presence of Ph_3PO (*) as an internal standard (**minor residual P_4).

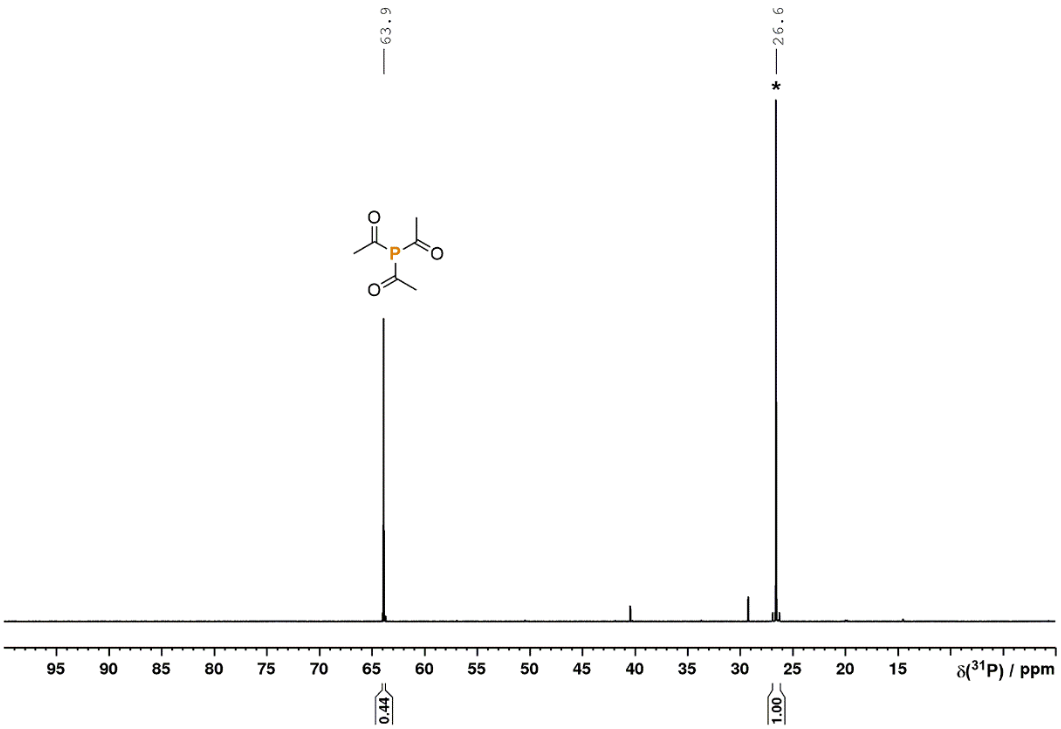

Supplementary Figure 89. Quantitative $^{31}P\{^{1}H\}$ NMR spectrum (D1 = 22 s) of $P(C(O)Me)_3$ (**13**) generated *via* hydrostannylation of P_4 in PhMe followed by acylation, in the presence of Ph_3PO (*) as an internal standard.

Supplementary Method 24: Synthesis and isolation of [Bn$_4$P]Br (14) (without KHMDS)

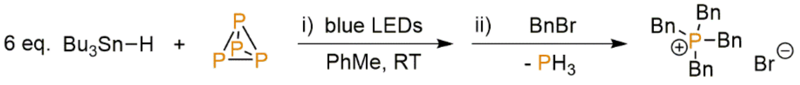

14

80% yield

To a 50 mL flat-bottomed Schlenk were added P_4 (62.0 mg, 0.5 mmol) and PhMe (25 mL). After stirring to obtain a homogeneous solution Bu_3SnH was added (847 µL, 3.15 mmol). The resulting colorless solution was stirred under irradiation with blue LED light (7X Osram OSLON SSL80, 455 nm (±15 nm), 20.3 V 1000mA) for 22 h, during whichch time the Schlenk tube was placed in a block cooled by circulating water to maintain near-ambient temperature. Benzyl bromide (2.4 mL, 20 mmol) was added and the reaction mixture heated to 60 °C with stirring for 3 days. After cooling to room temperature the pale yellow suspension was evaporated to dryness, and the resulting solid was washed with pentane (2 x 20 mL) and extracted with acetone (4 x 15 mL ; undried, 'bench' acetone was used). Removal of volatiles under vacuum yielded the target product as a white solid (380 mg, 80%).

^{1}H NMR (400 MHz, 300 K, CD_3CN) : δ = 7.36 ppm (3H, m), 7.15 ppm (2H, m), 3.73 ppm (d, $^2J(^{31}P-^1H)$ = 14.3 Hz).

$^{31}P\{^1H\}$ NMR (121 MHz, 300 K, CD_3CN) : δ = 25.8 ppm (s).

^{31}P NMR (121 MHz, 300 K, CD_3CN) : δ = 25.8 ppm (nonet, $^2J(^{31}P-^1H)$ = 14.3 Hz).

$^{13}C\{^1H\}$ NMR (101 MHz, 300 K, C_6D_6): δ = 130.7 (d, $J(^{31}P-^1H)$ = 5.3 Hz), 129.3 (d, $J(^{31}P-^1H)$ = 2.9 Hz), 128.4 (d, $J(^{31}P-^1H)$ = 3.5 Hz), 127.8 (d, $J(^{31}P-^1H)$ = 8.1 Hz), 26.4 ppm (d, $J(^{31}P-^1H)$ = 43.2 Hz).

MS (ESI, MeCN): *m/z* = 395.1940 (PBn_4^+).

NMR data are consistent with previous reports of the chloride salt $[Bn_4P]Cl$.[20]

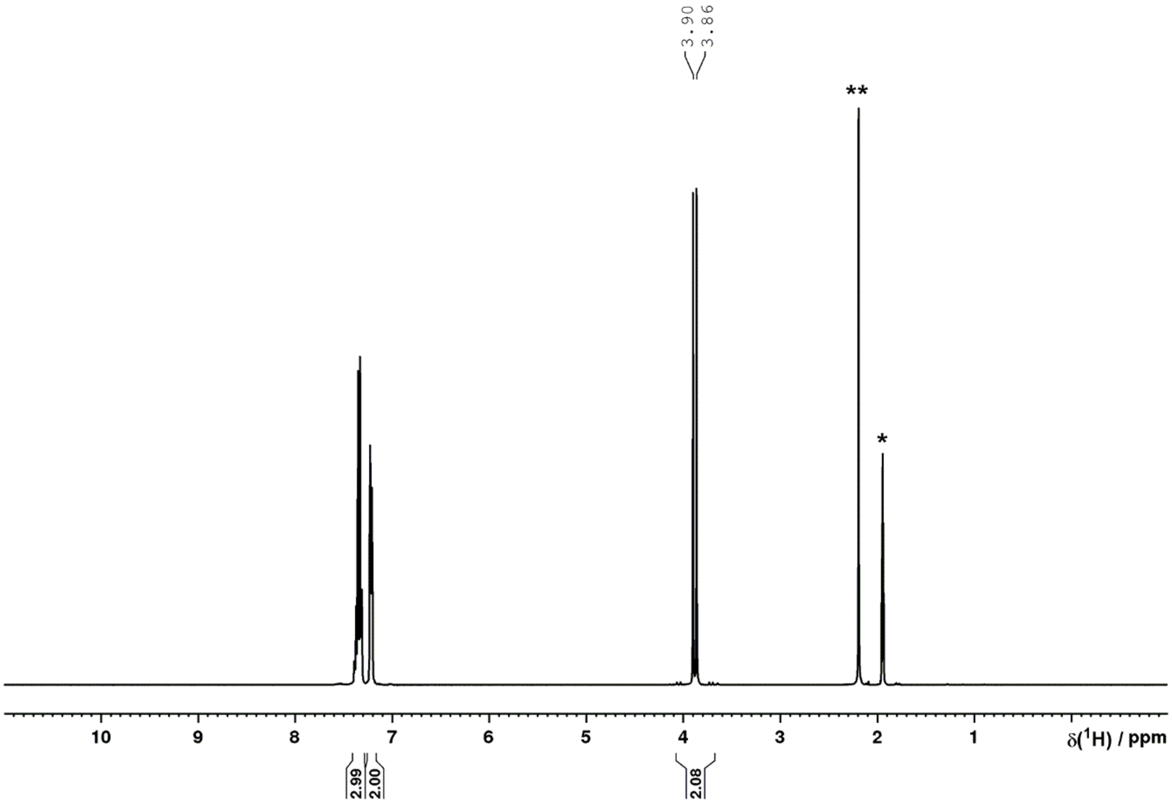

Supplementary Figure 90. ^{1}H NMR spectrum of $[Bn_4P]Br$ (**14**) in CD_3CN (*solvent, **H_2O).

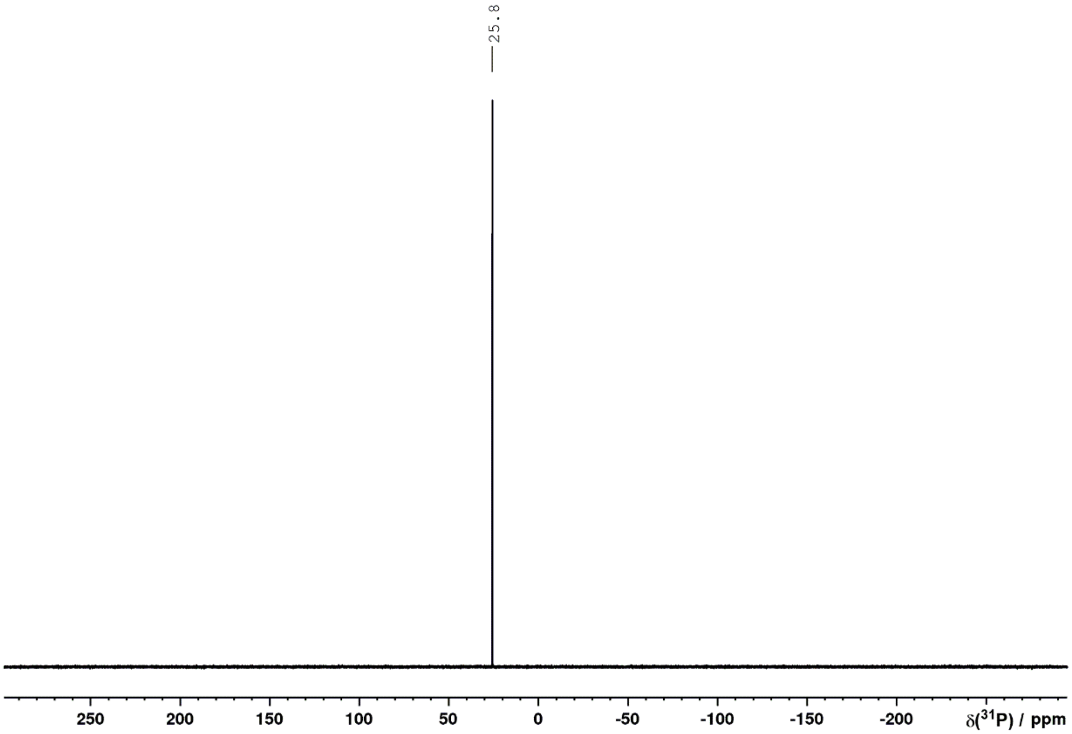

Supplementary Figure 91. $^{31}P\{^1H\}$ NMR spectrum of [Bn$_4$P]Br (**14**) in CD_3CN.

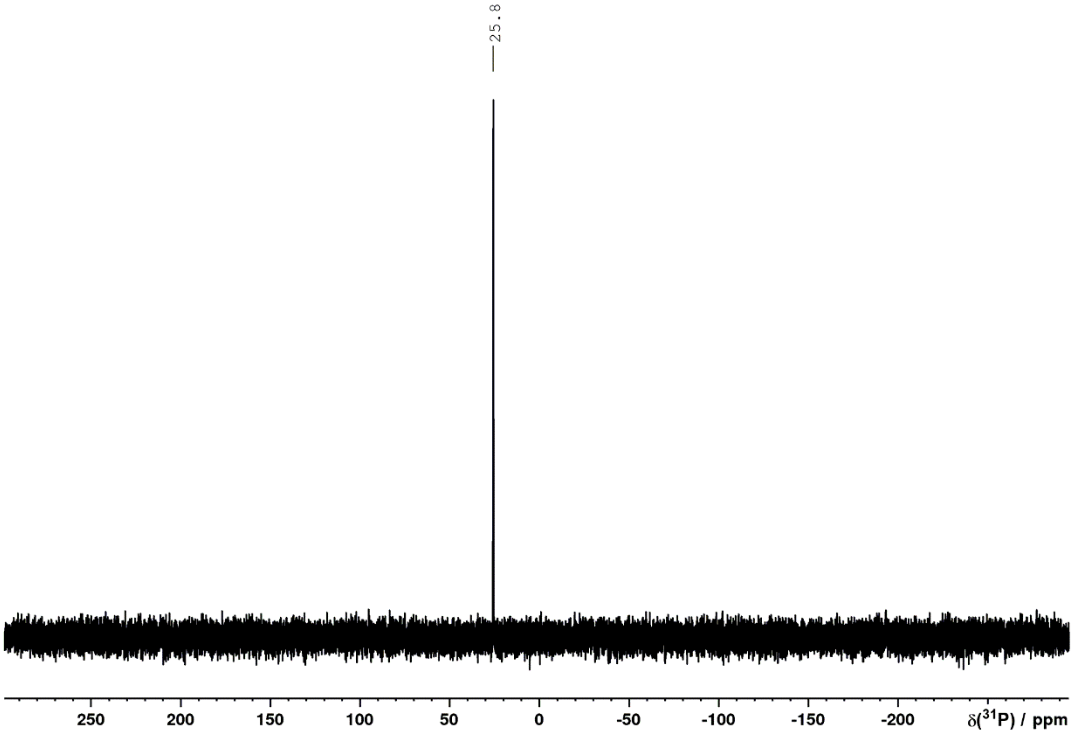

Supplementary Figure 92. ^{31}P NMR spectrum of [Bn$_4$P]Br (**14**) in CD_3CN.

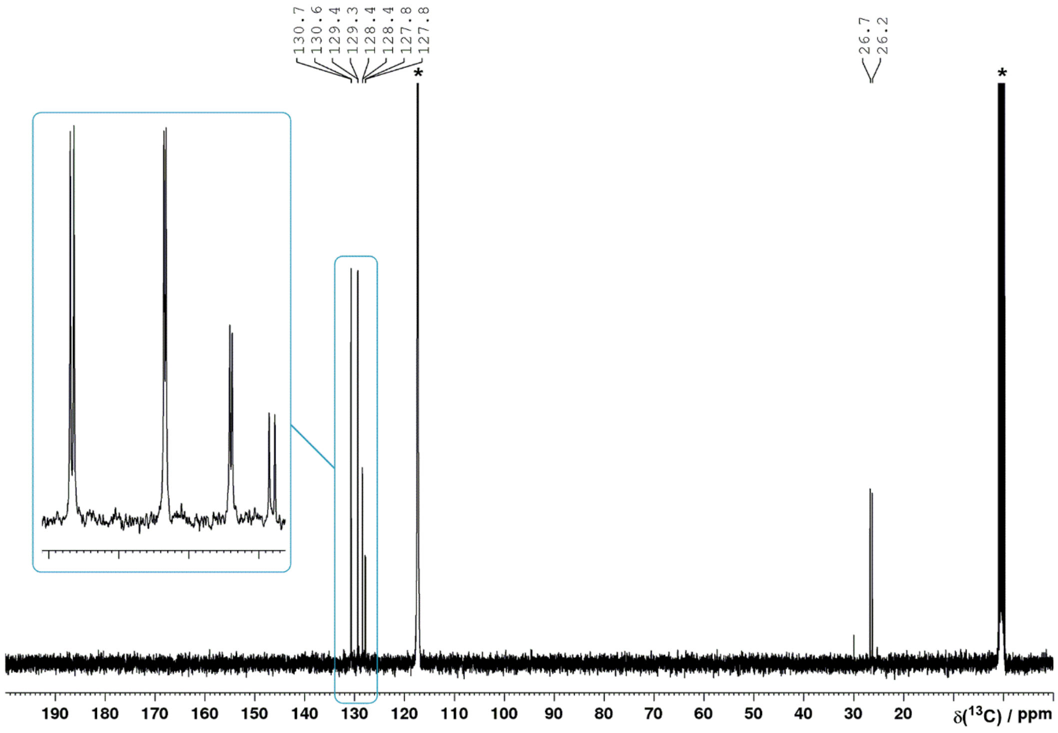

Supplementary Figure 93. $^{13}C\{^1H\}$ NMR spectrum of $[Bn_4P]Br$ (**14**) in CD_3CN. Solvent resonances (*) truncated for clarity.

Supplementary Method 25: Synthesis and isolation of $[Et_4P]Br$ (15)

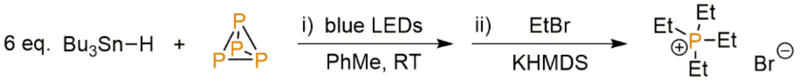

15

65% yield

To a 50 mL flat-bottomed Schlenk were added P_4 (62.0 mg, 0.5 mmol) and PhMe (25 mL). After stirring to obtain a homogeneous solution Bu_3SnH was added (847 µL, 3.15 mmol). The resulting colorless solution was stirred under irradiation with blue LED light (7X Osram OSLON SSL80, 455 nm (±15 nm), 20.3 V 1000mA) for 22 h, during which time the Schlenk tube was placed in a block cooled by circulating water to maintain near-ambient temperature. Ethyl bromide (741 µL, 10 mmol) and KHMDS (798 mg, 4.0 mmol) were added and the reaction mixture heated to 100 °C with stirring for 3 days. After cooling to room temperature the pale yellow suspension was filtered, and the remaining solid was washed with PhMe (2 x 20 mL) and extracted into acetonitrile (3 x 20 mL). Removal of volatiles under vacuum yielded the target product as a white solid (295 mg, 65%).

^{1}H NMR (400 MHz, 300 K, CD_3CN) : δ = 2.21 ppm (2H, dq, $^1J(^{31}P-^1H)$ = 13.0 Hz, $^3J(^1H-^1H)$ = 7.7 Hz), 1.19 ppm (3H, dt, $^2J(^{31}P-^1H)$ = 18.0 Hz, $^3J(^1H-^1H)$ = 7.7 Hz).

$^{31}P\{^1H\}$ NMR (121 MHz, 300 K, CD_3CN) : δ = 42.3 ppm (s).

^{31}P NMR (121 MHz, 300 K, CD_3CN) : δ = 42.3 ppm (m).

$^{13}C\{^1H\}$ NMR (101 MHz, 300 K, C_6D_6): δ = 11.7 (d, $^1J(^{31}P-^1H)$ = 49.6 Hz), 5.7 ppm (d, $^2J(^{31}P-^1H)$ = 5.3 Hz).

MS (ESI, MeCN): *m*/*z* = 147.1295 (Et_4P^+).

NMR data are consistent with previous reports of $[Et_4P][BAr^F_4]$ (Ar^F = 3,5-bis(trifluoromethyl)phenyl).[21]

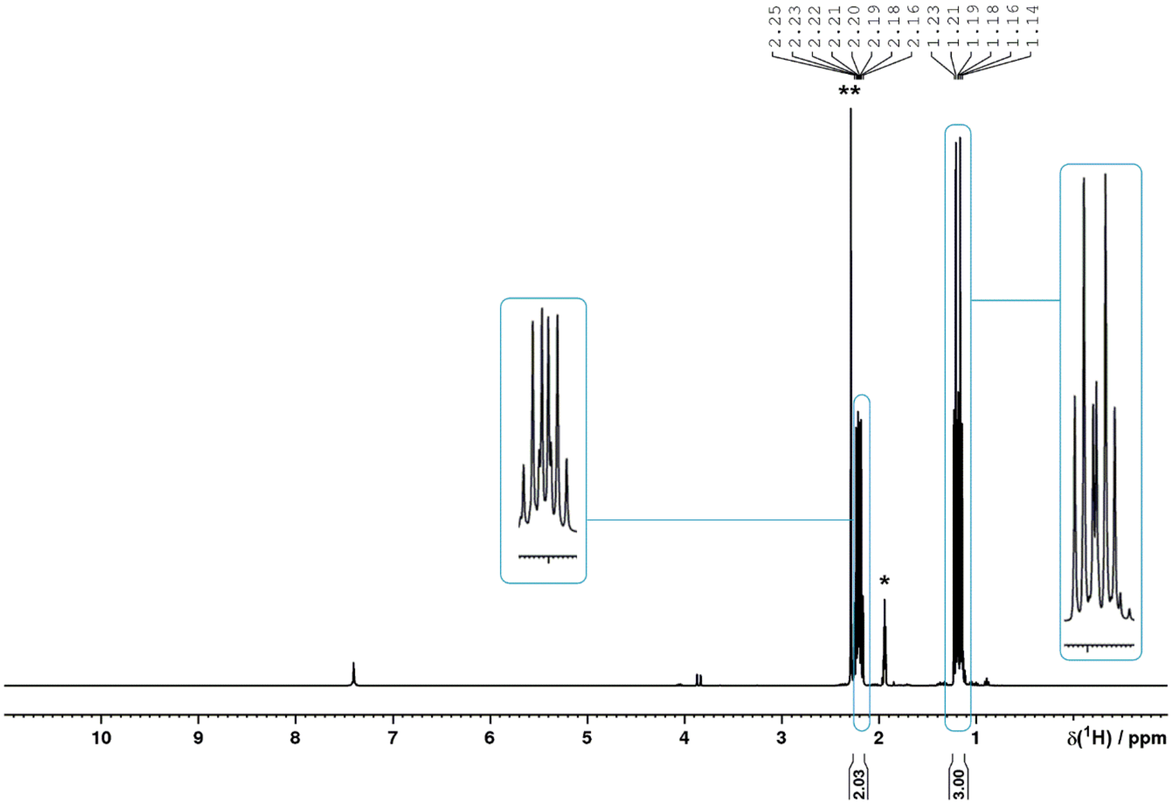

Supplementary Figure 94. ^{1}H NMR spectrum of $[Et_4P]Br$ (**15**) in CD_3CN (*solvent, **H_2O).

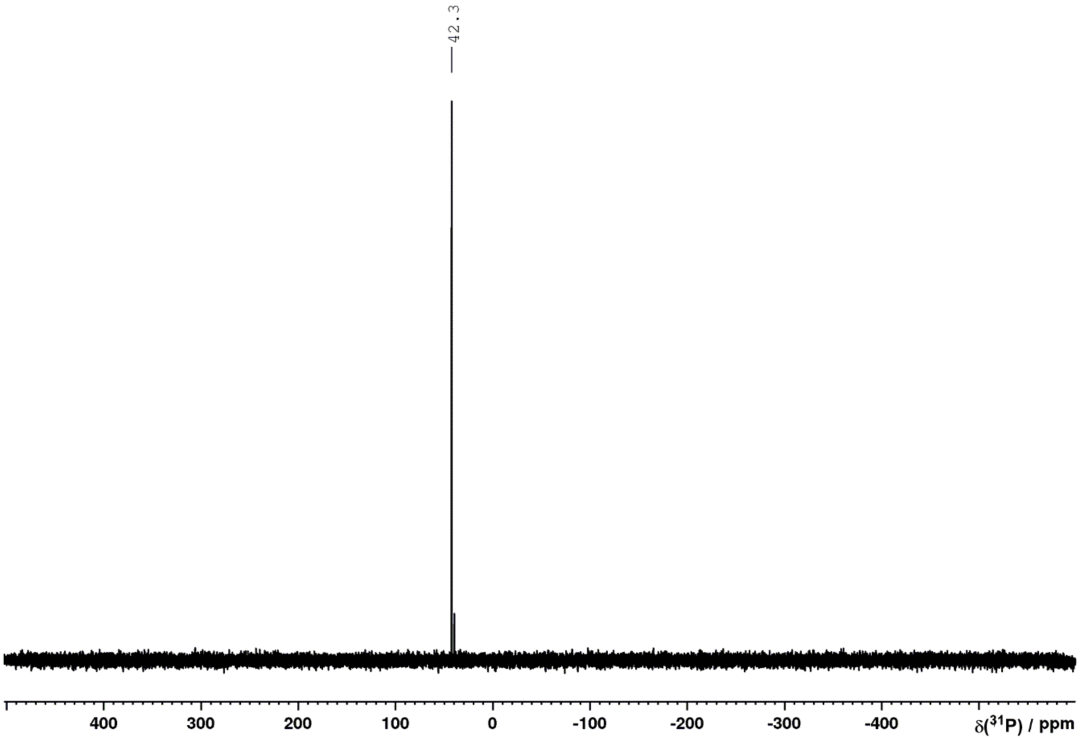

Supplementary Figure 95. $^{31}P\{^1H\}$ NMR spectrum of [Et_4P]Br (**15**) in CD_3CN.

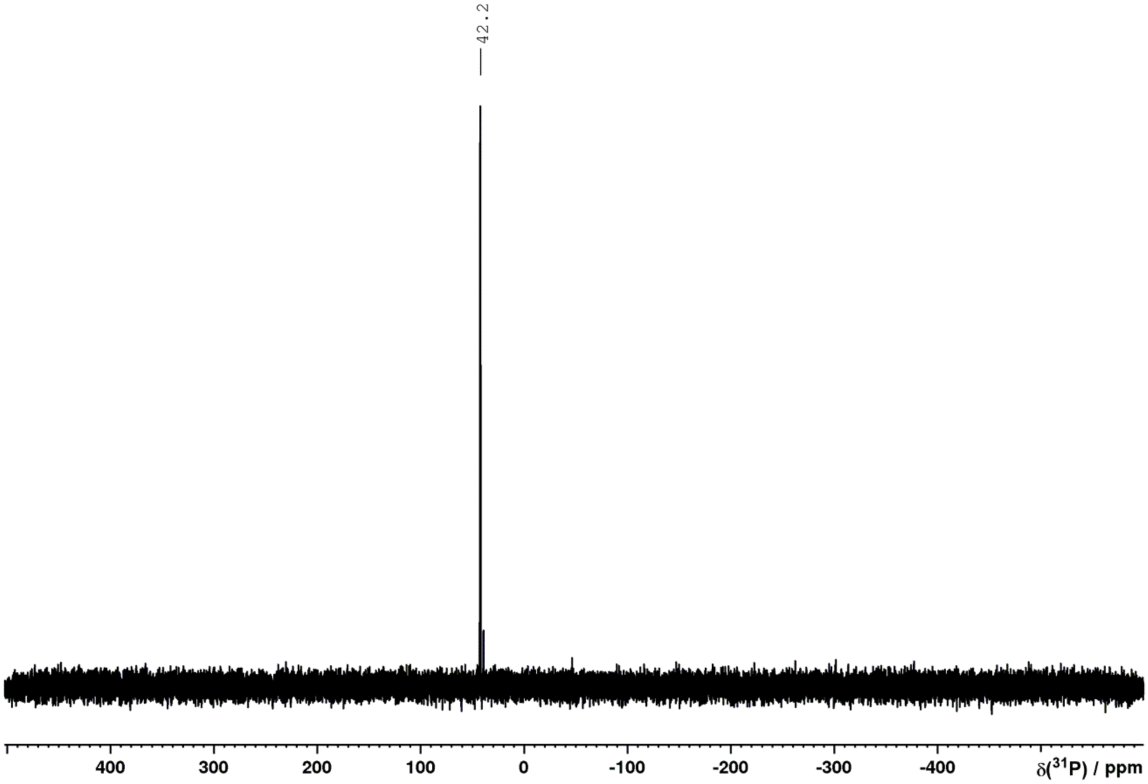

Supplementary Figure 96. ^{31}P NMR spectrum of [Et_4P]Br (**15**) in CD_3CN.

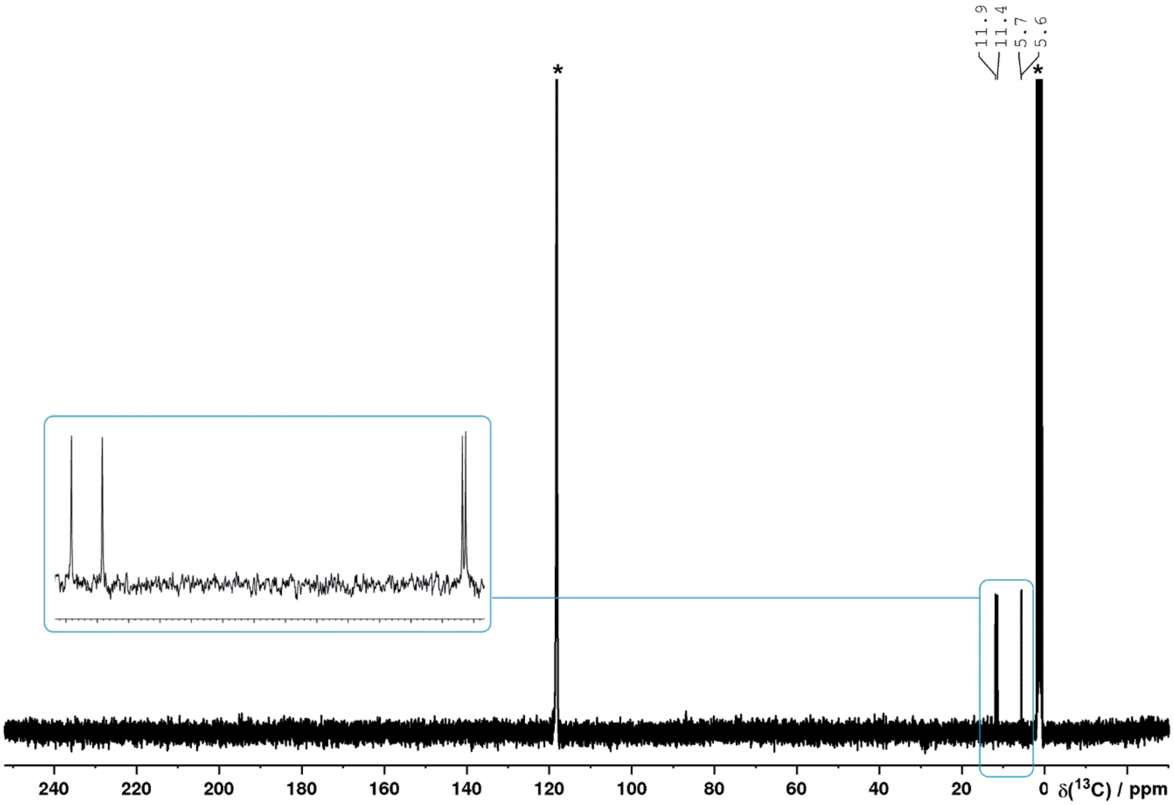

Supplementary Figure 97. ^{13}C{^{1}H} NMR spectrum of [Et$_4$P]Br (**15**) in CD$_3$CN. Solvent resonances (*) truncated for clarity.

Supplementary Method 26: Alkylation of (Bu$_3$Sn)$_x$PH$_{3-x}$ using RBr (R = 2-ethylhexyl)

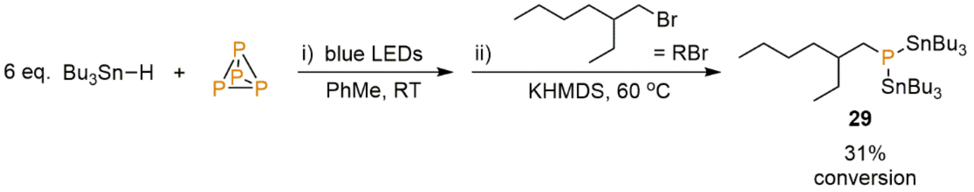

To a 10 mL, flat-bottomed, stoppered tube were added PhMe (500 µL), P$_4$ (0.01 mmol, as a stock solution in 77.4 µL PhH) and Bu$_3$SnH (16.1 µL, 0.06 mmol). The resulting colorless solution was stirred under irradiation with blue LED light (455 nm (±15 nm), 3.2 V, 700 mA, Osram OSLON SSL 80) for 18 h, during which time the tube was placed in a block cooled by circulating water to maintain near-ambient temperature. 3-(bromomethyl)heptane (35.1 µL, 0.20 mmol) and KHMDS (16.0 mg, 0.08 mmol) were added and the reaction mixture heated to 60 °C with stirring for 1 day. After cooling to room temperature, Ph$_3$PO (9.8 mg, 0.0352 mmol) was added as an internal standard, and the mixture analysed by ^{1}H, ^{31}P{^{1}H} and ^{31}P

NMR spectroscopy as shown in Supplementary Figures 98-100, below. The $^{31}P\{^1H\}$ and ^{31}P spectra indicated formation of one major P-containing species, characterised by a resonance at –208.4 ppm. Based on this upfield chemical shift, the presence of $^{117/119}Sn$ satellites ($^1J(^{31}P\text{-}^{117}Sn) = 796$ Hz, $^1J(^{31}P\text{-}^{119}Sn) = 832$ Hz), the intensity of these satellites, and the absence of $^1J(^{31}P\text{-}^1H)$ splitting in the proton-coupled spectrum, this species can reasonably be assigned as the mono-alkylated product $RP(SnBu_3)_2$ (**29**).[22] Using quantitative $^{31}P\{^1H\}$ NMR spectroscopy (D1 = 30 s; Supplementary Figure 101), a total conversion of P_4 to this product of 31% was determined.

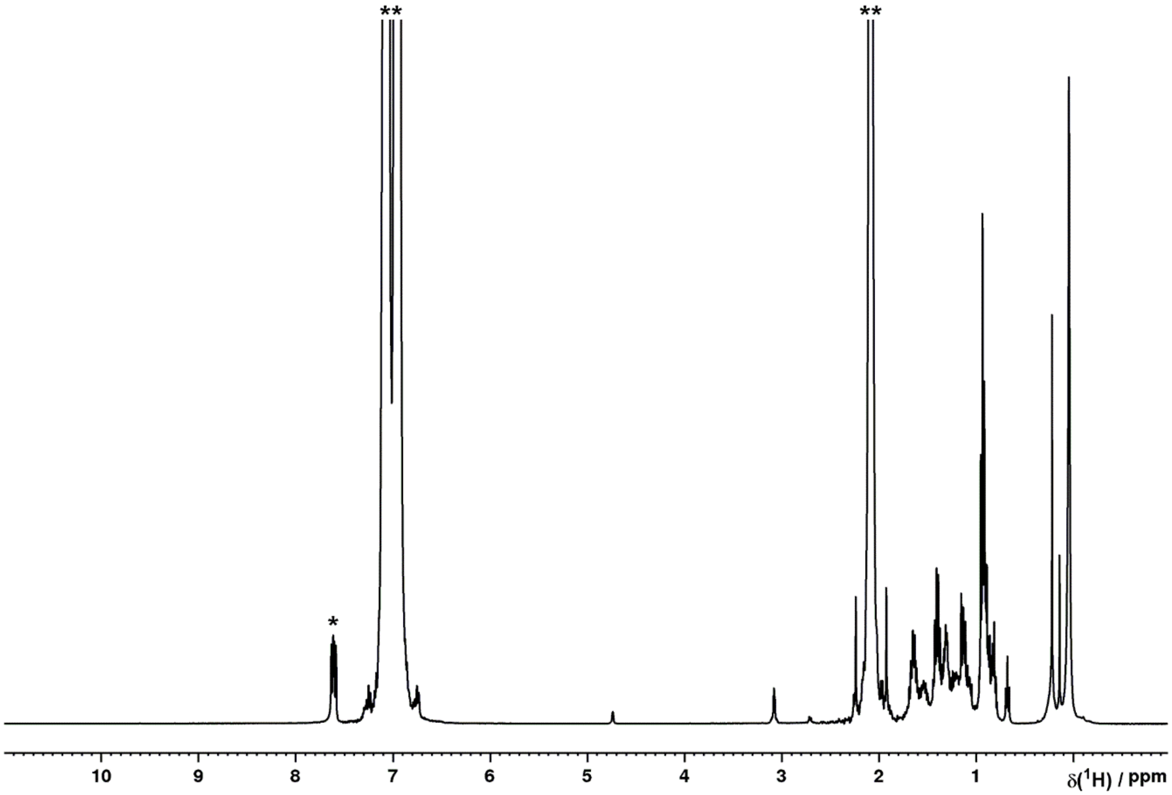

Supplementary Figure 98. ^1H NMR spectrum for the hydrostannylation of P_4 in PhMe, followed by *in situ* alkylation with RBr and KHMDS and addition of Ph_3PO (*) as internal standard. Solvent resonances (**) truncated for clarity.

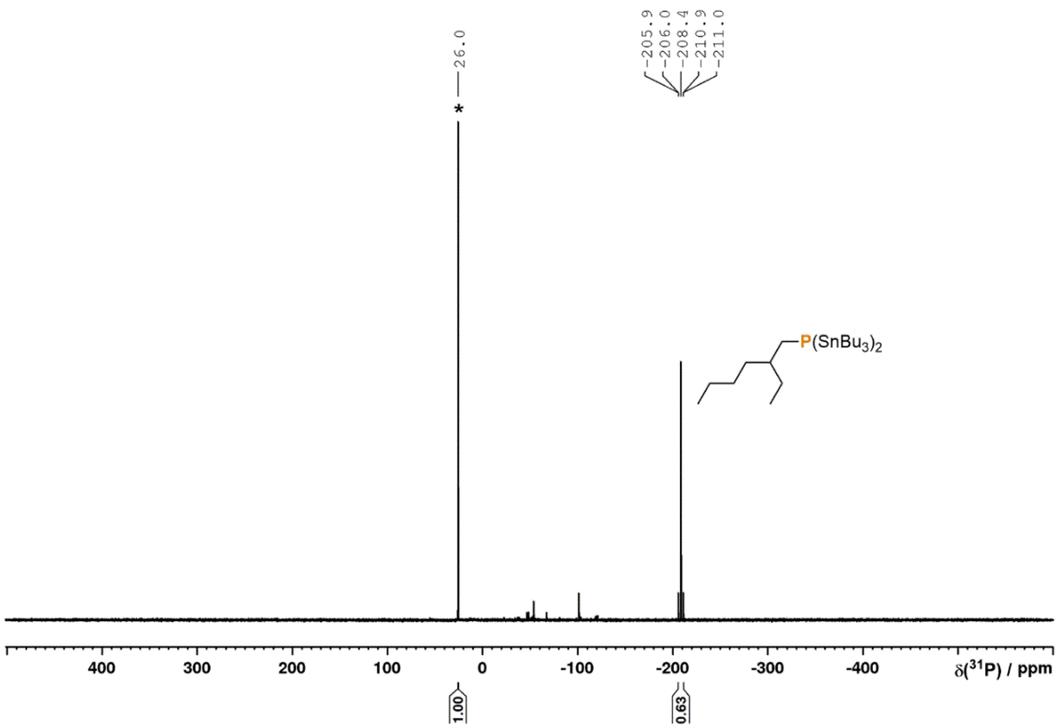

Supplementary Figure 99. $^{31}P\{^1H\}$ NMR spectrum for the hydrostannylation of P_4 in PhMe, followed by *in situ* alkylation with RBr and KHMDS and addition of Ph_3PO (*) as internal standard.

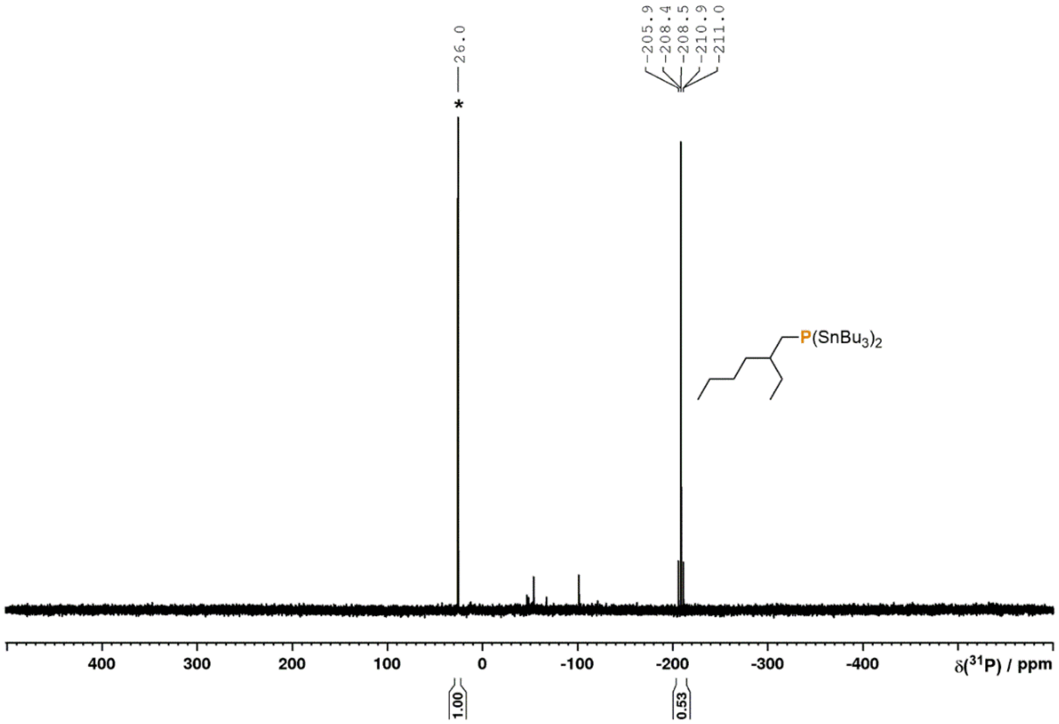

Supplementary Figure 100. ^{31}P NMR spectrum for the hydrostannylation of P_4 in PhMe, followed by *in situ* alkylation with RBr and KHMDS and addition of Ph_3PO (*) as internal standard.

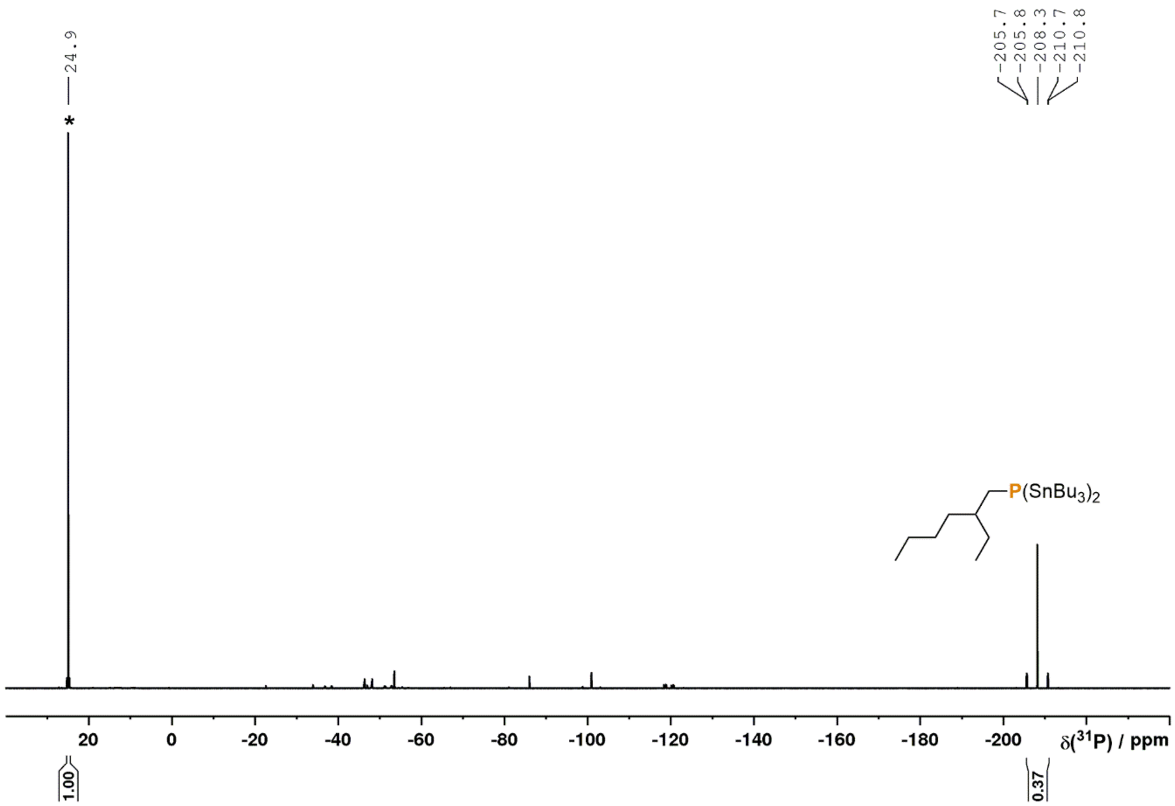

Supplementary Figure 101. Quantitative $^{31}P\{^1H\}$ NMR spectrum (D1 = 30 s) for the hydrostannylation of P_4 in PhMe, followed by *in situ* alkylation with RBr and KHMDS and addition of Ph_3PO (*) as internal standard.

Supplementary Method 27: Alkylation of $(Bu_3Sn)_xPH_{3-x}$ using R'Br (R' = 2,4,4-trimethylpentyl)

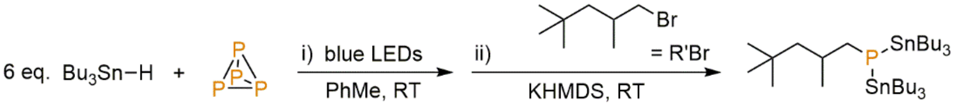

30

44% conversion

To a 10 mL, flat-bottomed, stoppered tube were added PhMe (500 µL), P_4 (0.01 mmol, as a stock solution in 77.4 µL PhH) and Bu_3SnH (16.1 µL, 0.06 mmol). The resulting colorless solution was stirred under irradiation with blue LED light (455 nm (±15 nm), 3.2 V, 700 mA, Osram OSLON SSL 80) for 18 h, during which time the tube was placed in a block cooled by circulating water to maintain near-ambient temperature. 1-bromo-2,4,4-trimethylpentane (27.9 µL, 0.16 mmol) and KHMDS (12.0 mg, 0.06 mmol) were added and the reaction mixture was stirred at room temperature for 3 days. Ph_3PO (9.3 mg, 0.0334 mmol) was then added as an internal standard, and the mixture analysed by ^1H, $^{31}P\{^1H\}$ and ^{31}P NMR spectroscopy as shown in Supplementary Figures 102-104, below. The $^{31}P\{^1H\}$ and ^{31}P spectra indicated formation of one major P-containing species, characterised by a resonance at –209.3 ppm. Based on this upfield chemical shift, the presence of $^{117/119}Sn$ satellites ($^1J(^{31}P\text{-}^{117}Sn)$ = 794 Hz, $^1J(^{31}P\text{-}^{119}Sn)$ = 830 Hz), the intensity of these satellites, and the absence of $^1J(^{31}P\text{-}^1H)$ splitting in the proton-coupled spectrum, this species can reasonably be assigned as the mono-alkylated product $R'P(SnBu_3)_2$ (**30**).[22] Using quantitative $^{31}P\{^1H\}$ NMR spectroscopy (D1 = 30 s; Supplementary Figure 105), a total conversion of P_4 to this product of 44% was determined.

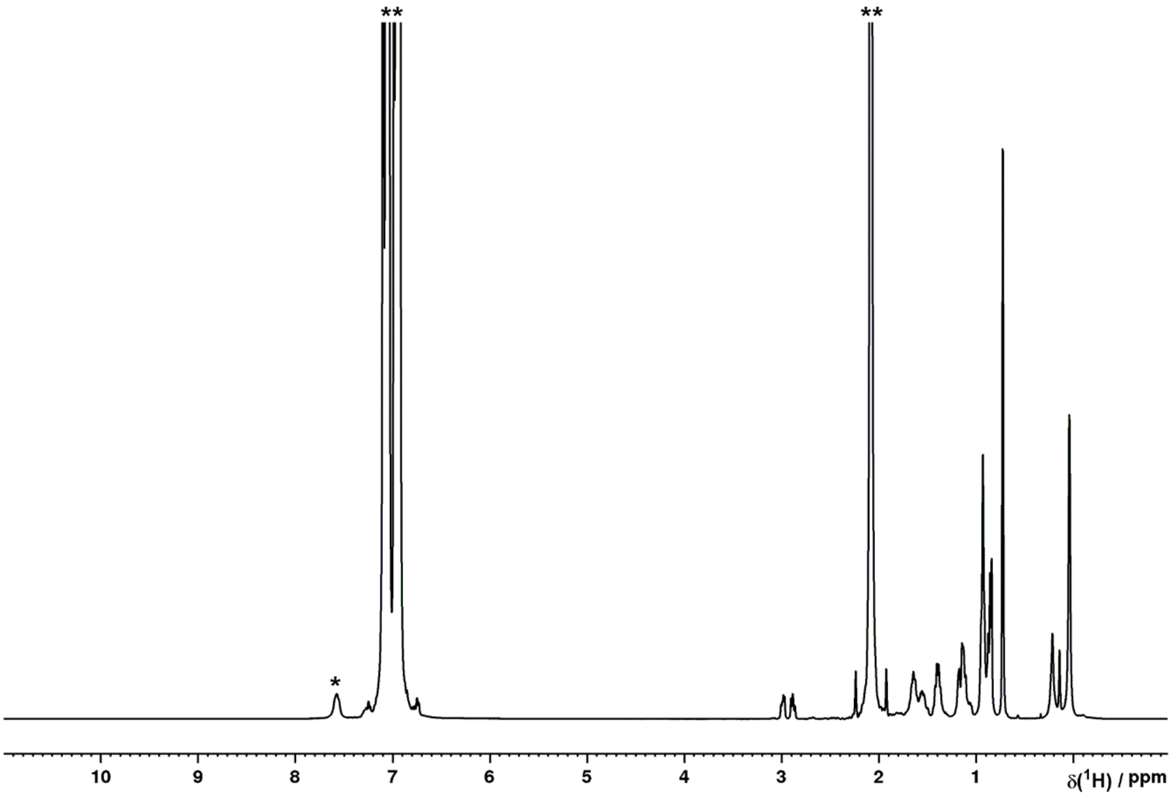

Supplementary Figure 102. ^1H NMR spectrum for the hydrostannylation of P_4 in PhMe, followed by *in situ* alkylation with R'Br and KHMDS and addition of Ph_3PO (*) as internal standard. Solvent resonances (**) truncated for clarity.

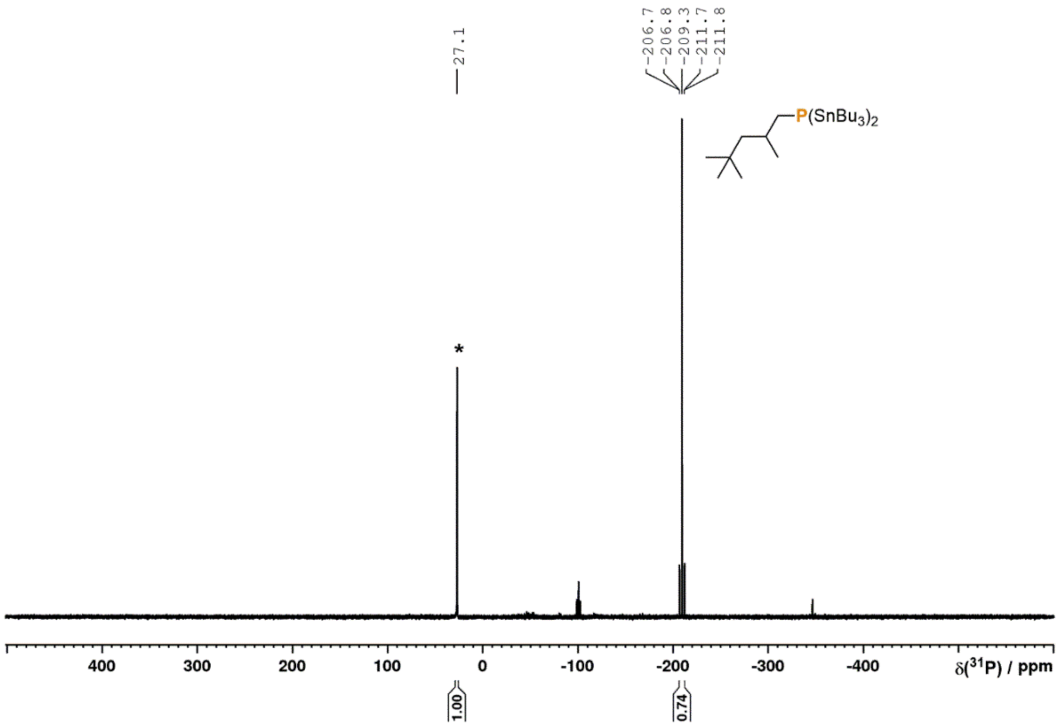

Supplementary Figure 103. $^{31}P\{^{1}H\}$ NMR spectrum for the hydrostannylation of P_4 in PhMe, followed by *in situ* alkylation with R'Br and KHMDS and addition of Ph_3PO (*) as internal standard.

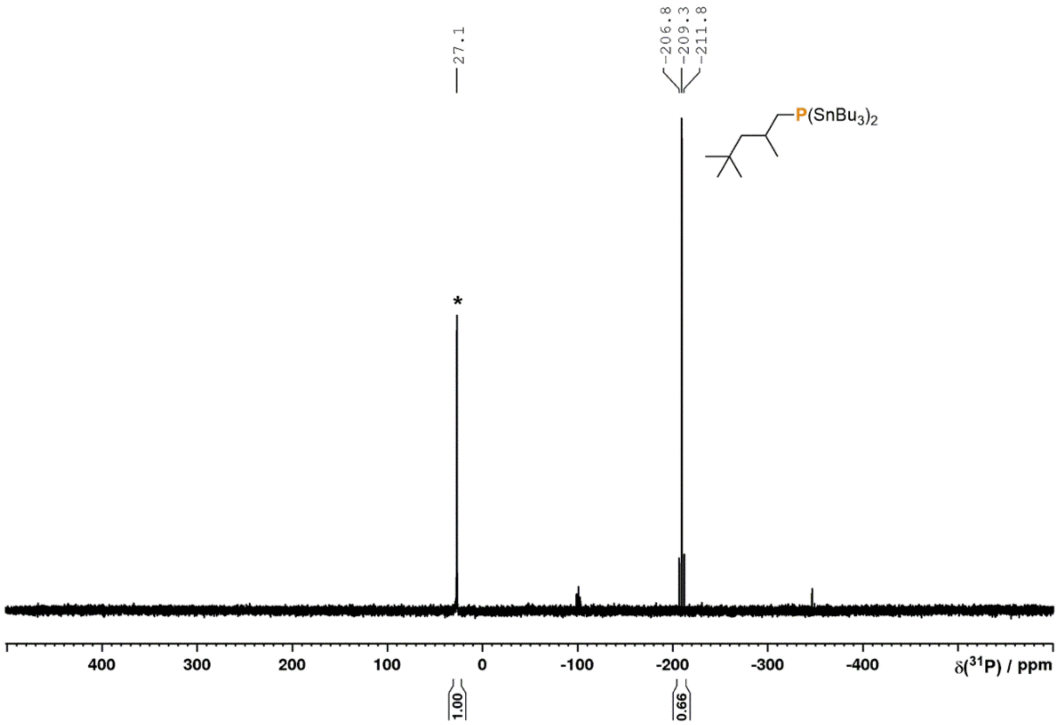

Supplementary Figure 104. ^{31}P NMR spectrum for the hydrostannylation of P_4 in PhMe, followed by *in situ* alkylation with R'Br and KHMDS and addition of Ph_3PO (*) as internal standard.

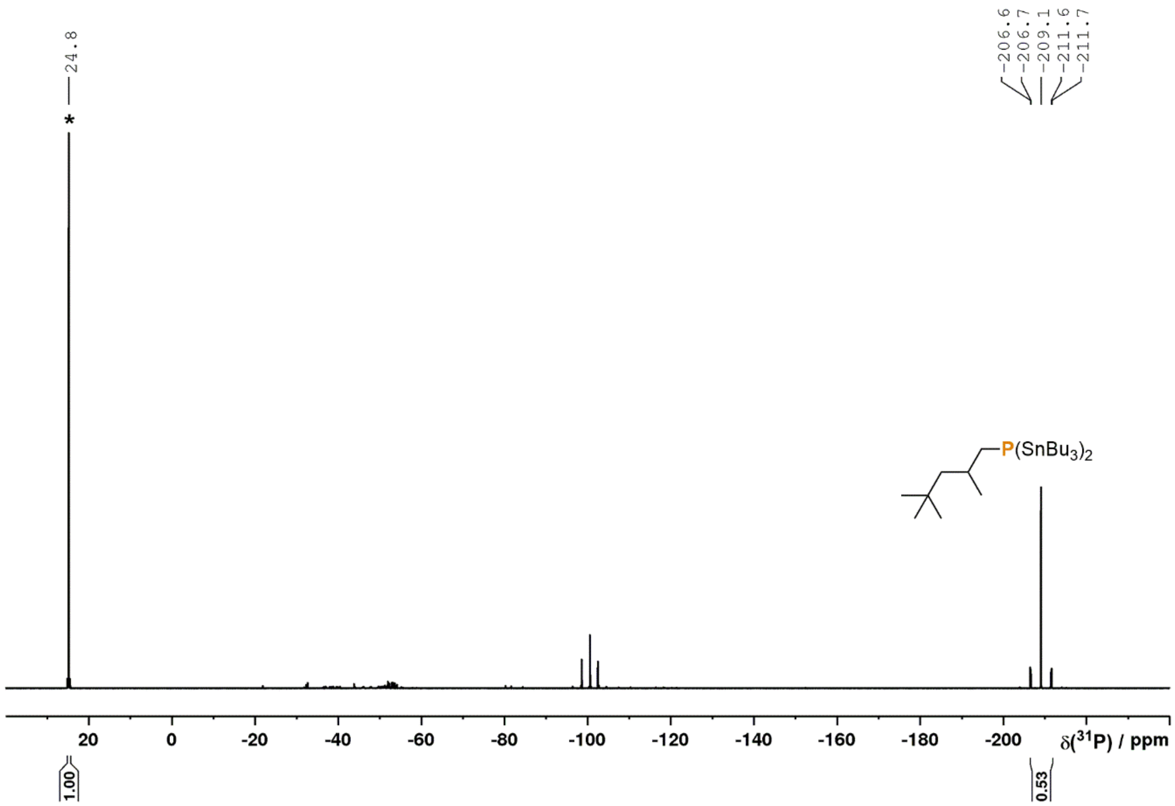

Supplementary Figure 105. Quantitative $^{31}P\{^1H\}$ NMR spectrum (D1 = 30 s) for the hydrostannylation of P_4 in PhMe, followed by *in situ* alkylation with R'Br and KHMDS and addition of Ph_3PO (*) as internal standard.

Supplementary Method 28: Attempted arylation of $(Bu_3Sn)_xPH_{3-x}$ using PhBr

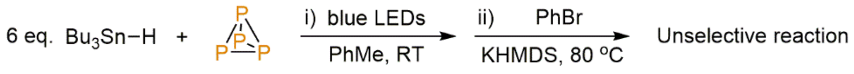

To a 10 mL, flat-bottomed, stoppered tube were added PhMe (500 µL), P_4 (0.01 mmol, as a stock solution in 77.4 µL PhH) and Bu_3SnH (16.1 µL, 0.06 mmol). The resulting colorless solution was stirred under irradiation with blue LED light (455 nm (±15 nm), 3.2 V, 700 mA, Osram OSLON SSL 80) for 18 h, during which time the tube was placed in a block cooled by circulating water to maintain near-ambient temperature. PhBr (8.4 µL, 0.8 mmol) and KHMDS (12.0 mg, 0.06 mmol) were added and the reaction mixture was heated to 80 °C with stirring for 3 days. After cooling to room temperature, Ph_3PO (10.0 mg, 0.0359 mmol) was added as an internal standard, and the mixture analysed by ^1H, $^{31}P\{^1H\}$ and ^{31}P NMR spectroscopy as shown in Supplementary Figures 106-108, below. $^{31}P\{^1H\}$ and ^{31}P spectra, including a quantitative $^{31}P\{^1H\}$ spectrum (D1 = 30 s; Supplementary Figure 109), did not reveal any major new products (no new peaks whose conversion from P_4 would exceed *ca*. 15%). Analogous experiments using PhI or PhCl in place of PhBr were similarly unsuccessful, as were reactions at other temperatures.

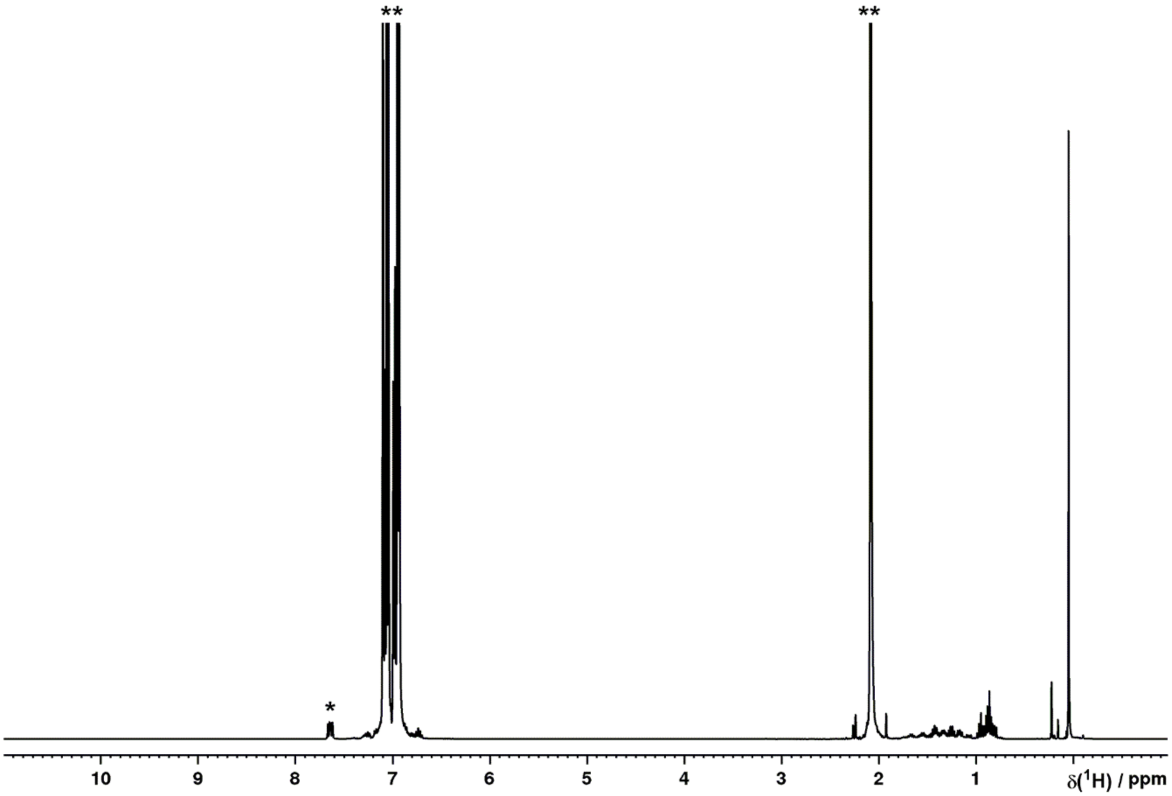

Supplementary Figure 106. ^1H NMR spectrum for the hydrostannylation of P_4 in PhMe, followed by attempted *in situ* arylation with PhBr and KHMDS and addition of Ph_3PO (*) as internal standard. Solvent resonances (**) truncated for clarity.

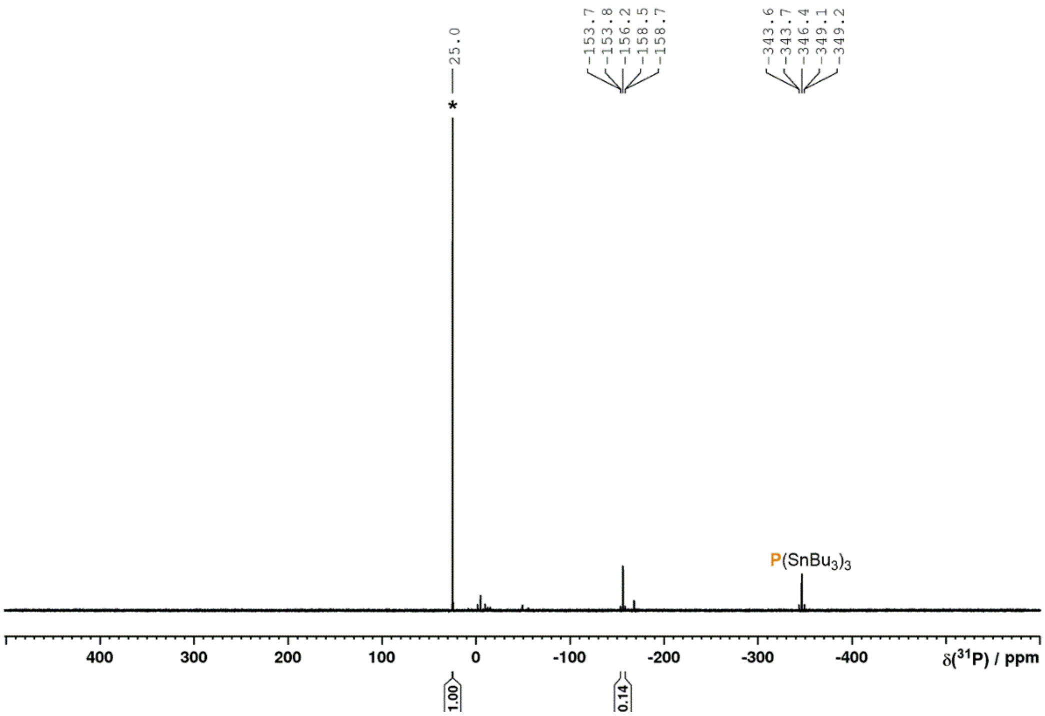

Supplementary Figure 107. $^{31}P\{^1H\}$ NMR spectrum for the hydrostannylation of P_4 in PhMe, followed by attempted *in situ* arylation with PhBr and KHMDS and addition of Ph_3PO (*) as internal standard.

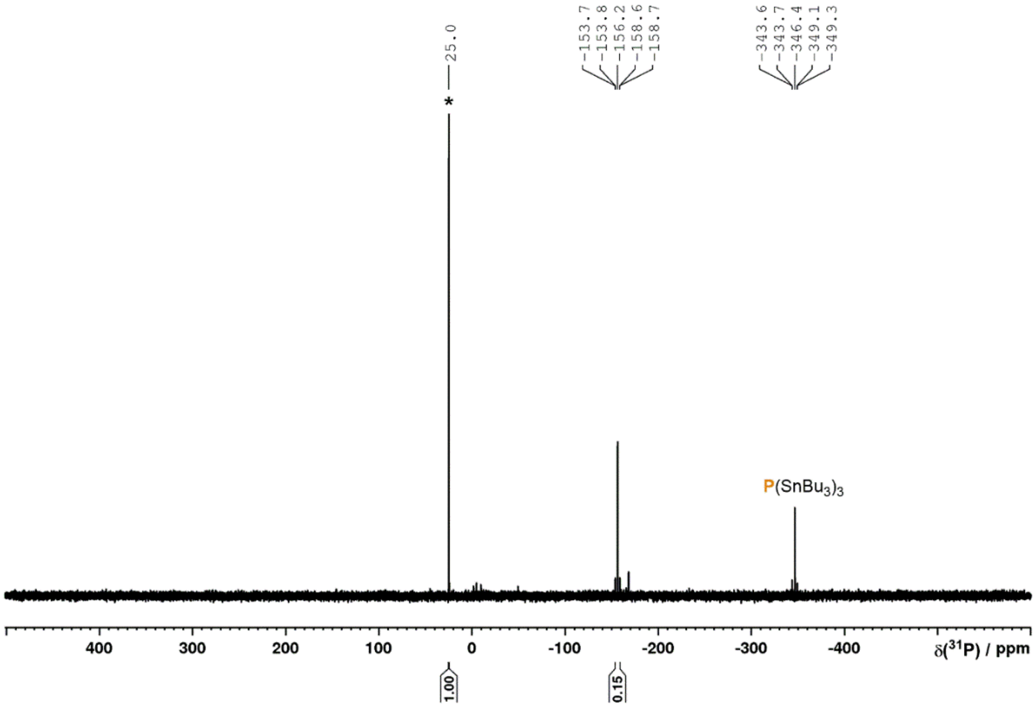

Supplementary Figure 108. ^{31}P NMR spectrum for the hydrostannylation of P_4 in PhMe, followed by attempted *in situ* arylation with PhBr and KHMDS and addition of Ph_3PO (*) as internal standard.

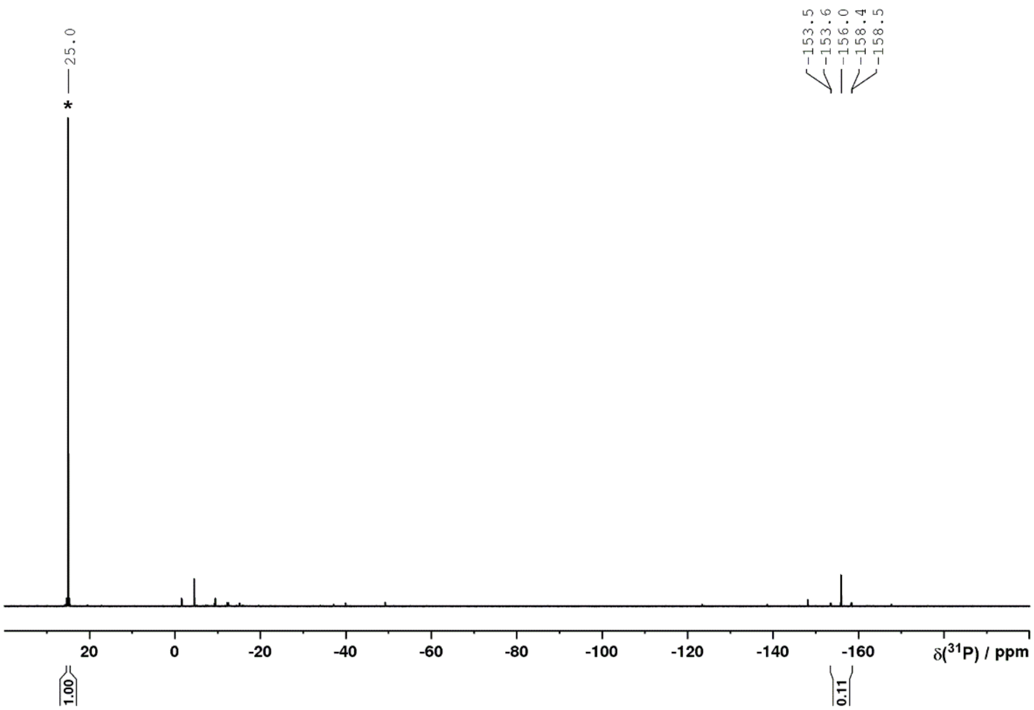

Supplementary Figure 109. Quantitative $^{31}P\{^1H\}$ NMR spectrum (D1 = 30 s) for the hydrostannylation of P_4 in PhMe, followed by attempted *in situ* arylation with PhBr and KHMDS and addition of Ph_3PO (*) as internal standard.

Supplementary Method 29: Synthesis and isolation of THP (16)

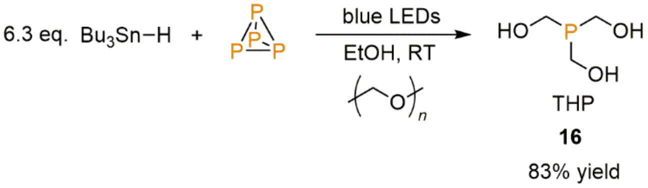

To a 50 mL flat-bottomed Schlenk were added P_4 (62.0 mg, 0.5 mmol) and PhH (5.0 mL). After stirring to obtain a homogeneous solution, EtOH (25 mL), Bu_3SnH (847 µL, 3.15 mmol) and paraformaldehyde (180 mg, 6.0 mmol) were added. The resulting suspension was stirred under irradiation with blue LED light (7X Osram OSLON SSL80, 455 nm (±15 nm), 20.3 V 1000mA) for 22 h, during which time the Schlenk tube was placed in a block cooled by circulating water to maintain near-ambient temperature. The resulting suspension was filtered and volatiles were removed under vacuum. To the oily residue thus obtained was added PhMe (20 mL) and degassed H_2O (20 mL). The biphasic mixture was thoroughly stirred for 30 min, the toluene phase was removed, and the aqueous phase was washed with further PhMe (2 x 20 mL).

Following removal of volatiles from the aqueous phase under vacuum, THP was obtained as a colourless oil (206 mg, 83%).

^{1}H NMR (400 MHz, 300 K, D_2O) : δ = 3.99 ppm (d, $^2J(^{31}P\text{-}^1H)$ = 5.2 Hz).

$^{31}P\{^1H\}$ NMR (121 MHz, 300 K, D_2O) : δ = –23.6 ppm (s).

^{31}P NMR (121 MHz, 300 K, D_2O) : δ = –23.6 ppm (s).

$^{13}C\{^1H\}$ NMR (101 MHz, 300 K, D_2O): δ = 56.4 ppm (d, $^1J(^{31}P\text{-}^{13}C)$ = 8.5 Hz).

MS (APCI, EtOH): *m/z* = 125.0364 ([M+H]$^+$).

NMR data are consistent with previous reports.[23]

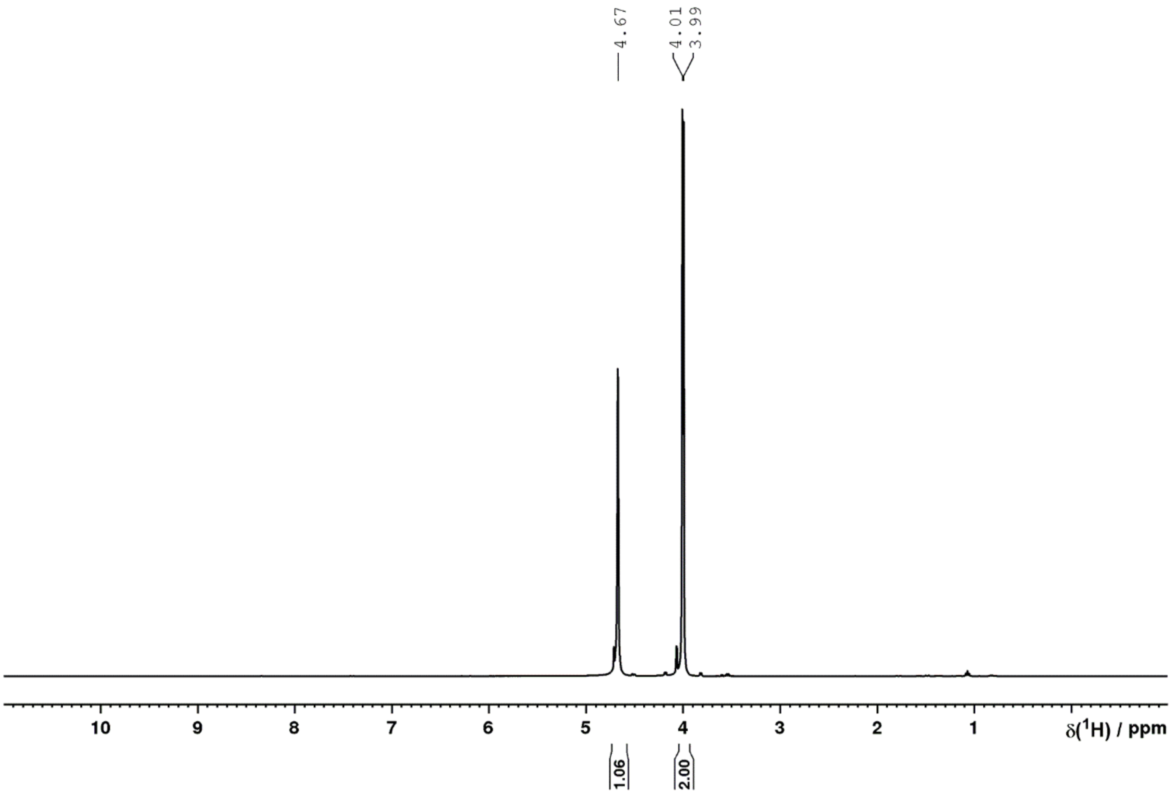

Supplementary Figure 110. ^{1}H NMR spectrum of THP (**16**) in D_2O.

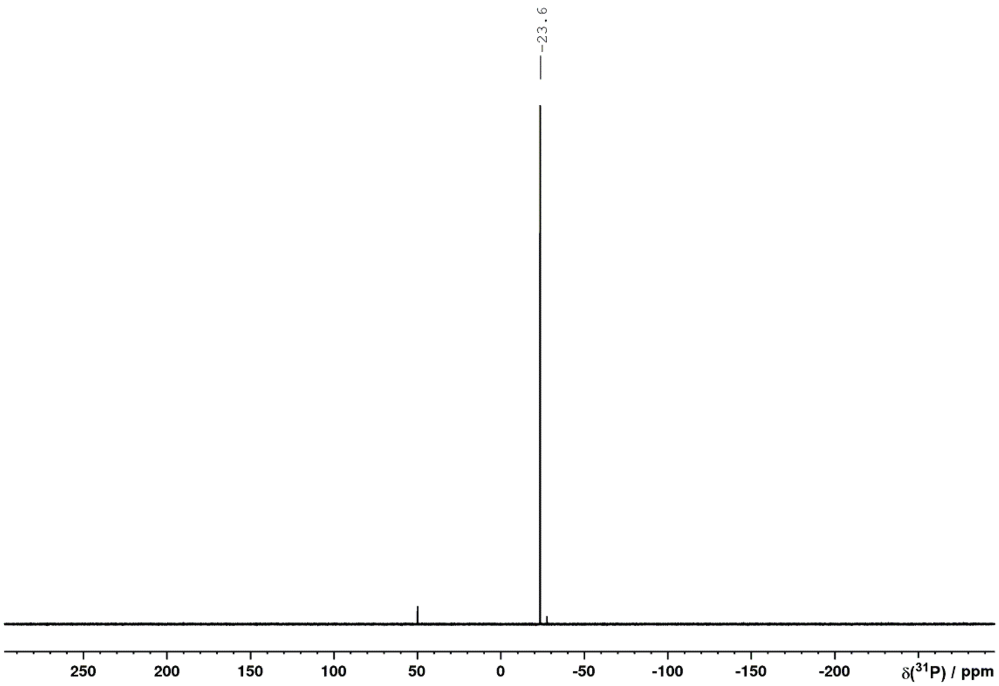

Supplementary Figure 111. $^{31}P\{^1H\}$ NMR spectrum of THP (**16**) in D_2O.

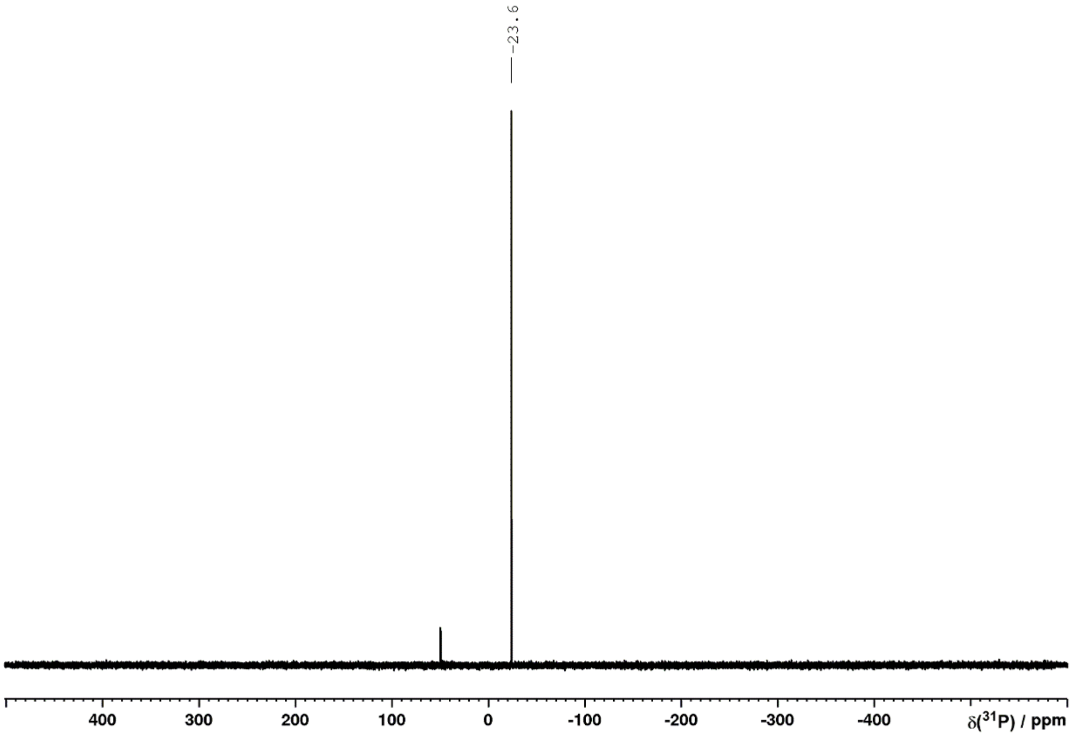

Supplementary Figure 112. ^{31}P NMR spectrum of THP (**16**) in D_2O.

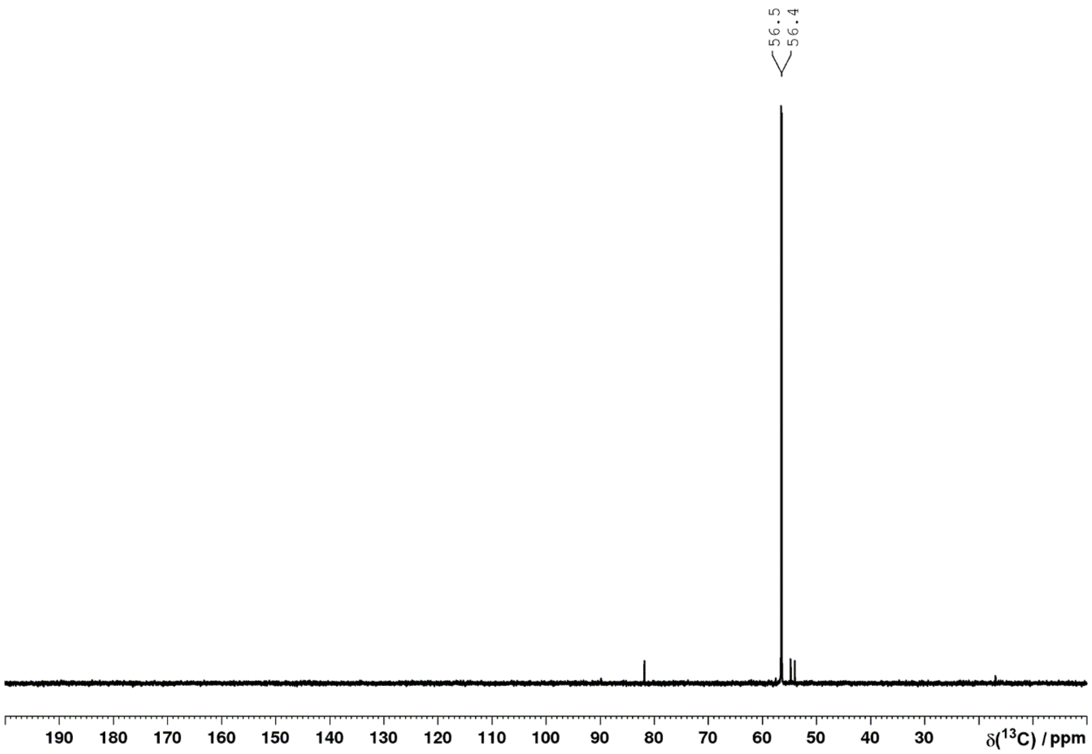

Supplementary Figure 113. $^{13}C\{^1H\}$ NMR spectrum of THP (**16**) in D_2O.

Supplementary Method 30: Synthesis and isolation of THPC (17) *via* hydrostannylation under blue LEDs in PhMe, with recovery of Bu_3SnCl (20)

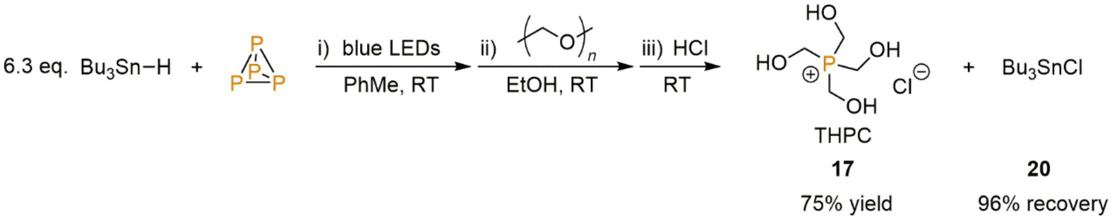

The product THPC (**17**) was prepared as described in the Methods section of the main manuscript. Characterisation data are provided below:

<u>Spectroscopic data of THPC (**17**):</u>

^1H NMR (400 MHz, 300 K, D_2O) : $\delta = 4.67$ ppm (d, $^2J(^{31}P\text{-}^1H) = 1.8$ Hz).

$^{31}P\{^1H\}$ NMR (121 MHz, 300 K, D_2O) : δ = 27.0 ppm (s).

^{31}P NMR (121 MHz, 300 K, D_2O) : δ = 27.0 ppm (s).

$^{13}C\{^1H\}$ NMR (101 MHz, 300 K, D_2O): δ = 49.1 ppm (d, $^1J(^{31}P\text{-}^{13}C)$ = 51.3 Hz).

NMR data are consistent with previous reports.[24]

Spectroscopic data of recovered Bu_3SnCl (**20**):

^1H NMR (400 MHz, 300 K, $CDCl_3$) : δ = 1.77-1.51 (2H, m), 1.41-1.21 (4H, m), 0.92 ppm (3H, t, $^3J(^1H\text{-}^1H)$ = 7.3 Hz).

$^{119}Sn\{^1H\}$ NMR (149 MHz, 300 K, $CDCl_3$) : δ = 157.5 ppm.

$^{13}C\{^1H\}$ NMR (101 MHz, 300 K, $CDCl_3$): δ = 27.9 (s), 26.9 (s), 17.5 (s), 13.6 ppm (s).

NMR data are consistent with previous reports.[25]

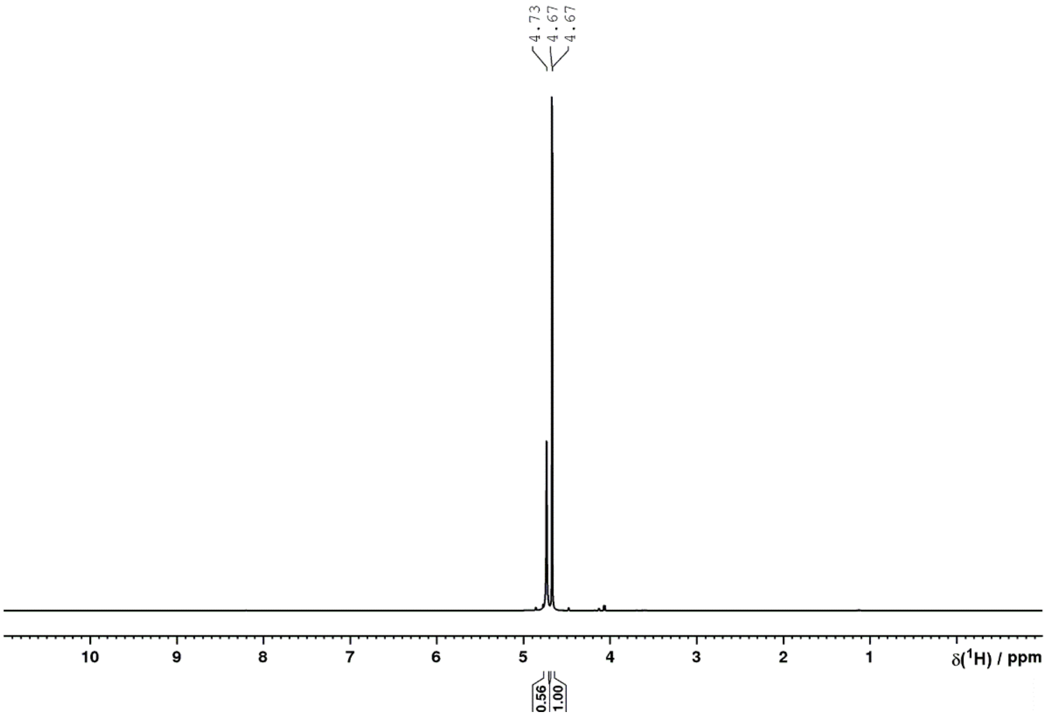

Supplementary Figure 114. ^1H NMR spectrum of THPC (**17**) in D_2O.

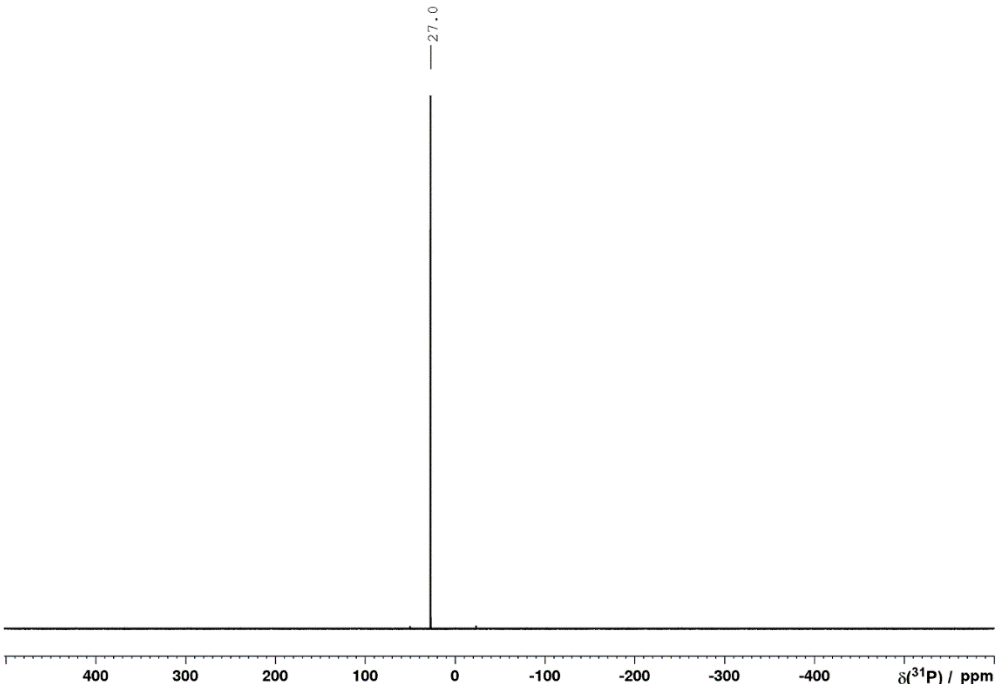

Supplementary Figure 115. $^{31}P\{^1H\}$ NMR spectrum of THPC (**17**) in D_2O.

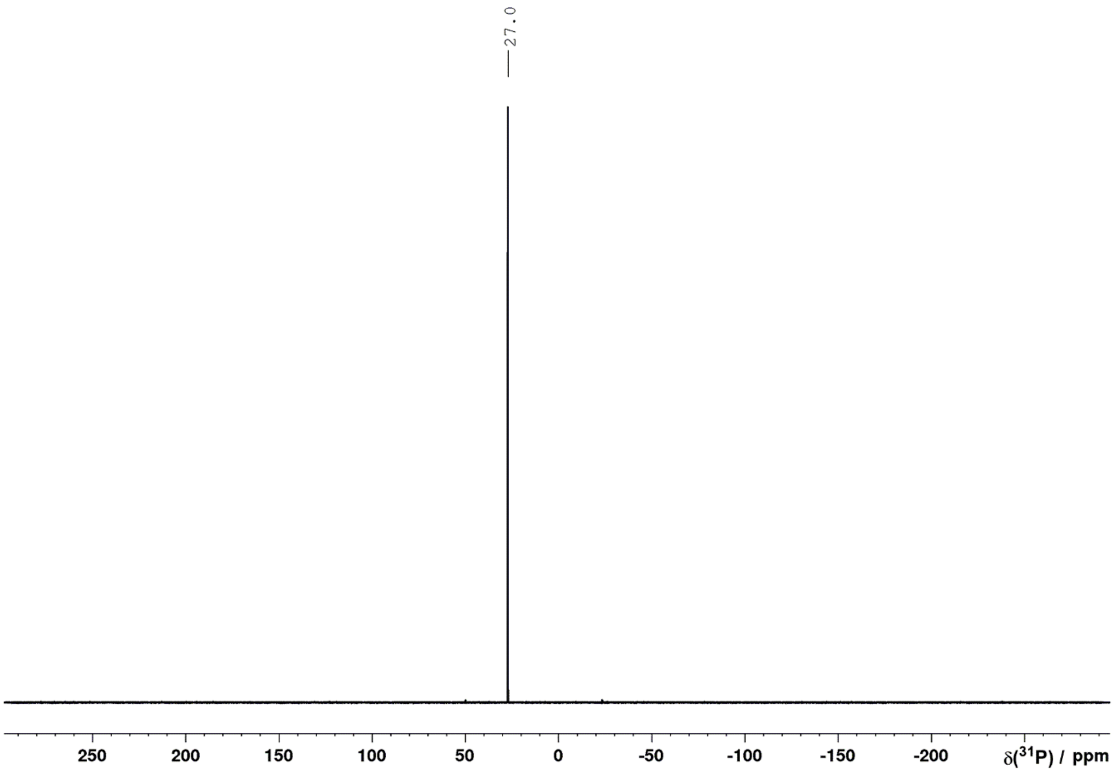

Supplementary Figure 116. ^{31}P NMR spectrum of THPC (**17**) in D_2O.

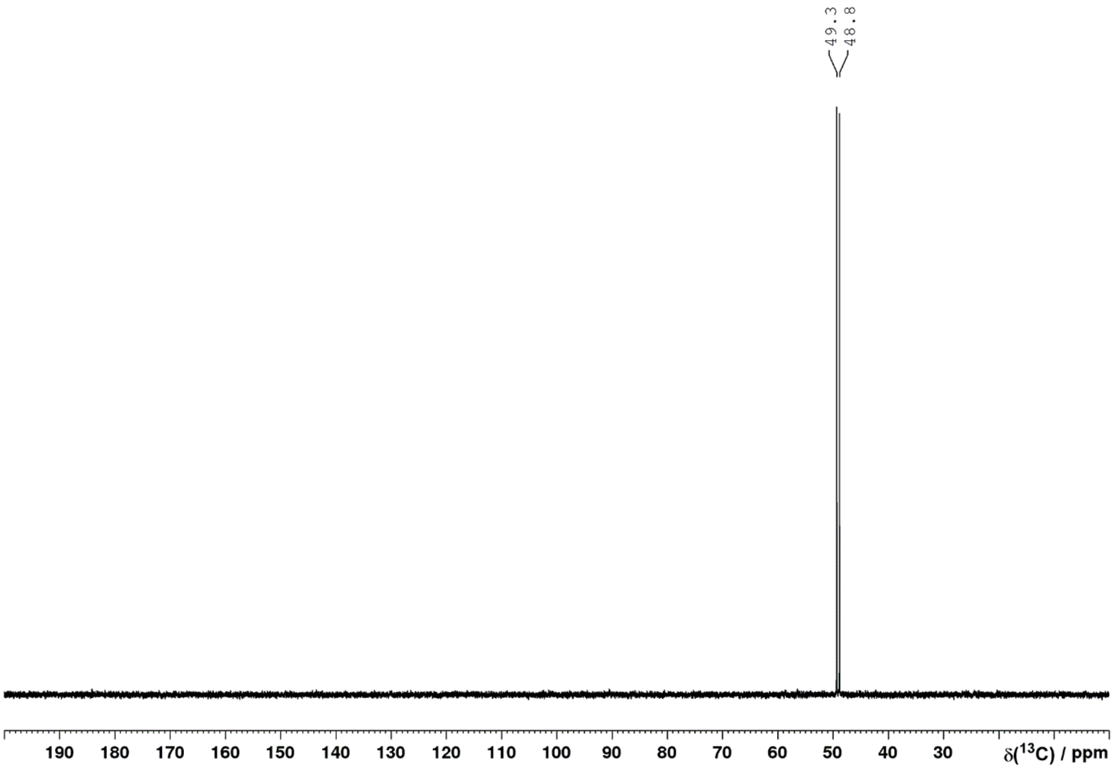

Supplementary Figure 117. $^{13}C\{^1H\}$ NMR spectrum of THPC (**17**) in D_2O.

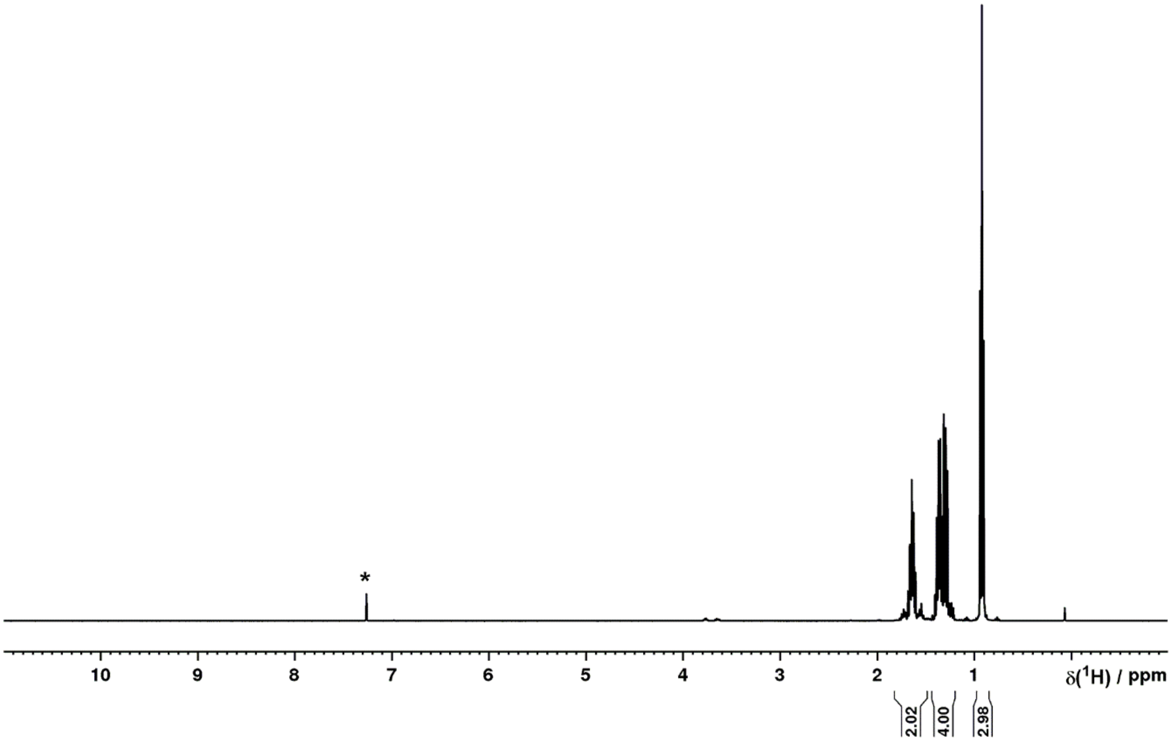

Supplementary Figure 118. ^1H NMR spectrum of Bu_3SnCl (**20**) in $CDCl_3$ (*).

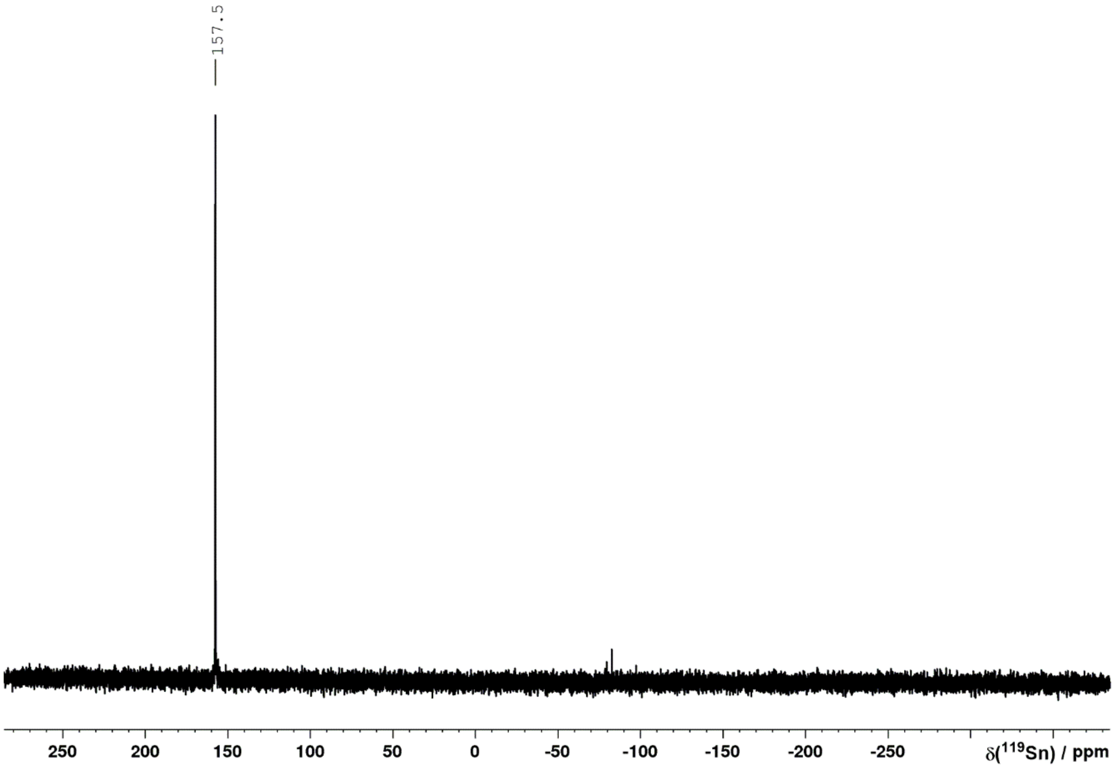

Supplementary Figure 119. $^{119}Sn\{^1H\}$ NMR spectrum of Bu_3SnCl (**20**) in $CDCl_3$.

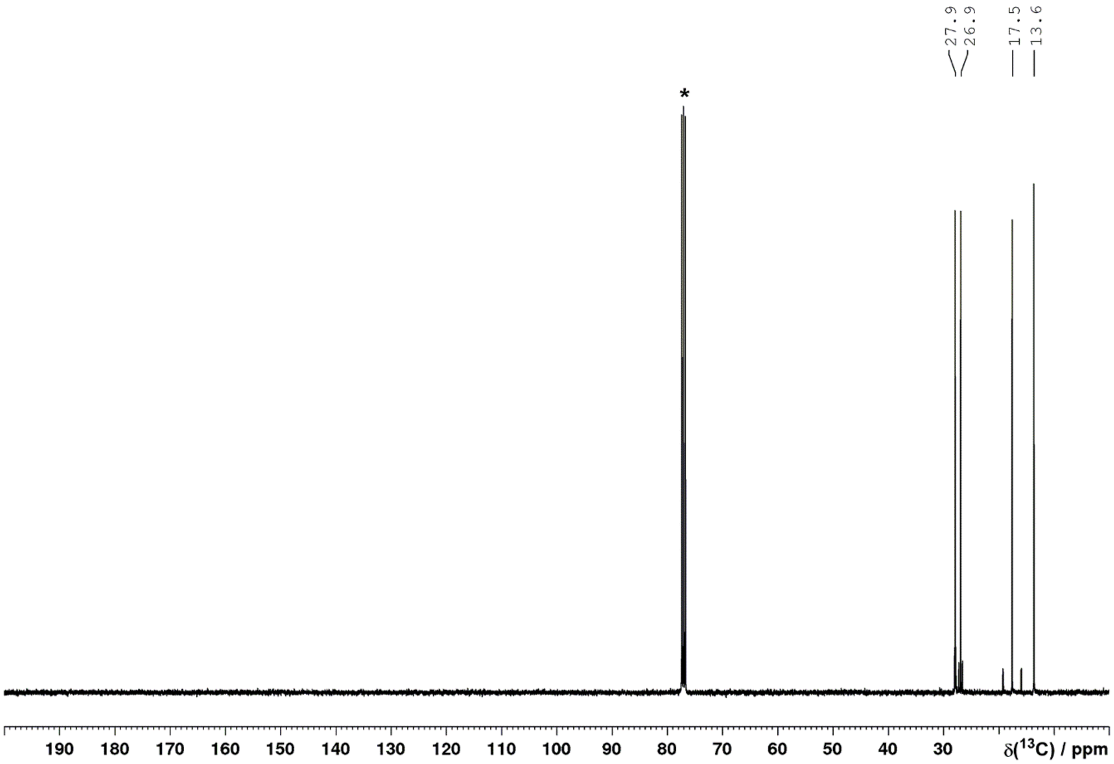

Supplementary Figure 120. $^{13}C\{^1H\}$ NMR spectrum of Bu_3SnCl (**20**) in $CDCl_3$ (*).

Supplementary Method 31: Synthesis and isolation of THPC (17) *via* hydrostannylation under blue LEDs in EtOH, with recovery of Bu_3SnCl (20)

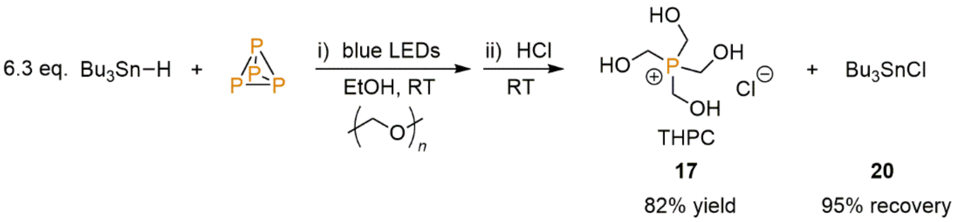

To a 50 mL flat-bottomed Schlenk were added P_4 (62.0 mg, 0.5 mmol) and PhH (5.0 mL). After stirring to obtain a homogeneous solution, EtOH (25 mL), Bu_3SnH (847 μL, 3.15 mmol) and paraformaldehyde (750 mg, 25 mmol) were added. The resulting suspension was stirred under irradiation with blue LED light (7X Osram OSLON SSL80, 455 nm (±15 nm), 20.3 V 1000mA) for 22 h, during which time the Schlenk tube was placed in a block cooled by circulating water to maintain near-ambient temperature. The resulting mixture was frozen and HCl (4.0 M in 1,4-dioxane, 5 mL, 20 mmol) was added. After thawing, the reaction mixture was stirred for 2 h. The resulting suspension was filtered to give a colorless solution. Removal of volatiles under vacuum yielded an oily solid residue that was triturated with Et_2O (20 mL) overnight to give THPC (**17**) as a white solid (312 mg, 82%) after filtration, washing with additional Et_2O (20 mL) and drying under vacuum.

The combined Et_2O washes from the above reaction were dried under vacuum to afford Bu_3SnCl (**20**) as a pale yellow oil (980 mg, 95%).

NMR data of product THPC and recovered Bu_3SnCl are identical to those given in Supplementary Method 30.

Supplementary Method 32: Synthesis and isolation of THPC (17) *via* hydrostannylation using AIBN in PhMe (0.5 mmol scale)

To a 50 mL Schlenk tube were added P_4 (62.0 mg, 0.5 mmol) and PhMe (25 mL). After stirring to obtain a homogeneous solution, Bu_3SnH (847 µL, 3.15 mmol) and AIBN (8.2 mg, 0.05 mmol) were added. The Schlenk tube was immediately and thoroughly wrapped in Al foil to exclude any ambient light, and the stirred reaction mixture was then heated to 30 °C for 16 h. Following removal of volatiles under vacuum, EtOH (25 mL) and paraformaldehyde (750 mg, 25 mmol) were added, and the resulting suspension was stirred at room temperature for 16 h. The mixture was frozen in a liquid nitrogen bath and HCl (4.0 M in 1,4-dioxane, 5 mL, 20 mmol) was added. After thawing, the reaction mixture was stirred at room temperature for 2 h. The resulting yellowish suspension was filtered, and volatiles were removed under vacuum. The remaining oily solid residue was triturated with Et_2O (20 mL) overnight, to give THPC (**17**) as a white solid (330 mg, 87%) after filtration, washing with additional Et_2O (20 mL) and drying under vacuum.

NMR data are identical to those given in Supplementary Method 30.

Supplementary Method 33: Synthesis and isolation of THPC (17) *via* hydrostannylation using AIBN in PhMe (5 mmol scale)

To a 500 mL round-bottomed Schlenk flask were added P_4 (620 mg, 5 mmol) and PhMe (250 mL). After stirring to obtain a homogeneous solution, Bu_3SnH (8.5 mL, 31.5 mmol) and AIBN (82.1 mg, 0.5 mmol) were added. The Schlenk flask was immediately and thoroughly wrapped in Al foil to exclude any ambient light, and the stirred reaction mixture was then heated to 30 °C for 16 h. Following removal of volatiles under vacuum, EtOH (250 mL) and paraformaldehyde (7.51 g, 250 mmol) were added, and the resulting suspension was stirred at room temperature for 16 h. The mixture was frozen in a liquid nitrogen bath and HCl (4.0 M in 1,4-dioxane, 50 mL, 200 mmol) was added. After thawing, the reaction mixture was stirred at room temperature for 4 h. The yellowish suspension was filtered through a bed of Celite in a glass frit (P4) column, and volatiles were removed under vacuum. The remaining oily solid residue was triturated with Et_2O (200 mL) overnight, filtered and washed with additional Et_2O (2 x 25 mL). After drying thoroughly under vacuum, the desired product was obtained as an off-white solid (3.33 g, 87%).

NMR data are identical to those given in Supplementary Method 30.

Supplementary Method 34: Synthesis and isolation of THPO (18)

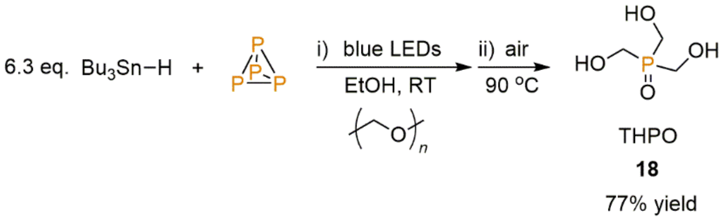

To a 50 mL flat-bottomed Schlenk were added P_4 (62.0 mg, 0.5 mmol) and PhH (5.0 mL). After stirring to obtain a homogeneous solution, EtOH (25 mL), Bu_3SnH (847 μL, 3.15 mmol) and paraformaldehyde (180 mg, 6.0 mmol) were added. The resulting suspension was stirred under irradiation with blue LED light (7X Osram OSLON SSL80, 455 nm (±15 nm), 20.3 V 1000mA) for 22 h, during which time the Schlenk tube was placed in a block cooled by circulating water to maintain near-ambient temperature. The resulting suspension was filtered and volatiles were removed under vacuum. Additional work-up was performed under air. To the oily residue thus obtained was added PhMe (20 mL) and H_2O (20 mL). The biphasic mixture was thoroughly stirred for 30 min and the aqueous phase was separated and washed with additional PhMe (3 x 15 mL), before being heated to 90 °C for 16 h while being kept open to air. Subsequent removal of volatiles yielded THPO (**18**) as a colourless oil (217 mg, 77%).

^1H NMR (400 MHz, 300 K, D_2O) : δ = 4.04 ppm (d, $^2J(^{31}P\text{-}^1H)$ = 3.0 Hz).

$^{31}P\{^1H\}$ NMR (121 MHz, 300 K, D_2O) : δ = 49.7 ppm (s).

^{31}P NMR (121 MHz, 300 K, D_2O) : δ = 49.7 ppm (s).

$^{13}C\{^1H\}$ NMR (101 MHz, 300 K, D_2O): δ = 54.3 ppm (d, $^1J(^{31}P\text{-}^{13}C)$ = 75.7 Hz).

MS (ESI, EtOH): *m/z* = 141.0312 ($[M+H]^+$).

NMR data are consistent with previous reports.[26]

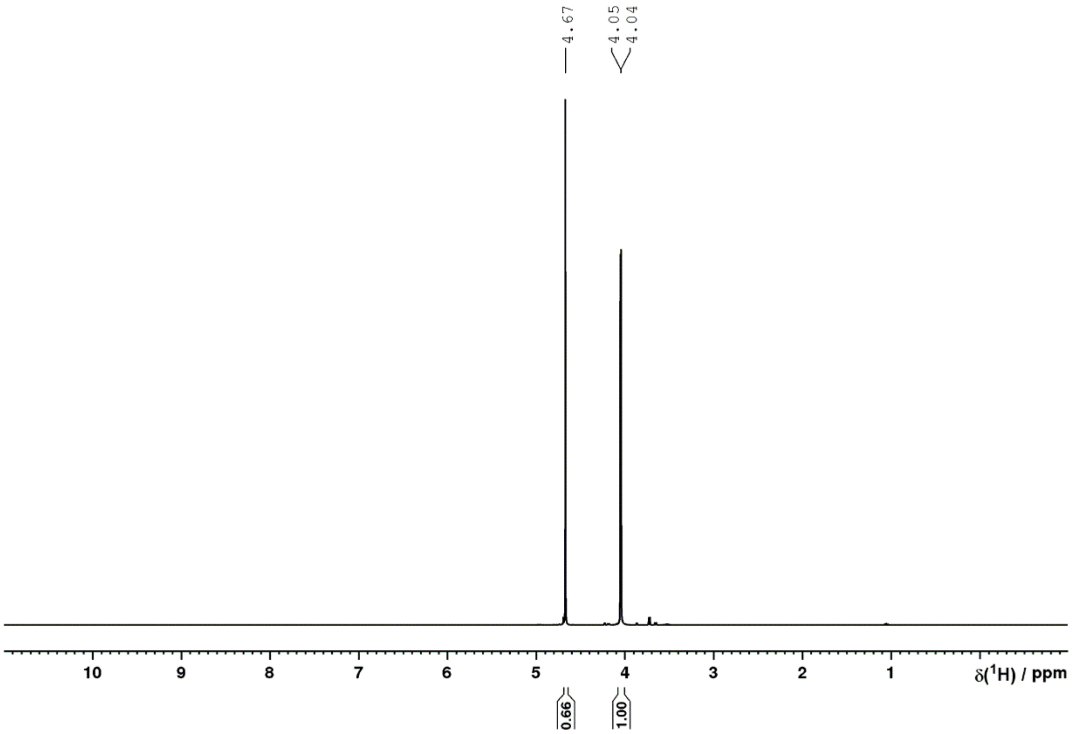

Supplementary Figure 121. ^{1}H NMR spectrum of THPO (**18**) in D_2O.

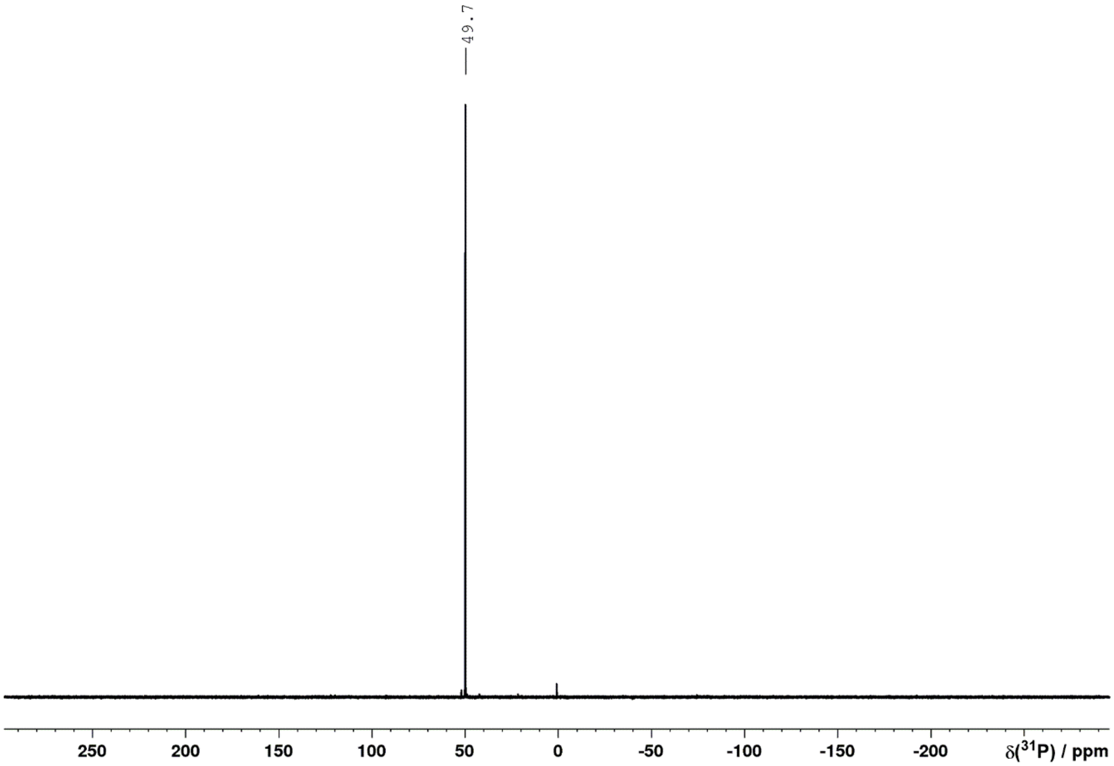

Supplementary Figure 122. $^{31}P\{^1H\}$ NMR spectrum of THPO (**18**) in D_2O.

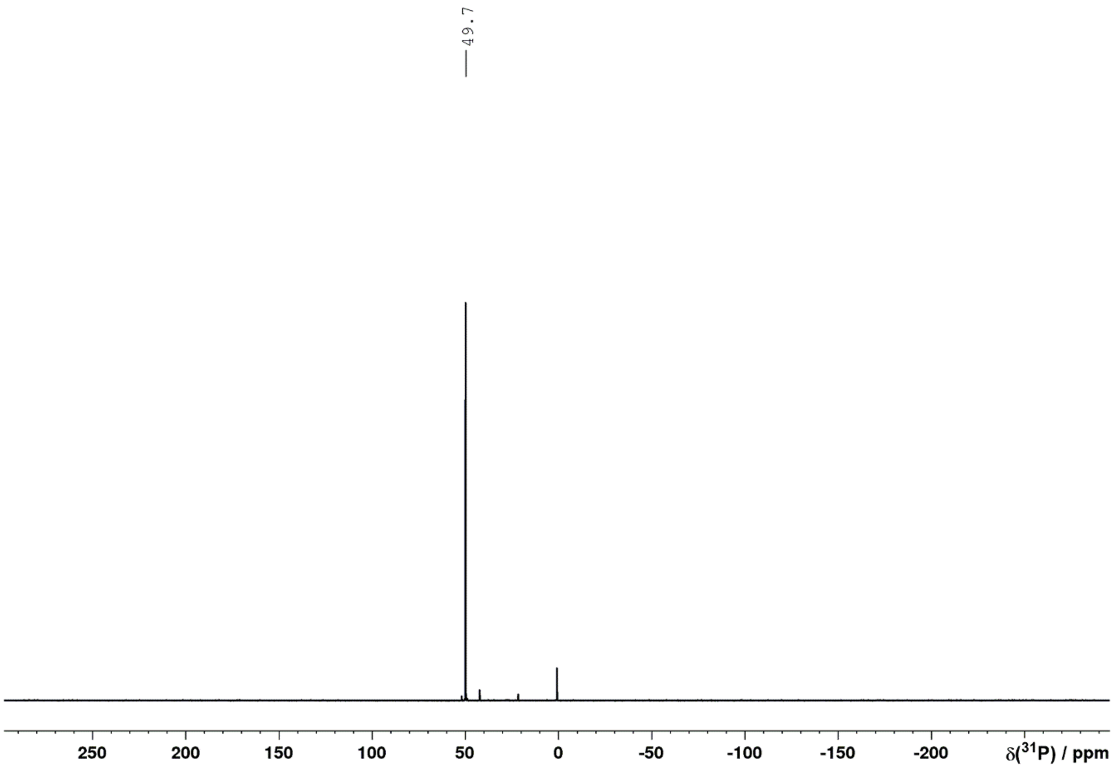

Supplementary Figure 123. ^{31}P NMR spectrum of THPO (**18**) in D_2O.

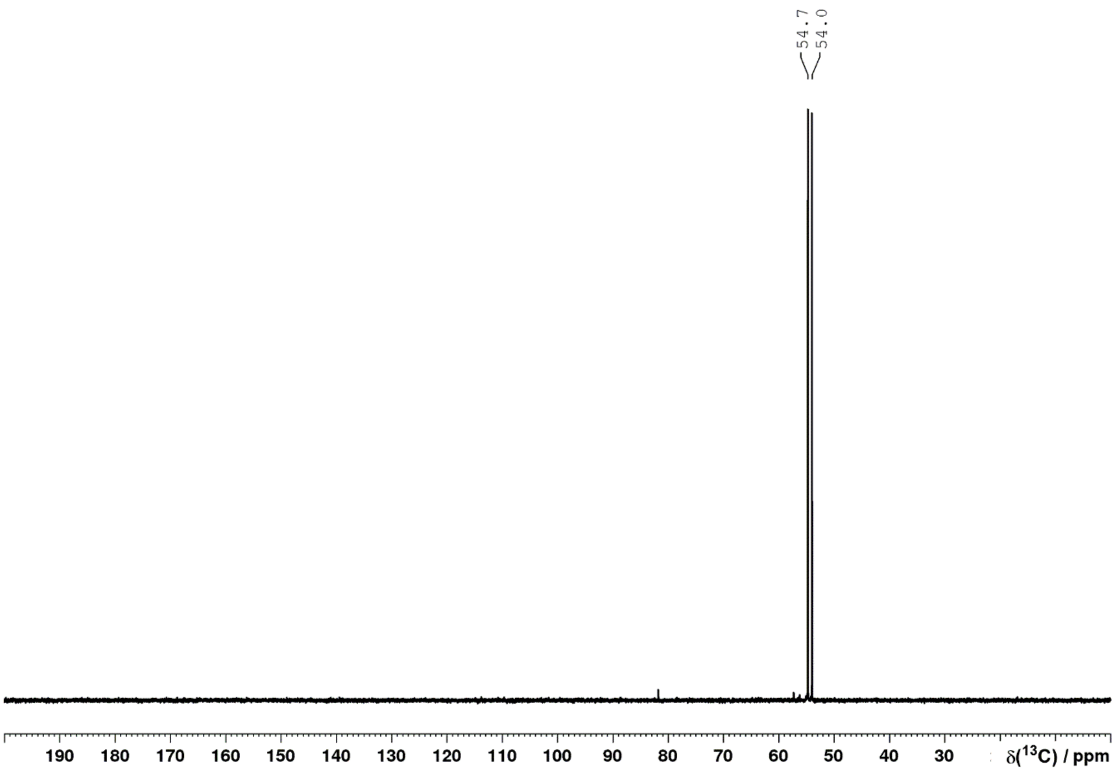

Supplementary Figure 124. ^{13}C{^{1}H} NMR spectrum of THPO (**18**) in D_2O.

Supplementary Method 35: Synthesis and isolation of HPA (19), with recovery of Bu_3SnCl (20)

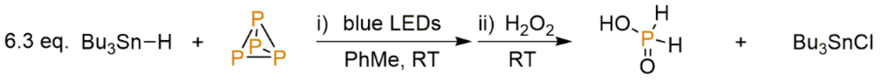

HPA

19

57% yield

20

93% recovery

The product HPA (**19**) was prepared as described in the Methods section of the main manuscript. Characterisation data are provided below:

<u>NMR data of HPA (**19**):</u>

^{1}H NMR (400 MHz, 300 K, CD_3CN) : δ = 10.84 (s), 7.05 ppm (d, $^1J(^{31}P\text{-}^1H)$ = 575 Hz).

$^{31}P\{^1H\}$ NMR (121 MHz, 300 K, CD_3CN) : δ = 13.9 ppm (s).

^{31}P NMR (121 MHz, 300 K, CD_3CN) : δ = 13.9 ppm (d, $^1J(^{31}P\text{-}^1H)$ = 575 Hz).

NMR data are consistent with previous reports.[27]

NMR data of Bu_3SnCl (**20**) were identical to those obtained with Supplementary Method 30.

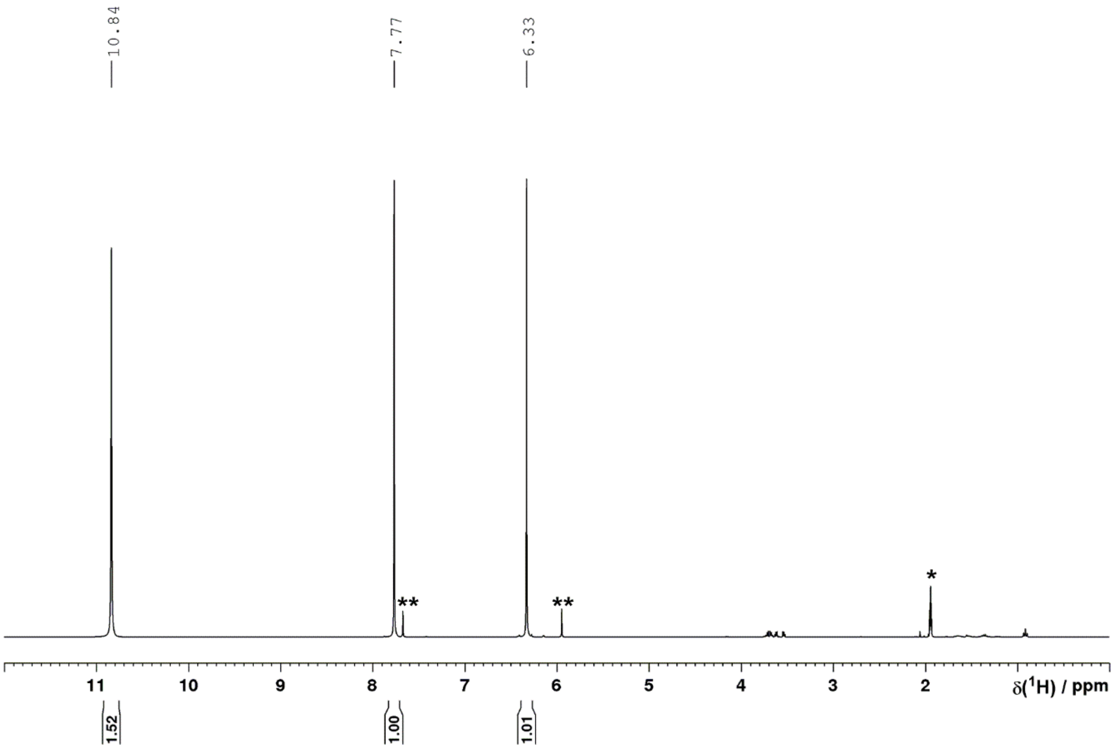

Supplementary Figure 125. ^{1}H NMR spectrum of HPA (**19**) in CD_3CN (*solvent, **minor $HP(O)(OH)_2$).

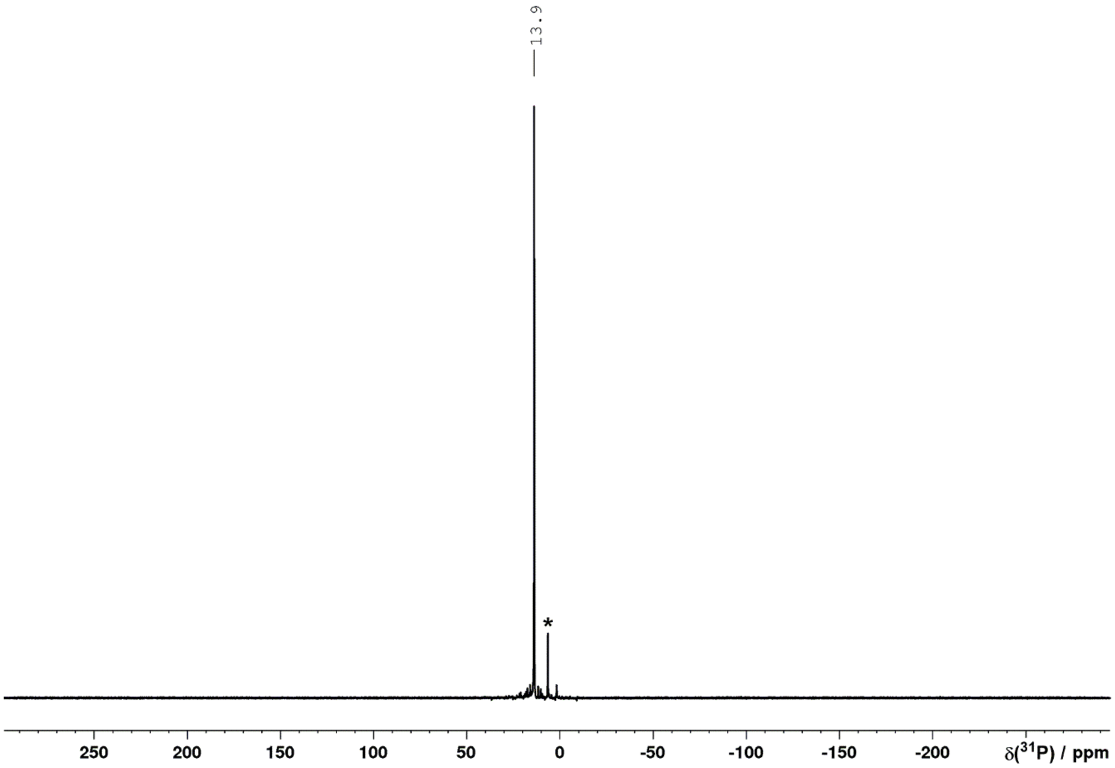

Supplementary Figure 126. $^{31}P\{^1H\}$ NMR spectrum of HPA (**19**) in CD_3CN (*minor $HP(O)(OH)_2$).

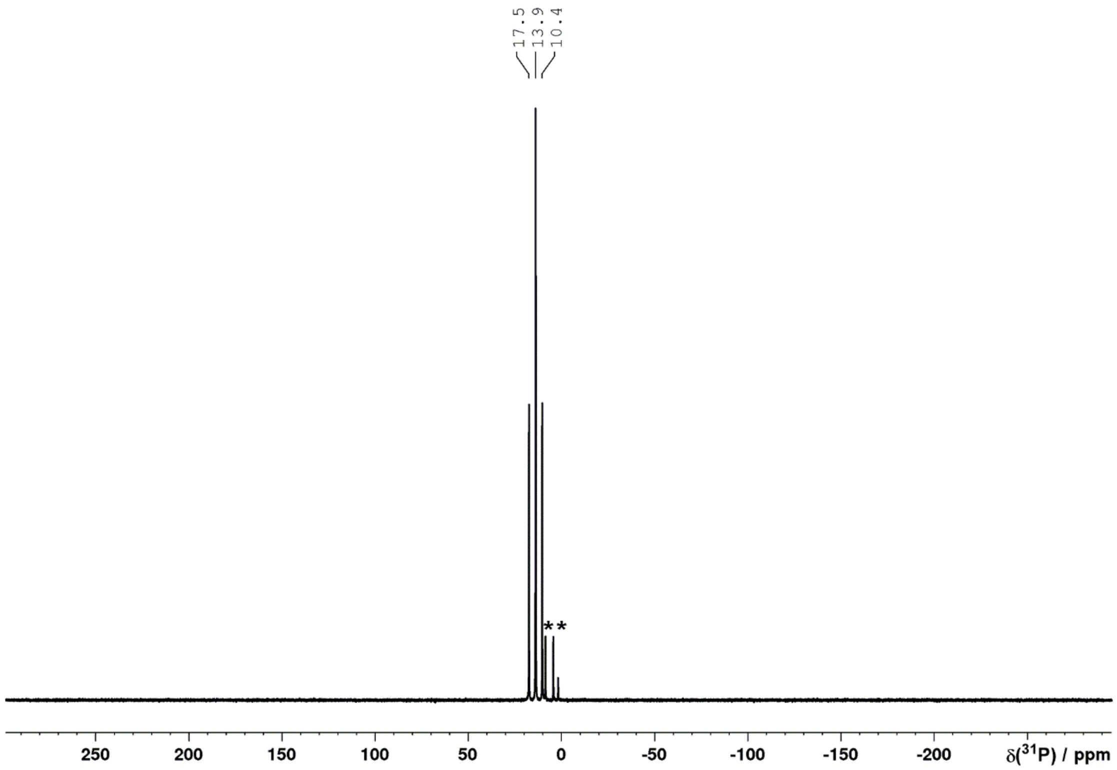

Supplementary Figure 127. ^{31}P NMR spectrum of HPA (**19**) in CD_3CN (*minor $HP(O)(OH)_2$).

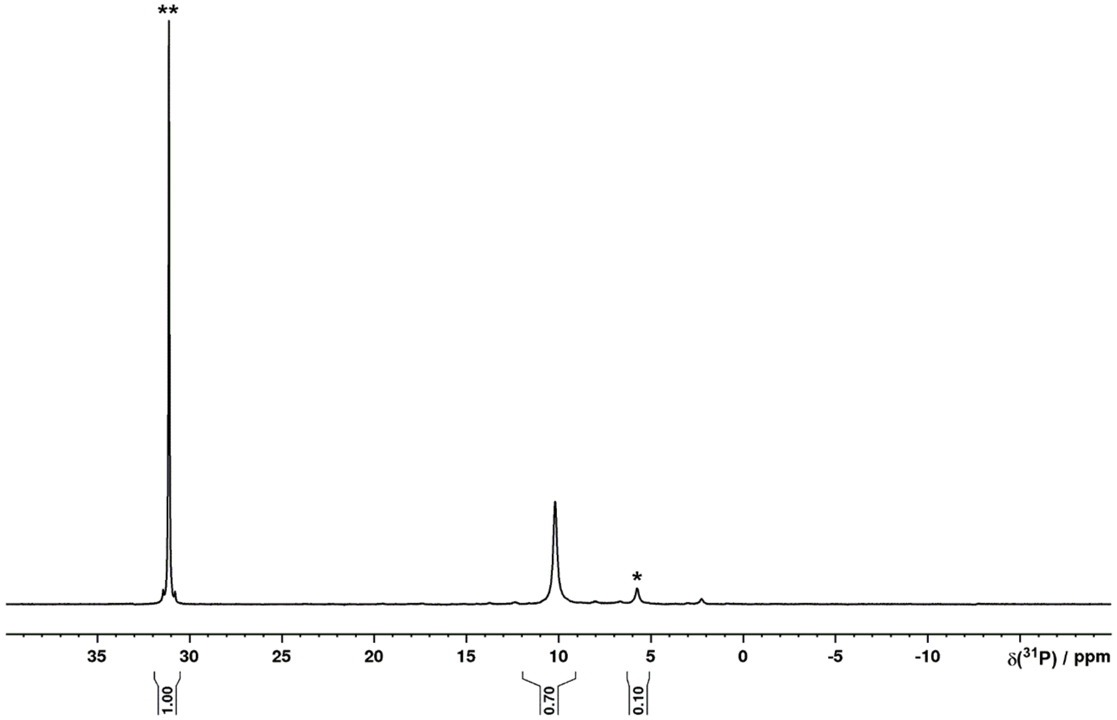

Supplementary Figure 128. Quantitative $^{31}P\{^1H\}$ NMR spectrum (D1= 14 s) of HPA (**19**; 6.5 mg) in CD_3CN (*minor $HP(O)(OH)_2$, **23.0 mg Ph_3PO).

In Situ Generation and Recycling of Bu_3SnH

Supplementary Method 36: Hydrostannylation of P_4 using Bu_3SnOMe and PMHS under blue LED irradiation (0.01 mmol scale)

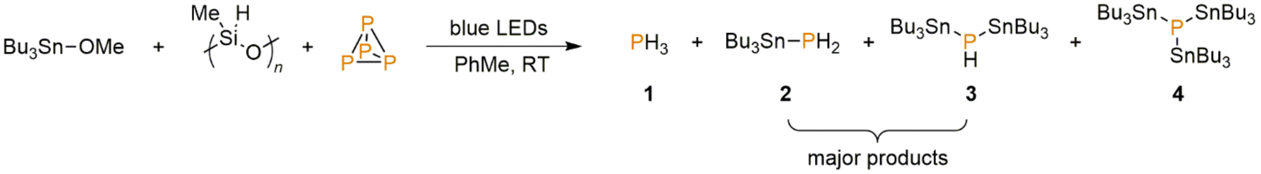

To a 10 mL, flat-bottomed, stoppered tube were added PhMe (500 µL), P_4 (0.01 mmol, as a stock solution in 77.4 µL PhH), Bu_3SnOMe (17.3 µL, 0.06 mmol), and PMHS (3.9 µL, 0.065 mmol). The tube was sealed, placed in a water-cooled block to maintain near-ambient temperature, and irradiated with blue light (455 nm (±15 nm), 3.2 V, 700 mA, Osram OSLON SSL 80) for 21 h. The resulting mixture was analysed by $^{31}P\{^1H\}$ NMR spectroscopy, as shown in Supplementary Figure 129 below.

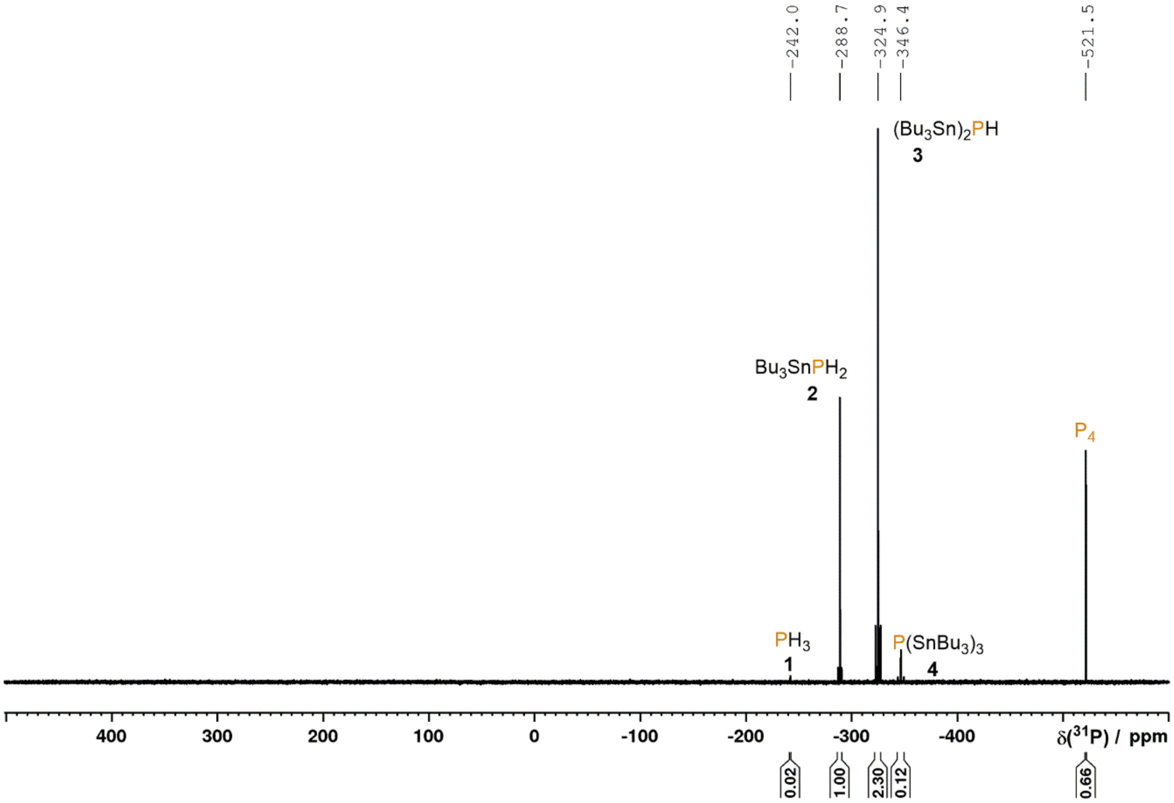

Supplementary Figure 129. $^{31}P\{^1H\}$ NMR spectrum for the reaction of P_4, 6 eq. Bu_3SnOMe and 6.5 eq. PMHS in PhMe, driven by 455 nm LED irradiation for 21 h.

The $^{31}P\{^1H\}$ NMR spectrum of the reaction clearly shows consumption of P_4, and concomitant formation of the hydrostannylation products $(Bu_3Sn)_xPH_{3-x}$ (x = 0-3), as is also observed when Bu_3SnH is used as starting material (for example, see Extended Data Figure 2). Close inspection, however, reveals a slightly increased fraction of $(Bu_3Sn)_2PH$ (**3**) relative to Bu_3SnPH_2 (**2**), as well as a significantly increased amount of residual, unreacted P_4. Both observations are attributed at least in part to a minor, competing side-reaction, in which the Bu_3SnOMe starting material reacts with Bu_3SnPH_2 to form $(Bu_3Sn)_2PH$ and MeOH, and is therefore unavailable for reduction by PMHS and subsequent P_4 hydrostannylation (Supplementary Figure 130). Similar reactivity is observed during the selective synthesis of $P(SnBu_3)_3$ (**4**; Supplementary Method 17). Furthermore, when the reaction was repeated using a two-fold excess of Bu_3SnOMe (12 eq.) under otherwise identical conditions, almost full P_4 consumption was observed, alongside formation of $(Bu_3Sn)_2PH$ as the clear major product (Supplementary Figure 131). The feasibility of the reaction was further confirmed by independent addition of Bu_3SnOMe to an isolated sample of Bu_3SnPH_2 at RT in PhMe.

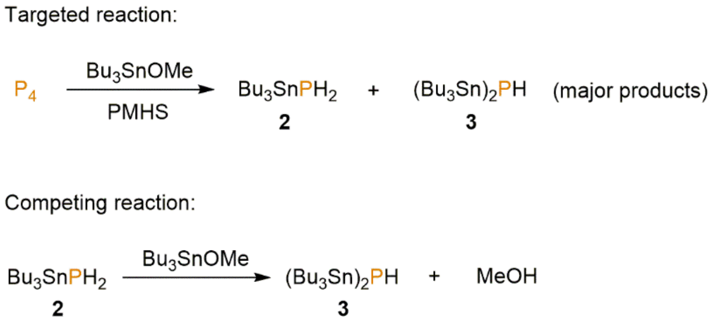

Supplementary Figure 130. Proposed side-reaction during the hydrostannylation of P_4 mediated by Bu_3SnOMe and PMHS.

As a result of the above side-reaction a slight excess (8 eq.) of both Bu_3SnOMe and PMHS was used, in order to achieve improved reactivity, and near-complete P_4 conversion (Supplementary Figure 132).

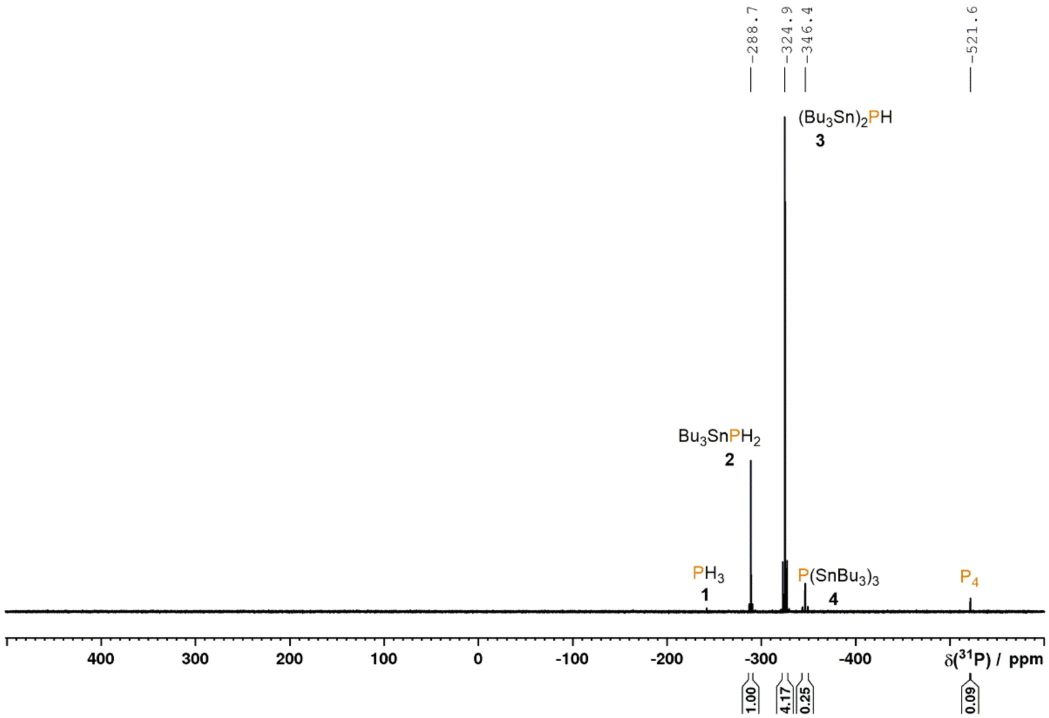

Supplementary Figure 131. $^{31}P\{^{1}H\}$ NMR spectrum for the reaction of P_4, 12 eq. Bu_3SnOMe and 6.5 eq. PMHS in PhMe, driven by 455 nm LED irradiation for 21 h.

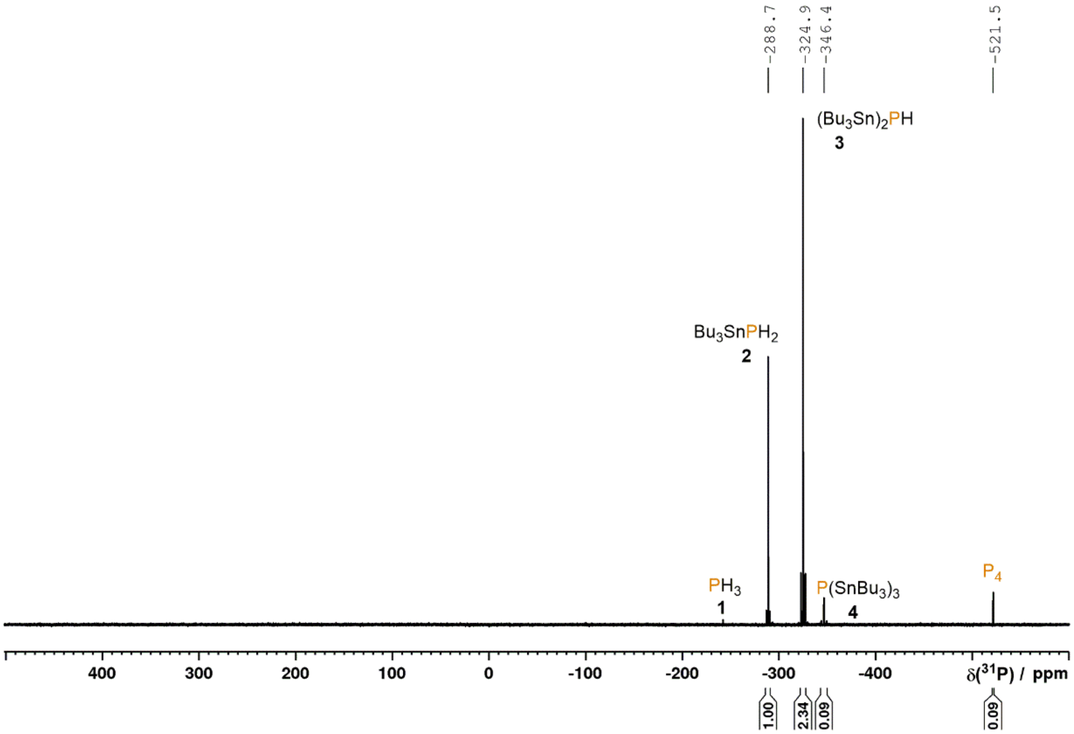

Supplementary Figure 132. $^{31}P\{^{1}H\}$ NMR spectrum for the reaction of P_4, 8 eq. Bu_3SnOMe and 8 eq. PMHS in PhMe, driven by 455 nm LED irradiation for 21 h.

Supplementary Method 37: Hydrostannylation of P_4 using Bu_3SnOMe and PMHS initiated by AIBN (0.01 mmol scale)

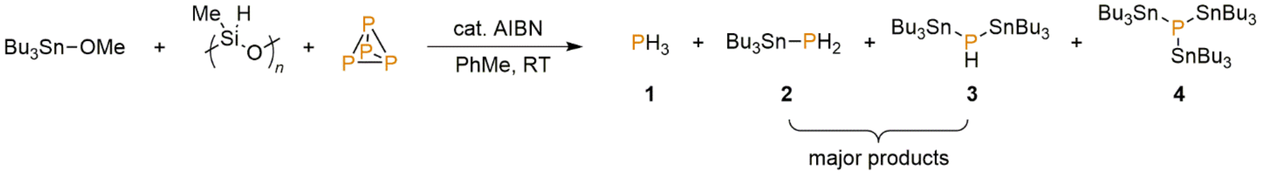

As for the blue LED-driven reactions, AIBN-initiated P_4 hydrostannylation was found to proceed in a very similar manner when Bu_3SnH was replaced with Bu_3OMe and PMHS. Again, however, slight modification of the initial reaction conditions was found to give improved performance.

To a 10 mL, flat-bottomed, stoppered tube were added PhMe (500 µL), P_4 (0.01 mmol, as a stock solution in 77.4 µL PhH), Bu_3SnOMe (23.0 µL, 0.08 mmol), PMHS (4.8 µL, 0.08 mmol) and AIBN (0.001 mmol, as a stock solution in 49.3 µL PhH). The tube was sealed, wrapped in Al foil to exclude light, and heated to 40 °C for 19 h. The resulting mixture was analysed by ^{1}H, $^{31}P\{^{1}H\}$ and ^{31}P NMR spectroscopy, as shown in Supplementary Figure 133, below.

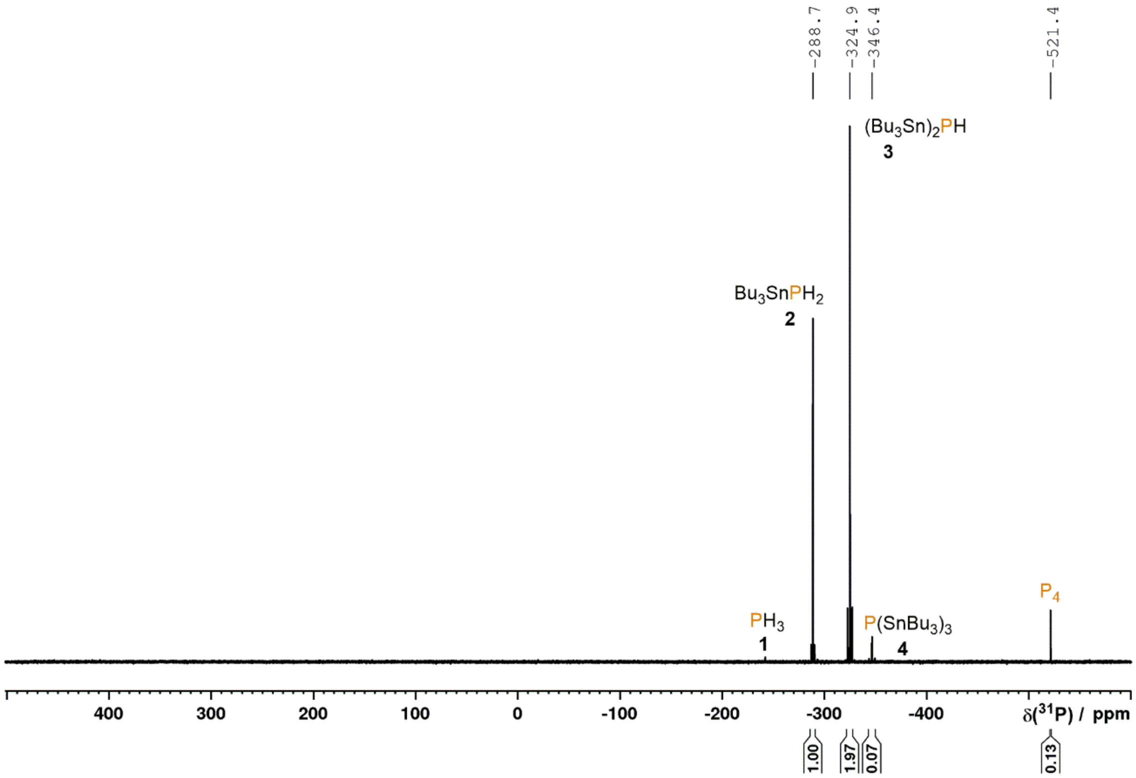

Supplementary Figure 133. $^{31}P\{^{1}H\}$ NMR spectrum for the reaction of P_4, 8 eq. Bu_3SnOMe and 8 eq. PMHS in PhMe, driven by AIBN initiation at 40 °C for 19 h.

Supplementary Method 38: Hydrostannylation of P_4 using $(Bu_3Sn)_2O$ and PMHS

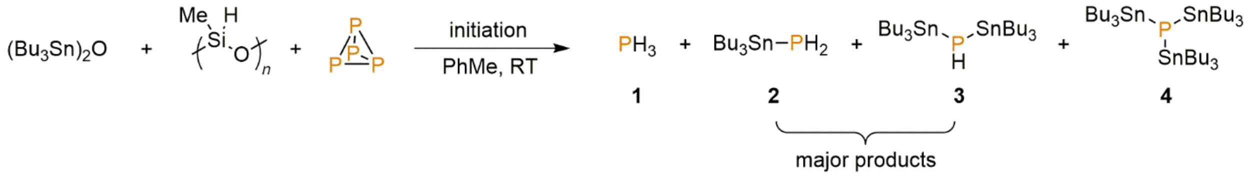

To a 10 mL, flat-bottomed, stoppered tube were added PhMe (500 µL), P_4 (0.01 mmol, as a stock solution in 86.0 µL PhH), $(Bu_3Sn)_2O$ (15.3 µL, 0.03 mmol) and PMHS (3.9 µL, 0.065 mmol). The tube was sealed, placed in a water-cooled block to maintain near-ambient temperature, and irradiated with blue light (455 nm (±15 nm), 3.2 V, 700 mA, Osram OSLON SSL 80) for 21 h. The resulting mixture was analysed by $^{31}P\{^1H\}$ NMR spectroscopy, as shown in Supplementary Figure 134, below.

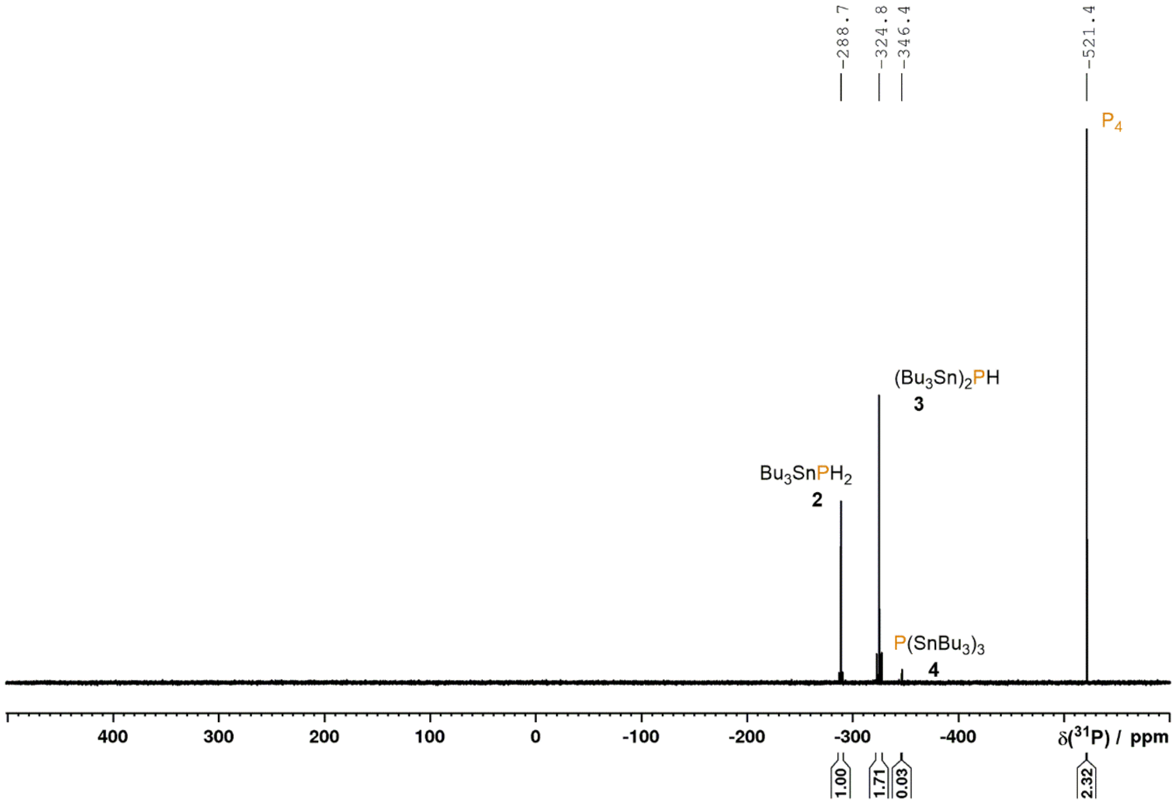

Supplementary Figure 134. $^{31}P\{^1H\}$ NMR spectrum for the reaction of P_4, 3 eq. $(Bu_3Sn)_2O$ and 6.5 eq. PMHS in PhMe, driven by 455 nm LED irradiation for 21 h.

In contrast to reactions using Bu_3SnOMe (Supplementary Methods 36 and 37), and despite the known ability of $(Bu_3Sn)_2O$ to act as a source of Bu_3SnH upon treatment with PMHS,[28] attempts to hydrostannlyate P_4 *via* reaction with a mixture of $(Bu_3Sn)_2O$ and PMHS were initially found to give significantly inferior results, with very significant amounts of P_4 remaining (for example, see Supplementary Figure 134, above). Nevertheless, satisfactory reactivity could be achieved by using ACN as an initiator under modified, and still relatively mild reaction conditions (Supplementary Figure 135, below).

To a 10 mL, flat-bottomed, stoppered tube were added PhMe (500 µL), P_4 (0.01 mmol, as a stock solution in 77.4 µL PhH), $(Bu_3Sn)_2O$ (20.4 µL, 0.04 mmol), PMHS (4.8 µL, 0.08 mmol) and ACN (0.002 mmol, as a stock solution in 96.2 µL PhH). The tube was sealed, wrapped in Al foil to exclude light, and heated to 80 °C for 3 days. The resulting mixture was analysed by $^{31}P\{^1H\}$ NMR spectroscopy, as shown in Supplementary Figure 135, below.

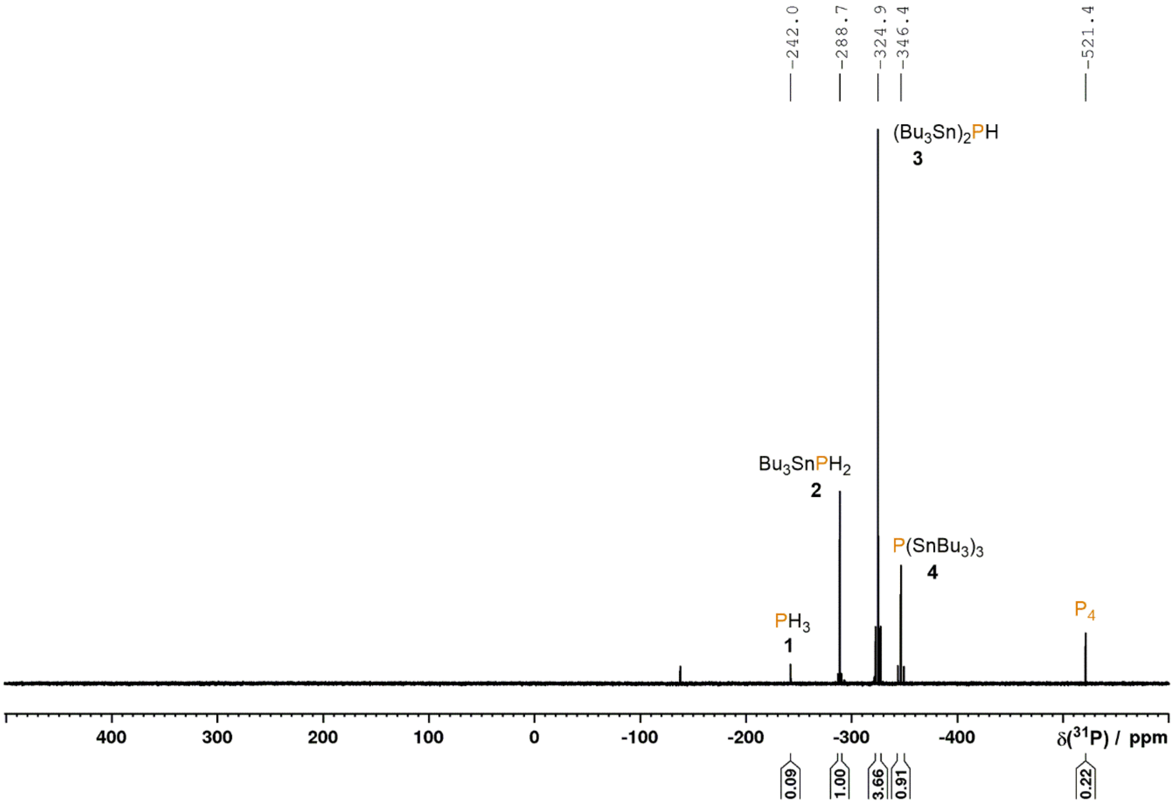

Supplementary Figure 135. $^{31}P\{^1H\}$ NMR spectrum for the reaction of P_4, 4 eq. $(Bu_3Sn)_2O$ and 8 eq. PMHS in PhMe, driven by ACN initiation at 80 °C for 3 days.

Supplementary Method 39: Synthesis and isolation of THPC (17) *via* hydrostannylation starting from Bu_3SnOMe

To a 50 mL flat-bottomed Schlenk tube were added P_4 (62.0 mg, 0.5 mmol) and PhMe (25 mL). After stirring to obtain a homogeneous solution, Bu_3SnOMe (1.15 mL, 4 mmol) and PMHS (239 µL, 4 mmol) were added. The resulting colourless, homogeneous mixture was stirred under irradiation with blue LED light (7X Osram OSLON SSL80, 455 nm (±15 nm), 20.3 V 1000mA) for 16 h, during which time the Schlenk tube was placed in a block cooled by circulating water to maintain near-ambient temperature. Following removal of volatiles under vacuum, EtOH (25 mL) and paraformaldehyde (750 mg, 25 mmol, 50 eq.) were added, and the resulting suspension was stirred at room temperature for 16 h. The mixture was frozen in a liquid nitrogen bath and HCl (4.0 M in 1,4-dioxane, 5 mL, 20 mmol) was added. After thawing, the reaction mixture was stirred at room temperature for 2 h. The pale yellow suspension was filtered, and volatiles were removed under vacuum. The oily solid residue was triturated with *n*-pentane (20 mL) overnight, filtered and washed with Et_2O (20 mL). The resulting white solid was then again dissolved in EtOH (2 x 20 mL). Following filtration, removal of volatiles under vacuum afforded the desired product as a white solid (330 mg, 87%).

NMR data are identical to those reported in Supplementary Method 30.

Supplementary Method 40: Synthesis and isolation of THPC (17) *via* hydrostannylation starting from $(Bu_3Sn)_2O$, with recycling of Bu_3SnCl (20) (0.5 mmol scale)

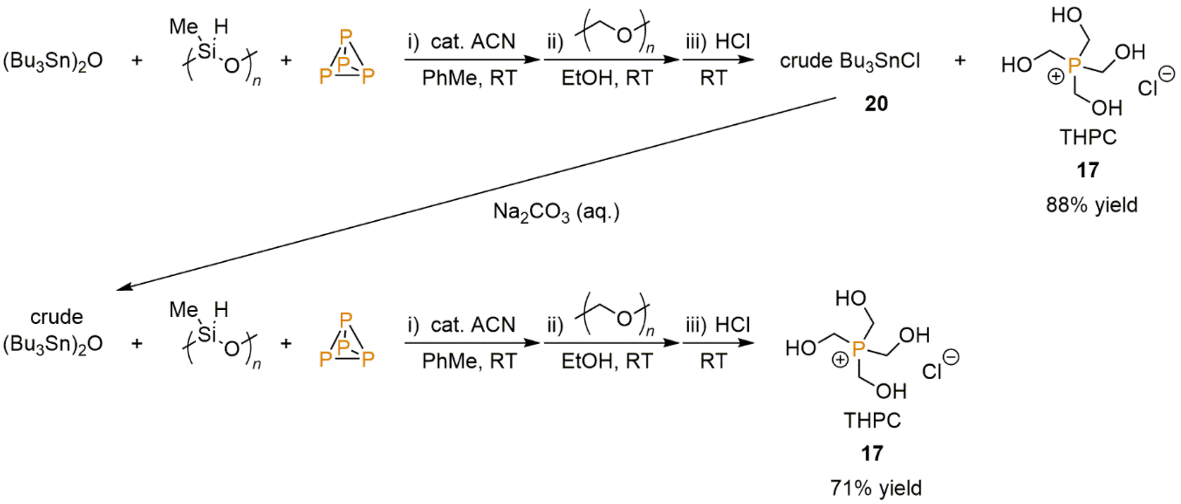

To a 50 mL Schlenk tube were added P_4 (62.0 mg, 0.5 mmol) and PhMe (25 mL). After stirring to obtain a homogeneous solution, $(Bu_3Sn)_2O$ (1.02 mL, 2 mmol), PMHS (239 µL, 4 mmol) and ACN (24.4 mg, 0.1 mmol) were added. The Schlenk tube was immediately and thoroughly wrapped in Al foil to exclude any ambient light, and the stirred reaction mixture was then heated to 80 °C for 3 days. Following removal of volatiles under vacuum, EtOH (25 mL) and paraformaldehyde (750 mg, 25 mmol) were added, and the resulting suspension was stirred at room temperature for 16 h. The mixture was frozen in a liquid nitrogen bath and HCl (4.0 M in 1,4-dioxane, 5 mL, 20 mmol) was added. After thawing, the reaction mixture was stirred at room temperature for 2 h. The pale yellow suspension was filtered, and volatiles were removed under vacuum. The remaining oily solid residue was triturated with Et_2O (20 mL) overnight, filtered and washed with further Et_2O (20 mL). The resulting white solid was then again dissolved in EtOH (2 x 20 mL). Following filtration and removal of volatiles under vacuum, the desired product was obtained as a white solid (335 mg, 88%).

NMR data are identical to those reported in Supplementary Method 30.

To the combined Et_2O washes from the above reaction was added a saturated aqueous solution of Na_2CO_3 (40 mL). The resulting biphasic mixture was stirred under open bench conditions for 16 h, and the organic phase was separated and washed with H_2O (4 x 15 mL). The organic phase was transferred into a 50 mL Schlenk tube and volatiles were removed under vacuum. The remaining procedure was performed under an inert atmosphere. A solution of P_4 (62.0 mg, 0.5 mmol) pre-dissolved in PhMe (25 mL) was added, followed by PMHS (239 µL, 4 mmol) and ACN (24.4 mg, 0.1 mmol). The Schlenk tube was immediately and thoroughly wrapped in Al foil to exclude any ambient light, and the stirred reaction mixture was then heated to 80 °C for 3 days. Following removal of volatiles under vacuum, EtOH (25 mL) and paraformaldehyde (750 mg, 25 mmol) were added, and the resulting suspension was stirred at room temperature for 16 h. The mixture was frozen in a liquid nitrogen bath and HCl (4.0 M in 1,4-dioxane, 5 mL, 20 mmol) was added. After thawing, the reaction mixture was stirred at room temperature for 2 h. The pale yellow suspension was filtered, and volatiles were removed under vacuum. The remaining oily solid residue was triturated with Et_2O (20 mL) overnight, filtered and washed with further Et_2O (20 mL). The resulting white solid was then again dissolved in EtOH (2 x 20 mL). Following filtration and removal of volatiles under vacuum, the desired product was obtained as a white solid (270 mg, 71%).

NMR data are identical to those reported in Supplementary Method 30.

Supplementary Method 41: Catalytic hydrostannylation of P_4 using Bu_3SnOMe and PMHS under near UV LED irradiation

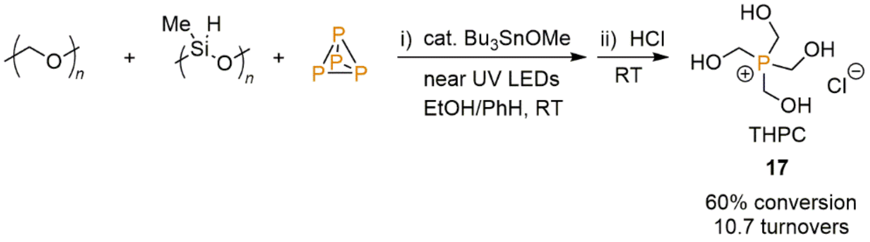

The catalytic transformation of P_4 into THPC (**17**) was performed (and the conversion and turnover number calculated) as described in the Methods section of the main manuscript. Relevant NMR data are provided below.

A proposed mechanism for the catalytic reaction is outlined in Extended Data Figure 7. Complete hydrostannylation of P_4 is suggested to occur prior to H_2CO insertion and subsequent ethanolysis. This is supported by the lack of observable, partially-hydrostannylated intermediates in previous experiments (see Supplementary Method 1, for example). Nevertheless, analogous insertion of H_2CO into these transient intermediates is also possible, and this option cannot be definitively excluded.

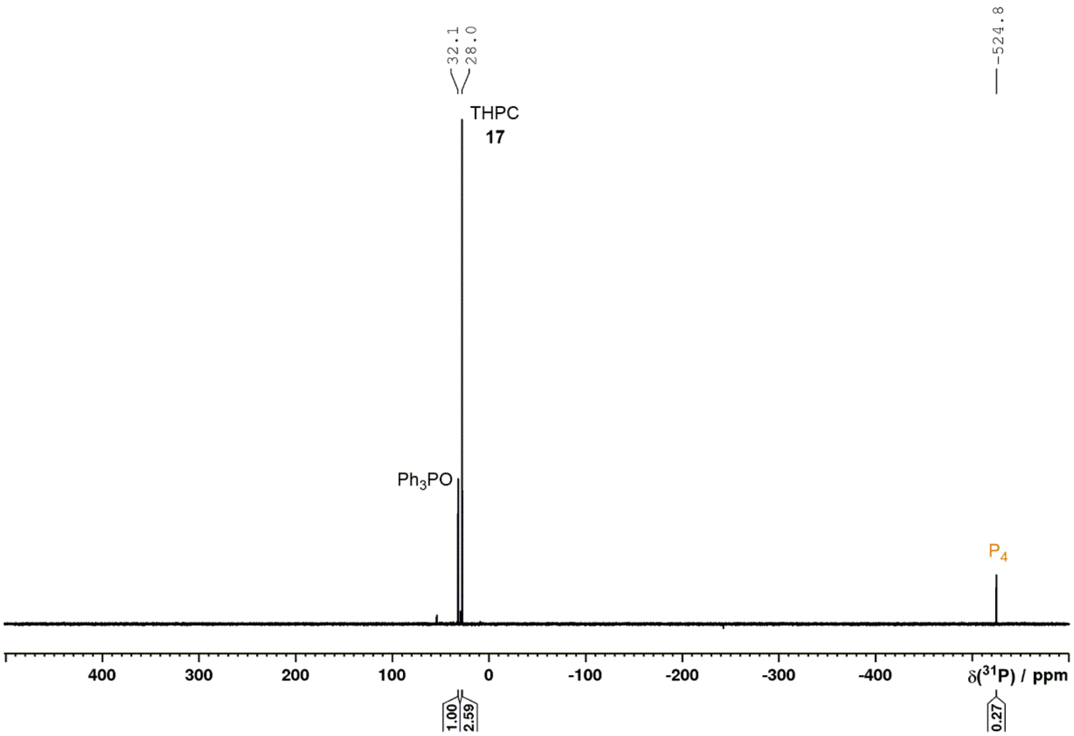

Supplementary Figure 136. $^{31}P\{^1H\}$ NMR spectrum for the catalytic transformation of P_4 into THPC (**17**) *via* THP (**16**), driven by 455 nm LED irradiation.

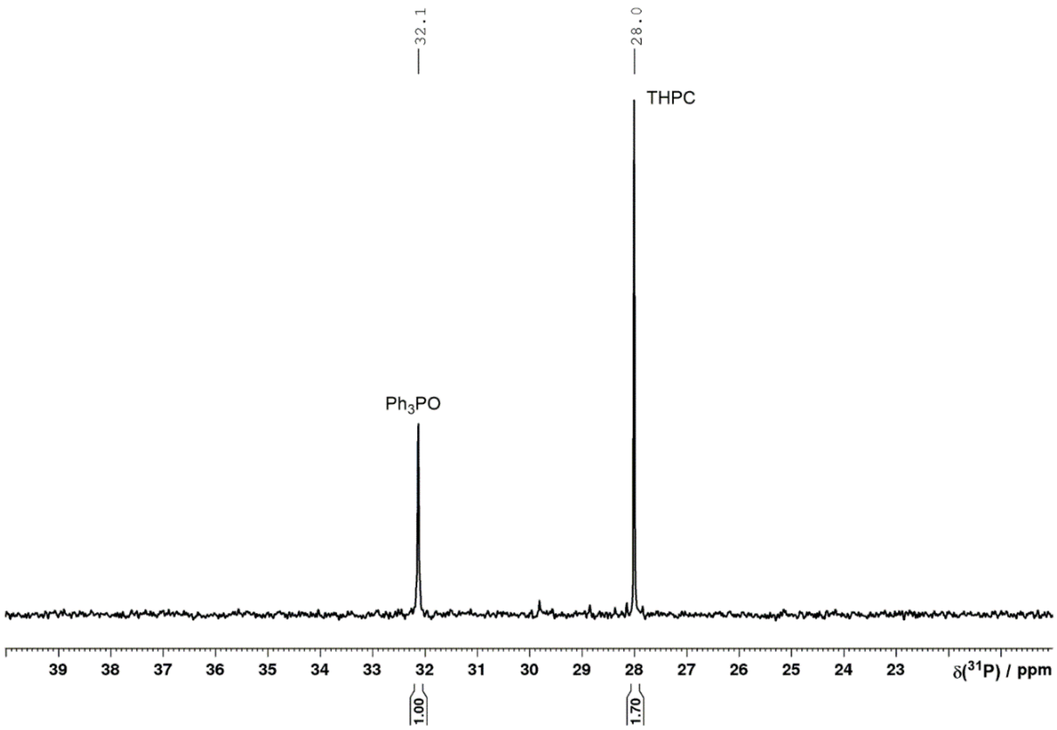

Supplementary Figure 137. Quantitative single-scan, inverse-gated $^{31}P\{^1H\}$ NMR spectrum for the catalytic transformation of P_4 into THPC (**17**) *via* THP (**16**), driven by 455 nm LED irradiation.

Supplementary Method 42: Catalytic hydrostannylation of P_4 using Bu_3SnOMe and PMHS initiated by AIBN

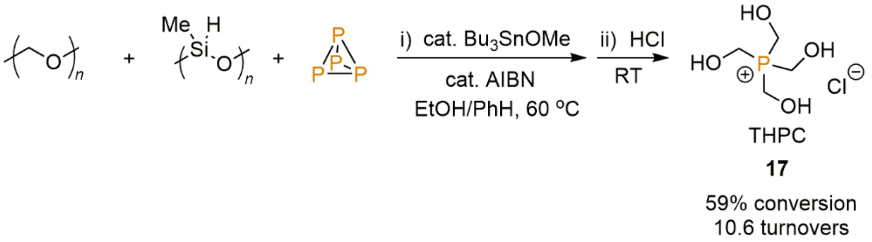

To a 10 mL, flat-bottomed, stoppered Schlenk tube were added EtOH (500 µL), P_4 (0.03 mmol, as a stock solution in 190 µL PhH), Bu_3SnOMe (2.9 µL, 0.01 mmol), PMHS (57.4 µL, 0.96 mmol), AIBN (0.01 mmol, as a stock solution in 37.0 µl PhH) and paraformaldehyde (30 mg, 1.0 mmol). The tube was sealed, wrapped in Al foil to exclude light, and heated to 60 °C for 65 h. The mixture was then frozen in a liquid nitrogen bath and HCl (4.0 M in 1,4-dioxane, 0.1 mL, 0.4 mmol) was added. After thawing, the reaction mixture was stirred at room temperature for 2 h. Following addition of Ph_3PO (0.04 mmol, as a stock solution in 497 µL MeCN) as an internal standard, the resulting mixture was analysed by $^{31}P\{^1H\}$ NMR spectroscopy, as shown in Supplementary Figure 138, below. The chemical shift observed for THPC (**17**) in these spectra is *ca.* 1 ppm downfield of that observed in spectra of isolated samples, which is attributed to solvent effects and the presence of excess HCl. That these peaks correspond to THPC was unambiguously confirmed by subsequent addition of an authentic sample to one representative reaction, which clearly increased the intensity of this peak.

Accurate conversion to THPC was measured by integration of a single-scan, inverse-gated $^{31}P\{^1H\}$ NMR spectrum (Supplementary Figure 139), in line with our previously-described methodology.[29] For two independent runs, conversions of 58% and 60% were determined.

Turnover numbers (TONS; 10.4 and 10.9, respectively, for an average of 10.6) were calculated from these conversions by factoring in the 1:6 stoichiometry of the reaction between P_4 and Bu_3SnH. Because of this stoichiometry, full consumption of 1 eq. of P_4 relative to Bu_3SnOMe requires six turnovers of the catalyst (i.e. it must be used to regenerate Bu_3SnH six times). Equivalently, formation of 1 eq. of THPC (from 0.25 eq. P_4) requires 1.5 turnovers of the catalyst. The TON is therefore calculated as 1.5 times the molar ratio between the THPC formed and the Bu_3SnOMe catalyst employed.

A proposed mechanism for the catalytic reaction is outlined in Extended Data Figure 7.

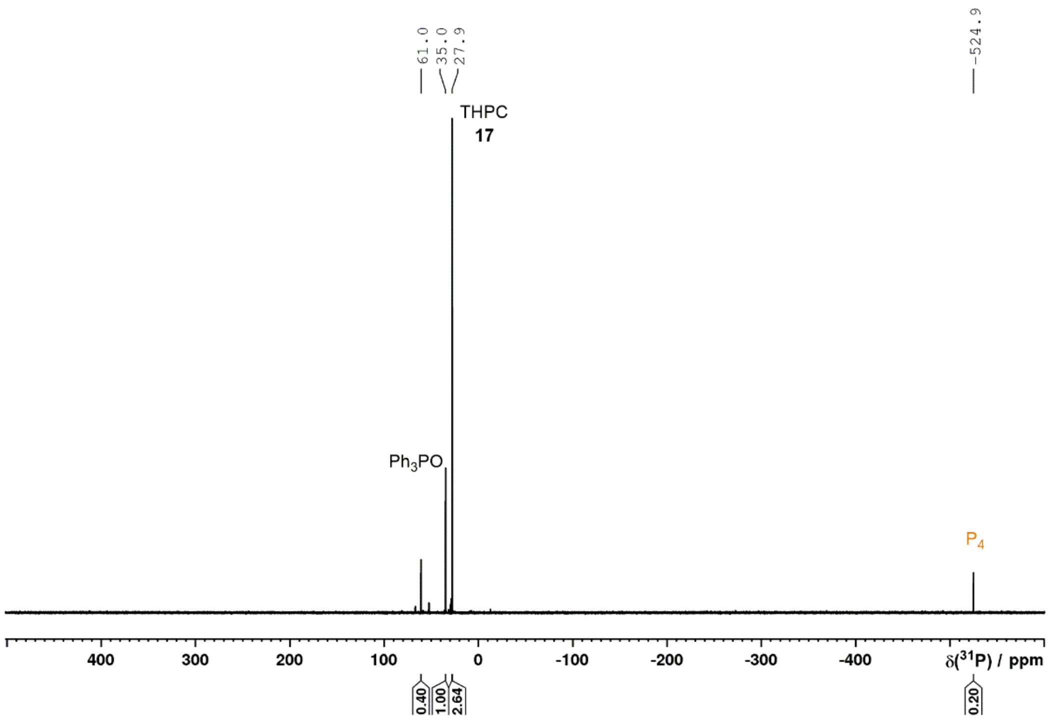

Supplementary Figure 138. $^{31}P\{^{1}H\}$ NMR spectrum for the catalytic transformation of P_4 into THPC (**17**) *via* THP (**16**), driven by AIBN initiation.

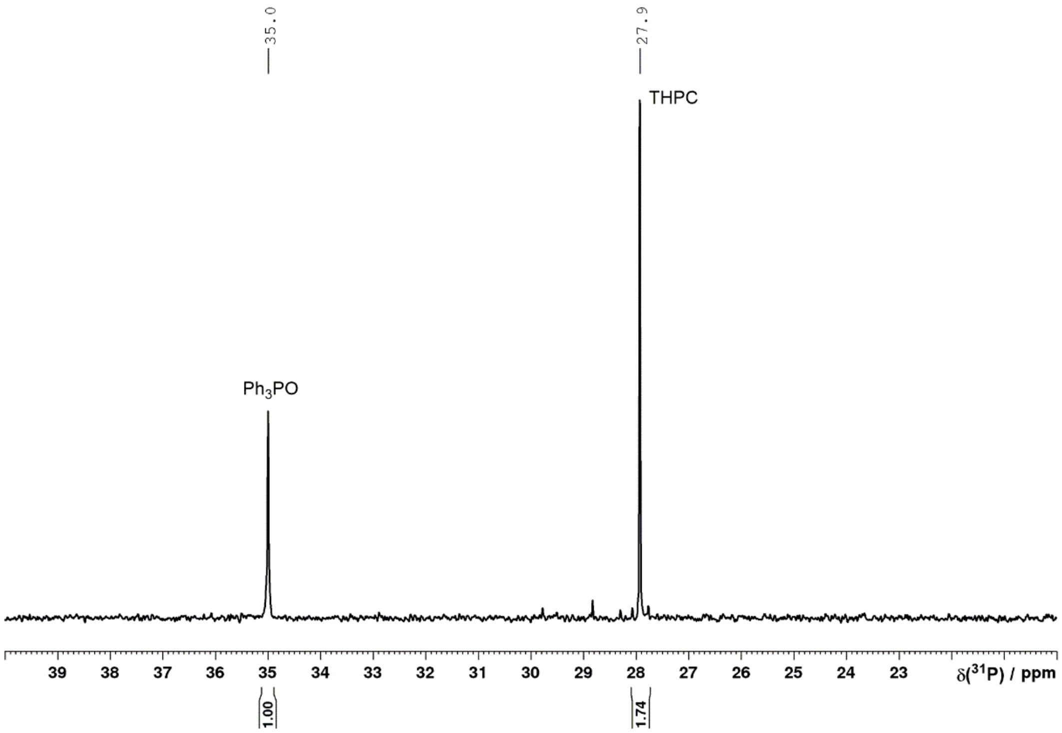

Supplementary Figure 139. Quantitative single-scan, inverse-gated $^{31}P\{^{1}H\}$ NMR spectrum for the catalytic transformation of P_4 into THPC (**17**) *via* THP (**16**), driven by AIBN initiation.

Supplementary References

1. Nakajima, M. et al. A direct $S_0 \rightarrow T_n$ transition in the photoreaction of heavy atom-containing molecules. *Angew. Chem. Int. Ed.* **59**, 6847-6852 (2020).

2. Julliard, M. & Chanon, M. Photoelectron-transfer catalysis: its connections with thermal and electrochemical analogs. *Chem. Rev.* **83**, 425-506 (1983).

3. Thompson, S. M. & Schubert, U. Dehydrogenative stannane coupling by platinum complexes. *Inorg. Chim. Acta* **350**, 329-338 (2003).

4. Bumagin, N. A., Gulevich, Y. V. & Beletskaya, I. P. Synthesis of hexaalkyl(aryl)distannanes and their reaction with organic halides under conditions of catalysis by palladium complexes. *Izv. Akad. Nauk SSSR, Ser. Khim.* **33**, 1044-1049 (1984).

5. Mitchell, T. N., Amamria, A., Killing, H. & Rutschow, D. Palladium catalysis in organotin chemistry: addition of hexaalkylditins to alkynes. *J. Organomet. Chem.* **304**, 257-265 (1986).

6. Neumann, W. P., Schneider, B. & Sommer, R. Über den Austausch nucleophiler Reste am Zinn und eine vielseitige Synthese für organische Distannane. *Liebigs Ann. Chem.* **692**, 1-11 (1966).

7. Norman, A. D. The synthesis of (trimethylstannyl)phosphine: the observation of phosphorus-tin nuclear spin-spin coupling. *J. Organometal. Chem.* **28**, 81-86 (1971).

8. Kai, Y., Oku, S., Tani, T., Sakurai, K. & Tsuchimoto, T. A Drastic Effect of TEMPO in Zinc-Catalyzed Stannylation of Terminal Alkynes with Hydrostannanes via Dehydrogenation and Oxidative Dehydrogenation. *Adv. Synth. Catal.* **361**, 4314-4323 (2019).

9. Evans, C. M., Evans, M. E. & Krauss, T. D. Mysteries of TOPSe revealed: insights into quantum dot nucleation. *J. Am. Chem. Soc.* **132**, 10973-10975 (2010).

10. Li, Y., Chakrabarty, S., Mück-Lichtenfeld, C. & Studer, A. Ortho-Trialkylstannyl Arylphosphanes by C–P and C–Sn Bond Formation in Arynes. *Angew. Chem. Int. Ed.* **55**, 802-806 (2016).

11. Harrison, P. G., Ulrich, S. E. & Zuckerman, J. J. A Nuclear Magnetic Resonance Investigation of the Bonding in Fourth-Group Phenylphosphines. *Inorg. Chem.* **11**, 25-28 (1972).

12. Laneman, S. A., Fronczek, F. R. & Stanley, G. G. Structural characterization of 1,2,4,5-tetraphenylcyclo-3,6-dicarba-1,2,4,5-tetraphosphine: a highly folded chair conformation. *Phosphorus, Sulfur, and Silicon* **42**, 97-102 (1989).

13. Becker, G., Rössler, M. & Uhl, W. Acyl- und alkylidenphosphane. XII. Synthese und Eigenschaften des 2,2-Dimethylpropionylphosphans und einiger Derivate. *Z. Anorg. Allg. Chem.* **473**, 7-19 (1981).

14. Becker, G., Rössler, M. & Uhl, G. Acyl- und Alkylidenphosphane. XX. Bis(2,2-dimethylpropionyl)phosphan und Bis(2,2dimethylpropionyl)phosphide. *Z. Anorg. Allg. Chem.* **495**, 73-88 (1982).

15. Geeson, M. B. & Cummins, C. C. Phosphoric acid as a precursor to chemicals traditionally synthesized from white phosphorus. *Science* **359**, 1383-1385 (2018).

16. Ebsworth, E. A. V., Hutchison, D. J., Macdonald, E. K. & Rankin, D. W. H. Some di- and tri-phosphines containing PF_2-groups. *Inorg. Nucl. Chem. Letters* **17**, 19-21 (1981).

17. Cossairt, B. M. & Cummins, C. C. Radical synthesis of trialkyl, triaryl, trisilyl and tristannyl phosphines from P_4. *New J. Chem.* **34**, 1533-1536 (2010).

18. Becker, G. Bildung und Eigenschaften von Acylphosphinen. II. Verbindungen aus der Reaktion von Tris(trimethylsilyl)phosphin mit Pivaloylchlorid. *Z. Anorg. Allg. Chem.* **430**, 66-76 (1977).

19. Macdonnell, G. D. et al. The barrier to carbon–phosphorus bond rotation in triaroylphosphines. *Tetrahedron Lett.* **19**, 857-860 (1978).

20. Geeson, M. B., Ríos, P., Transue, W. J. & Cummins, C. C. Orthophosphate and sulfate utilization for C-E (E = P, S) bond formation via trichlorosilyl phosphide and sulfide anions. *J. Am. Chem. Soc.* **141**, 6375-6384 (2019).

21. Kaphan, D. M., Levin, M. D., Bergman, R. G., Raymond, K. N. & Toste, F. D. A supramolecular microenvironment strategy for transition metal catalysis. *Science* **350**, 1235-1238 (2015).

22. Schumann, H. Organogermyl, organostannyl, and organoplumbyl phosphines, arsines, stibines, and bismuthines. *Angew. Chem. Int. Ed.* **8**, 937-950 (1969).

23. Caporali, M., Gonsalvi, L., Zanobini, F. & Peruzzini, M. Synthesis of the water-soluble bidentate (P,N) ligand PTN(Me) (PTN(Me) - 7-phospha-3-methyl-1,3,5-triazabicyclo[3.3.1]nonane). *Inorganic Syntheses* **35**, 96-102 (2010).

24. Vullo, W. J. Studies concerning the neutralization of tetrakis(hydroxymethyl)phosphonium chloride and the reaction of tris(hydroxymethyl)phosphine with formaldehyde. *J. Org. Chem.* **33**, 3665-3667 (1968).

25. Davies, A. G., Sella, A. & Sivasubramaniam, R. Can mono- or di-butyltin chlorides produce tributyltin chloride at elevated temperatures? Implications for applications in chemical vapour deposition. *J. Organomet. Chem.* **691**, 3556-3561 (2006).

26. Tan, Z. et al. Phosphorus-containing polymers from tetrakis-(hydroxymethyl)phosphonium sulfate III. A new hydrolysis-resistant tris(allyloxymethyl)phosphine oxide and its thiol-ene reaction under ultraviolet irradiation. *RSC Adv.* **4**, 41705-41713 (2014).

27. Golubev, N. S., Asfin, R. E., Smirnov, S. N. & Tolstoi, P. M. Study of hydrogen bonds of hypophosphorous acid by ^{1}H, ^{2}H, ^{31}P, and ^{15}N NMR spectroscopy under slow exchange conditions. *Russ. J. Gen. Chem.* **76**, 915-924 (2006).

28. Hayashi, K., Iyoda, J. & Shiihara, I. Reaction of organotin oxides, alkoxides and acyloxides with organosilicon hydrides. New preparative method of organotin hydrides. *J. Organomet. Chem.* **10**, 81-94 (1967).

29. Lennert, U. et al. Direct catalytic transformation of white phosphorus into arylphosphines and phosphonium salts. *Nat. Catal.* **2**, 1101-1106 (2019).